Studies of the Role of Versican Expression and Turnover in the Control of Axonal Growth in the Chick Embryo

Dissertation
zur
Erlangung der naturwissenschaftlichen Doktorwürde
(Dr. sc. nat.)

vorgelegt der
Mathematisch-naturwissenschaftlichen Fakultät
der
Universität Zürich

von

Estelle Cassoly

aus Frankreich

Promotionskomitee

Prof. Dr. Esther Stöckli (Vorsitz)
Prof. Dr. Dieter Zimmermann (Leitung der Dissertation)
Prof. Dr. Stephan Neuhauss

Zürich, 2011

À mes parents,

À ma grand-mère, Jacqueline Boussard.

1. Summaries

1.I. Summary

The coordinated action of multiple guidance cues controls the migration of neural crest cells (NCC) and outgrowth of axons in embryonic development to build a functional peripheral nervous system (PNS). Previous studies from our laboratory have shown that the particular isoforms (V0/V1) of the extracellular matrix hyalectan 'versican' are selectively associated to barrier tissues of migrating NCC and growing axons in the embryonic chick hind limb *in vivo* and act as potent inhibitors of NCC migration *in vitro*. Moreover, the V0/V1 versican splice-variants widely expressed in early hind limbs disappear when axons invade the embryonic limb suggesting an involvement of the proteases of the ADAMTS family (a disintegrin and metalloprotease with thrombospondin type 1 motifs), which specifically cleave some hyalectans including versican.

To elucidate the role of versican function and its turnover in axonal guidance of the PNS, we first analysed the inhibitory effect of versicans V0/V1 on neurite growth of dorsal root ganglia *in vitro* and showed that ectopic injection of versican into the chick hind limb *in ovo* severely disturbs the patterns of growing axons. Furthermore, we detected an intriguing correlation between ADAMTS9 expression, versican disappearance and axons extension. However, no versican processing was observed with different chick recombinant ADAMTS9 variants *in vitro*. Besides, versican turnover and axonal guidance of developing axons *in vivo* were not affected, when chick ADAMTS9 cDNA expression constructs were in vivo-electroporated in the hind limb or in the spinal cord of chick embryos. These results suggest that versicans V0/V1 act as axon guidance molecules in the peripheral nervous system and indicates that ADAMTS9 alone may not be the major protease involved in versican turnover during innervation of limb bud.

Recent genetic studies have revealed collaborative functions of ADAMTS members for versican processing *in vivo.* Interestingly, the versicanase ADAMTS5 was described to be specifically expressed in the peripheral nerve components during mouse embryogenesis. Taking together these studies and our results, in which a clear spatio-temporal correlation was established between the expression profile of ADAMTS9, versican distribution and outgrowing axons in chick hind limb development, let us suspect that ADAMTS9 expressed in mesenchymal tissues of the developing limb bud might interact with ADAMTS5 and/or other versicanases to regulate versican function in axonal guidance *in vivo*.

1.II. Zusammenfassung

Um ein funktionelles peripheres Nervensystem (PNS) zu bilden, ist die koordinierte Tätigkeit verschiedenster Moleküle in der embryonalen Entwicklung nötig. Dabei müssen die Neuralleistenzellen (NCC) in die vorgesehene Richtung migrieren und das axonale Wachstum muss präzise gelenkt werden. Frühere Studien unserer Gruppe haben gezeigt, dass bestimmte Versican Isoformen (V0/V1), welche zur Familie der extrazellulären Matrix Hyalektane gehören, mit Barrierengeweben von migrierenden NCCs und wachsenden Axone in den Beinanlagen von Hühnerembryonen assoziiert sind und dass aufgereinigte Versicane die Migration von NCCs und das Wachstum von Neuriten *in vitro* unterdrückt. Die Versicane V0/V1, die in den frühen Beinanlagen weit verbreitet sind, verschwinden kurz vor dem Eindringen der Axone in die embryonale Hinterextremität. Dieses Verschwinden weist auf einen Abbauprozess hin, der zur Regulation von Versican-Funktionen möglicherweise Metalloproteasen der ADAMTS Familie (a disintegrin and a metalloprotease with thrombospondin type 1 motif) involviert.

Um die Rolle von Versican in der Lenkung von Axonen des PNS aufzuklären, haben wir zuerst den hemmenden Effekt von Versican V0/V1 auf das Neuritenwachstum der Rückenwurzelganglien *in vitro* analysiert. In weiteren Experimenten *in ovo* konnten wir zudem zeigen, dass die Injektion von Versican in das Hühnerhinterbein die Profile der auswachsenden Nervenbahnen ernsthaft stört. Des Weiteren haben wir eine klare Korrelation zwischen dem Auftreten der Metalloprotease ADAMTS9 und dem Abbau von Versicanen in der unmittelbaren Umgebung von wachsenden Axonen detektiert. In *in vitro* Experimenten konnten wir jedoch keinen Versican-Abbau durch rekombinantes ADAMTS9 beobachten. Ausserdem haben wir nach Injektion und *in vivo*-Elektroporation von ADAMTS9 cDNA Expressionskonstrukten in Hinterbein oder Rückenmark von Hühnerembryonen weder eine Beeinflussung des Versican-Abbaus noch des Axonwachstums festgestellt. Diese Ergebnisse lassen darauf schliessen, dass Versican V0/V1 zwar als Leitmolekül im PNS fungieren kann, dass ADAMTS9 - trotz passendem Expressionsmuster - als Einzelenzym aber eher nicht als regulatorisches Protein dieser Versican-Funktion in Frage kommt.

Neuere genetische Studien haben tatsächlich funktionelle Wechselwirkungen verschiedener ADAMTS Metalloproteasen in der Prozessierung von Versican *in vivo* aufgedeckt. Interessanterweise wurde beschrieben, dass ADAMTS5 während der Embryogenese von Mäusen in peripheren Nervenzellen ebenfalls hochreguliert wird. Zusammen mit unseren Ergebnissen zeigen sie eine deutliche räumliche und zeitliche Korrelation zwischen der Expression dieser ADAMTSs, dem Versican-Abbau und dem Einwachsen von Axonen in die Hinterbeinanlagen. Diese Resultate lassen vermuten, dass ADAMTS9 die Funktion von Versican in der Axonlenkung *in vivo* allenfalls nur zusammen mit ADAMTS5 und/oder anderen Versicanasen reguliert.

2. Introduction

2.I. Axon pathfinding

During development of the peripheral nervous system, trunk neural crest cells emigrate from the dorsal neural tube and differentiate into distinct cellular subpopulations including sensory and sympathetic neurons. These newly formed neurons interact with each other and other neuronal and non-neuronal cells to participate in the building of a functional network. One of the big challenges of the set-up of the nervous system consists in the difficult task of neuronal processes to reach their individual targets. The growth cone, a highly dynamic structure at the tip of the axons plays a key role in the pathfinding by selectively responding to multiple extracellular signals. This has already been realised more than a century ago by Ramón y Cajal, who described the growth cone as the element able to interpret chemotactic cues to steer the axons. Indeed, the growth cone recognises guidance cues via specific cell-surface receptors, integrates the different signals and promptly remodels the cytoskeleton to finally adjust the trajectory of the axon (reviewed in (Lowery and Van Vactor, 2009)). In consequence, the growing axons follow stereotypic pathways and eventually extend over considerable distances to reach their proper targets. On the lumbosacral level of the trunk for instance, sensory axons originating from the dorsal root ganglions join the motor axons exiting from the ventral neural tube and form together the crural and the sciatic plexuses from where they innervate the hind limb (reviewed in (Bonanomi and Pfaff, 2010)). In the spinal cord, motoneurons are arranged into longitudinal columns along the rostro-caudal axis. The lateral motor columns (LMC) contain also the limb-innervating motor neurons that project to the plexus at the base of the limb. As the axons emerge from the plexus region, their trajectories bifurcate either ventrally or dorsally within the limb mesenchyme. The lateral division of LMC send axons to dorsally derived muscles, whereas the motor neurons from the medial LMC project axons to ventral limb muscles. This initial bifurcation in the proximal limb tissue is followed by numerous additional pathway decisions at selective choice-points until the final target has been reached by the navigating growth cone.

Another impressive example of a highly precise axon guidance process can be observed at the spinal cord midline (reviewed in (Chedotal, 2010)). The commissural neurons extend their axons from the dorsal part of the spinal cord, first laterally then ventrally to reach and cross the midline. Afterwards they turn to project rostrally towards the brain.

How do axons from the same pool of motoneurons select their specific pathways? How do the commissural axons recognise their predetermined ventral trajectory and cross only once the midline before projecting rostrally? To respond to these questions, the molecular basis of axon pathfinding has been extensively studied during the last three decades. Many guidance cues have been discovered and the subjacent cellular mechanisms have been partially

described (reviewed in (Chilton, 2006; Dickson, 2002; Kolodkin and Tessier-Lavigne, 2010; Tessier-Lavigne and Goodman, 1996)).

In the current concepts, guidance molecules are divided in short and long-range cues, which participate in four principle types of regulatory mechanisms: contact attraction, chemoattraction, contact repulsion, and chemorepulsion (Fig.1).

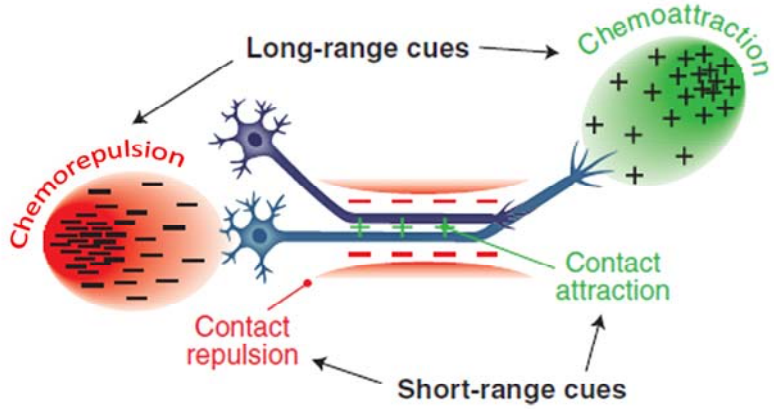

Figure 1. Different guidance molecules control the trajectories of the axons to their targets. All together, short (by contact) and long-range (by chemotropism) cues mediate the axon pathfinding (from (Kolodkin and Tessier-Lavigne, 2010)).

The repulsive cues push the axons and may provoke turning, collapse and retraction of the growth cone, while diffusible chemoattractants serve to pull the growing axons to particular regions. In an otherwise permissive environment, the repulsive cues permit to channel and thus, direct axons or to enforce route selection of pioneer axons and nerve fascicules at specific choice-points. Both repulsive and attractive short-range signals play together to maintain the growing axons in their predetermined corridors. In the following chapter I will present the principal molecules involved in axon guidance and growth, considering the two examples mentioned above as main model processes.

2.I.1 "Classical" guidance molecules

2.I.1.a Netrins

In vertebrates Netrins build a family of four secreted (1-4) and two membrane-bound molecules (G1-G2). Secreted Netrins form concentration gradients that are interpreted by navigating axons to reach their targets (Killeen and Sybingco, 2008; Livesey, 1999). In vertebrates, Netrins were first found as factor(s) secreted from the floor plate that selectively attract commissural neurons to the ventral midline (Tessier-Lavigne et al., 1988). Later, Netrin-1 and -2 were purified from chick brain or expressed as recombinant proteins and shown to exhibit chemoattractant properties for the commissural axons (Kennedy et al., 1994; Serafini et al., 1994).

The sequences of these two vertebrate netrins (Netrin-1 and Netrin-2) turned out to be highly homologous to the *Caenorhabditis elegans* Uncoordinated-6 (UNC-6) protein acting as a bi-functional axon guidance cue in conjunction with its receptors UNC-5 and UNC-40 (Hedgecock et al., 1990; Ishii et al., 1992). The worm mutants for the *unc-5*, *unc-6* and *unc-40* genes display all deficiencies in circumferential movement of cells and pioneer axons: unc-40 affects mainly the ventral migration, unc-5 the dorsal migration, and unc-6 both directions. UNC-6 and the vertebrate netrins primarily serve as diffusible attractive ligands (Kennedy et al., 1994). Interestingly, netrins were later recognised also as chemorepellents for certain types of neurons (Colamarino and Tessier-Lavigne, 1995; Varela-Echavarria et al., 1997), for example the trochlear motoneurons (Colamarino and Tessier-Lavigne, 1995). The first receptors for netrin to be identified belong to the DCC (Deleted in Colorectal Cancer) family (Keino-Masu et al., 1996), including UNC40 in *C.elegans* and Frazzled in *Drosophila* (Chan et al., 1996; Kolodziej et al., 1996). The vertebrate homologue of UNC-40, DCC is required for the functioning of Netrin as attractant (Keino-Masu et al., 1996). Unc-5 on the contrary, is necessary to mediate the repulsive effect of Netrin (Leonardo et al., 1997) (Fig.2). The immunoglobulin repeats of Unc-5 proteins are required for Netrin binding (Geisbrecht et al., 2003). Vertebrates have four Netrin-1 receptors (Unc5A-D) that are homologous to the UNC-5 receptor present in *C.elegans* (Hedgecock et al., 1990; Leonardo et al., 1997).

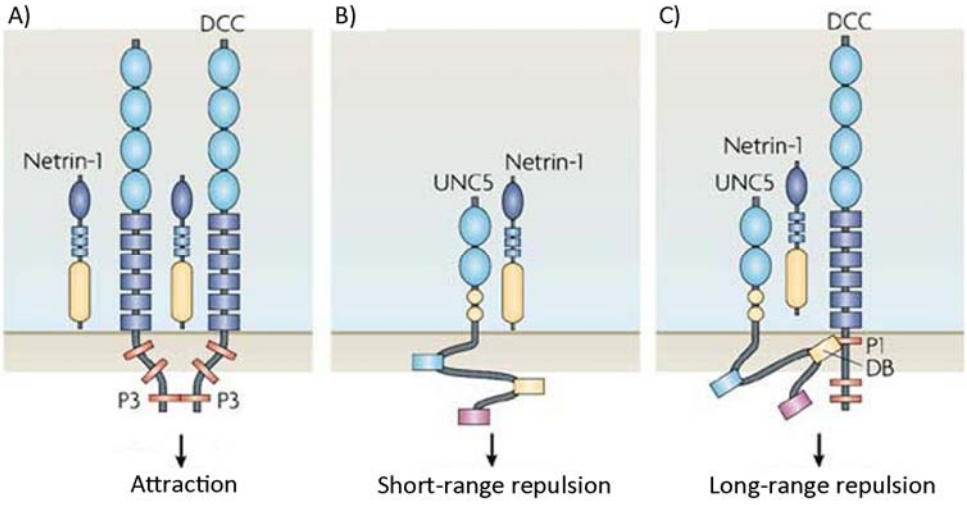

Figure 2. Bi-functionality of Netrin-1 is mediated through the interactions with UNC-5 and DCC receptors in the CNS (from (Cirulli and Yebra, 2007).
Attraction is triggered by Netrin-1 interacting exclusively with DCC receptors that permits their clustering via their P3 cytoplasmic domains (panel A), while repulsion is either mediated at short-range by UNC-5 alone (panel B) or UNC-5 and DCC, UNC5 interacting with the P1 intracellular domain of DCC impedes the DCC clustering and this complex mediated long-range repulsion (panel C).

More recently, another putative receptor for Netrins has been described. The Down's syndrome cell adhesion molecule (DSCAM) is a type I transmembrane receptor that

contains ten immunoglobulin domains and six fibronectin III repeats in its extracellular domain (Yamakawa et al., 1998). DSCAM may functions as an additional receptor for Netrin-1 and contributes to the netrin-dependent axon guidance during development (Andrews et al., 2008; Liu et al., 2009; Ly et al., 2008). Netrin-1 binds to the Ig domains of DSCAM *in vitro* (Ly et al., 2008). DSCAM is expressed by commissural axons in invertebrates and vertebrates as they extend to and across the floor plate (Andrews et al., 2008; Liu et al., 2009; Ly et al., 2008). Epitope-tagged recombinant Netrin protein from fruit fly, chick or human bind to recombinant *Dscam*/DSCAM in a cell overlay assay (Andrews et al., 2008; Liu et al., 2009; Ly et al., 2008). Liu *et al.* showed that the netrin-induced axon outgrowth is almost abolished by introducing DSCAM-specific siRNA into neurons of a spinal cord explant culture and that the downregulation of DSCAM inhibits the commissural axon attraction mediated by Netrin-1 in a commissural axon turning assay. Moreover, they have demonstrated that the knockdown of DSCAM *in ovo* interferes with commissural axon pathfinding in the chick neural tube (Andrews et al., 2008; Liu et al., 2009; Ly et al., 2008). Besides, Ly and colleagues put in evidence that the turning of axons is only completely abolished, when the DCC expression is down-regulated simultaneously. They also showed that DCC and DSCAM could interact in a heterophilic complex in the dorsal spinal cord. This complex seems, however, to dissociate in the presence of Netrin-1 (Andrews et al., 2008; Liu et al., 2009; Ly et al., 2008). From these data, it appears that DSCAM and DCC collaborate in the floor plate-attraction of commissural axons in response to Netrin-1 (Andrews et al., 2008; Liu et al., 2009; Ly et al., 2008).

2.I.1.b Slits and the Roundabout receptors (Robos)

Genetic analyses of the *Drosophila* mutants led to first identification of the Robos, receptors of a repellent guidance cue at the ventral midline. In *Robo* mutants, commissural axons are insensitive to midline repulsion and consequently cross and re-cross several times the midline, generating a "roundabout" phenotype (Seeger et al., 1993). The Robos, a novel receptor subfamily of the immunoglobulin superfamily, control the axon crossing of the midline in vertebrates and invertebrates (Kidd et al., 1998; Zallen et al., 1998). Later, secreted glycoproteins named Slits were recognised as the Robo ligands.

Twenty years ago, Slit had already been identified as a secreted factor from the midline glia, which is necessary for the proper path finding of commissural axons (Rothberg et al., 1990). In *Slit* mutants, axons never cross the midline and join together into a single longitudinal bundle in *Drosophila* (Kidd et al., 1999). It has been shown that mammalian Slit2 is able to bind Robos in a co-culture system and it was demonstrated that olfactory bulb axons from

mouse embryos turn away from cells expressing recombinant Slit (Li et al., 1999). These and other observations indicated that Slits are directly involved in axonal repulsion in *Drosophila* and vertebrates (Brose et al., 1999; Kidd et al., 1999; Li et al., 1999). Another role for Slit as branching factor for sensory axons in vertebrates has been described (Wang et al., 1999). The branching activity of Slits, observed for both axons and dendrites, is also mediated by Robo family members (Ma and Tessier-Lavigne, 2007; Whitford et al., 2002).

Slits and Robos have been found in the nervous system from invertebrates such as *Drosophila* and *C.elegans* to vertebrates (Brose et al., 1999; Hao et al., 2001; Itoh et al., 1998; Long et al., 2004). From the collected data of the different species, a concept has emerged, in which axonal tips carrying the Robo receptor are repelled by the Slit-ligand present in the floor plate. To allow the initial crossing of the midline, Robo is first virtually absent from the growth cone of the commissural axons approaching the floor plate. It is, however, upregulated as soon as the axons are reaching the contralateral side. The increasing robo-slit interactions subsequently prevent the re-crossing of the longitudinally turning and extending axons (Kidd et al., 1998).

Another protein, Commissureless (Comm) seems to participate in the Robo-Slit guidance at the midline in *Drosophila*. By disrupting the expression of the protein Comm via gene mutation, all left-right connections are abolished in the ventral nerve cord, the fly homolog of the spinal cord (Tear et al., 1996). By silencing axon responses to the midline repellent Slit, Comm promotes midline crossing (Gilestro, 2008; Keleman et al., 2002). Comm seems to do so by controlling the trafficking of Robo receptor and thus, regulate its exposure on the surface of the commissural growth cones (Fig.3).

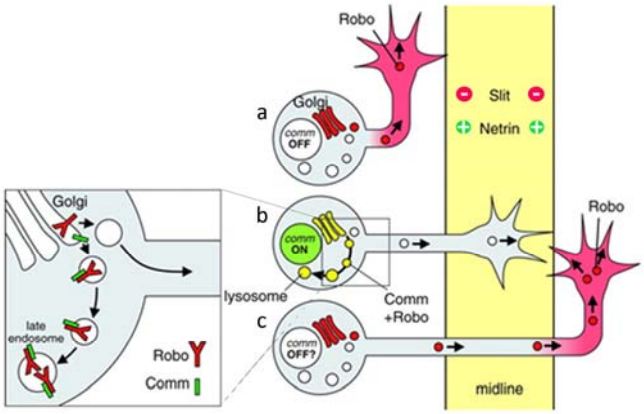

Figure 3. Comm controls the coordinated actions of Slit/Robos and Netrin at the *Drosophila* midline (adapted from (Dickson and Gilestro, 2006)).

The ipsilateral neurons, which do not express Comm display Robo receptors at their growth cones and are consequently repelled from crossing the midline by Slit ligands (a). As the growth cones of commissural axons reach the midline, Comm is expressed and triggers the Robo in the endosomes (b and insert). That impedes the Slit/Robo interaction and allows axons to go across. After crossing, Comm is down-regulated in commissural axons permitting the new synthesised Robo to be accumulated in the growth cones and to interact with Slit (c). Thus, Slit/Robo interaction hampers axons attracted by Netrin to re-cross the midline.

In *comm* mutants the Robo receptors appear on the axonal tip already on the ipsilateral side and interact with Slit secreted at the midline too early. Consequently, the axons project ipsilaterally while being prevented from crossing the midline. In wildtype flies commissural neurons begin to express the protein Comm as they approach the midline, and then reduce Comm expression after crossing to allow a continuous axonal growth (Gilestro, 2008).

No Comm homolog has yet been found in vertebrates, but a different mechanism seems to regulate the crossing at the midline. In vertebrates, the Robo family member Robo3 possesses a splice variant, Robo3.1, which seems to neutralise the repulsive actions of Robo1 and Robo2, when axons approach and cross the midline (Chen et al., 2008; Marillat et al., 2004; Sabatier et al., 2004; Tamada et al., 2008) (Fig.4). Robo3.1 is expressed at high levels on commissural axons until they have crossed the floor plate, while the concentrations of Robo1 and Robo2 increase only after axons have reached the contralateral side (Chen et al., 2008; Marillat et al., 2004; Sabatier et al., 2004; Tamada et al., 2008). A similar "anti-Robo" function of Robo2 has been proposed from genetic analyses in *Drosophila* as well (Spitzweck et al., 2010).

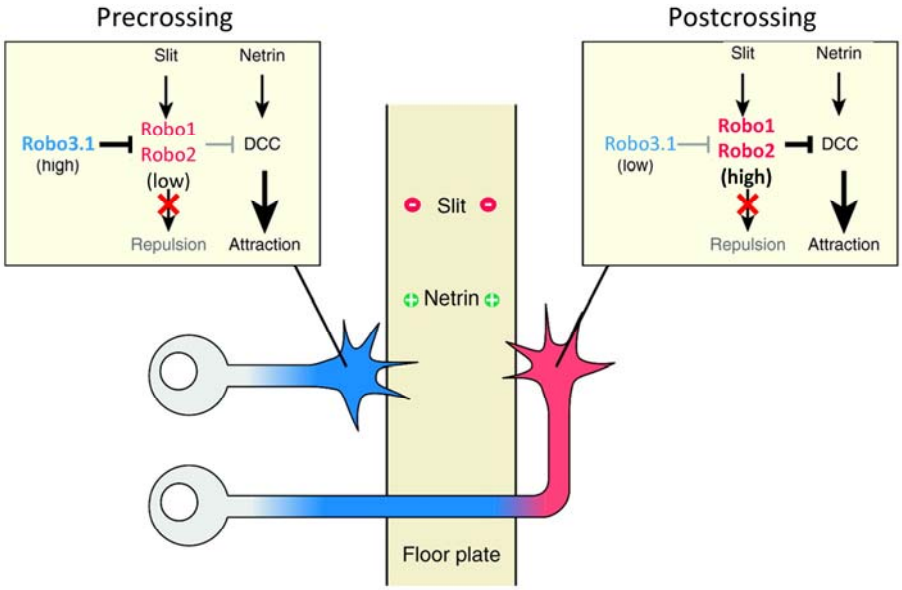

Figure 4. Coordinated actions of Slit/Robos and Netrin to control the midline crossing of commissural axons (adapted from (Dickson and Gilestro, 2006)).

Netrin attracts through DCC the growth cones of commissural axons to the floor plate. The commissural axons cross the midline. After crossing the Robo1 and Robo2 expression are up-regulated in the growth cones, the Robo1 and Robo2 interactions with Slit ligands distributed in the floor plate repel the commissural axons, preventing the re-crossing of the midline. Robo3.1, which is highly expressed before crossing and after that low expressed, participates in the control of the cross-guiding by down-regulating Robo1 and Robo2 expression.

2.I.1.c Semaphorins and their receptors

Semaphorins are a large family of phylogenetically conserved secreted and trans-membranous proteins (reviewed in (Raper, 2000; Yazdani and Terman, 2006)),

characterised by the sema domain, a specific cystein-rich region of about 500 amino acids length (Gherardi et al., 2004). Semaphorins members are regrouped in eight major classes: the classes 3, 4, 6 and 7 are found in vertebrates only, classes 1 and 2 are both present in invertebrates and vertebrates, while class V is specific to viruses. Sema-1 (previously named Fasciclin IV), the first member identified in the grasshopper embryo, was described as a preferential substrate to the growth cone of Ti1 neurons (Kolodkin et al., 1992). Isolated from chicken brain, collapsin 1, the chick orthologue of the mammalian Semaphorin3A (Sema3A), caused sensory ganglion growth cones to collapse *in vitro* (Luo et al., 1993).

Semaphorins function through multimeric receptor complexes (Raper, 2000). Membrane-associated Semaphorins bind to plexins (Winberg ML, 1998), whereas secreted class 3 Semaphorins interact with one of the four class A Plexins only in conjunction with the co-receptor of the Neuropilin (Npn) family (Sema3A/Npn1, Sema3F/Npn-2) (Chen et al., 1997; Giger et al., 1998; Kolodkin et al., 1997). Neuropilins act as the ligand-binding subunits, whereas plexins function as signal-transducting subunits. Plexin interactions with Neuropilin form a receptor complex that has a higher affinity for Semaphorin3A than Neuropilin alone (Takahashi et al., 1999). Semaphorins usually deflect axons from inappropriate regions, but some may also act as attractants. For instance, Wong and colleagues showed that trans-membranous Sema-1 ectopically expressed by epithelial cells in the grasshopper limb bud could promote axonal outgrowth during development, while the application of its extracellular domain as a soluble factor perturbed the axon pathfinding *in vivo* (Wong JT, 1999; Wong JT, 1997).

The secreted class 3 Semaphorins are the most studied group of axonal guidance molecules (reviewed in (Derijck et al., 2010; Mann and Rougon, 2007; Shim and Ming, 2007)). Secreted semaphorins are repulsive towards different types of neurons *in vitro*, including motor, sensory, olfactory and hippocampal neurons (reviewed in (Chilton, 2006)). Especially, the Sema3A/Npn-1 and Sema3F/Npn-2 complexes control distinct steps of motor axon growth and guidance during the formation of spinal motor connections (Huber AB, 2005). In Npn-1^{Sema-} knockout mice the absence of Sema3A/Npn-1 signalling leads to an aberrant defasciculation of the axons of LMC neurons and an early projection into the limb mesenchyme. In Npn-2-$^{Sema-}$ mutants no impairment of fasciculation was observed and the axons enter into the limb at the right time-point but the axons from the LMCm neurons show aberrant projections in the dorsal part of the limb. Moreover, the ectopic expression of Nnp-2 in LMC neurons promotes the selection of a ventral axonal trajectory into the forelimb. In summary, Sema3A/Npn-1 signalling seems to regulate the timing of motor axon growth into the forelimb. Sema3A possibly acting through a “surround repulsion” mechanism maintains fasciculation as axons grow toward the plexus and into the forelimb (Fig.5). The restricted expression of Sema3F in the dorsal part of the limb later in development, finally pushes the

motor axons expressing Npn-2 away from the dorsal towards the ventral region of the limb. Recently, Sema3F has been also described as a bifunctional guidance cue for axons of dopaminergic neurons in the mesodiencephalon (mdDA) of mouse embryos (Kolk et al., 2009). During early developmental stages, Sema3F chemorepulsion controls certain aspects of mdDA axons pathway development through both Npn-2-dependent (axon fasciculation and channelling) and Npn-2-independent (rostral growth) mechanisms. Later on, chemoattraction mediated by Sema3F and Npn-2 is required to orient mdDA axon projections in the cortical plate of the medial prefrontal cortex.

2.I.1.d Ephrins and Eph receptors

The Eph receptors and the ephrin ligands are cell-surface signalling molecules that play important roles in a large number of developmental events including axon guidance (reviewed in (Klein, 2004)). The EphA and EphB proteins are receptors tyrosine kinases, grouped together on the basis of high sequence similarities of their extracellular domains and on their preferential *in vitro*-binding to the GPI-linked ephrinA and transmembrane ephrinB ligand families, respectively (Pasquale, 2004). Ephrin-Eph heterodimers have to further cluster to engage bi-directional signalling. Soluble Ephrins released from the cell surface, do not appear to activate the Eph receptors. Consequently, ephrins and Eph receptors are thought to function only as short-range cues. The dimmer complexes can progressively aggregate, first to tetramers and then to larger clusters. This permits a modulation of the Eph-ephrin signalling in a concentration-dependent manner (reviewed in (Pasquale, 2005)).
The Eph-ephrin complexes function usually as repellents for some axons, but can also be attractants for others (Eberhart et al., 2004; Hansen et al., 2004; McLaughlin et al., 2003). Ephrin signalling plays an important role in topographic mapping of different sensorial systems, as the visual or the olfactory system (reviewed in (Klein, 2004)). In the optic tectum (chick, frog) or in the retina and in the superior colliculus (in mammals), gradients of EphA and EphrinA influence the topographic mapping along the anterioposterior tectal axis, while EphB and Ephrin B gradients control the dorsoventral projection pattern (Frisen et al., 1998; Hindges et al., 2002; Mann et al., 2002; Monschau et al., 1997; Nakamoto et al., 1996). Eph-ephrins complexes participate as well in the pathfinding of motor axons (Fig.5). Genetic analyses of multiple mouse mutants and the study of the overexpression or downregulation of different Eph-ephrins complexes in the hindlimb mesenchyme in chick embryo, have provided evidence that EphB1 and EphB3 are key contributors to the ventral trajectory of LMC axons within the developing limb (Luria et al., 2008). Luria and colleagues demonstrated that EphB receptors are concentrated on the axons of medial LMC neurons while the ephrin-B2 ligand is preferentially expressed by cells of the dorsal limb mesenchyme. They showed that axons of medial LMC neurons expressing EphB are indeed

repelled by ephrin ligands concentrated dorsally in the limb. In fact, they revealed a molecular symmetry in the dorsoventral guidance of the medial and lateral LMC axons: EphB-ephrinB signalling directing medial LMC axons ventrally, and EphA-ephrinA signalling directing lateral LMC axons dorsally. The reduction in EphA4 levels promotes the selection of ventral trajectories by LMC axons in both lumbar plexuses, but only under conditions of low EphA4 expression. A concomitant elevation of EphB1 levels and a reduction of EphA4 levels in lateral LMC neurons direct a significantly larger proportion of lateral LMC axons into the ventral nerve than reduced EphA4 expression alone. This emphasises the importance of a concerted action of EphB-ephrinB and EphA-ephrinA receptor-ligand pairs at this dorsoventral branch-point.

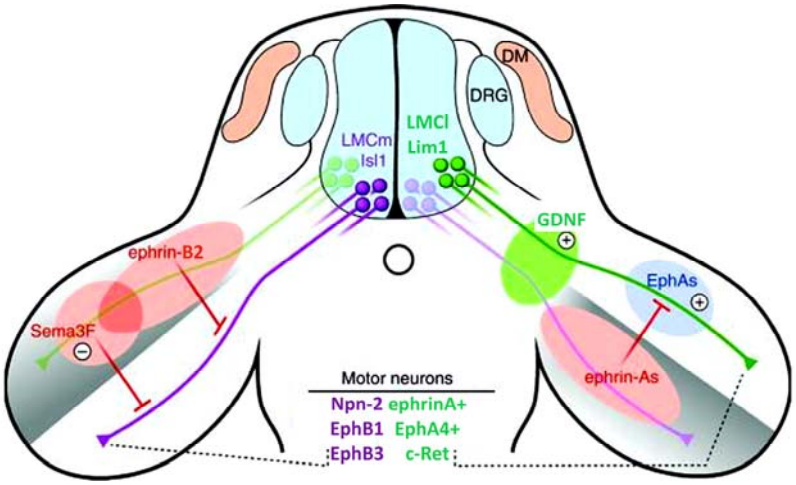

Figure 5. Coordinated actions of Sema3F/Npn-2, ephrinBs/EphBs, ephrinAs/EphAs and GDNF/c-Ret control the ventral and dorsal pathfindings of motor axons innervating the limb (adapted from (Bonanomi and Pfaff, 2010)).
The axons from medial LMC (LMCm) Isl1 positive neurons expressing EphB1, EphB3 and Npn-2 receptors are repelled from the dorsal limb by ephrin-Bs ligands such as ephrinB2 and Sema3F preferentially expressed in dorsal limb mesenchyme. Conversely, ephrin-As in ventral mesenchyme repel lateral LMC axons (LMCl Lim1 positive) through axonal EphA4 to the dorsal region. The EphAs expressed in the dorsal limb push forward the LMCl axons expressing ephrinAs. GDNF concentrated at the base of the limb drives dorsally extending LMCl axons through interaction with the c-Ret receptors.

2.I.2 Morphogens acting as guidance molecules

Morphogens are secreted proteins produced in a restricted region of a tissue and move away from their source to form a long-range concentration gradient. They act in concentration-dependent manner on susceptible groups of precursor cells to induce their differentiation to a specific cell fate (reviewed in (Teleman et al., 2001)). Recently, four morphogen families have been described to play a second role later in development by acting as guidance cues for some growing axons: the Hedgehog-, the Wnt-, the DPP/bone morphogenic protein/transforming growth factor-β (TGFβ)- and the fibroblast growth factor

(FGF)- families (Stoeckli, 2006). In this section I will mainly focus on the involvement of Hedgehog-, Wnt- and TGFβ-signalling (Fig.6).

Sonic hedgehog (Shh in mammals, Hh in *Drosophila*) is a Hedgehog family member secreted by the notochord and by floor-plate cells at the ventral midline of the neural tube and functions as a graded signal for the generation of distinct classes of ventral neurons along the dorsoventral axis of the neural tube (Ingham and McMahon, 2001; Jessell, 2000; Marti and Bovolenta, 2002). For this purpose, Shh acts through the receptor Patched (Ptc), which is bound to the Smoothened (Smo) protein. Inactivation of Ptc by interaction with Shh activates Smo, which in turn activates the transcription factors of Shh target genes (Ci in Drosophila and Gli in mammals). Smo associates directly with Ci-containing complex (kinesin costal2 (Cos2) and the protein Fused (Fu) to specify the fate of particular cells (reviewed in (Lum and Beachy, 2004)).

The roof-plate cells express members of Wnt family. Wnt ligands can activate several different signal transduction pathways (reviewed in (Endo and Rubin, 2007)). The most extensively studied is the canonical Wnt pathway, which controls gene expression by stabilising β-catenin. The Frizzled (Fz) proteins are seven-transmenbrane-domain molecules that function as Wnt receptors. When Wnts are absent, β-catenin is phosphorylated by GSK3β activity, thus stabilizing β-catenin. Accumulated β-catenin converts the lymphoid enhancer factor LEF/TcF from a transcriptional repressor to an activator. In addition of the canonical signalling, Wnt presents two non-canonical pathways, the Wnt/Ca^{2+} pathway and the planar cell polarity (PCP) pathway. The PCP pathway involves a non-canonical, β-Catenin-independent, Wnt/Fz pathway that requires Dsh. The Wnt/Ca^{2+} pathway functions via heterotrimeric G-proteins to mobilise intracellular Ca^{2+} and to stimulate the protein kinase C (PKC). Another receptor can transduce Wnt-signals: the Ryk receptor related to tyrosine kinase receptor carrying a glycosylated extracellular domain (reviewed in (Bovolenta et al., 2006)).

DPP/BMP/TGFβ members are also secreted from the roof plate at the dorsal midline of the neural tube around the time when dorsal neurons are generated (Augsburger 1999). In their classical signalling pathways, BMPs members signal through heterodimeric complexes of type I and II BMP receptors belonging to the serine/threonine kinases, to specify the cell fate (Ebendal et al., 1998; Irving et al., 2002). After ligand binding, this BMPR complex phosphorylates the receptor-regulated Smads (R_Smads) (Heldin et al., 1997). After release from the receptor, the phosphorylated Smad proteins associate with the related protein Smad4, which acts as a shared partner. This complex translocates into the nucleus and participates in gene transcription with other transcription factors (Chen et al., 2004).

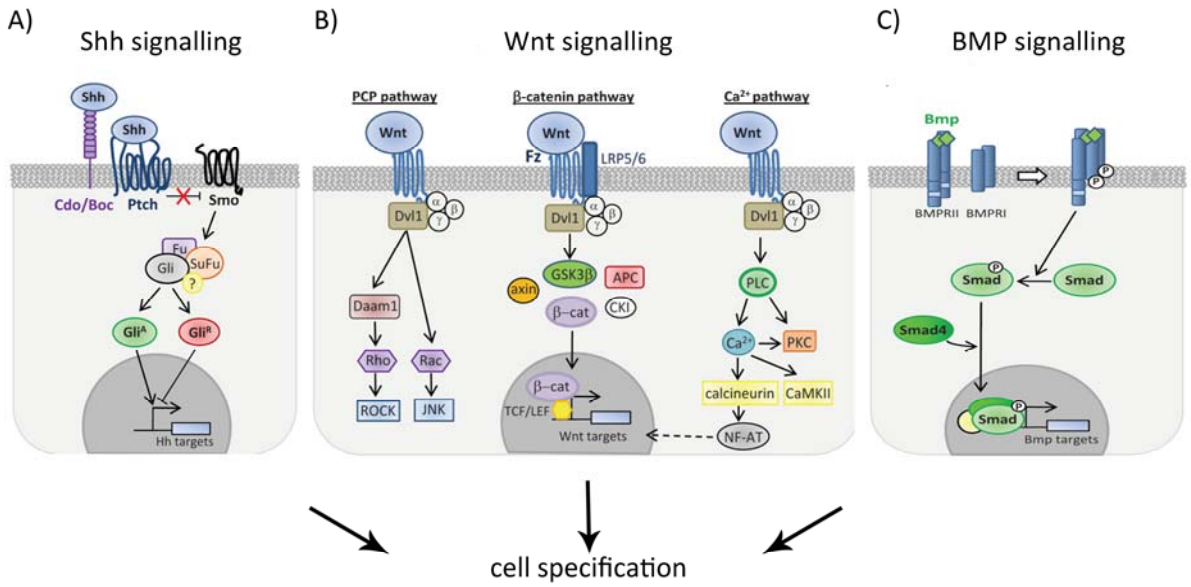

Figure 6. Morphogens signalling pathways involved in the cell specification (adapted from (Sanchez-Camacho and Bovolenta, 2009)).

A) Shh by binding to the twelve transmembrane Patched (Ptch) receptors relieves Ptch inhibition of the transmembrane Smo protein. Smo in absence of Shh binding is inactivated and processed repressor forms of the Gli family (GliR) inhibit the transcription of Hh target genes. After Shh binding, Smo is activated inducing accumulation of GliA forms, which activate Hh target genes.

B) The Wnt binding to Frizzled seven transmembrane proteins activates either the canonical β-catenin pathway, the planar cell polarity (PCP) pathway or the Ca^{2+} pathway. The canonical β-catenin pathway promotes nuclear translocation of β-catenin through inhibition of the GSK3β to activate Wnt target genes. The PCP pathway induces cytoskeleton changes by activation of small GTPases Rho and Rac, which activate the Rho kinase (ROCK) and the c-JNK (JNK), respectively. The Ca^{2+} pathway induces activation of protein kinase C (PKC), calmodulin dependent protein kinase II (CamKII) and calcinurin, which activate the nuclear factor of activated T cells (NF-AT).

C) TGFβ /BMP signalling induce dimerisation of BMPR type I and type II receptors that induce phosphorylation of BMPRI and in turn activate the phosphorylation of Smad proteins, which associate with co-Smad proteins to translocate to the nucleus and regulate the transcription of target genes.

2.I.2.a The Hedgehog family in axonal guidance

Shh is a chemoattractant for precommissural axons in rodents

As mentioned earlier, commissural axons, which differentiate in the dorsal neural tube, send axons that project toward and subsequently across the floor plate, forming axon commissures. These axons project toward the midline because they are attracted by Netrin-1 (Placzek et al., 1990; Serafini et al., 1994; Tessier-Lavigne et al., 1988). In mice mutants for Netrin 1 or its receptor DCC, many commissural axon trajectories fail to invade the ventral spinal cord and are misrouted (Fazeli et al., 1997; Serafini et al., 1996). However, some of them reach the midline, suggesting that another chemoattractant guides these axons. Further analyses of the mice mutants have shown that the floor plate expresses an additional diffusible guidance cue for commissural axons, Shh (Charron et al., 2003; Serafini et al., 1996). Shh was indeed shown to function as an axonal chemoattractant that can mimic the Netrin-1 independent chemoattractant activity of the floor plate in *in vitro* assays (Charron et

al., 2003). Like floor plate cells and COS cells expressing secreting Netrin-1, COS cells secreting Shh can reorient and attract the growth of commissural axons within explants of E11 rat spinal cord. This effect is blocked by cyclopamine, a specific inhibitor of Smo, indicating the requirement for Smo in mediating this effect. Similarly, when embryonic spinal axons from *Xenopus* are exposed to a gradient of a bioactive fragment of Shh, N-Shh, the growth cones turned toward the source of N-Shh. While cyclopamine neutralised the effect of Shh, it did not affect the axonal attraction induced by BDNF in the *Xenopus* spinal axon turning assay. Moreover, the growth cones of isolated *Xenopus* spinal axons were similarly attracted by recombinant N-Shh in a cyclopamine-dependent manner. Taken together, these results prove that Shh can act as a chemoattractant to the commissural axons via a Smo signalling mechanism *in vitro* (Charron et al., 2003). Besides, Charron and colleagues showed that the projections of commissural axons in the ventral spinal cord were also disturbed in a conditional KO mouse model in which the *Smo* expression in the dorsal spinal cord was specifically deleted. These results suggest that *in vivo*, these axons are normally guided by a Smo-dependent Shh pathway (Charron et al., 2003) (Fig.7).

In another *in vitro* assay, Yam *et al.* confirmed that Shh can act as a chemoattractive guidance cue for axons from primary DRG and commissural rat neurons (Yam et al., 2009). These dissociated neurons exposed to a stable Shh-gradient in a Dunn cultivation chamber turned to the source of Shh in a few minutes. The velocity of Shh effect on axon turning suggests that the effect may be independent of transcriptional activity and does not trigger a downstream transcriptional regulation. They argue that a new non-canonical Shh-induced pathway mediates this chemoattraction involving members of the Src-Family kinases (SFKs). SFKs were present in the growth cone of commissural axons and the level of phospho-SFK was increased in presence of Shh in a polarised manner, the distribution of phospho-SFK being more concentrated on the side of the growth cone exposed to higher Shh levels. Moreover, the specific inactivation of SFKs blocked the ability of commissural axons to turn up to the Shh gradient in the *in vitro* Dunn chamber assay (Fig.7).

The attractive effect of Shh in guidance of commissural axons go through binding to Boc and Ptc receptors, which then activate Smo (Charron et al., 2003; Okada et al., 2006). The activation of Smo would activate SFKs in a graded manner. The activated SFKs can mediate signalling to rearrange the cytoskeleton of the growth cone and play a role in Eph or Netrin guidance pathways. They hypothesise that the Shh gradient interferes through a non-canonical pathway with the remodelling of growth cone cytoskeleton and consequently adapt the growth cone trajectory according to the Shh gradient (Fig.7).

Shh is a chemorepellent for post-commissural axons in chicken

In early stage of development, Shh morphogen secreted from the floor plays a role in cell patterning. Bourikas *et al.* showed that it is again expressed later in development during a restrictive time window corresponding to the time-point of commissural axon crossing (Bourikas et al., 2005). By *in vitro* and *in vivo* experiments, they showed that Shh expression has a direct effect on the longitudinal guidance. When Shh was downregulated, instead of turning rostrally the commissural axons stalled at the exit point of the midline or turned randomly to caudal or rostral side. The ectopic expression of Shh in the thoracic and upper lumbosacral levels on one side of the spinal cord interfered with the normal crossing pathway as well. In presence of high Shh concentrations most of the commissural axons either could not leave the floor plate or turned caudally after crossing to avoid the high level of Shh protein. This repulsive activity of Shh was also demonstrated *in vitro*. Spinal cord explants were cultivated in collagen gels and exposed to beads coated with Shh. In this assay, no commissural axons were growing from the side of the explant in presence of Shh or they turned away to avoid the Shh-coated beads. Finally, Bourikas *et al.* showed that the repulsive effect of Shh on postcommissural axons is mediated by the Hip receptor, while its chemoattractive activity on precommissural axons is transduced by the Ptc-Smo complex, whose expression is downregulated when they reach the floor plate (Fig.7).

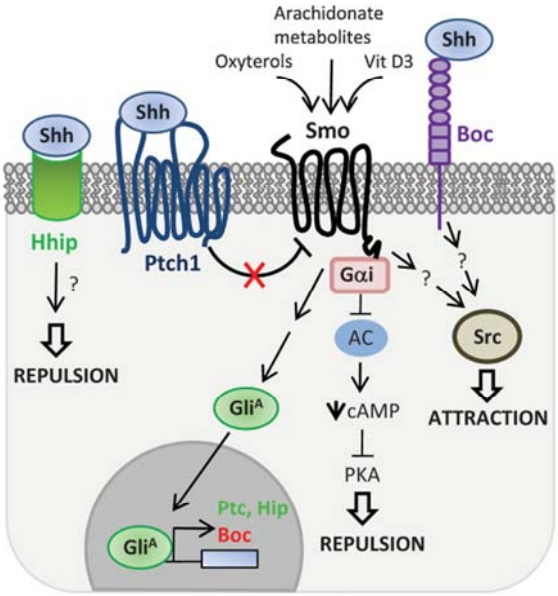

Figure 7. Shh signalling components involved in axon guidance (from (Sanchez-Camacho and Bovolenta, 2009)).
Shh mediates attraction of pre-commissural axons by recruitment of Boc and Smo to activate the kinases of Src family. Smo is constitutively inactived by Ptch1 in absence of Shh. Oxyterols, arachidonates metabolites and Vitamine D3 can mediate Smo activation. The activated signalling pathway induces modifications of intracellular cAMP concentration and inhibition of PKA leading to the repulsion of growth cones. Shh by interacting with Hhip receptor inhibits the growth of post-commissural axons.

2.I.2.b The Wnt family in axonal guidance

Wnt4 controls the antero-posterior guidance of commissural axons in mice (post-crossing)

Lyuksyutova and colleagues found that Wnt4 mRNA is expressed in a decreasing anterior-to-posterior gradient in the floor plate of mouse embryos, and that a directed source of Wnt4 protein attracted post-crossing commissural axons in explant cultures (Lyuksyutova et al., 2003). Commissural axons in mice lacking the Wnt receptor Frizzled3 have normal pre-crossing commissural axon behaviour, but display anterior-posterior guidance defects after midline crossing. Thus, Wnt-Frizzled signalling participates in the guidance of commissural axons along the anterior-posterior axis of the spinal cord. A recent study suggests that an atypical protein kinase C (aPKC) is required to further transduce the Wnt4/frzz3 guidance signalling (Wolf et al., 2008) (Fig.8).

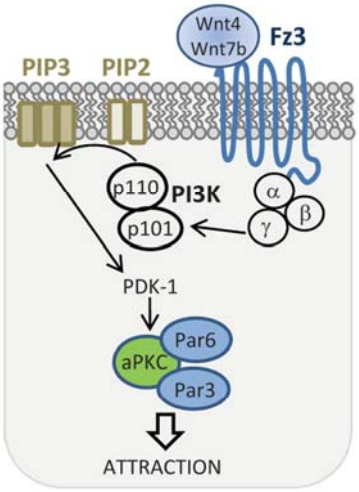

Figure 8. Wnt signalling pathway involved in axon guidance of post-commissural axons (from (Sanchez-Camacho and Bovolenta, 2009)).
Wnt4 and Wnt7b by binding to the Frizzled3 transmembrane protein activate a non-canonical pathway, which induces activation of the aPKC complex and leads to attraction of commissural axons.

Wnt5a and Wnt7a are attractive cues for post-crossing commissural axons regulated by Shh

In the chick embryo Wnt5a and Wnt7a are expressed in and adjacent to the floor plate, respectively, while Wnt4 is completely absent from this region. The downregulation of Wnt5a and Wnt7a by *in ovo* RNAi indeed disturbs the routing of post-crossing commissural axons, suggesting a direct role in longitudinal axonal guidance. Unlike the graded expression of Wnt4 in mouse, Wnt5a and Wnt7a in chick are uniformly distributed along the anteroposterior axis in the lumbosacral region. In contrast, inhibitors of Wnt receptors, Secreted frizzled-related protein (Sfrp) family members, are expressed in a rostrocaudal gradient in the chick spinal cord. *In vitro*, the attractive effect of recombinantly expressed Wnt5a and Wnt7a on post-crossing commissural axons is blocked by recombinant Sfrp1. Along with the growth-promoting effect, the preferred outgrowth of post-crossing commissural axons towards rostral floor plate explants in relation to their caudal counterpart is lost upon addition of Sfrp1-

containing medium as well. The ectopic expression of Sfrps1 at thoracic and upper lumbosacral level of the spinal cord *in vivo*, induces turning of commissural axons at the upper lumbosacral levels. Taken together, the post-crossing commissural axons are guided by a functional gradient of Wnt-signalling linked to a graded expression of the inhibitory Sfrp. As mentioned above, a Shh repulsive gradient participates in the longitudinal guidance of commissural axons (Bourikas et al., 2005). Interestingly, an ectopic expression of Shh in the developing spinal cord also induces Sfrp1 and Sfrp2 expression *in ovo*. These results taken together, strongly suggest that a caudo-rostral gradient of Shh controls directly the commissural axons guidance by repulsion and indirectly by generating a functional rostro-caudal gradient of Wnt5a- and Wnt7a-signalling (Domanitskaya et al., 2010) (Fig.9).

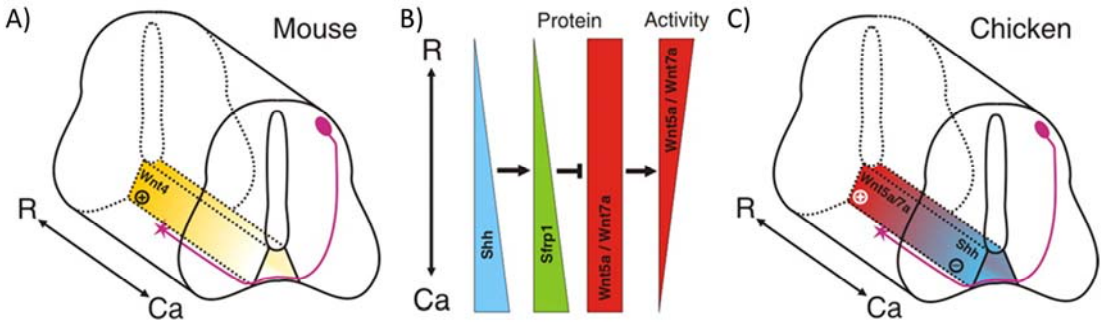

Figure 9. Wnts gradient controls post-commissural axons guidance (from (Domanitskaya et al., 2010)).

A) In mouse embryo, Wnt4 gradient attracts post-commissural axons to the rostral part of the spinal cord.

B) In chick embryo, the Wnt5a and Wnt7a are homogeneously expressed along the spinal cord. The graded expression of Shh in the floor plate induced as well a graded expression of the Wnt antagonist Sfrp1 that regulates in turn the Wnt activity in a graded manner.

C) Consequently, the post-commissural axons repelled by Shh at the floor plate are directed along the spinal cord by Wnt5a and Wnt7a highly active in the rostral region.

R, Rostral; Ca, caudal.

2.I.2.c The Dpp/BMP/TGFβ family in axonal guidance

BMPs are chemorepellents for commissural axons

Butler and co-workers provided evidence for a repulsive role of BMP family members in the guidance of commissural axons in vertebrates (Augsburger et al., 1999; Butler and Dodd, 2003; Yamauchi et al., 2008). The commissural axons originating close to the roof plate extend their axons away from the dorsal midline suggesting that the floor plate participates by chemorepulsion. Indeed, explants of the roof plate repel the commissural axons *in vitro*. Intriguingly, three members of BMP morphogen family (BMP7, BMP6 and GDF7) are expressed by the roof plate in the rat spinal cord at the time (E11-E13), when the commissural axon extension occurs (Augsburger et al., 1999). Particularly BMP7 deviates the trajectories of commissural axons from spinal cord explants, mimicking the chemorepellent activity of the roof plate *in vitro* without causing changes in neuronal cell fate

at the doses required for chemorepulsion. The repulsion is neutralised by soluble inhibitors of BMP activity, BMP7-blocking antibodies and by genetic inactivation of Bmp7. This indicates, that of the three BMPs expressed in the roof plate, only BMP7, but not BMP6 or GDF7 alone, are able to exert a chemorepellent activity towards commissural axons (Augsburger et al., 1999).

BMP7 induces the collapse of commissural axon growth cones eliciting a rapid change in cytoskeletal organisation of dissociated dorsal spinal cord cell culture (Augsburger et al., 1999). Genetic inactivation studies of single and double knockout mouse mutants of the BMPs members, BMP7, BMP6 and GDF7, have later revealed that the expression of both, BMP7 and GDF7 is required for the fidelity of commissural axon growth *in vivo* (Butler and Dodd, 2003). Moreover, they showed that BMP7 and GDF7 heterodimerize *in vitro* and that, under these conditions, GDF7 enhances the axon-orienting activity of BMP7. They finally conclude that a GDF7:BMP7 heterodimer functions as the roof plate-derived repellent that adds to the establishment of the initial ventral trajectory of commissural axons (Butler and Dodd, 2003).

The BMP signalling pathway, which controls cellular specification during early neural development, seems to act via transcriptional activation. In contrast, the BMP pathway that triggers growth cone collapse and thus regulates axon routing seems to be too rapid to involve transcription in the regulatory process (Augsburger et al., 1999) (Fig.10).

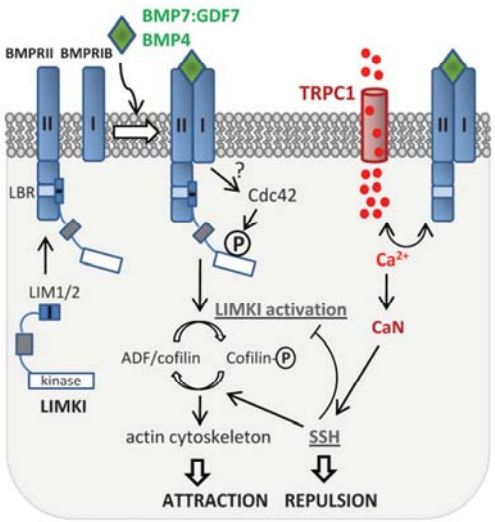

Figure 10. BMP signalling components involved in axon guidance (from (Sanchez-Camacho and Bovolenta, 2009)).

Attraction and repulsion of the growth cones can be mediated through BMPRII receptors. BMPRII interacting with LIM kinase1 inhibits its activity. Ligand binding activates LIMKI, cdc42 and Rho GTPase that induces cytoskeleton changes and attraction of the growth cone. The repulsion is mediated by calcium signalling and activation of Shh, which in turn inhibits the LIMK1 activation and the cofilin signalling.

Yamauchi and colleagues recently demonstrated that both pathways depend on the type I and type II BMP-receptors. Nevertheless, using loss and gain-of-function approaches, they provided evidence that the BMP7/GDF7-induced chemorepulsion of the commissural axons is principally mediated by BMPRIB/BMPRII-heteromeric complexes (Yamauchi et al., 2008), while both, BMPRIA/BMPRII- and BMPRIB/BMPRII-heterodimers, control the cell fate earlier in embryogenesis (Yamauchi et al., 2008).

A connection between the chemorepulsion mediated by Netrin and by members of the TGFβ family has been previously proposed by Culotti and co-workers who searched in *C.elegans* for genes functionally linked with *unc-5*, a receptor for UNC-6/Netrin. The molecule they found indeed participated in axon guidance along the dorso-ventral axis and was identified as the TGFβ related gene *unc-129* (Colavita and Culotti, 1998; Colavita et al., 1998). They recently provided further evidence that UNC-129 facilitates the long-range axonal repulsion exerted by UNC-6 by enhancing the more effective "UNC-5 + UNC-40" signalling in comparison to "UNC-5 alone" signalling. They also showed that UNC-129 interacts with the UNC-5 but not with UNC-40 receptor and consequently modulates the UNC-6 repulsion via UNC-5. These results provide some hints on how the sensitivity of growth cones of motor axons to UNC-6/Netrin in *C.elegans* could be regulated as they simultaneously migrated up the UNC-129 gradient and down the UNC-6 gradient (MacNeil et al., 2009). In vertebrates a similar coordinated long-range repulsion is unlikely to guide commissural axons, which grow in the opposite direction, but may direct the axons of spinal accessory motoneurons.

2.I.3 Neurotrophic factors

Several neurotrophins and some growth factors are required to promote neuronal survival, growth cone motility and axon outgrowth. Even if they could not be defined as emblematic guidance cues, a variety of neurotrophic factors take part in attraction of specific populations of axons in the peripheral and central nervous systems of vertebrates. They consist of nerve growth factor (NGF), brain-derived neurotrophic factor (BDNF), neurotrophin-3 and -4 (NT-3, NT-4), glial-derived neurotrophic factor (GDNF), neuregulin (NRG), hepatocyte growth factor (HGF), and stem cell factor (SCF) (Kolodkin and Tessier-Lavigne, 2010). Each of the vertebrate neurotrophins interacts with one or more members of the Trk family of receptor tyrosine kinase (TrkA, TrkB and TrkC) and the p75 neurotrophin receptor (reviewed in (Reichardt, 2006)). The p75 neurotrophin receptor ($p75^{NTR}$), a transmembrane protein of the tumour necrosis receptor superfamily, regulates three major signalling pathways by interacting with different proteins. Some promote neuronal survival, while others activate apoptosis (NfkB and c-Jun kinase, respectively). The p75 receptor can upon binding with neurotrophins activate the Rho pathway that controls the growth cone motility. Recently, its role in retinal mapping via interaction with EphrinA has been

demonstrated. Therefore, the p75 receptor appears as a multifunctional modulator either promoting or inhibiting axon growth and guidance according to its partners (Schecterson and Bothwell, 2008).

The first neurotrophin identified was NGF from snake venom. It was shown to promote axon growth and survival on sensory and sympathetic axons *in vitro* (Gundersen and Barrett, 1979; Levi-Montalcini and Cohen, 1956). Barde *et al.* isolated BDNF from pig brain. This neurotrophin was later in combination with NT-3 recognised as component of the Maxillary factor, promoting growth of trigeminal sensory axons *in vitro* and permitting them to reach their targets (O'Connor and Tessier-Lavigne, 1999). HGF, a diffusible ligand of the c-Met receptor tyrosine kinase, acts as chemoattractant for the motoraxon outgrowth in developing limb bud (Ebens et al., 1996). GDNF and its receptor Ret were shown to mediate the signalling pathway of the lateral motor column axons that are repelled from the ventral limb mesoderm (Kramer et al., 2006). In motor axons guidance of EphA4 expressing neurons, GDNF/ret cooperates with ephrinA/EphA4 signalling to direct motoraxons into the dorsal limb mesenchyme (Kramer et al., 2006) (shown in Fig.5).

Another growth factor, SCF, has been identified as a guidance cue for commissural axons (Gore et al., 2008). Gore and colleagues demonstrated by genetic studies on mice that interactions between SCF secreted from the floor plate and the Kit receptor expressed by commissural axons are required for the exit of commissural axons from the floor plate. Furthermore, they showed that recombinant SCF could promote the outgrowth only of post-crossing commissural axons indicating a restricted guidance role of SFC after midline crossing.

2.I.4 Cell adhesion molecules

First studies on axon guidance focused on the potential role of the cell adhesion molecules (CAMs). Indeed, the CAMs (IgCAM and cadherins) expressed by developing neurons at their growth cones signal through homophilic or heterophilic interactions in diverse processes during nervous system development. The action on axon growth has often also been demonstrated with their recombinant soluble forms, indicating that CAMs do not act solely as adhesives between cells, but also as specific cues that activate specific signalling pathways to enhance distinct growth cone control mechanisms participating in axonal guidance.

The roles of CAMs in fasciculation, axon growth and guidance, synaptogenesis and synapse plasticity have been particularly described (reviewed in (Chedotal and Richards, 2010; Kolodkin and Tessier-Lavigne, 2010; Skaper, 2005)). The function of axonin-1 and NrCAM as cooperative short attractive guidance cues for commissural axons was demonstrated *in*

vivo in chick embryos (reviewed in (Stoeckli and Landmesser, 1998)). Indeed, injection of soluble axonin-1 or function-blocking antibodies against axonin-1 and NrCAM into the spinal cord strongly disturbed the pathfinding of commissural axons that extend to the floor plate causing their inappropriate turning on the ipsilateral side. Landmesser and coworkers established that axonin-1 expressed on the growth cone of commissural axons interacts with NrCAM present on the floor plate, permitting axons to cross the midline. Moreover, they showed that in absence of a functional balanced interaction between these two proteins, the short negative guidance cues emanating from the floor plate prevail and impede the commissural axons from entering the floor plate. More recent studies revealed that the NrCAM and L1-proteins participate as co-receptors in Semaphorin receptor complexes to guide commissural axons crossing the midline (reviewed in (Mann et al., 2007)). Lately, a soluble form of CAM (sNrCAM) has been described to mediate the Sema3B/Nrp2 repulsion pathways signalling at the vertebrate ventral midline (Nawabi et al., 2010). In the brain, close homologue of L1 (CHL1) and Neurofascin 186, both members of L1-CAM family control the targeting of different interneurons (reviewed in (Chedotal and Richards, 2010)).

Homophilic binding of N-cadherin guides the optic nerve fibers. Like NCAM and L1, N-cadherin can also interact with the fibroblast growth factor receptor (FGFR) in neurons to stimulate axon growth (Doherty et al., 2000). After FGFR activation, the local calcium level in the growth cone is changed and triggers the response by activating different signalling pathways to adapt the actin cytoskeleton. Other cadherins were shown to play a role in motor axon patterning, like the calcium–dependent cell surface T-cadherin for spinal motor neurons. T-cadherin expression is restricted to the caudal half of the sclerotome suggesting that T-cadherin acts as negative guidance cue for the sensory and motor axon projections. Indeed, T-cadherin inhibits motor axon growth *in vitro* (Fredette et al., 1996). Spinal motor neurons from explants at different stages of chick development were only inhibited by T-cadherin substrata at stages when the axons usually grow across the sclerotome. The inhibitory responses corresponded to neuronal T-cadherin expression in the axons, suggesting a homophilic binding mechanism. Sympathic and sensory ganglion neurons in culture were inihibited by T-cadherin substrata as well. Other cadherins (cadherin-7 and cadherin-6B, cadherin-11) can also regulate axon guidance. For instance, cadherin-11 promotes axon growth and impedes the interactions between growing axons (Marthiens et al., 2005). Consistent with their different expression profiles (cadherin-7 and cadherin-6B in early and late phases of chick branchiomotor neuron development, respectively), they play different roles in guidance and branching of cranial motor axons. Cadherin-7 promotes the growth of a single unbranched axon and regulates axon guidance at early stages, whereas cadherin-6B promotes later axon branching, acting via the phosphatidylinositol 3-kinase (PI3K) pathway (Barnes et al., 2010).

2.I.5 ECM associated molecules in development

During nervous system development, the extracellular matrix molecules laminin and fibronectin simply support axonal growth, while other molecules such as tenascins appear to guide them (reviewed in (Barros et al., 2010)).

Laminin together with type IV collagen, nidogen and perlecan, is one of the main components of the basement membrane (Miner, 2008). Laminins are glycoproteins assembled in α-β-γ heterotrimers that interact with integrins and non-integrin receptors (reviewed in (Durbeej, 2010)). In vertebrates, fifteen isoforms of these cell adhesion proteins have been described. The laminins α-2, α-4 and α-5 are mainly expressed in the peripheral nervous system (reviewed in (Durbeej, 2010)). Laminins act as permissive substrates for cultured neurons. The neurite outgrowth promoting function occurs in a integrin-dependent manner (reviewed in (Barros et al., 2010)). Laminins have also been implicated in axonal guidance *in vivo*. For instance, downregulation of laminin A in *Drosophila* results in pathfinding errors of sensory nerves. Similarly in mice, mutants for α-2 laminin or α-4 laminin (constituents of laminins 2 and 10 from the basal lamina in the PNS) display several defects in axon branching, axon sorting and migration of neuronal cells. Only some of these observations were made, when the β1 subunit of integrin receptors was deleted in mice, suggesting that β1-containing integrins mediate only a part of the laminin function.

Fibronectin is another adhesive glycoprotein largely distributed in the ECM of mesenchymal tissues. Fibronectin can mediate cell migration, differentiation and adhesion by binding to other ECM components and to different integrin-receptors. During development, fibronectin is expressed in the CNS and the PNS. Like laminin, fibronectin also supports neurite outgrowth *in vitro* but the growth cones advance on fibronectin more slowly than on laminin (Kuhn et al., 1995).

Tenascins, another family of glycoproteins associated with the ECM, also participates in axonal growth. The tenascin family comprises TN-C, TN-R, TN-W, TN-X, TN-Y (reviewed in (Joester and Faissner, 2001)). Under physiological conditions, tenascins are expressed only during embryogenesis and tissue regeneration. Tenascin-R found only in the CNS, is expressed during late development by oligodendrocytes (Pesheva et al., 1997) and participates in the interaction between neurons and oligodendrocytes. Tenascin-C is expressed in the central nervous system as well, but at earlier stages and contributes to neuronal migration. Tenascin-C is, for instance, present in the barrel boundaries of the somato-sensory cortex and at the interface between compartments in the developing nigro-striatal pathway, when these structures are modified suggesting tenascin-C implication in these remodelling events.

The tenascins R and C can both promote or inhibit neurite growth *in vitro*, depending on the type of neurons. *In vivo*, no axonal pathfinding error was observed in tenascin-R deficient mice, whereas a repellent function for the growth of optic axons was suggested in zebrafish.

Some defects in peripheral nerves in tenascin-C mutant mice were described (Cifuentes-Diaz et al., 2002) and a recent study provided evidence for a role as boundary molecule in the developing olfactory bulb (Treloar et al., 2009).

Apart from laminins, fibronectin and tenascins, some of ECM-molecules with thrombospondin type1 repeats take part in axon growth and guidance (reviewed in (Barros et al., 2010)). For example, F-spondin secreted from the floor plate and expressed in developing nerves, promotes migration and outgrowth by inhibiting cellular adhesion. Another member of this family, thrombospondin-1 secreted by astroglia, promotes neurite outgrowth of many types of cultured neurons and facilitates migration of oligodendrocyte precursors.

Collagens are also expressed during nervous system development and participate in axon growth promotion (reviewed in (Hubert et al., 2009)). For instance, collagen I and collagen XVIII support neurite growth *in vitro*. Moreover, collagen IV regulates the axon targeting in zebrafish.

Finally, the proteoglycans, another group of extracellular matrix molecules, play an important role during development of the nerve system. These molecules will be discussed more into details in the next chapter.

In conclusion, many molecules directly participate in axon guidance and growth. Among them, some act as bi-functional cues, either attractive/permissive or repellent/inhibiting, depending on the partners and time they interact. Additionally, several cues that have antagonistic effects may be expressed in the same spatiotemporal context. Hence, a particular guidance response does not rely exclusively on a single cue, but is rather the result of the reinforced action of multiple guidance cues, which function via different growth cone receptors and their distinct intracellular signal transducing pathways.

2.II. Proteoglycans

2.II.1 Structure

Proteoglycans are major components of the cell surface and the extracellular matrix. They consist of a core protein, to which dissacharide polymers termed glycosaminoglycans (GAGs) are covalently linked at specific sites.

The glycosaminoglycan chains are composed of repeated units of alternating N-acetylated hexosamine and an uronic acid (glucuronic acid or iduronic acid) or a galactose. Except for hyaluronan (also hyaluronic acid; HA), these sugar polymers are usually sulphated at various positions and bound to a central protein core. The four main classes distinguished among the sulphated glycosaminoglycans are chondroitin sulphate (CS) and dermatan sulphate (DS) resulting from the epimerization of the glucuronic acid to iduronic acid in CS, heparan

sulphate (HS) and its epimerized counterpart heparin and finally keratan sulphate (KS), a sulphated N-acteyllactosamine polymer (Fig.11).

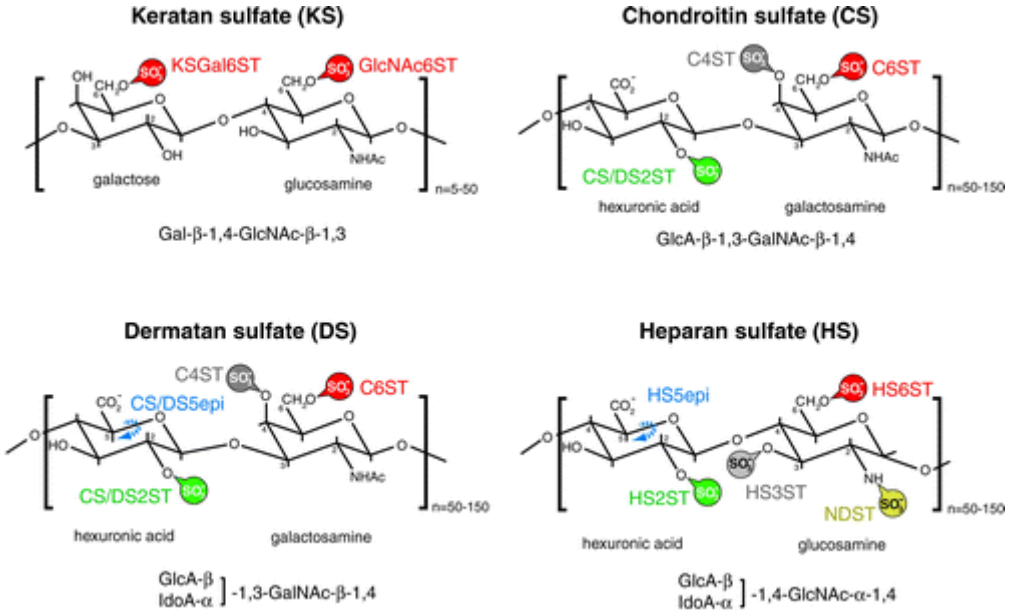

Figure 11. Types of dissacharide repeat units of glycosaminoglycans (GAGs).
Modifications and enzymes that catalyse the reactions are depicted in colour (modified from (Bulow and Hobert, 2006)).

2.II.2 Biosynthesis of proteoglycans

Apart from the hyaluronan that exists on the cell surface and in the extracellular matrix as a free high molecular weight glycosaminoglycan, the GAGs are covalently attached to a protein core. CS, DS and HS are linked to serine residues of the protein core via a specific tetrasaccharide (xylose-2xgalactose-glucuronic acid). The xylosyl transferase initiates the biosynthesis of these glycosaminoglycans by addition of xylose to a specific serine residue in the core protein and then two galactoses and one glucuronic acid are inserted by galactosyltransferase-I and II, and glucuronyltransferase I, respectively (Fig.12). Subsequently, specific co-polymerases elongate the disaccharides in the Golgi apparatus. In the case of chondroitin sulphate, six enzymes (three chondroitin sulphate synthases, one chondroitin sulphate glucuronyltransferase and two chondroitin sulphate N-acetylgalactosaminyl-transferase) may collaborate in the polymerisation process. Different sulphotransferases are involved in 2-O, 3-O, 4-O and 6-O-sulphation as well as in N-deacetylation/N-sulphations, while epimerases may catalyse the conversion of glucuronic acid to iduronic acid. The KS are attached to the core protein through an N-acetylglucosamine to asparagine or through N-acetylgalactosamine to serine or threonine residues.

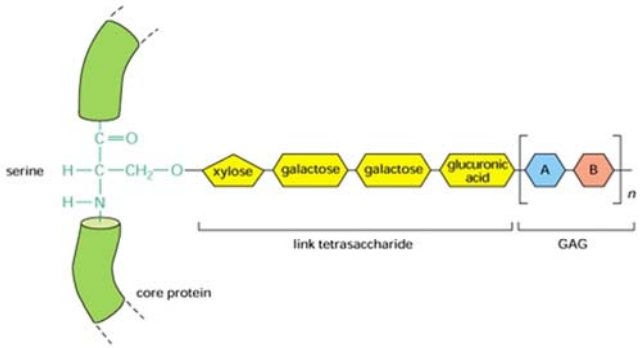

Figure 12. Tetrasaccharide linker region of the proteoglycans (from Molecular Biology of the Cell, 5th edition (Alberts B et al., 2008)).

Since proteoglycans could differ in terms of type, size and composition of GAG chains, primary sequence and domain arrangement of the protein core, degree of substitution of the GAG chains along the protein core, an enormous variety of proteoglycans is expressed and distributed in the tissues. Thus, the traditional GAG-oriented classification into **heparan sulphate proteoglycans** (HSPGs), **chondroitin/dermatan sulphate proteoglycans** (CSPG) and **keratan sulphate proteoglycans** (KSPGs) has meanwhile been superseded by a functionally more relevant separation into distinct families based on core protein homology. For instance, the cell surface associated HSPGs have been grouped into the trans-membranous syndecans and the GPI-linked glypicans and the major extracellular matrix CSPGs have been divided into the families of lecticans/hyalectans and SLRPs (small leucine-rich repeat proteoglycans). These subgroups include sometimes also "part-time" proteoglycans, which may or may not carry glycosaminoglycans depending on the physiological context.

2.II.3 Heparan sulphate proteoglycans in nervous tissues

HSPGs are generally known to interact with various guidance molecules and the deficient mouse for the gene encoding for the major HS glycosyltransferase (*Ext1*) displays severe defects in patterning and guidance of commissural tracts (Inatani et al., 2003). Since cell surface heparan sulphate proteoglycans may act as co-receptors for morphogens, neurotrophins and various growth factors they are good candidates to modulate different aspects of nervous system development (reviewed in (Holt and Dickson, 2005; Lee and Chien, 2004)) (Fig.13).

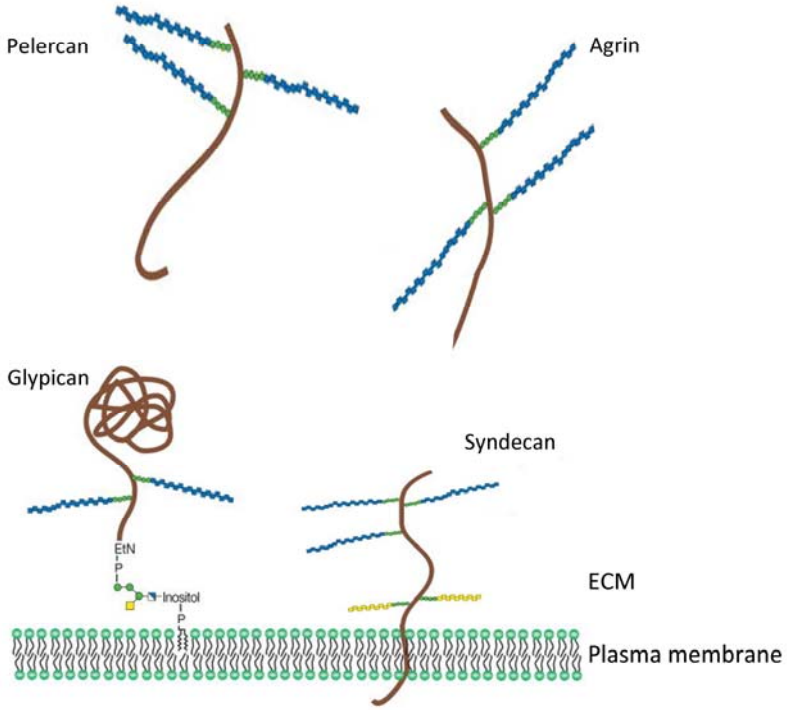

Figure 13. Examples of HSPGs family members (adapted from Essentials of Glycobiology, 2nd edition (Esko et al., 2009)).

Agrin is a heparan sulphate proteoglycan with a core protein of approximately 220 kDa. Agrin was first identified in the basal lamina of neuromuscular junctions being involved in clustering of acetylcholine receptors and formation of synapses at this site (Nitkin et al., 1987; Smith et al., 1987). Indeed the secreted isoform, neural agrin expressed by embryonic motoneurons participates in stabilisation of the synapses (Magill-Solc and McMahan, 1988; Ngo et al., 2007). Agrin downregulation in mutant mice leads to striking defects in postsynaptic differentiation such as a reduction in size and number of AchR aggregates at the neuromuscular junctions. Agrin-deficient mice die at E18 (Gautam et al., 1996).

Perlecan another secreted HSPG is abundantly expressed in basal lamina. This large proteoglycan (core protein of about 400 kDa) may bind cellular receptors such as integrins and α-dystroglycan. Perlecan-null mice are not viable and die either around E10-12 or at birth because of heart and cephalic development impairment or respiratory defects, respectively (Arikawa-Hirasawa et al., 1999; Costell et al., 1999). Indeed, perlecan expressed in the choroid plexus and in the neuroepithelium during development is needed to separate the brain tissue from the overlaying ectoderm. In deficient mice, the absence of perlecan leads to diverse cerebral development defects because of the fusion of the brain tissue with the adjacent mesenchyme resulting in abnormal expansion of the neuroepithelium, neuronal ectopias and exencephaly. More recently, a role for perlecan, potentially interacting with Shh and FGF2, has been suggested for the neurogenesis of the cortical progenitors (Giros et al., 2007).

Among the HSPGs, the families of glypicans and syndecans are cell-surface associated molecules linked via a GPI anchor or embedded by a type I transmembrane domain, respectively.

The **Glypican** family is constituted of six members in vertebrates and two in *Drosophila* and *C.elegans*. All of them are expressed at least transiently in the nervous system. Glypican-1 is the most abundant in developing brain (Litwack et al., 1998; Litwack et al., 1994; Niu et al., 1996). It is present in neuroepithelial precursors and differentiated neurons and participates in FGF signalling during early neurogenesis (Jen et al., 2009). The glypican-2 expression is restricted to the developing brain. It is particularly found in immature neurons disappearing after completion of cell migration and axon outgrowth (Stipp et al., 1994). Interestingly, glypican-2 is present on a polarised way on growth cones of axons suggesting a role in axon guidance (Ivins et al., 1997). Glypican-1 binds Slit *in vitro* and both molecules co-localise on the surface of reactive astrocytes in a model of injured brain (Hagino et al., 2003; Liang et al., 1999). Furthermore, glypican-1 is upregulated and mainly presented on the cellular membrane of sensory neurons after injury in either PNS or CNS, while Slit1 and Robo2 are upregulated in DRGs after peripheral axotomy (Bloechlinger et al., 2004; Yi et al., 2006). These data suggest a participative role for glypican in axonal growth control and guidance mediated by the Slit/Robo pathways.

Syndecans are small type I transmembrane cell surface heparan sulphate proteoglycans with core protein sizes of 20 to 40 kDa. In mammals, four syndecans are present. All vertebrate syndecans are expressed during development in the brain by different cell populations (Hsueh and Sheng, 1999). They are involved in neural migration, axonal growth and synaptic plasticity (reviewed in (Hacker et al., 2005; Reizes et al., 2008)). Syndecan 2 and syndecan 3 are expressed by neurons but are distributed in a distinct manner on the neuronal surface. The syndecan 2 distribution is restricted to the dendrites, while syndecan 3 is present mainly on axons. Syndecan 2, phosphorylated in neurons by EphB2, takes part in the maturation of the synapse inducing the formation of mature dendritic spines (Ethell et al., 2001; Ethell and Yamaguchi, 1999).
Syndecan 3 seems to participate in axonal growth and synaptogenesis processes, since syndecan 3 expression on the axon surface is specifically downregulated once the axons have reached their targets. Recently, the role of syndecan 3 in promoting cortical neuron migration and neurite outgrowth by interacting with the GDNF has also been shown (Bespalov et al., 2011). Besides in a co-culture model system, syndecan 3 expressed by Schwann cells is enriched at the nodes of Ranvier, but syndecan 3-deficient mice do not

display particular defects in node formation (Asundi et al., 2003; Melendez-Vasquez et al., 2005). Different studies in *Drosophila* indicate a role of syndecans in Slit/Robo signalling by facilitating the Slit/Robo interaction (Johnson et al., 2004; Steigemann et al., 2004). In *C.elegans* the sole syndecan controls the neural migration and the guidance of growing axons of midline interneurons and motoneurons (Rhiner et al., 2005).

2.II.4 Chondroitin sulphate proteoglycans in nervous tissues

Chondroitin sulphate proteoglycans represent the principal group of proteoglycans in the nervous system. Among them, members of the lectican (hyalectan) family are the main components of a unique ECM found only in the central nervous system (reviewed in (Yamaguchi, 2000; Zimmermann and Dours-Zimmermann, 2008)). During brain development, the proteoglycans play a role in morphogenesis by regulating the interactions between cells, of the cells to the extracellular matrix and to growth factors and morphogens of the environment. The function of CSPGs (hyalectans, NG2 and phosphacan) in the control of axonal growth and neural regeneration has been investigated in different *in vitro* models.

2.II.4.a NG2 and Phosphacan, two CSPGs involved in development and regeneration of the nervous tissues

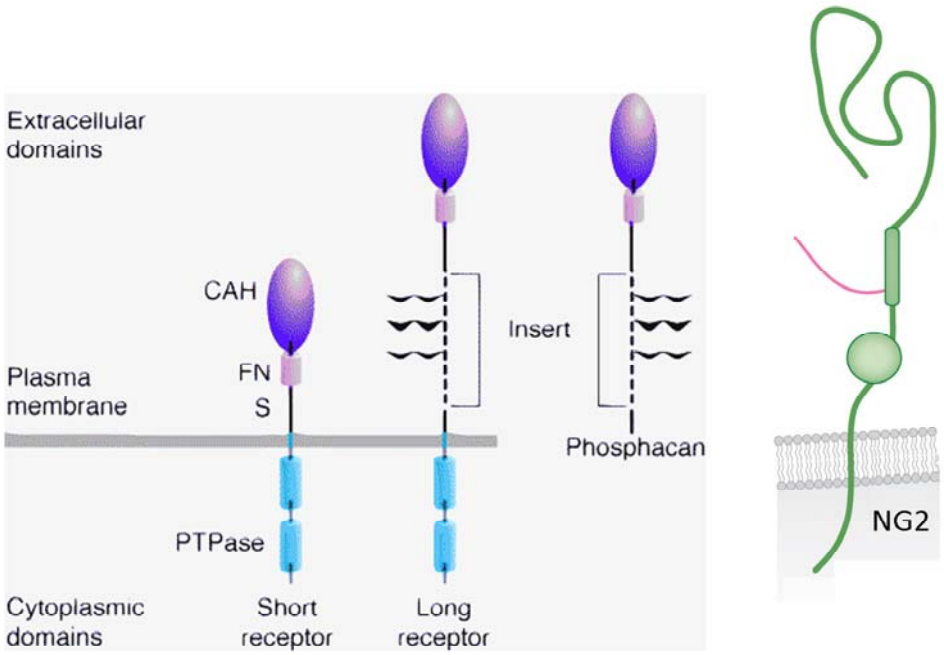

Figure 14. Depiction of NG2 and receptor-like protein tyrosine phosphatase β (RPTPβ) isoforms (adapted from (Couchman, 2010; Peles et al., 1998)).

NG2 is a membrane proteoglycan with a large core protein (330kDa) (Fig.14). During development also some non-neural cells display NG2 expression for example also chondroblasts. In adult mammalian brain and spinal cord, NG2 is expressed mainly by progenitors of glial cells such as the oligodendrocytes precursor cells that give rise *in vitro* to

the mature oligodendrocytes and the type II astrocytes (Nishiyama et al., 1991). These progenitors are called *in vivo* polydendrocytes because of their astrocyte-like structure and their oligodendrocyte antigenic features (Nishiyama et al., 1991; Nishiyama et al., 2002). The intracellular domain of NG2 may bind to the glutamate receptor interacting protein-1 GRP1 mediating clustering of NG2 and AMPA glutamate receptors to potentially modulate the glial neuronal signalling (reviewed in (Trotter et al., 2010)). Role of NG2 during nervous system development and brain regeneration is not yet well understood. Several studies provided evidence for a NG2 inhibitory function on neurites and axon growth *in vitro* and suggested a role in inhibiting axonal regeneration in CNS after injury (Chen et al., 2002; de Castro et al., 2005; Dou and Levine, 1994; Fidler et al., 1999; Jones et al., 2002; Ughrin et al., 2003). A recent study showed a putative role of NG2 in blocking the conduction in axons after spinal injury (Hunanyan et al., 2010). Even if the increased expression of NG2 in injury sites of CNS is unequivocal, the function and consequences of that increment are not clear. More recently, accumulating data have identified NG2 as promoter of nerve regeneration. NG2-deficient mice generated by Stallcup and colleagues did not show any obvious defects, neither in nervous system development nor later in adult (Grako et al., 1999). However, in a model of spinal axon injury, axons seemed to penetrate the developing scar tissue more easily in wild-type mice than in NG2 knockout mutants, suggesting a stimulatory function of NG2 in nerve regeneration (de Castro et al., 2005). In another study, NG2-cells promoted the extension of regenerating axons in a graft after spinal cord injury (Jones et al., 2003). In line with these results, Yang *et al*. demonstrated that rat polydendrocytes did not repel growing axons from hippocampal and cortical neurons, but promoted their growth *in vitro* (Yang et al., 2006). In addition, they showed that *in vivo*, growing axons were in a much bigger proportion directly in membrane-contact with NG2 cells than with astrocytes of the developing corpus callosum. Besides, NG2 appears also to be involved in glioma progression (reviewed in (Stallcup and Huang, 2008)).

PTPζ/RPTBβ/Phosphacan

PTPζ/RPTBβ is a receptor-type protein tyrosine phosphatase that is synthesized as a chondroitin sulphate proteoglycan. Alternative splicing of the single gene coding for PTPζ/RPTBβ generates three isoforms (Levy et al., 1993; Maeda et al., 1995; Margolis et al., 1996): the full length PTPζ/RPTBβ, a shorter receptor (sRPTBβ) missing the part carrying the attachment region of CS chains, and an extracellular secreted variant called phosphacan lacking the transmembrane and the intracellular domains. Phosphacan represents a major soluble chondroitin/keratan sulphate proteoglycan in the developing and adult brain and is mainly synthesized by glial cells (Canoll et al., 1993; Canoll et al., 1996; Maeda et al., 1995; Margolis et al., 1996; Maurel et al., 1994; Rauch et al., 2001; Sakurai et al., 1996). Indeed,

phosphacan seems to be involved in different developmental processes such as cell migration, axon growth and myelination (Garwood et al., 2003; Grumet et al., 1994; Harroch et al., 2002; Harroch et al., 2000; Maeda and Noda, 1998). The PTPζ/RPTBβ receptor is constituted of several domains, especially in the extracellular portion. These domains play also a role in the functions of phosphacan in cell migration and axonal growth. For instance, the CAH domain of phosphacan present in the longest transmembrane isoform of PTPζ/RPTBβ and in phosphacan functions as a ligand to contactin (Peles et al., 1995). The binding of phosphacan via CAH domain with the contactin/NrCAM complex on the neuronal surface induces neuritic growth of chick primary tectal neurons (Peles et al., 1995; Sakurai et al., 1997). By contrast, phosphacan binding neurons via Ng-CAM/L1, may also inhibit neurite outgrowth *in vitro* (Milev et al., 1994) and may suppress adhesion of glioma cells on their preferential Ng-CAM/L1 substrate. Similarly, Maeda and Noda showed that phosphacan acts as bi-functional molecule, promoting the outgrowth of neurites and dendrites of cortical neurons but not of thalamic neurons, while inhibiting adhesion of both types of neurons (Maeda and Noda, 1996). Phosphacan also interacts with pleiotrophin/HB-GAM via the spacer (S) domain and this binding interferes with the neurite outgrowth-inducing properties of pleiotrophin on cortical neurons (Maeda and Noda, 1998). Phosphacan can also bind the extracellular matrix molecule tenascin and form a complex which may participate in different mechanisms of development and repair of the nervous tissues (Barnea et al., 1994; Garwood et al., 2001; Grumet et al., 1994). Even if many *in vitro* studies indicate a significant role for phosphacan in different developmental and regenerative processes in the nervous system, no obvious effect of the deletion of the three isoforms has been observed in the knock-out mouse model. Only a slight impairment of long-term potentiation (LTP) associated with memory and learning has been described (Harroch et al., 2000; Niisato et al., 2005; Shintani et al., 1998).

2.II.4.b Expression and functions of lecticans/hyalectans in nervous tissues

In mammals, four lectican genes have been identified that encode aggrecan, versican and the two neuronal-tissue specific members, neurocan and brevican (Doege et al., 1991; Rauch et al., 1992; Yamada et al., 1994; Zimmermann and Ruoslahti, 1989) (Fig.15). All of them are spatially and temporally regulated during embryonic development and in the adult. Their core proteins share several structural domains. Close to the N-terminus, an Ig-like loop and two link-protein-like tandem repeats form the globular domain G1 that binds to hyaluronan and to different link proteins. Near the C-terminal end, another globular domain (G3) consists of one or two EGF-repeat domains, a C-type lectin element and a complement regulatory protein (CRP or Shushi) domain, respectively. The central core protein between the two terminal globular domains is quite flexible. This region carries the GAG chains and

numerous O- and N-glycans, which are covalently bound. The GAG-attachment domains of the distinct lecticans differ, greatly in primary sequence, peptide length as well as structure and number of the attached GAG chains. In addition, alternative splicing of the versican gene VCAN and the brevican gene BCAN enlarge the variety of the lecticans (versican isoforms V0, V1, V2, V3 and secreted and GPI-linked variants of brevican, respectively).

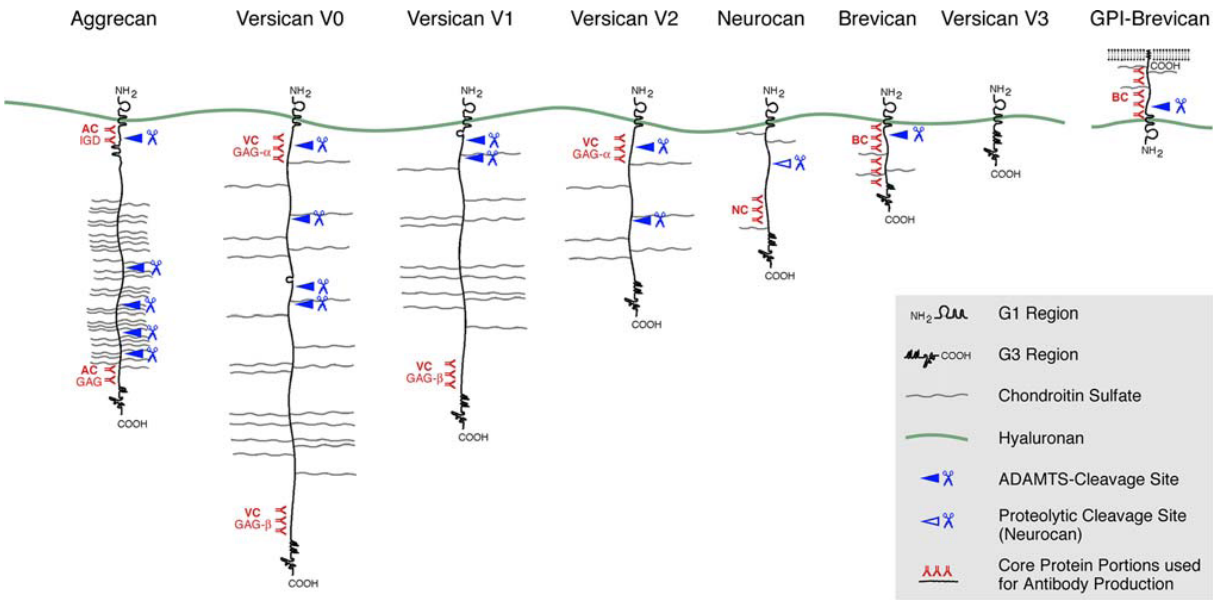

Figure 15. The lectican-family (from (Zimmermann and Dours-Zimmermann, 2008)).
ADAMTS: A disintegrin and metalloprotease with thrombospondin type 1 motif.

Brevican, a "part-time" proteoglycan (not always carrying GAGs), is restrained to the CNS and displays a much shorter central core protein domain than the other lectican members (Yamada et al., 1994). Brevican isoforms exist either as secreted or GPI-anchored proteoglycans (Seidenbecher et al., 1995). In adult, brevican is found in many regions of the brain associated with the perineural nets (PNNs), subcomponents of the central nervous ECM surrounding the soma and proximal neurites of large neurons (Bruckner et al., 2000). The secreted form is preferentially found in the gray matter structures, such as cerebellar and cerebral cortex, hippocampus and thalamic nuclei, while the GPI-anchored glycoproteins are mainly present in white matter and expressed by glial cells (Seidenbecher et al., 1998). The expression of secreted brevican is in rodents as well as in human upregulated during peri- and postnatal development. Brevican is deposited as long as the brain develops reaching a constant level only in mature brain. Its expression coincides spatio-temporally with the production of glial cells (Gary et al., 2000; Jaworski et al., 1995). Yet the GPI-anchored isoform displays the same level of expression during development. In case of gliomas, tumours derived from glial cells, both brevican isoforms are highly overexpressed with some preference for the secreted isoform (Gary and Hockfield, 2000). Furthermore, the role of cleaved brevican in mediating tumour invasion and reinforcing tumour expansion was

revealed in gliomas (Nutt et al., 2001; Zhang et al., 1998). Besides, a potential inhibitor function of purified brevican for neurite outgrowth has been demonstrated *in vitro* (Yamada et al., 1997). Together, these data suggest that this lectican may participate in the regulation of cell adhesion and migration during brain development with different functions in relation to the isoform being expressed. Surprisingly however, the knock-out mice display only mild defects in long term potentiaton (LTP) but no morphological or behavioural changes were noticeable (Brakebusch et al., 2002).

Neurocan, another nervous-tissue specific hyalectan, is secreted as an intact proteoglycan with a 275 kDa core glycoprotein during early rodent brain development. At the end of CNS development, it is mostly cleaved into two fragments, a N-terminal fragment of 130 kDa and a C-terminal fragment of 150 kDa, which are mainly detectable in adult tissues (Matsui et al., 1994; Milev et al., 1998b; Rauch et al., 1992). Neurocan expressed by neurons, astrocytes and oligodendrocytes displays *in vitro* neurite growth inhibitory activities (Asher et al., 2000; Engel et al., 1996; Friedlander et al., 1994; Sango et al., 2003). In the context of mechanical stress and injury, neurocan expression is also upregulated corroborating a potential inhibitory function in axon regeneration (Asher et al., 2000; Davies et al., 2004; Tang et al., 2003). Neurocan can bind to tenascins-C and -R, NCAM, Ng-CAM/L1 and TAG-1 proteins (Milev et al., 1998a; Milev et al., 1997; Milev et al., 1996). The interactions with NCAM and Ng-CAM/L1 are suggested to mediate the inhibitory functions of neurocan on axon growth and cell adhesion processes (Rauch et al., 2001). Besides, its participation in axonal pathfinding in retino-tectal mapping was suggested (Leung et al., 2004; Popp et al., 2004; Sango et al., 2003). Surprisingly, although neurocan is widely expressed in brain and appears to be involved in different processes during development, no particular defect has been identified in the neurocan-deficient mouse model except for some LTP deficits (Zhou et al., 2001).

Aggrecan, which has first been described and mainly known for its function in cartilage maintenance and the involvement of its degradation in arthritis, is also expressed by neurons and glial cells of the central nervous system ((Domowicz et al., 1996; Domowicz et al., 2008) and reviewed in (Kiani et al., 2002; Schwartz et al., 1996)). The nervous-tissue specific aggrecan carries only chondroitin sulphate chains and in general fewer glycosaminoglycans than the cartilage counterpart, its core protein runs at a relative size of about 370 kDa on SDS-PAGE. Aggrecan is present in the brain and the notochord of chick embryos and it forms aggregates with hyaluronan and link protein like in the ECM of cartilage. The expression in chick brain begins at HH-stage 31 to reach a plateau at HH39 and then decreases after HH42 to be absent post-hatching (Li et al., 1996). *In vitro*, cartilage-derived aggrecan and its respective core glycoprotein depleted of the GAG side chains can inhibit

axon growth from spinal cord in an injury assay (Lemons et al., 2003). Through its GAG chains, aggrecan may participate in adhesion and migration of neurons during development, since aggregating neurons in culture display high levels of aggrecan expression and removal of the GAG chains with chondroitinase ABC leads to smaller aggregates (reviewed in (Schwartz and Domowicz, 2004)). Besides, the expression pattern of aggrecan during development coincides with the formation of neuronal nuclei in the chick telencephalon.
In the mature CNS, aggrecan is the major proteoglycan expressed in the perineural nets (PNNs) (Carulli et al., 2006; Carulli et al., 2007). The PNNs are potential organisers of synaptic connections. Their formation after birth coincides with maturation of the synapses suggesting that PNNs may participate in the stabilisation of the synapses (reviewed in (Faissner et al., 2010)). Interestingly, aggrecan seems to modulate the function of the different PNNs, since its glycosylation pattern varies according to the types of neurons and the activity of those neurons (Giamanco et al., 2010; Matthews et al., 2002).

2.II.4.c Versican

(1) Gene structure and distribution of versican

Versican originally identified as large fibroblast proteoglycan was first cloned from a human placental cDNA library (Zimmermann and Ruoslahti, 1989) and later also characterised in other species, such as mouse, bovine, chick (previously named PG-M). As for the other lectican members, the gene structure follows a modular organisation in direct correlation between the exons and the different domains of versican core protein (Naso et al., 1994). The *versican* gene localised on the chromosome 5 in human is under control of a promoter displaying a typical TATA box and different binding sites for transcription factors such as AP2, CCAAT enhancer protein and cAMP-responsive element.
Four versican isoforms (V0, V1, V2 and V3) have been identified resulting from alternative splicing of a single gene (Fig.16). The two giant exons 7 and 8 code for the GAG-attachment domains (GAGα and GAGβ). The longest versican (V0) contains both exons, while only exon 8 is present in versican V1 and versican V2 possesses exon 7, but not exon 8 (Dours-Zimmermann and Zimmermann, 1994; Ito et al., 1995; Schmalfeldt et al., 1998; Shinomura et al., 1993). The smallest splice-variant V3 is not a proteoglycan, since both exons carrying the GAG attachment regions are absent (Zako et al., 1997a). A PLUS domain has exclusively been described for chick versican. It is located between the hyaluronan-binding region and the GAGα domain. The respective size of the transcripts and the core proteins of human versican isoforms are for V0 (11.8 kb - 372 kDa), V1 (8.2 kb - 265 kDa), V2 (5.9 kb - 182 kDa), V3 (2.1 kb - 75 kDa).

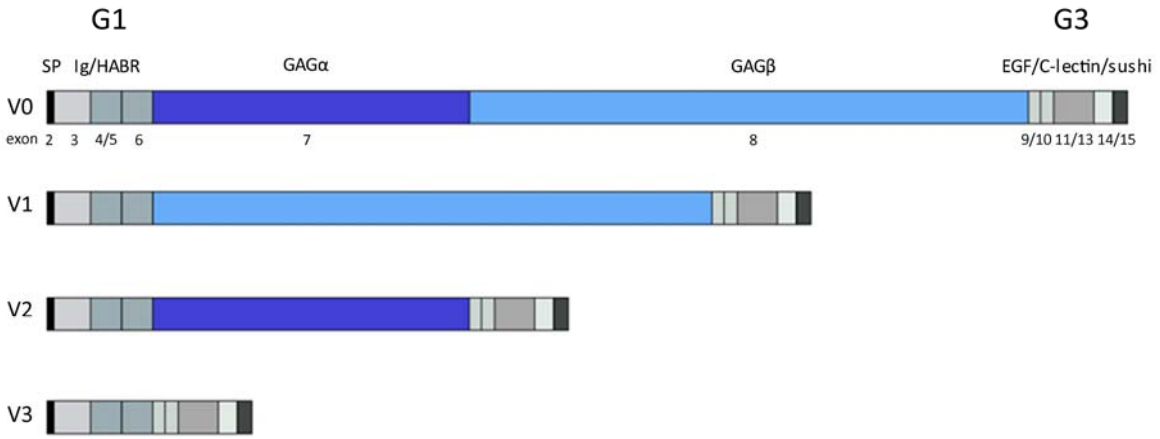

Figure 16. Gene structure of versican isoforms V0, V1, V2 and V3.
Exons encoding the different domains of versican splice-variants are mentioned below the respective motifs, and the globular domains in the proteoglycans are named above.

Versican is widely distributed in adult tissues and in almost all mesenchymal tissues at some stage during development (Bode-Lesniewska et al., 1996; Dours-Zimmermann and Zimmermann, 1994; Yamagata et al., 1993a; Zimmermann et al., 1994). Versican expression is subjected to a fine regulation, especially in regions actively modulated during development, such condensing mesenchyme in limb bud, the perinotochordal mesenchyme between notochord and neural tube or next to the basement membranes facing neuroepithelial cells (Kimata et al., 1986; Yamagata et al., 1993a; Yamagata et al., 1993b; Zako et al., 1997b).
In central and peripheral nervous systems, specific splice-variants are transiently expressed. Versican V2 is the major isoform in adult brain and is associated with myelin, while versican V0 and V1 are the main forms detected in the embryonic CNS and PNS (Dours-Zimmermann and Zimmermann, 1994; Landolt et al., 1995; Milev et al., 1998b; Schmalfeldt et al., 1998).

(2) Binding partners and putative functions

Versican can bind to several molecules including hyaluronan, tenascin-R and -C, fibulin-1 and -2, fibrillin, fibronectin, CD44, selectins, and link proteins through the different modules of the core protein or frequently also mediated by the GAG side chains (reviewed in (Wu et al., 2005)). In addition to functions in the structural assembly of the extracellular matrix, these interactions, may play important roles in different cellular processes such as migration, adhesion, proliferation and, in the specific context of the nervous tissues, in the control of neurite growth, axon regeneration and synaptogenesis (reviewed in (Wight, 2002; Yamaguchi, 2000; Zimmermann and Dours-Zimmermann, 2008)).

Versican and the ECM of the nervous system

By involving both globular domains G1 and G3, versican participates in assembling the specialised extracellular matrix in nervous tissues, especially at level of the nodes of Ranvier. The binding between hyaluronan and versican is stabilised by the interaction with link proteins such as HAPLN1/Ctrl1 (Matsumoto et al., 2006). In the brain, the protein Bral1 predominantly expressed by neurons joins the specific ECM at the nodes of Ranvier and reinforces the hyaluronan-binding of versican V2 expressed by oligodendrocytes (Bekku et al., 2010; Oohashi et al., 2002). Besides, versican also interacts via its C-type lectin with the fibronectin type III motif 3-5 of tenascin-R from oligodendrocytes (Aspberg et al., 1995; Aspberg et al., 1997), which in turn binds to phosphacan. Versican V2 in fact recruits tenascin-R and phosphacan for the specialised ECM at the nodes of Ranvier *in vivo* underlining its role in ECM assembly at this location (Dours-Zimmermann et al., 2009).

Versican and cell proliferation, cell adhesion

The expression of versican V0/V1 in the proliferating zone in the epidermis and its inverse correlation to cell density in culture suggests a role in cell proliferation (Zimmermann et al., 1994). Its colocalisation with hyaluronan, tenascin-C and CD44 in different fibroblasts cultures seems to be linked to the formation of a specialised pericellular matrix (Yamagata et al., 1993a). Indeed, the versican/hyaluronan/CD44 interaction involving the tandem loop in the G1 domain of versican and the link protein binding to its Ig-like domain seems to stimulate cell proliferation of astrocytoma cells and reduce the cell adhesion of NIH3T3 cells (Ang et al., 1999; Yang et al., 1999). Yang and colleagues confirmed the proliferative effect of full-length versican V1 expressed in NIH3T3 cells, which evidently upregulates the epidermal growth factor receptor (EGFR) expression and activates the Erk pathway (Sheng et al., 2005). This effect appears to be dependent on the GAGβ domain, while versican V2 containing only the GAGα domain inhibits EGFR signalling and by consequence the proliferation of NIH3T3 cells. Intriguingly, over-expression of versican V1, but not V2, in PC12 cells induces neuronal differentiation and promotes neurite outgrowth by enhancing EGFR and integrin expression (Wu et al., 2004). Similarly, co-culture of astroglia cells over-expressing versican V1 with neural stem cells or hippocampal neurons induce differentiation and neurite outgrowth, respectively. In line with a promoting function of versican in adhesion and differentiation of cells of the nervous system, recombinant expression of the versican G3 domain alone in glial cells promotes neural cell attachment and neurite growth of hippocampal neurons in culture (Xiang et al., 2006).

Versican and synaptogenesis

In parallel, G3 domain was shown to play a role in synaptogenesis as well, since neurons grown on G3 coated dishes displayed more dendritic spines and filopodia than on dishes coated with buffer alone (Xiang et al., 2006). An earlier study provided already evidence for an impact of versican on synaptogenesis of retinal ganglion cells (Yamagata and Sanes, 2005). *In vitro*, versican V0 inhibits neurite growth of retinal ganglion cells (RGC), but promotes the enlargement of presynaptic varicosities in retinal axons. Conversely, its downregulation by RNA interference results in smaller varicosities on retinal axons. In the chick optic tectum, versican V0 may provide a lamina-specific cue by regulating synapse structure and encouraging the presynaptic maturation on ingrowing retinal axons.

Versican and neural crest cells migration

Several studies indicated a putative function of versican in the migration of neural crest cells (NCCs). Versican is present in barrier tissues that inhibit the migration of the NCCs and the outgrowth of motor and sensory axons in the trunk of chick embryos. For instance, V0/V1 expressed in the posterior half of the sclerotome is completely absent from the regions invaded by the neural crest cells (Landolt et al., 1995). Perris and colleagues indicated that, in contrast to fibronectin, versican alone does not support the migration and adhesion of neural crest cells in culture (Perris et al., 1996). These observations suggesting a role for versican in guiding the migration of NCCs, were then challenged by Perissinotto *et al*, who suggested that neural crest cells actually invade versican-rich matrices and remove it from the pathways (Perissinotto et al., 2000). This latter hypothesis was again not confirmed by Dutt *et al.* demonstrating that isolated versican V0/V1 and versican V1 in fact override the migration promoting activity of fibronectin already at low concentrations in a stripe-choice assay (Dutt et al., 2006). No evidence for a function-inactivating versican-degradation by the neural crest cells was provided in this study. Also the phenotypic analysis of a Pax3 mutant mouse (*Splotch*) further supported the notion of a crucial role for versican in controlling neural crest cell migration (Henderson et al., 1997). In the *Splotch* mouse NCCs display aberrant migration patterns. In this Pax3-deficient mutant versican is abnormally expressed in the usual pathways and blocks or deviates migratory NCCs. Pax 3 appears to modulate the expression of the large versican isoforms (Mayanil et al., 2001) by regulating the TGFβ2 pathway in early embryonic development in mouse (Mayanil et al., 2006). Taken together, these data suggest that versican regulated by TGFβ2 signalling may interfere with neural crest cell migration.

Versican and neurite growth and axon regeneration

Versican is believed to play a significant role during development of the central nervous system and in impeding axon regeneration. Indeed, versican V2 expressed by oligodendrocytes or by precursors of oligodendrocytes can inhibit neurite growth of neurons from both central and peripheral nervous system in *in vitro* assays (Asher et al., 2002; Niederost et al., 1999; Schmalfeldt et al., 2000). In addition, since versican V2 is the main component of the extracellular matrix in the adult CNS and is late upregulated in brain development (Schmalfeldt et al., 1998), it could play a major function in suppressing excessive axonal growth and impede axon regeneration in CNS after traumas (Schmalfeldt et al., 2000). In accordance with that, versicans are upregulated in different models of neural tissues injury (Asher et al., 2002; Beggah et al., 2005). For instance, lesion in rat cerebral cortex induced versican upregulation around the injury site (Asher et al., 2002). Among the hyalectans present in the extracellular matrix of the dorsal root entry zone (DREZ), the border between PNS and CNS, versicans V1 and, to a lesser extent, V2 show an increased expression after injury of the dorsal root (Beggah et al., 2005; Waselle et al., 2009). These newly expressed proteoglycans can be detected during several days after lesion.

The diverse and sometimes opposing effects of versicans on cell migration, adhesion and proliferation observed *in vitro*, may be explained by the multitude of interactions between the different domains of the distinct versican isoforms and their binding partners, and emphasise the importance of *in vivo* studies. Nevertheless, the notion that the large versican isoforms may mainly function as an inhibitor of neural crest cell migration and axonal extension, has become little disputed lately. It is therefore tempting to assume that this lectican plays a role as a general cue in axonal guidance.

2.III. Catabolism of hyalectans

In the previous chapter, the different hyalectans expressed in the extracellular matrix of the nervous system during development and in adult were described. Their distributions vary during development and cleavage products are detected in physiological and pathological contexts. Moreover, like other molecules, proteoglycans are catabolised to permit the recycling of their subcomponents. Indeed, different proteases participate in the proteoglycan catabolism. Metzincin proteases appear to specifically degrade the hyalectans, in particular the ADAMTS family are involved in this process (reviewed in (Flannery, 2006)).

2.III.1 The ADAMTS family

The recently identified ADAMTSs (a disintegrin and metalloprotease with thrombospondin type I motifs) build a separate family among the metzincins clan (reviewed in (Apte, 2009)). At present, nineteen members have been identified in the human genome, with different roles in various biological processes such as homeostasis of connective tissues, angiogenesis, inflammation, ovulation and fertilisation or cleavage of von Willebrand factor (vWF). These enzymes are related to the surface-bound ADAMs and they likewise display sequence similarities with the reprolysin snake venom proteases. In addition to the classical domains present in ADAMs such as the pro-domain, the zinc ion-dependent metalloprotease domain, and the disintegrin-like domain, ADAMTSs contain also a distinctive thrombospondin type-1 like repeat (TSP-1) motif, which is followed by a cysteine-rich element and a cysteine-free sequence, the spacer region (Fig.17). Except for ADAMTS4, which terminates after this spacer region, at least one additional TSP-like motif is present in the C-terminal portion. Other domains as cubilin (CUB) module, protease and lacunin (PLAC) motif and mucin-like domain are as well included in some ADAMTS members.

The pro-domain of ADAMTS members ends with a furin cleavage site that is processed to activate the zymogen forms. This occurs commonly in the *trans*-Golgi or for ADAMTS9 at the cell-surface allowing the secretion of the active proteinases (Wang et al., 2004; Zeng et al., 2006).

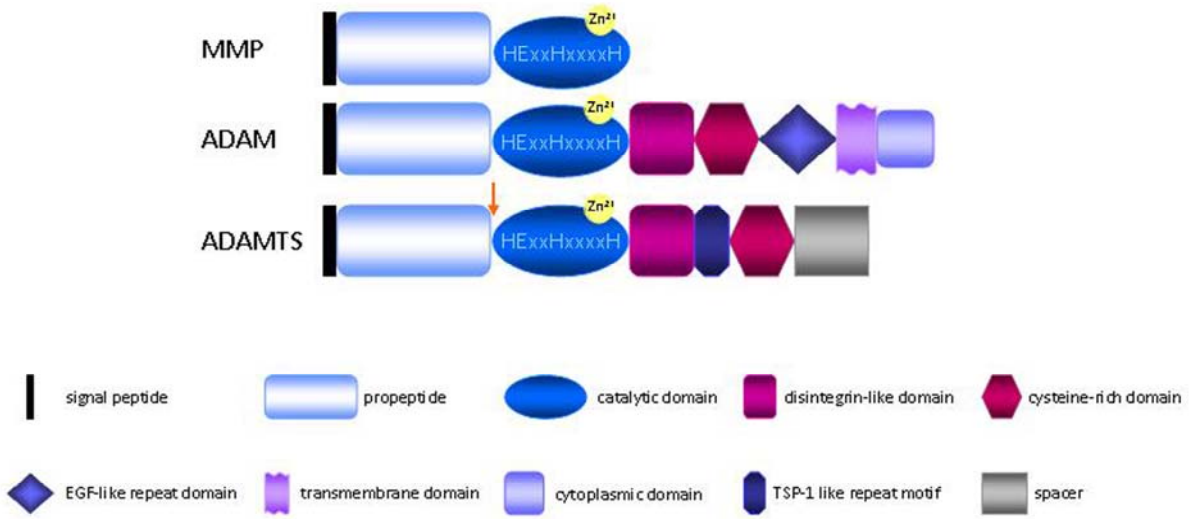

Figure 17. Domains structure of metzincin families MMP, ADAM and ADAMTS (modified from (Jones and Riley, 2005)).

Matrix metalloproteases (MMP), ADAMs (a disintegrin and metalloprotease) and ADAMTSs (a disintegrin and metalloprotease with thrombospondin type I motifs) comprise as typical metzincins the Zn^{2+} binding consensus sequence HExxHxxxxH in their catalytic domain. Prodomain of all ADAMTS contains at least one furin consensus cleavage site involved in regulation of the proteolytic activity (arrow). TSP-1: thrombospondin type-1 motif.

The catalytic domain contains an extended zinc-binding sequence (HExxHxxxxxHD) and provides generally the cleavage site specificity. Downstream of the reprolysin zinc-binding

consensus motif, a conserved methionine residue forms the characteristic “Met-turn” (VMA) arrangement that is believed to maintain the structural integrity of the catalytic domain. The ancillary domains usually supply the substrate-binding specificity and may participate in the modulation of the protease activity (Gao et al., 2002; Gendron et al., 2007; Kashiwagi et al., 2004; Somerville et al., 2003). Especially, the TSP-1 motifs can bind to heparin or heparan sulphate, and this binding is potentially involved in the interaction with the GAG chains of the proteoglycans.

Every ADAMTS (apart from ADAMTS4) are subjected to N-glycosylation in their ancillary domains and this post-translational modification is essential for ADAMTS9 secretion (Somerville et al., 2003). Akin to many metalloproteases, ADAMTS are inhibited by TIMP3 and their activity can be regulated by this classical metalloprotease inhibitor ((Wang et al., 2006; Westling et al., 2002) and reviewed in (Brew and Nagase, 2010)).

2.III.2 Different phylogenic and functional sub-groups of ADAMTS family

The nineteen members of ADAMTS family are regrouped in four clades suggesting an evolution by exon shuffling and duplication of ancestral genes. These different subgroups correlate quite precisely with the functional clustering derived from functional studies and mutation analyses (Fig.18).

ADAMTS2, -3 and -14 form a separate branch among the ADAMTS all exhibiting pro-collagen N-proteinase activities (Colige et al., 2002). They are able to cleave the specific Pro-Gln/Ala-Glu bound in different types of collagens (I, II and III), which is hydrolysed for converting the pro-collagens to the mature proteins. Mutations in the ADAMTS2 gene, the aminopropeptidase of procollagen I, II and III, result in the accumulation of non-fully processed type I procollagen, causing human Ehlers-Danlos syndrome type VIIC and dermatosparaxis (fragility of the skin) in animals (Colige et al., 2004). Besides, ADAMTS2, -3 and -14 are upregulated in the nodules of Dupuytren’s disease, a syndrome characterised by an abnormal thickening of the tissues beneath the skin corresponding to a fibrosis of the palmar fascia (Johnston et al., 2007).

The function of another member, ADAMTS13 was demonstrated by mutations analysis in a congenital disorder, the thrombotic thrombocytopenic purpura, in which mutations of *ADAMTS13* lead to defects in the regulation of von Willebrand factor proteolysis (Levy et al., 2001). ADAMTS13 is a distinctive member of the family by the presence of CUB motifs among its ancillary domains. It binds specifically through its spacer domain to the ultra-large vWF (ULVWF) multimers. The ULVWF multimers are involved in adhesion between platelets themselves and between platelets and the vascular subendothelium. To permit a right balance between haemorrhage and thrombosis, ADAMTS13 cleaves these multimers into

smaller fragments to avoid excessive platelet aggregation under shearing stress and thus properly adjusts coagulation (reviewed in (Zhou et al., 2010)).

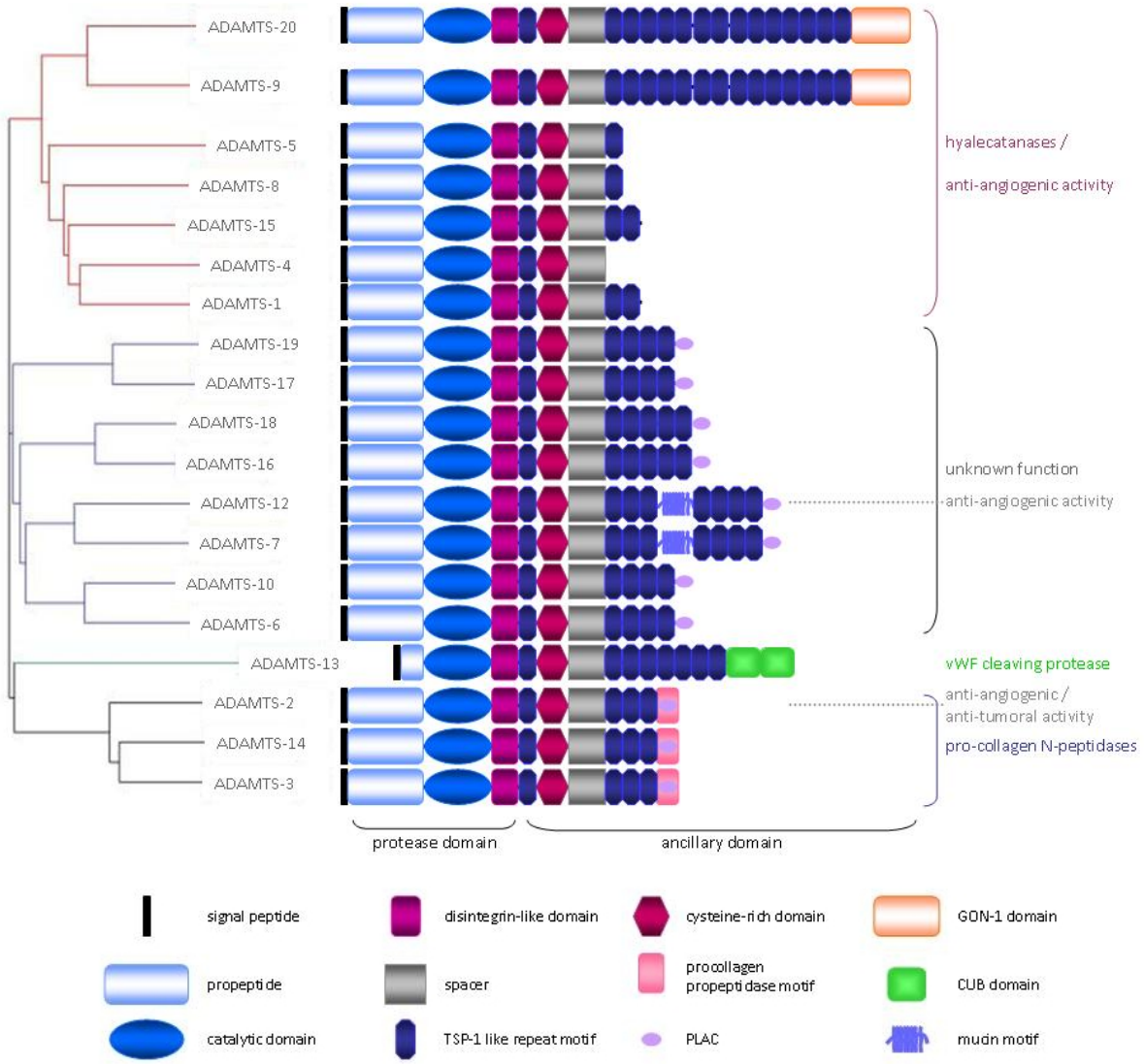

Figure 18. The human ADAMTS family, organisation and functions (adapted from (Apte, 2009; Jones and Riley, 2005).
The different members of ADAMTS (a disintegrin and metalloprotease with thrombospondin type I motifs) family are regrouped according to their evolutionary relationships and putative functions. PLAC: protease and lacunine; CUB: complement C1r/C1s, Uegf (epidermal growth factor-related sea urchin protein) and BMP-1 (bone morphogenic protein-1); vWF von Willebrand factor.

The ADAMTS7 and -12 are evolutionary related members, which represent another cluster. They are both identified as specific proteases of the cartilage oligomeric matrix protein COMP (reviewed in (Liu, 2009)).

ADAMTS1, -4, -5, -8, -9, -15 and -20 compose the largest clade, in which members have been first described to display anti-angiogenic properties or anti-tumoral activities. This group is actually defined and characterised by its proteoglycanase activity. Indeed, all these

ADAMTS members can actively process one or several lecticans in a specific manner (Table.1).

Table 1. Different identified cleavage-sites in human hyalectans and the respective hyalectanases

AGGRECAN		BREVICAN (rat)	VERSICAN	
(Glu^{373}-Glu^{374})	(Asn^{341}-Phe^{342}), (Glu^{1771}-^{1772})	(Glu^{395}-Glu^{396})	V1 (Glu^{441}-Ala^{442})	V0 (Glu^{1428}-Ala^{1429})
ADAMTS1	ADAMTS4	ADAMTS4	ADAMTS1	ADAMTS1
ADAMTS4	ADAMTS5		ADAMTS4	ADAMTS4
ADAMTS5			ADAMTS5	ADAMTS5
ADAMTS8			ADAMTS9	ADAMTS9
ADAMTS15			ADAMTS20	ADAMTS20

2.III.3 Hyalecatanase functions in development

The *ADAMTS-1* gene was first described in the mouse cachexigenic colon adenocarcinoma subline and then identified in human (Kuno et al., 1997). Further studies lead by Kuno and colleagues revealed that ADAMTS1 is an active metalloprotease, secreted and associated with the extracellular matrix through the TSP-1 motifs and the spacer domain (Kuno and Matsushima, 1998; Kuno et al., 1999). They and others also demonstrated that ADAMTS1 can cleave aggrecan at different sites *in vitro* (Kuno and Matsushima, 1998; Kuno et al., 2000; Kuno et al., 1999; Rodriguez-Manzaneque et al., 2002). ADAMTS1 is expressed in different tissues during development and in particular in the limb bud of mice (Kuno and Matsushima, 1998; Kuno et al., 1999; Thai and Iruela-Arispe, 2002). However, ADAMTS1-deficient mice did not show any defects in aggrecan turnover (Little et al., 2005).

ADAMTS4 and -5 were first identified as aggrecanases (aggrecanase-1 and aggrecanase-2 respectively) (Abbaszade et al., 1999; Tortorella et al., 1999). The ADAMTS4 activity is inhibited by fibronectin. The inhibition is mediated through the interaction of fibronectin with the spacer domain in the C-terminal region (Hashimoto et al., 2004). ADAMTS5 was identified as the main aggrecanase due to its abundant expression in cartilage and consequently considered prime candidate for a role in the etiology of arthritis (Stanton et al., 2005). Yet, careful analyses of single and double deficient mice for ADAMTS4 and ADAMTS5, provided evidences that aggrecan turnover *in vivo* is not only dependent of ADAMTS4 or ADAMTS5 processing (Ilic et al., 2007).

In addition of their aggrecanase activity, recombinant ADAMTS1 and ADAMTS4 are able to process a synthetic expressed versican GAGβ peptide *in vitro* producing two fragments, corresponding to a cleavage at the Glu^{441}-Ala^{442} bond in human versican V1 (Sandy et al., 2001). Moreover, using neo-epitope antibodies, related fragments are detected in human aorta. ADAMTS4 is indeed expressed in the aortic intima suggesting an active hyalectanase activity for this protease *in vivo*.

Moreover, in an *in vitro* assay, recombinant ADAMTS4 protease generates a 64 kDa and a 55 kDa N-terminal fragment of brain-derived versican and brevican, respectively (Westling et al., 2004). Of note, the 64 kDa peptide of versican V2 had first been identified as the glial hyaluronate binding protein (GHAP). The putative role of ADAMTS1 and -4 in cleavage of brevican *in vivo* was as well proposed in a model of chemical induced brain injury (Yuan et al., 2002). In these experiments, ADAMTSs were up-regulated after kainate injection and strong increases of the typical ADAMTS-cleavage products of brevican (size 55 kDa) were observed. These fragments co-localised with the ADAMTS transcripts.

A decade ago, *ADAMTS-9,* a new metalloprotease belonging to this family, was identified (Clark et al., 2000) and its expression was studied in detail during mouse development (Jungers et al., 2005). ADAMTS-9 displays a rather wide distribution in embryonic tissues and shows also a particularly strong expression in the limb buds. ADAMTS-20 composes together with ADAMTS9 a distinct subgroup among the ADAMTS being related to the *Caenorhabditis elegans* GON-1 enzyme (Somerville et al., 2003). The GON-1 metalloprotease is required for cell migration during gonadal morphogenesis in the worm suggesting a particular role for these enzymes in development. Versicanase activities of ADAMTS9 and ADAMTS20 were demonstrated in *in vitro* assays, in which versican was incubated with conditioned media containing the recombinant enzymes expressed by transiently transfected cells (Silver et al., 2008; Somerville et al., 2003). The ancillary domains are likely to play an important role in substrate and catalytic specificities, since neither versican nor aggrecan were cleaved by a truncated ADAMTS9 including only the catalytic domain (Somerville et al., 2003). Apart from these two versicanases, ADAMTS5 is transiently expressed in various tissues during development and, like the other ADAMTS-members, it is able to process versican *in vitro* (Longpre et al., 2009). In the last years, studies lead by Apte and colleagues brought some comprehensive inputs in regard to the functions of these three hyalectanases during development. By genetic analysis of the different mouse mutants, they demonstrated for instance a cooperative action of ADAMTS9, ADAMTS5 and ADAMTS20 in versican processing during the regression of interdigital webs (McCulloch et al., 2009b). The generation of the specific proteolytic fragments of versican appears to play a crucial role in this process, as the introduction of a recombinant peptide corresponding to an ADAMTS-cleavage product induced apoptosis in the webs of mice double-deficient for *Adamts5* and *Adamts20*. Based on these data, they suggested an active role for the versican fragments as anti-adhesive factors in this tissue remodelling during limb morphogenesis.

In a more recent study, they provided again strong genetic evidences for a similar functional association of ADAMTS9 and ADAMTS20 in cleaving versican during development of the secondary palate in mouse model (Enomoto et al., 2010). This structure separates the nasal

and oral cavities to isolate the respiratory ways from the digestive ones. Versican processed by ADAMTS9 and ADAMTS20 contributes to the mesenchymal proliferation occurring during the palate closure. Knockout mice heterozygous for ADAMTS9 and homozygous for ADAMTS20 consistently display cleft palates.
Two other ADAMTS members belonging to the hyalectanase cluster, ADAMTS8 expressed in cartilage and ADAMTS15 are only little characterised but may display aggrecanase activity (Cal et al., 2002; Collins-Racie et al., 2004).

Nowadays, the turnover of versican during various developmental remodelling processes is still poorly understood. Especially the rapid disappearance during peripheral nervous system development has not been analysed in detail. According to current knowledge, the hyalectanases ADAMTS-1,-4, -5, -9 and -20 are good candidates to actively control the distribution of versican isoforms and, thus, contribute to the specific regulation of the versican function when the nervous system is being built.

3. Aims of the project

During nervous system development, motor and sensory axons follow specific trajectories through permissive tissues delimited by non-permissive substrates. Previous work in our laboratory has shown that the hyalectan versican V0/V1, present in the barrier tissues to neural crest cell migration, inhibit the neurite extension from neural crest cells *in vitro* (Dutt et al., 2006). Moreover, versican V0/V1 isoforms are expressed in the whole hind limb before innervation of this structure, disappearing shortly later from the nerve pathways, while bordering the axons invading the limb bud of chick embryos (Landolt et al., 1995). Besides, particular metalloproteases from ADAMTS family have been described to specifically cleave hyalectan glycoproteins, such as versican (reviewed in (Apte, 2009)). In this context, we hypothesised that versican V0/V1 splice-variants and their turnover play a major role in axonal guidance of the peripheral nerve system.

In a first part of my PhD project, I have participated in the completion of an ongoing study analysing the effect of versicans V0/V1 on axonal growth of peripheral nerves by stripe choice and three-dimensional collagen matrix assays *in vitro*, and by ectopic injection of purified chick versican V0/V1 isoforms in the nerve pathways of the developing chick hind limb *in ovo*.
In the second and main part, I have focused on the identification and *in vitro*- and *in vivo*-characterisation of putative versicanases potentially involved in the processing of versican throughout chick embryogenesis.

We have formulated following aims for my PhD thesis:

i) to supplement previous *in vitro* and *in ovo* studies on the function versicans in PNS development and to complete this part of the project for publication;
ii) to clone two versicanase candidates, ADAMTS1 and ADAMTS9 in chick and to monitor their expression patterns in chick embryos by *in situ* hybridisation;
iii) to produce specific anti-sera against different epitopes of chick ADAMTS9;
iv) to generate different expression vectors for recombinant chick ADAMTS9 and truncated ADAMTS9 variants to investigate their functionality on versican processing *in vitro*;
v) to express chick recombinant ADAMTS9 in the hind limb and the spinal cord of chick embryos to elucidate its role in the turnover of versican *in vivo*.

4. Studies of versican function in axonal guidance of peripheral axons

4.I. Article

Versican V0 and V1 direct the growth of peripheral axons in the developing chick hind limb (Journal of Neuroscience - *accepted*).

Section: Cellular & Molecular Neuroscience

Versican V0 and V1 direct the growth of peripheral axons in the developing chick hind limb

(Abbreviated title: Versicans V0/V1 control limb innervation)

Shilpee Dutt[1,3], Estelle Cassoly[1], María T. Dours-Zimmermann[1], Mattia Matasci[1,4], Esther T. Stoeckli[2,5] and Dieter R. Zimmermann[1,5]

[1] Institute of Surgical Pathology, University Hospital Zurich, CH-8091 Zurich, Switzerland

[2] Institute of Molecular Life Sciences, University of Zurich, Zurich, Switzerland

[3] Present address: Tata Memorial Centre/ACTREC, Navi Mumbai-410210, India

[4] Present address: Laboratory of Cellular Biotechnology, École Polytechnique Fédérale de Lausanne, CH-1015 Lausanne, Switzerland

[5] both authors contributed equally

Corresponding author: Dieter R. Zimmermann, Institute of Surgical Pathology, University Hospital Zurich, Schmelzbergstrasse 12, CH-8091 Zürich, Switzerland. Email: dieterzi@pathol.uzh.ch

Numbers of figures / tables: **9 / none**
Numbers of pages: **22**
Numbers of words for Abstract / Introduction / Discussion: 149 / 443 / 1315

Keywords: Versican; Chondroitin Sulfate Proteoglycan; Lectican; Extracellular Matrix; PNA-binding; Peripheral Nervous System; Axon Guidance; Inhibitor

Acknowledgements

We thank Marie-Therese Abdou for preparing the tissue sections, Beat Kunz for practical help and excellent advice and Holger Moch and Philipp U. Heitz for their constant support during this project. Our work has been financed in part by grants from the Swiss National Science Foundation and from the Velux-Foundation to D.R.Z. and a grant from the Swiss National Science Foundation to E.T.S.

ABSTRACT

Peanut agglutinin-binding disaccharides and chondroitin sulfate mark transient mesenchymal barriers to advancing motor and sensory axons innervating the hind limbs during chick development. Here we show that the vast majority of these carbohydrates are at the critical stage and location attached to the versican splice-variants V0 and V1. We reveal that the isolated isoforms of this extracellular matrix proteoglycan suppress axon extension at low concentrations and induce growth cone collapse and rapid retraction at higher levels. Moreover, we demonstrate that versican V0 and/or V1, recombinantly expressed in collagen-I gels or ectopically deposited in the hind limbs of chicken embryos in ovo cause untimely defasciculation and axon stalling. Consequently, severe disturbances of nerve patterning are observed in the versican-treated embryos. Our experiments emphasize the inhibitory capacity of versicans V0 and V1 in axonal growth and evidence for their function as basic guidance cues during development of the peripheral nervous system.

INTRODUCTION

The establishment and stabilization of the neuronal circuitry during development and postnatal maturation greatly relies on a timely and spatially coordinated program regulating the delicate balance between axon growth-promotion and -inhibition. In the developing peripheral nervous system (PNS), the delineation of barrier tissues blocking axonal growth and forcing advancing axons into their designated trajectories constitutes one of the initial steps of the highly complex guidance process (Tosney, 1991). This early phase of motor and sensory innervation is at least partly accompanied by the selective deposition and turnover of inhibitory extracellular matrices (ECMs). Once pioneering axons have begun to invade permissive mesenchymal tissues and successive nerve fibers have followed by fasciculation, a refined system of diffusible and stationary attractants and repellents in combination with specific receptor sets on the advancing growth cones controls numerous branch point decisions and directs segregating axons towards their individual targets (Landmesser, 2001; Hanson et al., 2008).

The non-permissive mesenchymal tissues, consistently bordering the pathways of migratory neural crest cells and growing axons during early PNS development, are particularly rich in chondroitin sulfate proteoglycans (CSPGs) and peanut agglutinin (PNA)-binding glycoproteins (Tosney and Landmesser, 1985; Oakley and Tosney, 1991). In the trunk of the chicken embryo, these temporary boundaries include the posterior sclerotome, the perinotochordal region and the early subectodermal zone. CSPGs are also abundantly expressed in the developing hind limbs. The early limb bud tissue blocks innervation initially in its entirety and delays axonal extension from the plexus region by about 24 hours (Wang and Scott, 2000). After this period most of the non-permissive areas have regressed and are ultimately confined to the condensing mesenchyme of the pelvic girdle and other pre-chondrogenic areas.

Prominently represented in all these transient barriers of the trunk and limb anlage are the two largest splice-variants of the extracellular matrix CSPG versican, V0 and V1 (Landolt et al., 1995). Intriguingly, other members of the lectican/hyalectan family of CSPGs including the smaller versican isoform V2 are similarly expressed in non-permissive tissues of the developing or mature central nervous system (CNS) and exert potent axon growth inhibitory activity (Bandtlow and Zimmermann, 2000; Schmalfeldt et al., 2000; Zimmermann and Dours-Zimmermann, 2008). Despite this apparent analogy to axon growth suppressing roles of CSPGs in the CNS, a functional link between the selective expression and turnover of versican V0 and V1 and the non-permissive character of matrices flanking axon trajectories during PNS formation has not been established so far.

Therefore, we have isolated intact versican V0 and V1, explored their inhibitory potential in a series of functional analyses with dorsal root explants in vitro and analyzed their impact on axonal patterning in the developing limb by ectopical deposition in vivo.

MATERIALS AND METHODS

Antibodies and versican preparations

Polyclonal antibodies against specific domains of bovine, human, mouse and chick versican were affinity-purified from rabbit antisera previously prepared by our laboratory (Zimmermann et al., 1994; Landolt et al., 1995; Schmalfeldt et al., 1998; Schmalfeldt et al., 2000). The anti-proteoglycan Di-6S monoclonal antibody 3-B-3 was obtained from Seikagaku. The monoclonal antibody RMO-270 against neurofilament-160 kD (anti-NF-M; Invitrogen) and goat polyclonal antibodies against axonin-1 (Ruegg et al., 1989) were used for axon and growth cone labeling. Lectin- staining of tissue sections was done with Peanut agglutinin (PNA) and goat anti-PNA antibodies (both Vector Laboratories). Fluorescent secondary antibodies included a) Alexa Fluor-488 goat anti-rabbit IgG and Fluor-594 goat anti-mouse IgG for cell culture stainings, b) Alexa Fluor-488 donkey anti-rabbit IgG, Fluor-555 donkey anti-mouse IgG and Fluor-647 donkey anti-goat IgG (Invitrogen) for triple stainings of tissues sections and c) Cy-3 labeled goat anti-mouse secondary antibodies (Jackson ImmunoResearch) for whole mount NF-stainings, respectively. Secondary antibodies for immunoblotting experiments were also from Jackson ImmunoResearch.

Versican isoforms employed in the in vitro and in vivo studies were purified from conditioned medium of the human glioma cell line U251MG and from calf aorta as described (Dutt et al., 2006). Versican core glycoproteins used in some experiments were obtained by removal of the glycosaminoglycan chains through digestion with chondroitinase ABC (Seikagaku).

Blotting techniques

Extracts from Hamburger and Hamilton stage 21 to 22 (HH21/22, (Hamburger and Hamilton, 1951) chick trunks and hind limbs, conditioned media from E13 chick embryonic fibroblast and U251MG cell cultures as well as control extracts of P30 brains of wild type and versican V0/V2 knockout mice (Dours-Zimmermann et al., 2009) were analyzed by lectin- and immunoblotting. Samples were run on 4-15% Phastgels (GE Healthcare Life Sciences) and processed according to (Zimmermann et al., 1994). For the detection of PNA-binding proteins, proteoglycans and versicans we employed a DIG-Glycan Differentiation Kit (Roche Applied Science), a monoclonal antibody against chondroitin sulfate stubs or our polyclonal antibodies against versican, respectively.

Neurite outgrowth assays

Stripe-choice analyses of neurites extending from intact or dissociated explants of dorsal root ganglia (DRG) of E10 to E11 chick embryos were essentially done as described (Vielmetter et al., 1990; Schmalfeldt et al., 2000). In brief, surface-treated glass cover-slips were coated in alternating stripes covered with either test substrates admixed to 100 μg/ml laminin-1 or with 20 μg/ml laminin-1 alone (Invitrogen). The test substrate solutions contained, apart from laminin-1, intact or chondroitinase ABC-digested versican V1 or a versican V0/V1-mixture at concentrations of 10-100 μg/ml. The DRGs were placed onto the stripe pattern and cultured in DMEM/F12 1:1 medium containing 10% FCS, 2% chicken serum, 100 U/ml penicillin, 100 μg/ml streptomycin, 100 ng/ml nerve growth factor 7S (all Invitrogen), 10 mM cytosine arabinoside and 0.5% methylcellulose (both Sigma). After 2 to 3 days of incubation in a 5% CO_2 atmosphere at 37°C, the explant cultures were fixed in 4%

paraformaldehyde / 0.33% sucrose in PBS for 10 min and subsequently analyzed by immunofluorescence. For some experiments laminin-1 was replaced by fibronectin (Roche Diagnostics) as neurite growth-supporting substrate.

To test growth cone behavior in time-lapse video microscopy, half of a pre-treated glass cover-slip was first manually covered with a mixture of 100 µg/ml versican V0/V1 and 100 µg/ml laminin-1, followed by coating of the remaining surface with 20 µg/ml laminin-1 alone. The border of the test substrate area was delineated on the back of the slide with a marker pen. DRGs from E10 chick embryos were placed near the versican coated area and neurites were allowed to grow under a Leica DM IRBE wide field microscope equipped with a culture chamber controlling temperature and CO_2 conditions (37°C and 5%). Images of growth cone movement towards the versican-coated region were captured with a Hamamatsu Orca ER camera using a phase contrast PH1 N Plan L 20X/ 0.40 objective. Frames were captured every 30 seconds and analyzed with the Openlab 3.1.5 software.

Co-cultures of DRGs and transfected COS cells

COS cells were transiently transfected with either an empty pSecTagA vector (Invitrogen; mock transfection) or with a pSecTagA-construct, in which the reconstituted full-length cDNA of the mature human versican V1 core protein including its native stop codon had been inserted into the vector after the Ig secretory leader sequence (Zimmermann and Ruoslahti, 1989). COS cell aggregates were prepared in hanging drops as described (Kennedy et al., 1994). For co-cultures COS cell aggregates were placed in solidifying collagen I gels in close vicinity to DRGs from E10 chick embryos (Lumsden and Davies, 1983) and subsequently incubated at 37°C in DMEM/F12 (1:1) medium containing 10% FCS, 2% chicken serum, 2 mM L-glutamine, 100 U/ml penicillin, 100 g/ml streptomycin and 100ng/ml 7S NGF (all Invitrogen). After 3.5 to 4 days, the 3D-cultures were fixed in 4% paraformaldehyde / 0.33% sucrose in PBS and processed for immunofluorescence staining.

In ovo injections of versican

Hisex chick embryos were staged according to Hamburger and Hamilton (Hamburger and Hamilton, 1951). In ovo injections were performed as described previously (Stoeckli and Landmesser, 1995). After local removal of the extra-embryonic membrane, injections into the hind limb were done with a pointed glass capillary (tip diameter about 5 m) attached to Teflon tubing. The test substrates in PBS were mixed with Trypan Blue (Invitrogen; final concentration 0.04% v/v) to control localization and volume of the injection. Injections were done into the right hind limb at three different positions near the plexus region, two paraxial and one distal (Fig. 1). Less then 1 l of the test solution with versican concentrations of 180 or 400 g/ml (V1 and V0/V1 preparations, respectively) was deposited at each time point. First injections were done at HH18 to 19 and subsequently repeated in regular intervals for three to four times until the embryo reached HH22 to 23. After every manipulation, the eggs were resealed with paraffin and a glass cover slip and incubated at 39°C. At the end of the in ovo experiment (HH25/26), embryos were collected, eviscerated, freed of residual blood and fixed in 4% paraformaldehyde prior to whole mount staining.

Immunohistological and lectin-staining procedures

For the combined immunofluorescence- and PNA-stainings of chick embryo sections we adapted previously described protocols (Oakley and Tosney, 1991; Schmalfeldt et al., 2000). In brief, the isolated embryos were fixed overnight in 4% paraformaldehyde containing 0.5% cetylpiridinium chloride, afterwards dehydrated and paraffin-embedded. Glass slides carrying 4 μm-thick tissue sections were dewaxed and antigens were retrieved in 10 mM tri-sodium citrate, pH 6.0, under controlled conditions (antigen-retrieval device FSG 120-T/T; Milestone). Sections were then blocked with Carbo-Free™ blocking solution for 90 min and incubated with 10 μg/ml PNA in 10 mM HEPES, 150 mM NaCl, 1 mM $CaCl_2$, pH 7.5 for 3 h (all PNA-staining reagents from Vector Laboratories). The binding of the primary antibodies in PBS containing 0.5% BSA, 0.2% gelatin, 0.02% NaN_3 was allowed to proceed overnight at 4°C. The antibody-dilutions were 1:400 for anti-PNA, 1:500 for the antibodies against versican GAG-β and 1:2000 against neurofilament-M. The subsequent incubation with Alexa Fluor-labeled secondary antibodies (all 1:200 dilution, Invitrogen) for 1 to 2 hours was in some experiments followed by counterstaining with Hoechst H33258 bis-benzimide (Invitrogen). Primary and secondary antibody-binding of fixed dorsal root ganglia explant cultures was done analogously, however, antibodies were directly applied after initial blocking with 0.5% BSA, 0.2% gelatin, 0.02% NaN_3 in PBS (Schmalfeldt et al., 2000). Stained cell cultures and tissue sections were finally mounted in fluorescence mounting medium (Dako).

For whole mount-staining of nerve fibers, fixed embryos were washed in PBS and permeabilized in 1% Triton/PBS for 1 h at room temperature. After rinsing in PBS, they were incubated for 1 h in 20 mM lysine, 0.1 M sodium phosphate, pH 7.4, subsequently washed five times in PBS for 10 min and subjected to blocking in 10% fetal calf serum/PBS for at least 2 h at room temperature. Incubation with the monoclonal antibody against neurofilament-M (dilution 1:1500) was carried out for 48 h at 4°C. After five short and one last prolonged incubation in PBS (≥12 h), embryos were again submerged in blocking buffer for 2 h before binding of Cy3-labeled secondary antibodies (diluted 1:500) was done overnight at 4°C. Unbound antibodies were removed by six extensive PBS-washing steps at room temperature (at least 2 times for more than 2 h plus last incubation overnight). Finally, the embryos were dehydrated in an increasing methanol series (25%, 50%, 75% and 100%; each step for ≥30 min) and then transferred into 2:1-benzyl benzoate/benzyl alcohol.

Fluorescence photomicrographs were taken with an Olympus BX61 (cells / sections) or a SZX12 microscope (whole mounts) equipped with a F-view camera. Image capture and analysis was performed using the AnalySISPro software (Soft Imaging System, Germany). Monochromatic fluorescence images were imported into separate color channels in Photoshop and superimposed.

RESULTS

Independent histological studies by Oakley and Tosney and by our group have previously revealed strict complementarities between axonal growth patterns and the distribution of PNA-binding carbohydrates, chondroitin-6-sulfate (Oakley and Tosney, 1991) and the versican isoforms V0/V1 (Landolt et al., 1995) during motor and sensory innervation of the trunk and limbs in the chicken. Although the originally monochrome stainings were suggestive of a close association of these mesenchymal components with axon growth-impeding boundary tissues, particularly the interconnection between the PNA-binding molecule and the chondroitin sulfate-carrying versicans remained rather obscure. For this reason we have first attempted to clarify this relationship before embarking on extensive functional studies in vitro and in vivo.

Versicans are the major PNA-binding proteins in the developing trunk and limb buds

Our triple fluorescence stainings simultaneously detecting PNA-binding carbohydrates, versicans V0/V1 and neurofilaments, now clearly demonstrate a broad overlap of versican-specific immunoreactivity and PNA-binding sites in mesenchymal barriers and confirm the virtual absence of both components from the axonal pathways in the chick embryonic trunk and the developing hind limbs (Fig. 2). For instance, at stage HH22, when the growing motor and sensory axons have joined but are still locked within the plexus region, the entire hind limb is intensely labeled by both, PNA-lectin and versican-specific antibodies. At this time, considerable versican V0/V1 depositions are also found in the perinotochordal region, particularly in immediate vicinity to the notochord, whereas the staining of the PNA-lectin in this area appears more uniform and widespread. Unlike versican, PNA-binding is additionally detected within the neural tube and in the ectodermal layer. Later in hind limb development (HH26), versican and the PNA-binding carbohydrate become confined to the pelvic girdle, to the subectodermal region and to the condensing mesenchyme of the pre-chondrogenic zones. The trajectories of the advancing nerve fibers and the more distal areas of future axonal invasion are essentially free of PNA- and versican-staining. While PNA-binding carbohydrates are still present in the perinotochordal region, the versican V0/V1 immunoreactivity has greatly diminished in this area. At this stage, the PNA-binding activity also persists in the neural tube (except for the motor columns) and in the ectoderm.

The rather striking co-localization of PNA-binding molecules and the versican immunoreactivity within the early mesenchyme supports the hypothesis that the highly glycosylated versicans V0 and V1 might carry not only chondroitin sulfate but also galactosyl (□-1,3) N-acetylgalactosamine, the oligosaccharide recognized by PNA. We have therefore extracted early embryonic trunks and hind limb buds (HH21/22) with a detergent-containing high-salt buffer to solubilize extracellular matrix and cell surface molecules and we have subsequently performed PNA-lectin-blotting and versican V0/V1-specific immunoblotting (Fig. 3). Comparisons of these analyses demonstrate that versicans, and in particular the V0 isoform, in fact account for most of the PNA-binding activity in the early chick trunk and limb extracts. Moreover, nearly exclusive staining of versican V0 and V1 is observed on PNA lectin-blots of conditioned culture media from chick primary embryonic fibroblasts and from the human glioma cell line U251. Akin to the larger V0 and V1 isoforms, versican V2 seems to represent the major PNA-binding component of the mature CNS, as brain extracts of knockout mice selectively

lacking this isoform (Dours-Zimmermann et al., 2009) have lost virtually all of the PNA-reactivity along with the V2-variant.

Versican V0 and V1 are potent neurite outgrowth inhibitors in vitro

In order to examine the inhibitory capacity of the large versican isoforms, we have performed various functional assays with chick dorsal root ganglia (DRG) explants in vitro. In stripe choice experiments, we have first exposed the outgrowing sensory axons to alternating lanes coated either with the neurite growth-promoting ECM-glycoprotein laminin-1 alone or with mixtures of laminin-1 and intact versican V1- or versican V0/V1-preparations isolated as described (Dutt et al., 2006). In spite of the high laminin-level present on both surfaces, robust extension of DRG neurites is confined to the substrate-stripes that lack versican (Fig. 4). Versican overrides the axon growth promoting activity not only of laminin-1. Similar inhibitions can also be observed, when fibronectin (Fig. 5) or collagen-I (not shown) are used as growth promoting substrates in this assay. Because laminin-1 is the most effective substrate and therefore widely used for in vitro studies, we have performed the subsequent stripe-choice experiments with this standard neurite outgrowth promoter. Even under these optimal conditions, a partial reversion of the laminin-induced growth can already be observed, when as little as 10 □g/ml versican V1 or V0/V1-mixture is included in the 100 □g/ml laminin coating-solution (Fig. 6). At versican concentrations of 25 to 50 □g/ml the avoidance by the neurites is nearly complete. This inhibitory activity of versican V0 and V1 is reduced, but not abolished, when the chondroitin sulfate side chains are removed by chondroitinase ABC digestion. In comparison to the intact proteoglycan preparations, the coating concentrations of the core glycoproteins have to be approximately doubled to achieve similar axonal avoidance reactions.

While lower versican V0 and V1 concentrations may provoke stalling and/or turning of the axonal tip, higher concentrations induce growth cone collapse and rapid retraction. We have recorded this latter behavior by time-lapse video microscopy (Fig. 7), in which we confronted DRG neurites growing on a 100 □g/ml-coat of laminin-1 to a surface treated with laminin-1- and versican V0/V1 at dilutions of 100 □g/ml each. In these experiments the neurites advance on the laminin-1 substrate at a speed of 120 to 150 □m/hour and display extended growth cone morphologies. Once they have contacted the versican-containing zone however, the growth cones immediately collapse and the axons retract with a three to four times higher velocity. This retrograde movement slows down after a while, stops, the growth cones restore and axonal growth is re-initiated. Similarly, growth cones advancing on laminin-1 alone in the stripe-choice format constantly explore the neighboring lanes containing high versican concentrations, but invariably collapse, when they reach the end of the versican-free lane (Fig. 7).

In the final experiments of our in vitro series, we have analyzed the influence of versican deposition on axonal growth in three-dimensional collagen I matrices. Also in this more in vivo-like setting, we obtained clear evidence for a dominant inhibitory effect of versican overriding the axon growth promotion, this time exerted by the collagen substrate. In the collagen gel assay (Fig. 8) axons frequently extend from the DRG explants in form of robust nerve bundles. However, as soon as they approach the neighborhood of COS cells, which recombinantly express full-length versican V1, they

begin to defasciculate and then stop before reaching the aggregates. In contrast, mock-transfected control aggregates devoid of versican expression do not affect neurite outgrowth.

Ectopical deposition of versican V0 and V1 disturbs axon patterning in developing hind limbs in vivo

Untimely defasciculation and aberrant axon routings are also observed in vivo, when versican V1 or V0/V1 are ectopically deposited in the nerve pathways of the developing hind limb. Repeated in ovo injections of versicans between HH18 and HH23 resulted in aberrant branching of developing peripheral nerves at HH25/26. Whole mounts stained with anti-neurofilament antibodies were scored blind to the experimental condition for axonal branching in the developing hind limbs (Fig. 9). As main indicators, we scored abnormal exit points (criterion 1) and irregular branching of secondary nerve fibers (criterion 2) emerging from the dorsal trunk of the sciatic plexus. This way, we revealed moderate to severe disturbances (only one or both criteria fulfilled, respectively) of axonal growth behavior in the vast majority of the embryos, in which the natural formation of versican-free pathways was counteracted by our exogenous versican supply. Conversely, irregularities of sciatic nerve formation were only very rarely seen in control-injected embryos by the three independent observers of this blinded study.

In summary, all our analyses emphasize the inhibitory potential of versican V0 and V1 in axon growth regulation by inducing defasciculation, deflection and repulsion of neuronal processes depending on the concentration within the extracellular matrix.

Discussion

The guidance process that directs sensory and motor axons with utmost precision towards their individual targets in the hind limb operates on multiple levels. At the lowest level, general cues divide the early mesenchyme into permissive and non-permissive areas for axon growth (Tosney, 1991; Landmesser, 2001). Through short-range contact, they roughly indicate the prospective nerve routes and transiently block inappropriate and/or pre-mature innervation of differentiating tissues. Although the axons following these basic pathways intermingle initially in the spinal nerves, they subsequently segregate within the plexus region into separate pools, which already bear the capacity to later respond differentially to region-specific cues within the developing limbs. Rhythmic electrical bursts originating from the early spinal cord appear to sustain this axonal pooling and hence, further influence subsequent pathfinding decisions (Hanson et al., 2008). Controlled by this second level and more sophisticated guidance mechanism axon bundles enter the hind limb and stereotypically bifurcate into ventral and dorsal nerve trunks. More distally, the growth cones encounter several additional choice points, where selected subsets of nerve fibers continue to branch off and finally defasciculate at their predetermined target destination. This last step of innervation is likely regulated by the most complex and hitherto still largely unknown interplay of multiple receptors and corresponding guidance cues.

Commonly, the identification of guidance molecules that function at any stage of limb development has been rather difficult. Best characterized so far are ligand-receptor systems that cooperate in dorsoventral pathfinding decisions at the entrance of the hind limb. This includes pairs of ephrinA:EphA4- and ephrinB:EphB-receptors controlling selective axonal growth by repulsion (Helmbacher et al., 2000; Eberhart et al., 2002; Luria et al., 2008) and the ligand-receptor combination of glial cell-line derived neurotrophic factor (GDNF):Ret mediating axon attraction (Kramer et al., 2006). Mice lacking one or several of these signaling components indeed display different degrees of misrouting of motor axons at the dorsoventral choice-point, but the basic outline of the main nerve pathways remains unaffected (Helmbacher et al., 2000; Kramer et al., 2006; Luria et al., 2008). These findings clearly establish their role as specific cues yet, they indicate that other molecules operate on a more general level of axonal guidance.

Owing to their consistent association with barrier tissues, PNA-binding glycoproteins and chondroitin-6 sulfate (CS6)-carrying proteoglycans have generally been considered the prime candidates for such a universal role, namely as inhibitors of neural crest cell migration and axonal growth in the periphery (Oakley and Tosney, 1991; Oakley et al., 1994). The best match in the search for the CSPG component is versican, since its splice-variants V0 and V1 show a highly similar temporospatial distribution in the developing trunk and hind limbs (Landolt et al., 1995) and because it impedes the migration of neural crest stem cells in vitro (Dutt et al., 2006). We now demonstrate that these two versican isoforms are also the main carriers of PNA-reactive carbohydrates at the corresponding locations and therewith tie our versican findings to the knowledge of PNA-binding barrier components. This integration may as well encompass the only partly characterized growth cone collapse-inducing 48 and 55 kDa glycoproteins, which have previously been isolated by PNA-affinity chromatography from extracts of cultured somitic strips (Davies et al., 1990). Considering our current lectin-blots with almost exclusive staining of the versican core glycoproteins in embryonic trunk extracts, it appears unlikely that these former preparations of PNA-binding protein contained no

versicans. They must have rather evaded detection due to their large sizes and dispersion in gel electrophoresis. It seems therefore likely that at least parts of the growth cone collapsing activity ascribed to these smaller PNA-binding glycoproteins has emanated from 'contaminating' versicans. Whether the 48 and 55 kDa components represented chondroitin sulfate-free proteolytic fragments of versican remains presently open.

In a few tissues of the early trunk, such as the ectoderm and the neural tube, PNA-binding and versican V0/V1 immunostaining do not co-localize. Moreover, the initially expressed versicans, but not the PNA-affinity sites, disappear from the greater surrounding of the notochord after HH22 to 23. At this time and location, versican is progressively being substituted by its close relative, aggrecan (Oettinger et al., 1985; Domowicz et al., 1995). Like versicans, it carries chondroitin sulfate side chains and numerous mucin-type O-glycans, some of which might maintain the PNA-reactivity at this particular site. Yet, the early notochordal aggrecan of the trunk region seems to bind only little PNA according to our blotting experiments. Aggrecan and versican V0/V1 probably share some inhibitory functions during the initial stages of PNS formation. While aggrecan may prevent neural crest cells and neuronal projections from invading the perinotochordal region (Perris and Johansson, 1990; Snow et al., 1990), versicans V0 and V1 seem to be primarily responsible for the non-permissive properties of the posterior somite, the early limb bud and pelvic girdle. Only later in development, when versican V0/V1 has long been cleared from the axonal pathways and when cartilage begins to form, aggrecan and some other chondroitin sulfate proteoglycans, such as decorin and type IX collagen, replace versican in the skeletal primordia of the limb (Shinomura et al., 1984; Lennon et al., 1991; Yamagata et al., 1993). Of note, defects in versican turnover lead at this advanced stage to digit malformations (McCulloch et al., 2009).

Despite their intriguing association with barrier tissues during nervous system development, the exploration of the putative guidance roles of the two largest versican variants has long been hampered by their extraordinary structural and biochemical properties. In addition, attempts to approach functional aspects by gene knockout experiments in mice or by over-expression and knockdown in chick embryos have been frustrating due to the early lethality of versican null mice (Mjaatvedt et al., 1998) and due to the relative inefficiency of in ovo electroporation of mesenchymal cells in the early limbs, respectively (own observations). Only the recent elaboration of protocols to isolate larger quantities of intact V0 and V1 isoforms (Dutt et al., 2006) has enabled us to study the inhibitory potential of versicans in peripheral axon growth in vitro and in vivo. In every assay of our present study, versican V0/V1 proved to override the axon growth promotion of extracellular matrix components such as laminin-1 and collagen-I. Most of this inhibitory potential appears to reside in the versican core protein structure, as complete removal of the chondroitin sulfate chains cannot neutralize this function. Nevertheless, the glycosaminoglycans and mucin-type O-glycans are certainly required for the structural integrity, which might explain the partial reduction of the inhibitory capacity of versicans after chondroitinase digestion.

The axonal response induced upon encounter of versican V0/V1-containing areas is highly concentration-dependent and ranges in our functional experiments from rapid retraction and deflection to defasciculation and growth arrest. These latter forms of attenuated versican inhibition are frequently observed in the collagen gel assays in vitro and in the injected hind limbs in vivo. In comparison with

their endogenous counterparts, the ectopically positioned versicans V0/V1 are usually limited in quantity. Moreover, they are in vivo confronted with emerging proteolytic processes typically clearing the proteoglycans from future nerve pathways. By repeating the injections in regular intervals we could at least partly circumvent this problem as illustrated by the clear inhibitory effects of versican observed in our in ovo study.

Interestingly, a similar concentration-dependency of versican seems to control axonal behavior in the developing optic tectum of the chicken CNS (Yamagata et al., 1995). Here graded levels of versicans V0/V1 are involved in the pathway-restriction of retinal axons and in the regulation of lamina-specific arborization and presynaptic maturation.

Whether versican V0 and V1 act alone or in concert with other factors in the different boundary tissues is currently not known. However, concepts of direct functional links between these proteoglycans and semaphorins (Kantor et al., 2004; Huber et al., 2005) and/or ephrins (Wang and Anderson, 1997) in certain selective axonal barriers seem highly realistic and thus, should be included in future strategies to explore the guidance processes in the developing nervous system.

References

Bandtlow CE, Zimmermann DR (2000) Proteoglycans in the developing brain - new conceptual insights for old proteins. Physiol Rev 80:1267-1290.

Davies JA, Cook GM, Stern CD, Keynes RJ (1990) Isolation from chick somites of a glycoprotein fraction that causes collapse of dorsal root ganglion growth cones. Neuron 4:11-20.

Domowicz M, Li H, Hennig A, Henry J, Vertel BM, Schwartz NB (1995) The biochemically and immunologically distinct CSPG of notochord is a product of the aggrecan gene. Dev Biol 171:655-664.

Dours-Zimmermann MT, Maurer K, Rauch U, Stoffel W, Fassler R, Zimmermann DR (2009) Versican V2 assembles the extracellular matrix surrounding the nodes of ranvier in the CNS. J Neurosci 29:7731-7742.

Dutt S, Kleber M, Matasci M, Sommer L, Zimmermann DR (2006) Versican V0 and V1 guide migratory neural crest cells. J Biol Chem 281:12123-12131.

Eberhart J, Swartz ME, Koblar SA, Pasquale EB, Krull CE (2002) EphA4 constitutes a population-specific guidance cue for motor neurons. Dev Biol 247:89-101.

Hamburger V, Hamilton HL (1951) A series of normal stages in the development of the chick embryo. J Morphol 88:49-92.

Hanson MG, Milner LD, Landmesser LT (2008) Spontaneous rhythmic activity in early chick spinal cord influences distinct motor axon pathfinding decisions. Brain Res Rev 57:77-85.

Helmbacher F, Schneider-Maunoury S, Topilko P, Tiret L, Charnay P (2000) Targeting of the EphA4 tyrosine kinase receptor affects dorsal/ventral pathfinding of limb motor axons. Development 127:3313-3324.

Huber AB, Kania A, Tran TS, Gu C, De Marco Garcia N, Lieberam I, Johnson D, Jessell TM, Ginty DD, Kolodkin AL (2005) Distinct roles for secreted semaphorin signaling in spinal motor axon guidance. Neuron 48:949-964.

Kantor DB, Chivatakarn O, Peer KL, Oster SF, Inatani M, Hansen MJ, Flanagan JG, Yamaguchi Y, Sretavan DW, Giger RJ, Kolodkin AL (2004) Semaphorin 5A is a bifunctional axon guidance cue regulated by heparan and chondroitin sulfate proteoglycans. Neuron 44:961-975.

Kennedy TE, Serafini T, de la Torre JR, Tessier-Lavigne M (1994) Netrins are diffusible chemotropic factors for commissural axons in the embryonic spinal cord. Cell 78:425-435.

Kramer ER, Knott L, Su F, Dessaud E, Krull CE, Helmbacher F, Klein R (2006) Cooperation between GDNF/Ret and ephrinA/EphA4 signals for motor-axon pathway selection in the limb. Neuron 50:35-47.

Landmesser LT (2001) The acquisition of motoneuron subtype identity and motor circuit formation. Int J Dev Neurosci 19:175-182.

Landolt RM, Vaughan L, Winterhalter KH, Zimmermann DR (1995) Versican is selectively expressed in embryonic tissues that act as barriers to neural crest cell migration and axon outgrowth. Development 121:2303-2312.

Lennon DP, Carrino DA, Baber MA, Caplan AI (1991) Generation of a monoclonal antibody against avian small dermatan sulfate proteoglycan: immunolocalization and tissue distribution of PG-II (decorin) in embryonic tissues. Matrix 11:412-427.

Lumsden AG, Davies AM (1983) Earliest sensory nerve fibres are guided to peripheral targets by attractants other than nerve growth factor. Nature 306:786-788.

Luria V, Krawchuk D, Jessell TM, Laufer E, Kania A (2008) Specification of motor axon trajectory by ephrin-B:EphB signaling: symmetrical control of axonal patterning in the developing limb. Neuron 60:1039-1053.

McCulloch DR, Nelson CM, Dixon LJ, Silver DL, Wylie JD, Lindner V, Sasaki T, Cooley MA, Argraves WS, Apte SS (2009) ADAMTS metalloproteases generate active versican fragments that regulate interdigital web regression. Dev Cell 17:687-698.

Mjaatvedt C, Yamamura H, Capehart A, Turner D, Markwald R (1998) The *cspg2* gene, disrupted in the *hdf* mutant, is required for right cardiac chamber and endocardial cushion formation. Dev Biol 202:56-66.

Oakley RA, Tosney KW (1991) Peanut agglutinin and chondroitin-6-sulfate are molecular markers for tissues that act as barriers to axon advance in the avian embryo. Dev Biol 147:187-206.

Oakley RA, Lasky CJ, Erickson CA, Tosney KW (1994) Glycoconjugates mark a transient barrier to neural crest migration in the chicken embryo. Development 120:103-114.

Oettinger HF, Thal G, Sasse J, Holtzer H, Pacifici M (1985) Immunological analysis of chick notochord and cartilage matrix development with antisera to cartilage matrix macromolecules. Dev Biol 109:63-71.

Perris R, Johansson S (1990) Inhibition of neural crest cell migration by aggregating chondroitin sulfate proteoglycans is mediated by their hyaluronan-binding region. Dev Biol 137:1-12.

Ruegg MA, Stoeckli ET, Kuhn TB, Heller M, Zuellig R, Sonderegger P (1989) Purification of axonin-1, a protein that is secreted from axons during neurogenesis. EMBO J 8:55-63.

Schmalfeldt M, Dours-Zimmermann MT, Winterhalter KH, Zimmermann DR (1998) Versican V2 is a major extracellular matrix component of the mature bovine brain. J Biol Chem 273:15758-15764.

Schmalfeldt M, Bandtlow CE, Dours-Zimmermann MT, Winterhalter KH, Zimmermann DR (2000) Brain derived versican V2 is a potent inhibitor of axonal growth. J Cell Sci 113:807-816.

Shinomura T, Kimata K, Oike Y, Maeda N, yano S, Suzuki S (1984) Appearance of distinct types of proteoglycan in a well defined temporal and spatial pattern during early cartilage formation in the chick limb. Dev Biol 103:211-220.

Snow DM, Lemmon V, Carrino DA, Caplan AI, Silver J (1990) Sulfated proteoglycans on astroglial barriers inhibit neurite outgrowth in vitro. Exp Neurol 109:111-130.

Stoeckli ET, Landmesser LT (1995) Axonin-1, Nr-CAM, and Ng-CAM play different roles in the in vivo guidance of chick commissural neurons. Neuron 14:1165-1179.

Tosney KW (1991) Cells and cell-interactions that guide motor axons in the developing chick embryo. Bioessays 13:17-23.

Tosney KW, Landmesser LT (1985) Development of the major pathways for neurite outgrowth in the chick hindlimb. Dev Biol 109:193-214.

Vielmetter J, Stolze B, Bonhoeffer F, Stuermer CAO (1990) In-Vitro Assay to Test Differential Substrate Affinities of Growing Axons and Migratory Cells. Exp Brain Res 81:283-287.

Wang G, Scott SA (2000) The "waiting period" of sensory and motor axons in early chick hindlimb: its role in axon pathfinding and neuronal maturation. J Neurosci 20:5358-5366.

Wang HU, Anderson DJ (1997) Eph family transmembrane ligands can mediate repulsive guidance of trunk neural crest migration and motor axon outgrowth. Neuron 18:383-396.

Yamagata M, Herman JP, Sanes JR (1995) Lamina-specific expression of adhesion molecules in developing chick optic tectum. J Neurosci 15:4556-4571.

Yamagata M, Saga S, Kato M, Bernfield M, Kimata K (1993) Selective distributions of proteoglycans and their ligands in pericellular matrix of cultured fibroblasts. Implications for their roles in cell-substratum adhesion. J Cell Sci 106:55-65.

Zimmermann DR, Ruoslahti E (1989) Multiple domains of the large fibroblast proteoglycan, versican. EMBO J 8:2975-2981.

Zimmermann DR, Dours-Zimmermann MT (2008) Extracellular matrix of the central nervous system: from neglect to challenge. Histochem Cell Biol 130:635-653.

Zimmermann DR, Dours-Zimmermann MT, Schubert M, Bruckner-Tuderman L (1994) Versican is expressed in the proliferating zone in the epidermis and in association with the elastic network of the dermis. J Cell Biol 124:817-825.

FIGURES AND LEGENDS

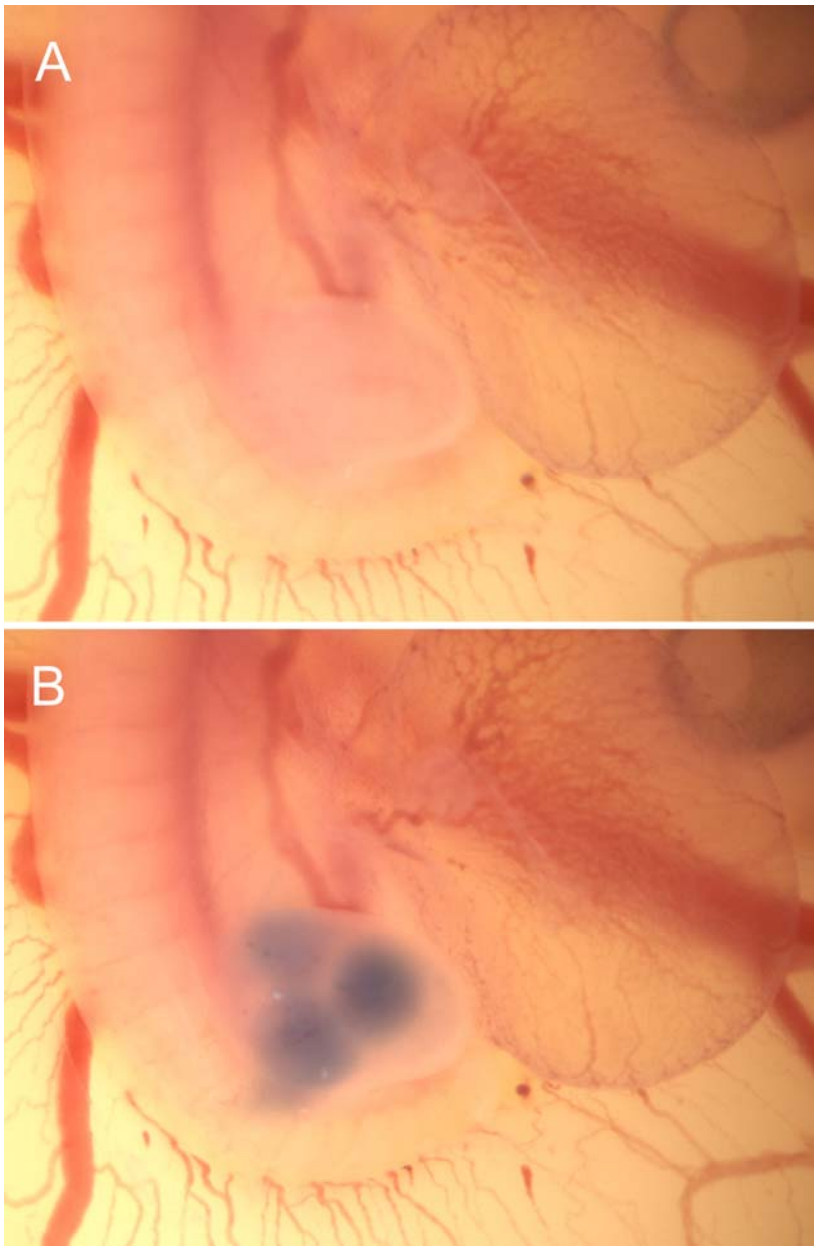

M_Figure 1*. Chick embryo at HH21/22 before (A) and after in ovo-injection (B) of the Trypan Blue-containing versican solution.*

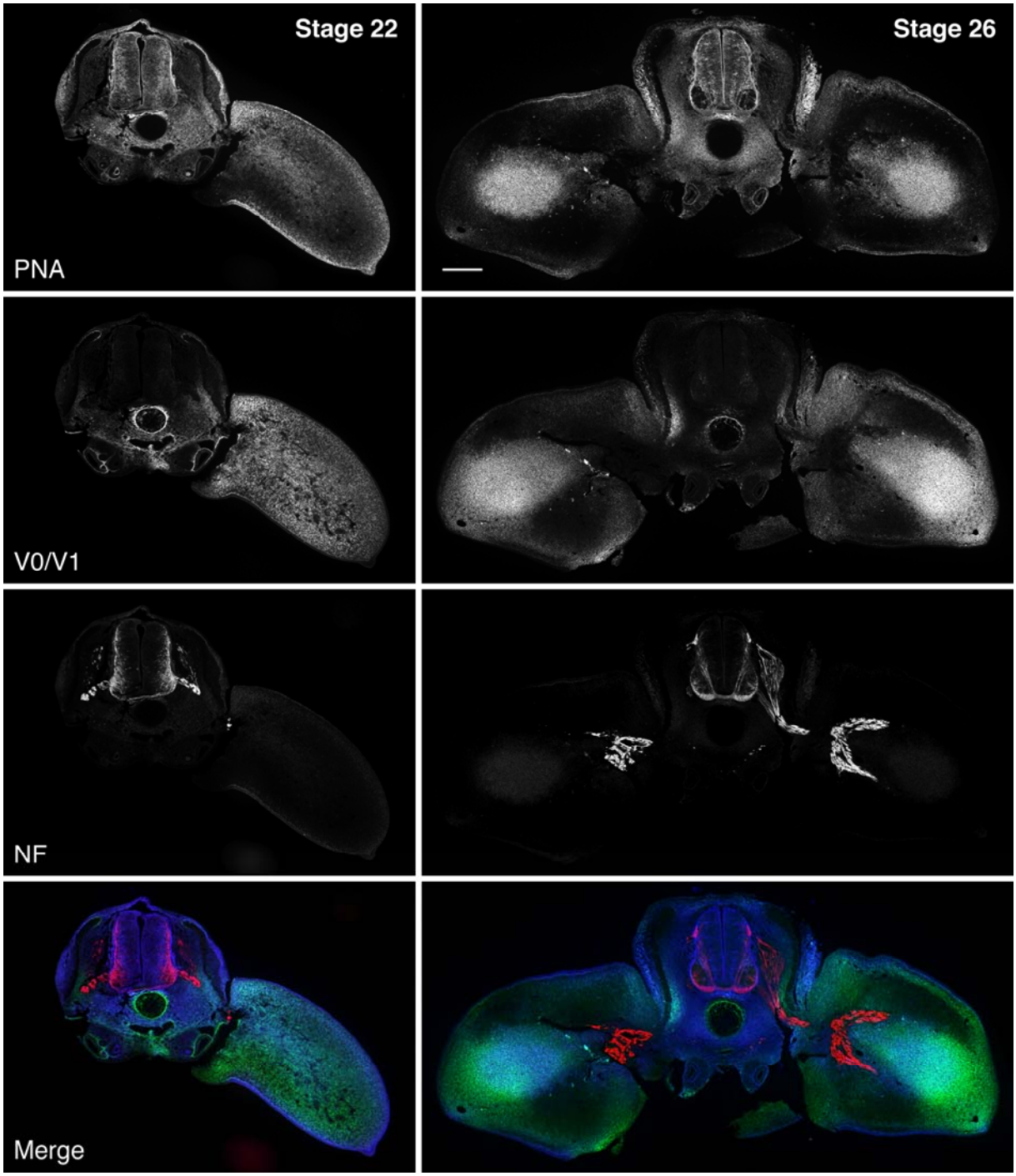

***M_Figure 2**. Temporospatial relationship of PNA-binding sites, versican V0/V1 and axonal growth in the developing hind limb.* Triple lectin/immunofluorescence stainings of cross-sections of HH22 and 26 chicken embryos at hind limb level reveal the largely overlapping patterns of PNA-ligands (dark blue in merged image) and versican V0/V1 (green). At HH22 both components are ubiquitously distributed in the perinotochordal region and the early limb bud, but absent from the pathways of motor and sensory axons (red), which have reached the plexus region and are momentarily hindered from entering the limb. At HH26 versican and PNA-binding sites have disappeared from the prospective axon routes, while persisting in the pelvic girdle precursor, in the forming dermis and the condensing mesenchyme adumbrating the future leg bones. Bar: 200 μm.

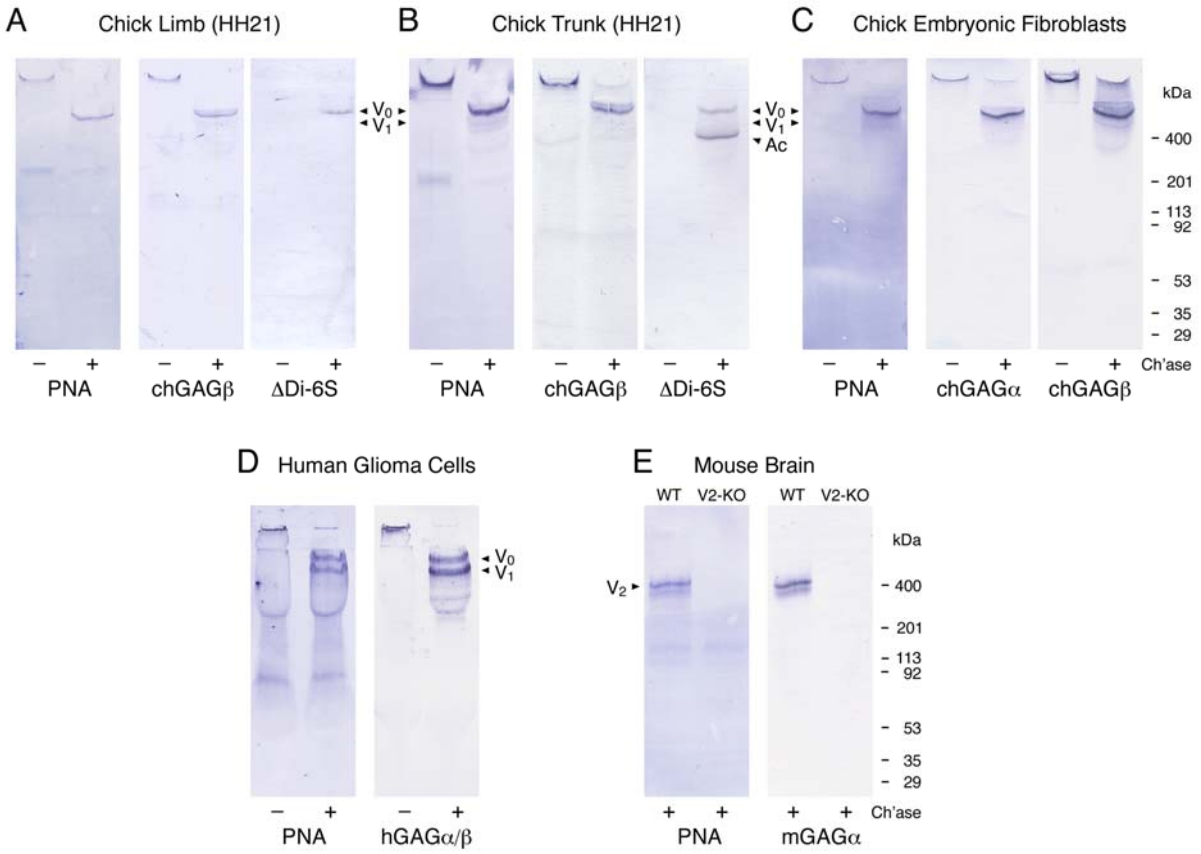

M_Figure 3*. Identification of versicans as major PNA-binding proteins*. Extracts of hind limbs (A) and trunks (B) from HH21-chick embryos, supernatants of chick embryonic fibroblasts (C) and of human U251 glioma cell cultures (D) and brain-extracts of P30-wild type (WT) and versican V0/V2-knockout mice (E) were analyzed by lectin- and immunoblotting with PNA and antibodies against versicans and against chondroitin 6-sulfate stubs (ΔDi-6S), respectively. Some of the samples were digested with chondroitinase ABC (+) to remove the GAG side-chains. The domain-specific antibodies against versican are reactive with the chick variants V0/V1 (chGAGβ), the chick and mouse isoforms V0/V2 (chGAGα, mGAGα) or all proteoglycan variants of human versican (hGAGα/β). The bands of the different core glycoproteins of versicans (V0, V1 and V2) and of aggrecan (Ac) are indicated by arrowheads.

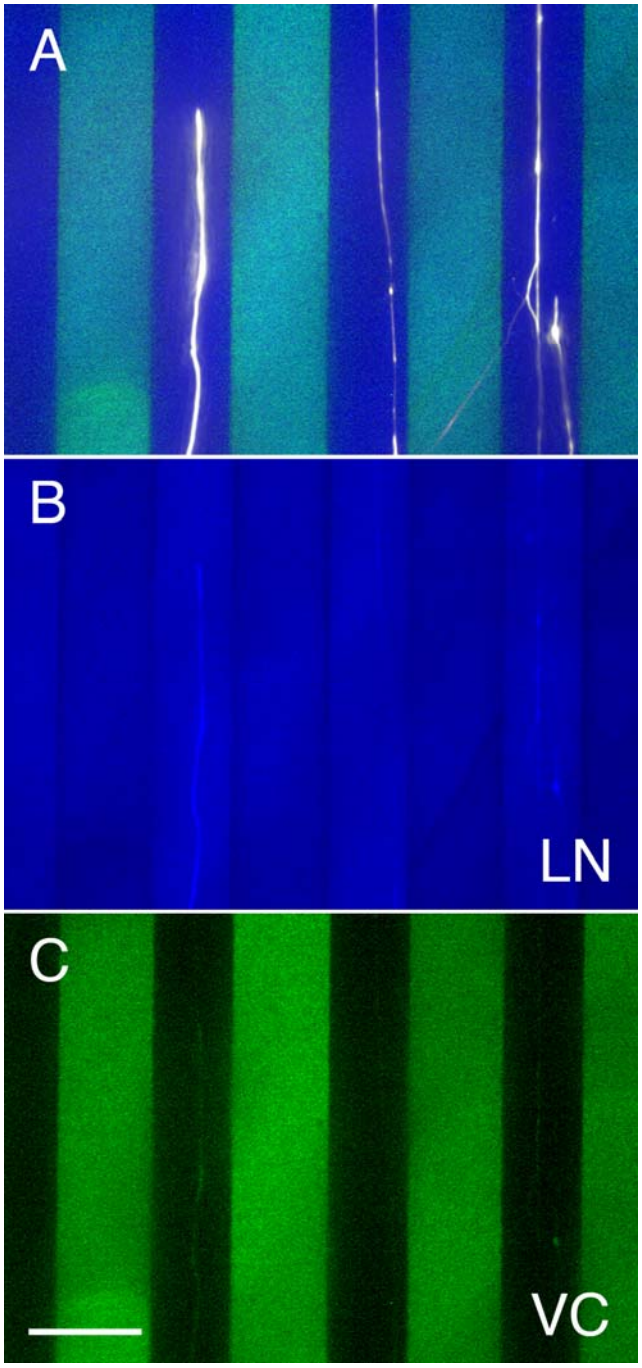

***M_Figure 4**. Versican overrides the neurite growth promoting activity of laminin-1 in a stripe-choice assay*. (A) Overlay of false color images of a triple immunofluorescence staining of laminin-1 (LN; blue), versican (VC; green) and neurofilaments (white). Despite the rather uniform distribution of the growth promoting substrate laminin-1, neurites from E10 chick dorsal root ganglions avoid stripes coated with laminin-1 plus versican V0/V1 (100 μg/ml coating concentration) and advance on lanes coated with laminin-1 alone. The laminin- and the versican-specific stainings are also depicted separately in (B) and (C), respectively. Bar: 50 μm.

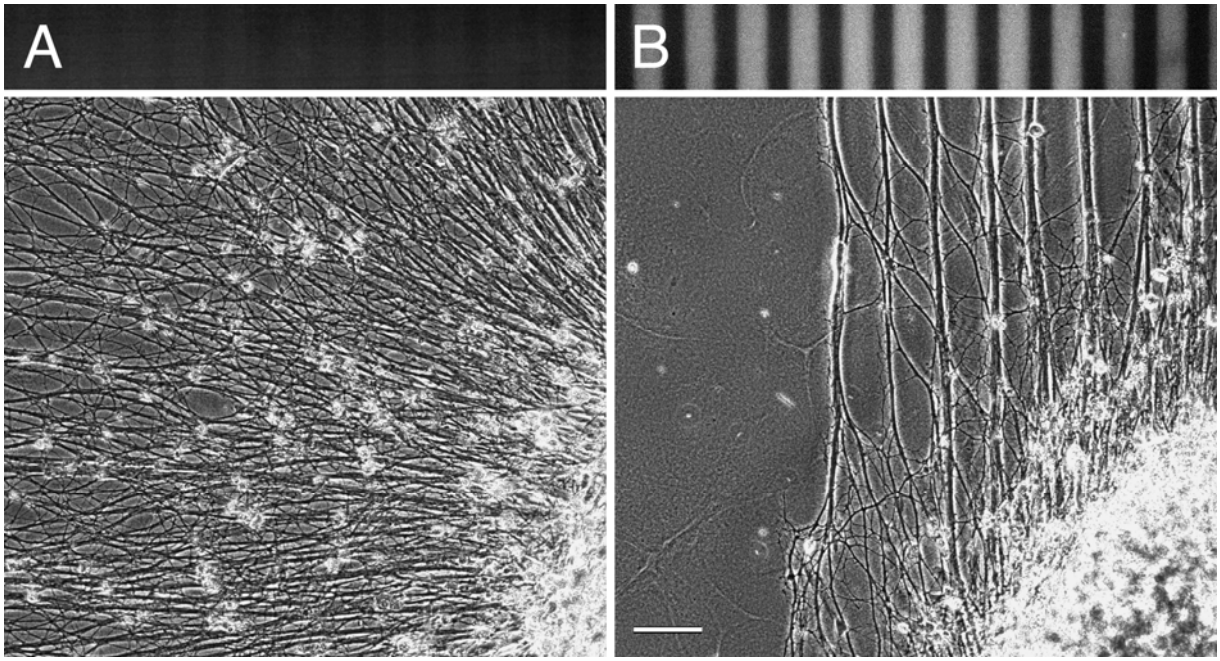

M_Figure 5*. Versican-mediated inhibition of neurite outgrowth on fibronectin.* While neurites from an E10 chick dorsal root ganglion extend freely on alternating substrate-stripes coated with 20 and 100 μg/ml fibronectin (A), they are rapidly forced into versican-free lanes on alternating stripes of fibronectin alone (coated with 20 μg/ml) and fibronectin plus versican V0/V1 (100 μg/ml each) substrates (B). Phase-contrast and versican-specific immunofluorescence images. Bar: 100 μm.

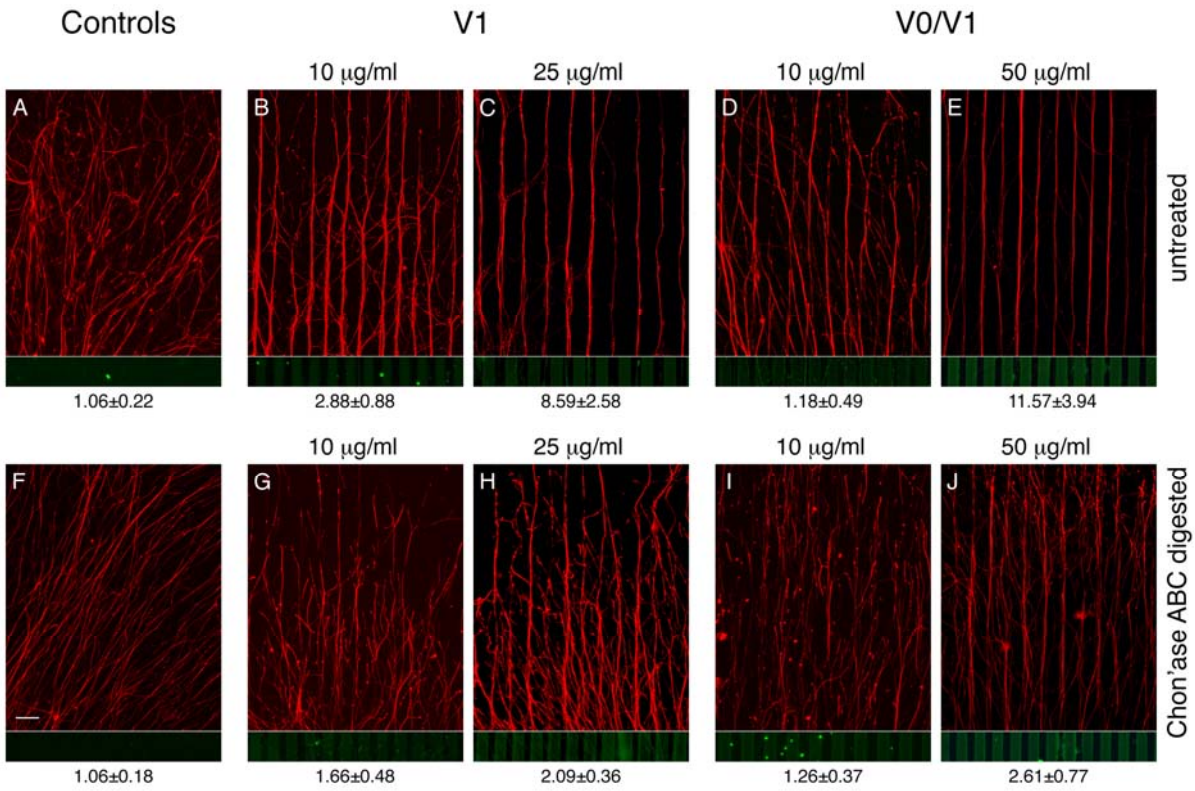

M_Figure 6*. Inhibitory potential of versican V0/V1 on neurite outgrowth in stripe-choice assays*. Neurites from E10 chick dorsal root ganglions grow on laminin-1 stripes, but avoid alternating lanes coated with laminin-1 plus intact or core glycoprotein preparations of versican V1 (B, C and G, H, respectively) or of a V0/V1-mix (D, E and I, J). For the coating of the test stripes a 100 μg/ml laminin-1 solution was supplemented with variable amounts of versican. The corresponding versican concentrations are indicated above the panels. On the versican-free control lanes 20 μg/ml laminin-1 was applied. The stripe patterns of the control assays (A, F) were prepared analogously, but versican was omitted in the test stripes; control (F) included in addition chondroitinase and enzyme buffer in the test lanes. Neurofilaments (red) and versican (green) have been visualized by double immunofluorescence staining. Ratios (±SD) of averaged grey values of the axon-specific red fluorescence in versican-free versus the adjacent versican-containing lanes are shown below the panels. Bar: 100 μm.

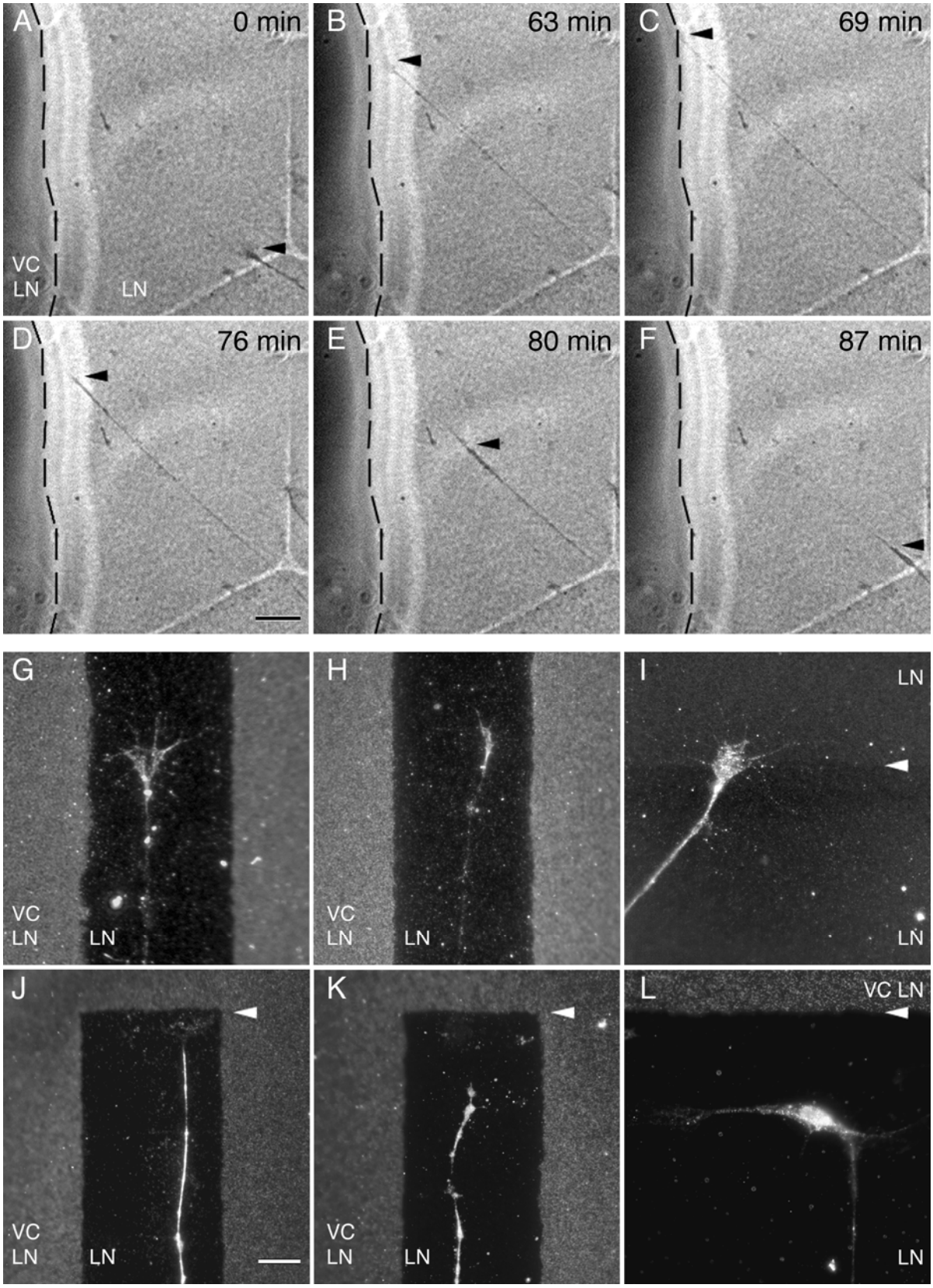

***M_Figure 7**. Growth cone collapse and retraction of DRG neurites after contact with versican containing substrate*. Still images from time lapse video microscopy (A-F) documenting the axon growth behavior of E10 chick DRG axons on a laminin-1 (LN) substrate either containing or lacking versican V0/V1 (VC). The boundary to the area coated with laminin plus versican V0/V1 (100µg/ml each) is marked with a stippled line. At 0 and 63 minutes the growth cone (arrowhead) is moving forward in direction of the versican containing region. Contacting versican after 69 min, it collapses

and the axon rapidly retracts back towards the cell body. After 87 min the original position is reached (F). Bar (A-F): 25 μm. Immunofluorescence-overlays of substrate-stainings of versican (G, H, J-L) or laminin-1 (I) and axonin-1-specific neurite-labelling reveal growth cones with partly to fully extended structures during advancement on a versican-free zone in between versican-containing stripes (G, H) or across the border of two differentially coated laminin-1 control areas (I; 100 μg/ml coating above and 20 μg/ml below arrowhead). A fully collapsed morphology is, however, invariably observed near the ends of versican-free lanes (arrowheads J, K). (L) A neuronal cell body near the versican-containing surface projects a long neurite perpendicularly away from versican while a short second process extends strictly parallel to the border. Bar (G-L): 10 μm.

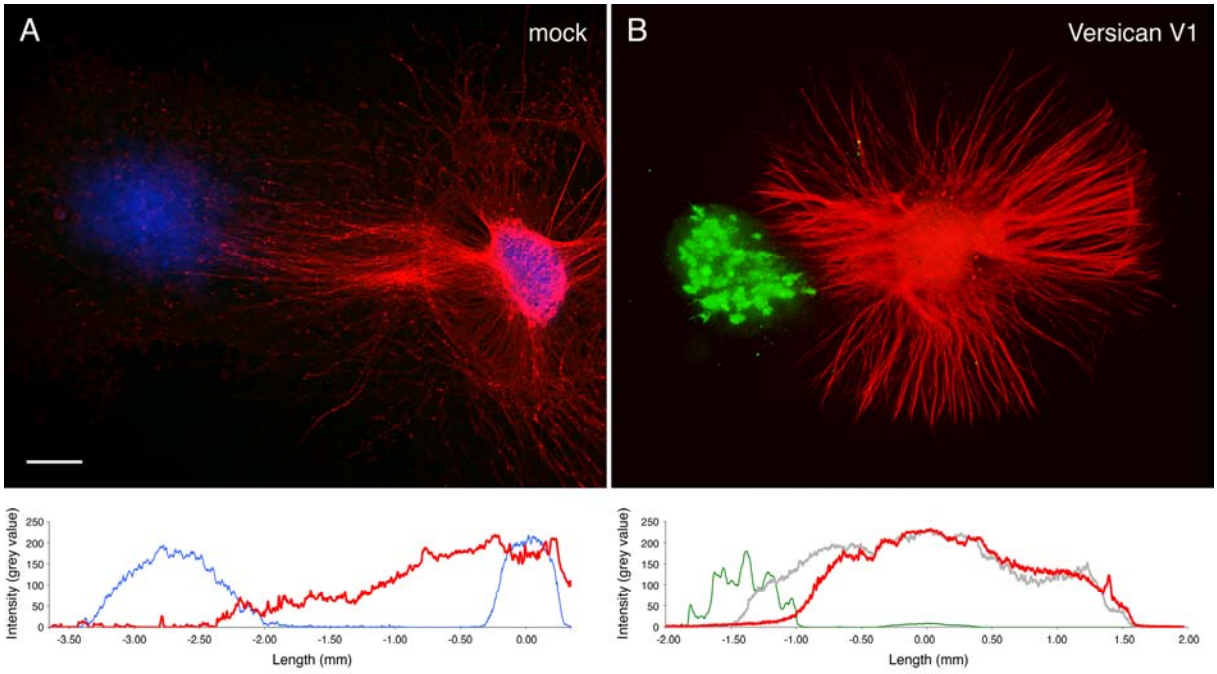

***M_Figure 8**. Inhibition of axonal outgrowth by versican V1-expressing COS aggregates in collagen-I gel.* Neurites from E10 chick DRG extend radially within the collagen gel, but defasciculate and stop near the COS cell aggregate recombinantly expressing versican V1. No such effect is observed in the control experiment with a COS cell aggregate transfected with the empty vector. Neurofilaments (red) and versican (green) are visualized by double immunofluorescence staining. Hoechst nuclear stain (blue) reveals the cellular localizations in the control. Fluorescence profiles averaged over a bandwidth of 200 μm reveal the decline of neurite density (red line in panel B) already 0.5 mm away from the versican-expressing (green line) COS cells in relation to the profile of a nearby control sector, where neurites pass by the aggregate unhindered (gray line). Profiles of neurites and COS aggregates are virtually non-overlapping contrasting the control experiment (A; Hoechst: blue line / neurites: red line). Bar: 400 μm.

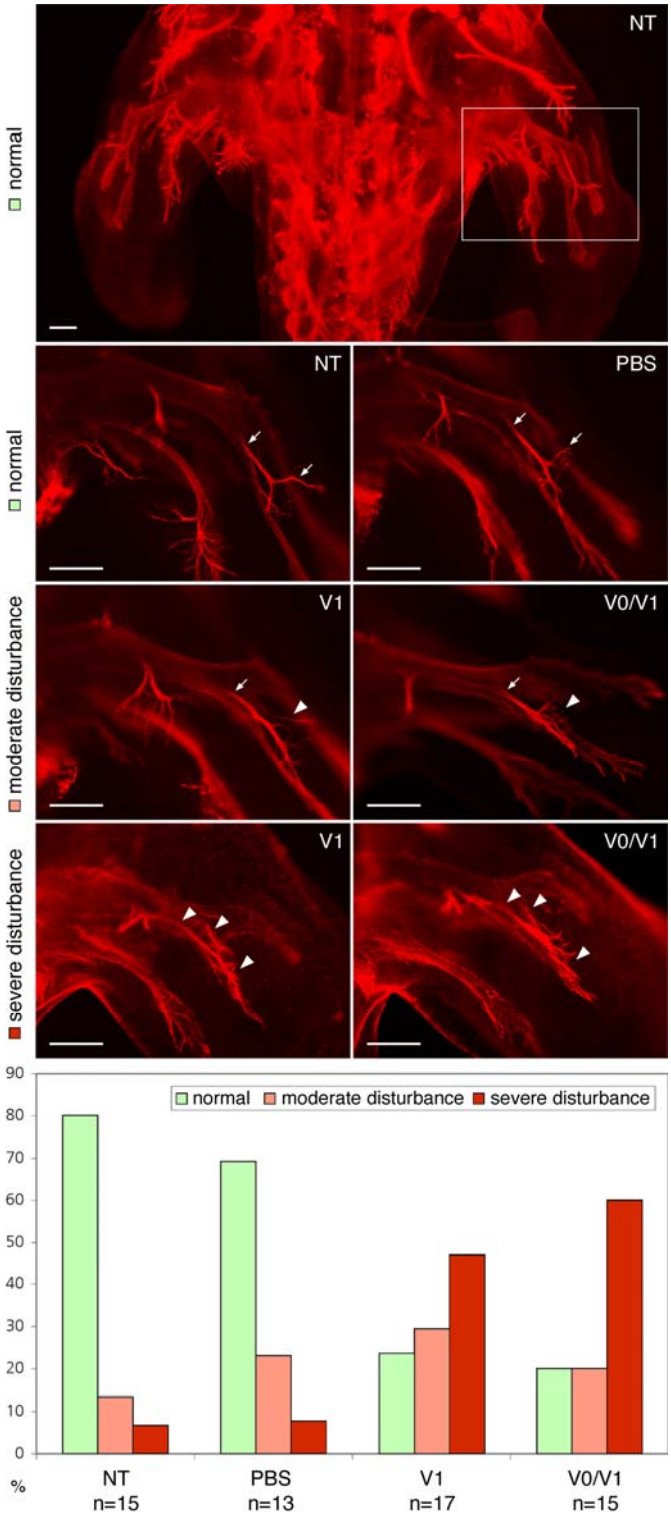

***M_Figure 9**. Consequences of ectopic deposition of versicans in developing chick hind limb in ovo.* Whole mount immunofluorescence stainings of neurofilaments in HH25 embryos injected beforehand with PBS, versican V0/V1- or versican V1-preparations into the hind limb are compared to not-treated controls (NT). The ectopic deposition of versican V0/V1 and V1 interferes with the normal growth, fasciculation and branching of secondary nerve fibers emerging from dorsal trunk of the sciatic plexus. Normal branch-points are indicated with arrows and aberrations with arrowheads (Bars: 200 µm). The proportions of normal, moderately and severely disturbed growth patterns were recorded in a blind study revealing the clear effect of the versican injections.

5. Identification of ADAMTS members in chick embryo: cloning and analysis of their expression patterns in developing hind limb.

5.I. Introduction

The development of a functional nervous system requires in all organisms from invertebrates to vertebrates a highly coordinated organisation for the establishment of a specific and precise neuronal network. During this process the axonal growth is tightly controlled by numerous attractive and repellent guidance cues, permitting the neuronal extensions to find their corresponding pathways and to reach their proper targets (reviewed in (Tessier-Lavigne and Goodman, 1996)). In the particular case of the hind limb innervation, the trajectories of motor and sensory axons follow a series of pathfinding decisions. The axons growing out from the spinal cord extend first to the base of the limb. On their way they pass through the dorsal-anterior sclerotome while they avoid the posterior halves of the somites and the perinotochordal mesenchyme (Tosney and Oakley, 1990). After reaching the plexus region, the motor- and sensory axons first stall for about 24 hours. During this waiting period, the extracellular matrix of the early hind limb, which acts as barrier to the growing axons, is being remodelled (Tosney and Landmesser, 1985). Once this has occurred, axons then are able to enter the proximal limb mesenchyme, where they are directed either ventrally or dorsally at the first choice point they encounter in this tissue (Ferguson, 1983; Whitelaw and Hollyday, 1983). Among the non-permissive components of the extracellular matrix, the chondroitin sulphate proteoglycan (CSPG) versican V0/V1 is present all along the border of the nerve tracks. Landolt et *al.* have shown that this hyalectan is at an early stage of chick development highly expressed in the entire hind limb (Landolt et al., 1995), being finally only concentrated within the precartilage mesenchyme starting from Hamburger and Hamilton stage 25 (HH25; (Hamburger and Hamilton, 1951)). In addition to the presence in axonal barrier tissues, the early versican V0/V1 expression co-localised also with boundaries to neural crest cell migration in the developing trunk.

The sequential disappearances of versican from the presumptive axonal pathways in the developing limb seems to be the result of an active proteolytic turn-over process, which may involve a novel family of metalloproteases, the ADAMTSs (a disintegrin and metalloprotease with thrombospondin type I motifs). These secreted enzymes are characterised by the presence of a zinc metalloproteinase domain and a C-terminal ancillary domain containing at least one thrombospondin type 1 repeat (reviewed in (Apte, 2009)). Some ADAMTS proteases, ADAMTS-1, ADAMTS-4, ADAMTS-5, ADAMTS-9 process a number of substrates within the ECM, including CSPGs such aggrecan and versican *in vitro* (Jungers et al., 2005; Kuno et al., 2000; Longpre et al., 2009; Rodriguez-Manzaneque et al., 2002; Sandy et al., 2001). Recombinant ADAMTS-1 cleaves versican at the Glu^{441}-Ala^{442} bond (Sandy et al.,

2001) and is widely expressed in embryonic tissues including the mesenchyme along the distal edge of the limb bud in mouse (Thai and Iruela-Arispe, 2002). During murine development ADAMTS-9 is expressed in several tissues and, for us of particular interest, within the developing limb bud (Jungers et al., 2005).

Consequently, we have focused our work on ADAMTS members, which might be involved in the turnover of versican and could this way contribute to the remodelling of the axonal growth-impeding ECM during the chick hind limb development. For this purpose, we first identified and cloned the cDNAs encoding the chick orthologues of ADAMTS-1 and ADAMTS-9. We then studied the expression of these two ADAMTSs by *in situ* hybridisation and we finally compared their distribution with the changing versican localisation in the leg anlage of chicken embryos between HH23 and HH27 stages.

5.II. Material and methods

5.II.1 Cloning of *ADAMTS1* and *ADAMTS9*

5.II.1.a Identification and assembling of chick ADAMTS1 and ADAMTS9 cDNAs

In order to clone the chicken *ADAMTS1* and *ADAMTS9* cDNAs, the described sequences of the human and mouse orthologues (access numbers: human *ADAMTS1* ENSG00000154734; mouse *ADAMTS1* ENSMUSG00000022893; human *ADAMTS9* ENSG00000163638; mouse *ADAMTS9* ENSMUSG00000030022) were compared to the partially completed genome sequences of the *Gallus gallus* project (release 36) annotated in the Ensembl Genome Browser. Based on the putative exon sequences at the two locations identified in the chick genome (chick *ADAMTS1*: ENSGALT00000025465; ENSGALP00000025419 chick *ADAMTS9*: ENSGALT00000011955), primers for RT-PCR amplification of the corresponding cDNAs were designed with Oligo6 software. Total RNA or mRNA prepared from primary cultures of chick fibroblasts or total RNA from head of HH38/39 chick embryos (Hamburger Hamilton stage 38/39) served as templates. To isolate total RNA and mRNA, Midi Easy Protect and Oligotex mRNA kits (both Qiagen) were used, respectively. Some of the cDNA fragments could be directly amplified from total RNA or mRNA preparations with a Qiagen One-Step Step RT-PCR kit (Table.2), while a two-step RT-PCR protocol was required to isolate the others. In this case, the mRNA preparations were first reverse-transcribed with AMV reverse transcriptase (Roche) and a specific reverse primers mix and then PCR amplified with Taq Gold polymerase (Roche) and a specific primer pair.

Table 2. Primers and conditions used to clone *ADAMTS1* and *ADAMTS9* cDNAs

	Fragment name	Primer name	Primer sequence	Annealing temp. °C	Product length bp	RT-PCR type	Template	Cycle number
ADAMTS1	1_ADAMTS1	1_cATS1 forward 1_cATS1 reverse	CTGGAGCTGGAGCCCGAC GCCCCGCAACGAGAAGG	62	207	one-step	total RNA chick fibroblasts	35
	2_ADAMTS1	2_cATS1 forward 2_cATS1 reverse	CCGGGAGACGACCTC CGGGGGCTGGAGACGAA	62	335	one-step	total RNA chick fibroblasts	40
	3-ADAMTS1	3_cATS1 forward 3_cATS1 reverse	CGCTGCGCCGTGACCGA GCAGACGAGCAGTCCTCCCGAA	68	915	one-step	total RNA chick fibroblasts	35
	4-ADAMTS1	4_cATS1 forward 4_cATS1 reverse	CCGGCACGCTGTATGAT CTAGGGCCTTCTCTGCTGA	66	1760	one-step	total RNA chick fibroblasts	35
ADAMTS9	1_ADAMTS9	1_cATS9 forward 1_cATS9 reverse	AGAAAGGGGCGAGAAAA CTGATGACGGCGGTGTG	58.6	586	two-step	mRNA chick fibroblasts	35
	2_ADAMTS9	2_cATS9 forward 2_cATS9 reverse	ACCGGGGGCACGTCAAC CACCAAAGTCGCCGACA	60	1174	one-step	total RNA chick embryo	35
	3_ADAMTS9	3_cATS9 forward 3_cATS9 reverse	TCATCAAGAACTTACGCT ATGTGCCACCTTAATTC	53.5	1325	one-step	total RNA chick fibroblasts	40
	4_ADAMTS9	4_cATS9 forward 4_cATS9 reverse	CAGCCCGACCCAATAA CTTCCCACACGTTGC	58	834	one-step	total RNA chick fibroblasts	35
	5_ADAMTS9	5_cATS9 forward 5_cATS9 reverse	AACAGTCCCGAAGCCAAG TCTCATCCACGCAGAAC	58.3	922	two-step	mRNA chick fibroblasts	35
	6_ADAMTS9	6_cATS9 forward 6_cATS9 reverse	GCAATGTGCAGGACTG CCTCTCCTCGGGTTTCA	61	530	two-step	mRNA chick fibroblasts	35
	7_ADAMTS9	7_cATS9 forward 7_cATS9 reverse	GTGCCTGACCAACG ACACTTCCCACAGTAACC	55.7	658	two-step	mRNA chick fibroblasts	35

Following steps and conditions were employed in the amplification experiments:

One-step RT-PCR: mRNA template (200 ng) or total RNA template (400 ng) from total embryo or chick fibroblast or chick embryo legs was added to 1x OneStep RT-PCR buffer, 400 µM dNTPs, 0.6 µM specific primers and 0.8 µl RT-PCR Enzyme mix in a 25 µl reaction volume (reverse transcription: 30 min at 50°C; inactivation of reverse transcriptase: 15 min at 95°C; cycling conditions: 1 min at 95°C, 1 min at the corresponding annealing temperature (Table.2), 1 min at 72°C; final extension for 10 min at 72°C).

Two-*step RT-PCR:* Reverse transcription was performed with 100 or 200 ng mRNA template, a mix of specific reverse primers at different ratios of primers to RNA (1/300, 1/1000 and 1/3000), 1X reaction buffer, 5 mM $MgCl_2$, 1 mM dNTPs, 1 µl RNAse Inhibitor (50U) and 0.8 µl AMV reverse transcriptase (20U) in a 25 µl total volume (annealing: 10 min at 25°C, reverse transcription: 60 min at 42°C, AMV inactivation and denaturation: 5 min at 99°C). Subsequent PCR-amplification from 60 pg to 3 ng chick cDNA template was done in a 25 µl reaction volume containing 1X buffer, 2.5 mM $MgCl_2$, 0.2 mM dNTPs, 0.2 µM primers, 1.25 U Taq GOLD Polymerase (initial denaturation: 10min at 95°C, cycling conditions: 1 min at 94°C, 1 min at annealing temperature, 1 min 30 sec at 72°C, final extension: 8 min at 72°C).

5.II.1.b Cloning, sequencing

The RT-PCR products were subcloned into pGEM ®T-Easy vector (Promega), propagated in XL_1 Blue Bacteria or Sure Bacteria strains (Invitrogen) and then Sanger sequenced and analysed with BLAST (Basic local alignment search tool) (http://blast.ncbi.nlm.nih.gov/Blast.cgi) to verify that no mutation artefacts were incorporated during PCR amplification.

The full length sequence of *ADAMTS9* was assembled from the overlapping cDNA fragments in a pGEM ®T-Easy vector. Briefly, the fragments were sequentially integrated into intermediate vectors using shared restriction enzyme sites. The vector A was constituted by ligation of the insert from the plasmid containing 3_ADAMTS9 and the vector containing 4_ADAMTS9, both previously digested with *NcoI* and *NruI* enzymes. The insert from the plasmid 1_ADAMTS9 and the plasmid 2_ADAMTS9, both digested with *SacII* and *BamHI* were ligated together in vector B. The predicted sequence coding for the last five TSP-1 submotifs presented some differences with what we obtained. For that reason, we first separately amplified the fragments 5_ADAMTS9 and 6_ADAMTS9. Afterwards, having functional primers in this region, we could obtain a long fragment corresponding to these two ones via One-Step RT-PCR (same conditions as described above, forward primer: 5_cATS9 forward; reverse primer: 6_cATS9 reverse; annealing temperature at 61 °C). The RT-PCR product was finally subcloned into a pGEM ®T-Easy vector, the vector C. The vector D was constituted of the insert from vector C and the plasmid containing the fragment 7_ADAMTS9, both double digested with *SacII* and *AvaI* restriction enzymes. Vectors B and D were put together in vector E via digestion with *SalI* and *BamHI* restriction enzymes. Finally, the vector E containing the 5' end and 3' end of the *ADAMTS9* cDNA was opened up with *BamHI* and the *BamHI* digested insert from the vector A containing the internal part of the sequence were ligated together into the vector F to obtain the full length *ADAMTS9* cDNA. Previous subsequent digestions, the vector C and the plasmid containing 7_ADAMTS9 fragment were digested with *EcoRI* restriction enzyme in order to have their sequences right oriented. The summary of the intermediate steps and the respective restriction enzymes used for the construction of the full length cDNA are presented in the figure 19 (table B).

To minimize the autoligation of the vector, each digested template used as host vector was dephosphorylated with 1 µl (150U) Bacterial Alkaline Phosphatase enzyme (Invitrogen) in 1X BAP buffer at 65°C for 1 hour in a 50 µl total volume and purified after agarose gel extraction. Then the ligation step was done at different ratios of vector to insert (2/5; 5/2;1/1) with 1 µl of the T4 ligase (10U) and 1X T4 ligase buffer (USB Europe) at 16°C for 16 hours in a 10 µl total volume.

A)

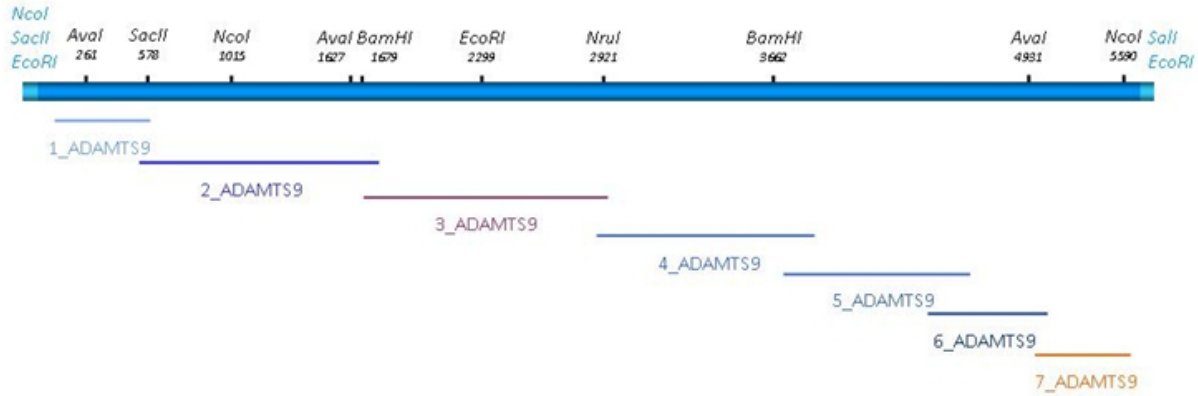

B)

Vector name	Assembled fragment	Restriction enzyme used for assembling
Vector A	3_ADAMTS9 (I) 4_ADAMTS9 (V)	*NcoI - NruI*
Vector B	1_ADAMTS9 (I) 2_ADAMTS9 (V)	*SacII - BamHI*
Vector C	5_ADAMTS9 6_ADAMTS9	via RT-PCR
Vector D	Vector C (I) 7_ADAMTS9 (V)	*SacII - AvaI*
Vector E	Vector B (V) Vector D (I)	*BamHI - SalI*
Vector F	Vector A (I) Vector E (V)	*BamHI*

C)

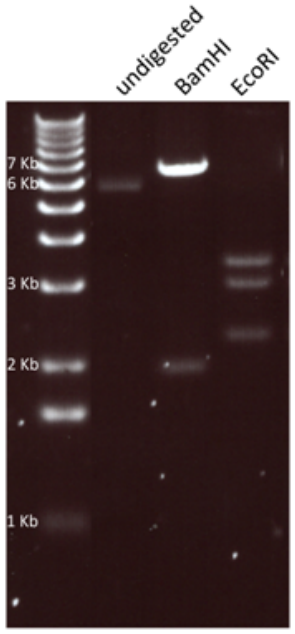

Figure 19. Cloning strategy for assembling the full length *ADAMTS9* cDNA.

A) Representation of the full length *ADAMTS9* cDNA integrated into the multiple cloning site (MCS) of the pGEM ®T-Easy vector.

The subcloned fragments are depicted under the schematic representation of the *ADAMTS9* cDNA into the pGEM ®T-Easy vector. The restriction enzyme sites used for the assembling of *ADAMTS9* full length are mentioned, in bright blue the cDNA coding for ADAMTS9 and in turquoise blue the Multiple Cloning Site of pGEM ®T-Easy vector are shown.

B) Table presenting the intermediate vectors generated in order to obtain the full length *ADAMTS9* cDNA.

The respective intermediate vectors and the different fragments are described, as well as the restriction enzymes used to obtain vector (V) and insert (I) parts.

C) Agarose gel representing digestion analysis of chick *ADAMTS9* cDNA cloned into pGEM ®T-Easy vector.

The undigested plasmid containing 8.7 Kb ran around 6 Kb corresponding to the circular form of the vector. After digestion, the vector was cut into two fragments (6.7 Kb, 2 Kb) and into three fragments (3.3 Kb, 3 Kb, 2.37 Kb) with *BamHI* and *EcoRI* restriction enzymes, respectively.

5.II.2 Distribution of chick *ADAMTS1* and *ADAMTS9* transcripts, localisation of versican in chick hind limb during development

5.II.2.a Preparation of the probes

For expression analysis of *ADAMTS1* and *ADAMTS9*, specific digoxygenin-labelled riboprobes were prepared from parts of the cloned cDNAs (Table.3). Briefly, plasmids containing cDNA fragment of interest were used as templates. Primer pairs with one primer carrying at the 5'end the T7 promoter sequence were designed and used to generate modified cDNA fragments by PCR. The PCR products were used as templates to produce DIG-labelled riboprobes with the DIG-labelling kit SP6/T7 (Roche Applied Science). 1 µg of each cDNA was mixed with 5 µl DIG RNA labelling mix (10 mM NTP), 5 µl 10x transcription buffer, 2.5 µl Protector RNase Inhibitor, 5 µl RNase polymerase T7 and RNase-free water up to a final volume of 50 µl. After incubation for 2 h at 37°C, the cDNA was eliminated by addition of 5 µl RNAse free DNAse I for 15 min at 37°C. The reaction was stopped by adding 5 µl EDTA (0.2 M). The cRNA probes were precipitated with 7.5M LiCl and dissolved in 50 µl of DEPC-treated H_2O.

Table 3. Primers used for preparing templates *in situ* hybridisation (ISH) riboprobes

	Primer name (ISH probe prep)	Primer sequence	Probe
ADAMTS 1	ISH_cATS1 forward	TGCGTGAAGGCTGGCTGT	ADAMTS1 anti-sense
	T7_ISH_cATS1 reverse	CGAAATTAATACGACTCACTATAGGGAGACGGTTTCTTGGAAGGCTC	
	T7_ISH_cATS1 forward	CGAAATTAATACGACTCACTATAGGGAGATGCGTGAAGGCTGGCTGT	ADAMTS1 sense
	ISH_cATS1 reverse	CGGTTTCTTGGAAGGCTC	
ADAMTS 9	ISH_cATS9 forward	ACCGGGGGCACGTCAACG	ADAMTS9 anti-sense
	T7_ISH_cATS9 reverse	CGAAATTAATACGACTCACTATAGGGAGATCCTTCGGGGTGGTTCTG	
	T7_ISH_cATS9 forward	CGAAATTAATACGACTCACTATAGGGAGAACCGGGGGCACGTCAACG	ADAMTS9 sense
	ISH_cATS9 reverse	TCCTTCGGGGTGGTTCTG	

5.II.2.b Preparation of tissue sections

Chicken embryos were collected at indicated embryonic HH-stages and dissected in PBS. After fixation in 4 % paraformaldehyde (PFA) in PBS for 1 to 2 h at room-temperature, the embryos were cryoprotected in 25% sucrose PBS over-night at 4°C. The cryo-protected embryos were embedded in Tissue-Tek OCT freezing compound (Sakura). 20 µm thick transversal sections were cut, mounted on SuperFrost Plus microscope slide (Menzel-Glaeser) and stored at -20°C until further use.

5.II.2.c In situ hybridisation (ISH)

The slides were dried for 10 min at room-temperature, post-fixed for exactly 30 min in 4% PFA in PBS, rinsed twice in PBS and once in H_20 for 5 min each. They were then acetylated for 10 min in 1% triethanolamine containing 0.25% acetic anhydride (vol/vol),

rinsed twice in PBS for 5 min and once in 2X SCC (0.3 M NaCl, 0.03 M tri-sodium citrate, pH 7) for 5 min. To block unspecific binding, the sections were pre-treated in hybridisation buffer (5X Denhardt's solution, 250 ug/ul yeast tRNA, 500 ug/ml herring sperm DNA, 5X SCC, 50% formamide) for 3 h. Finally, the hybridisation was done by incubating 600 ng riboprobe diluted in 300 µl hybridisation buffer per slide for at least 15 h. Both, prehybridisation and hybridisation were done at 56°C in humidified chamber. To avoid evaporation, slides were covered with a parafilm previously treated with 7% H_20_2 in H_20.

The hybridisation was followed by successive washings in 5X SSC (one short rinse and then another incubation for 5 min), in 2X SSC once for 5 min and in 0.25X SSC / 50% formamide for 20 min (all at 56°C). Finally, the slides were rinsed briefly in 0.2X SSC at room-temperature.

For probe detection, the sections were equilibrated in detection buffer containing 0.1 M tris-base, 0.15 M NaCl, pH 7.5 (2 incubations for 5 min each) and then incubated for 1 h in blocking buffer (detection containing 3% dry milk). These and all subsequent steps were done at room-temperature. The sections were next incubated for 1 h in blocking buffer supplemented with anti-DIG-AP Fab fragments polyclonal antibody (Roche) at a dilution of 1:5000. After this binding step, the preparations were rinsed by dipping shortly into detection buffer followed by two washings in the same buffer for 15 min. They were next equilibrated in 1X alkaline phosphatase (AP) buffer (0.1M Tris-base, 0.1M NaCl, 50 mM $MgCl_2$, pH 9.5). Afterwards the sections were covered with developing solution prepared by mixing equal volumes of Celvol 205 Polyvinyl alcohol (Celanese Chemicals) and 2X alkaline phosphatase (AP) buffer containing 100 mM $MgCl_2$, 337.5 µg/ml nitroblue tetrazolium (NBT; Roche), 175 µg/ml 5-bromo-4-chloro-3-indoyl- phosphate (BCIP, Roche), and 240 µg/ml levamisole (Sigma). Protected from light, the slides of the *ADAMTS1* and the *ADAMTS9* hybridisations were then incubated for 20 h and 16 h, respectively, until the colour reaction was stopped in TE buffer (one short dip and two 15 min washings). Finally, the sections were rinsed in H_20 before being cover-slipped with an aqueous mounting medium (Celvol). All the solutions used for pre- and hybridisation steps were prepared in RNase free-conditions. All developmental stages were processed identically.

5.II.2.d Immunofluorescence staining

Double immunofluorescence staining was done on embryo sections successive to the sections previously subjected to ISH. The cryo-sections were prepared as described above. Rabbit serum against chick GAG-β domain versican previously prepared in our laboratory (Landolt et al., 1995) and mouse monoclonal antibody RMO-270 against neurofilament-160kD (anti-NF_M; Invitrogen) were diluted in blocking buffer (0.2% gelatine, 0.5% BSA, 0.02% azide sodium in PBS) to 1:500 and 1:2000, respectively. Secondary antibodies used

in these stainings were goat anti-rabbit Alexa 488 and goat anti-mouse Alexa 594 (both Invitrogen) diluted to 1:200 in PBS. The cryo-sections were first dried for 15 min at room-temperature, then post-fixed in 4% PFA for 30 min, rinsed once shortly and then washed twice for 10 min in PBS. They were subsequently blocked in blocking buffer for 40 min at room-temperature and incubated with the primary antibody-mix (500 µl /slide) for at least 16 h at 4°C. Next, they were washed three times in PBS for 5 min and incubated with the secondary antibody-mix for 1 h under light protection (all at room-temperature). The sections were then rinsed again in PBS before counterstaining with Hoechst H33258 nuclear dye. After three washings in PBS for 5 min each, the sections were cover-slipped with fluorescence mounting medium (Dako).

5.II.2.e Immunofluorescence pictures and in situ hybridisation images

The ISH sections were scanned with the NanoZoomer 2.0 scanner (Hamamatsu). The images were similarly adjusted for brightness and contrast in Photoshop CS4. The immunofluorescence pictures were taken with an Olympus BX61 microscope coupled to an F-view camera. Red, green and blue channels were collected separately. The image analysis was done with the AnalysiSIS Pro software (Soft Imaging System, Germany). The contrast and brightness of the channels were similarly adjusted and the images were overlaid in Photoshop CS4.

5.III. Results

5.III.1 Identification and cloning of chick ADAMTS1 and ADAMTS9 cDNAs

The well characterised cDNA sequences of human and mouse *ADAMTS1* and *ADAMTS9* were used to identify orthologous sequences in the provisory *Gallus gallus* genome data base. The sequence alignments formed the basis to set-up PCR-approaches for their cloning.

5.III.1.a Chick ADAMTS1

In a first set of RT-PCR experiments with RNA from chick embryonic fibroblasts, we initially amplified two overlapping fragments containing in total 1653 bp of the chick ADAMTS1 cDNA including the translational stop codon. In subsequent RT-PCR rounds, we could extend this sequence towards the 5’ end by amplifying two smaller fragments, which covered an additional 422 bp of the cDNA sequence. The most 5' part of the coding sequence eluded amplification, however, even after multiple attempts employing random and specifically primed cDNA preparations as well as genomic DNA as PCR templates. Yet, the cDNA confirmed by our experiments encoded most of the pro-peptide and the entire

sequence of the mature enzyme. Some differences were observed with the predicted sequence in the Ensembl data base (Fig.20).

Figure 20. Putative cDNA and deduced peptide sequence of chick ADAMTS1.
The putative ADAMTS1 cDNA was assembled by aligning the Ensembl sequences of the predicted chick gene, the chick cDNA and the transcript of the human orthologue. The cloned and confirmed cDNA sequence is typed in black font. Italic letters indicate the 5' and 3' UTR regions. Putative sequences not covered by our clones are written in pink letters. Variations to the Ensembl sequences are depicted by blue characters (positions 677, 704, 1049, 1685, 1901 and 2108; all silent mutations). The position of a deletion (gccaga) observed in our cloned cDNA is marked by an asterisk. The yellow highlighted nucleotides display a two-basepair insertion in the 3'UTR. The amino sequence deduced from chick ADAMTS1 peptide (922 residues) is depicted below the cDNA sequence. The predicted signal peptide is indicated in bold font. Single-letter amino acid codes are used.

The sequences of our cloned cDNA fragments were confirmed by analysing independent RNA preparations from different embryos. Furthermore, sequence alignments of the fragments to ADAMTS1 cDNAs of other species with the Clustal W2 program (http://www.ebi.ac.uk/Tools/clustalw2/index.html) validated the specificity and accuracy of our isolated chick cDNA clones. The putative chick ADAMTS1 cDNA shared 69% identity with the human and 57% with the mouse orthologues. The deduced peptide sequence showed an even closer relationship (73% identity with human ADAMTS1 peptide and 72% with the murine orthologue). The comparison of the peptide sequence of the catalytic domain

revealed finally the highest similarity with an 82% and 78% identity with the corresponding domains in human and murine ADAMTS1, respectively (Fig.21).

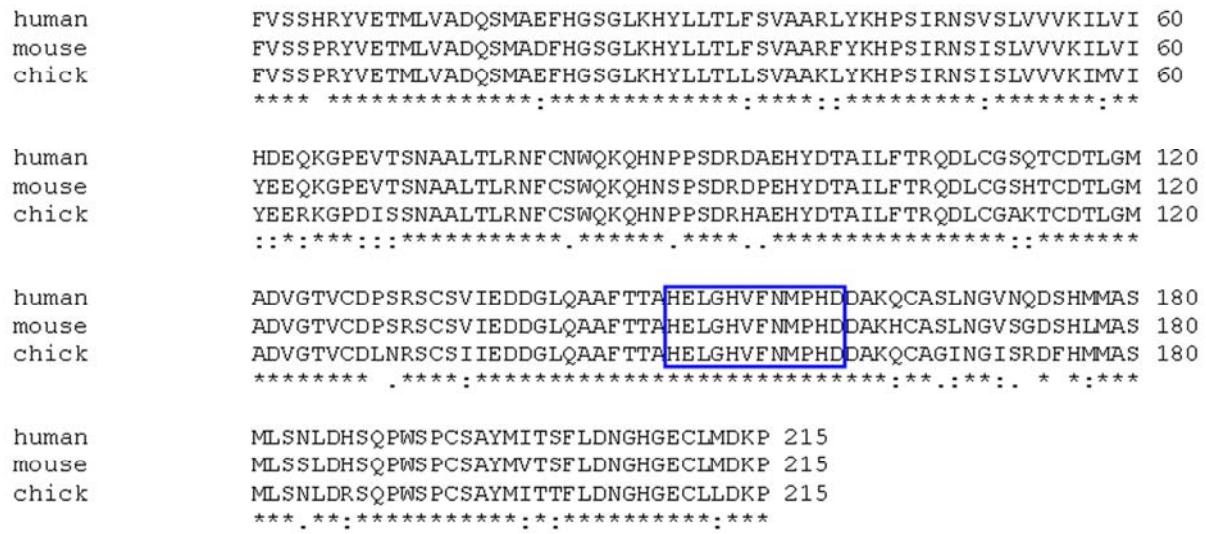

Figure 21. Comparison of the catalytic domains of human, mouse and chick ADAMTS1.
The amino sequences of the catalytic domains of ADAMTS1 in human, mouse and chick were aligned. The chick catalytic domain exhibits 82% and 78% identity with the human and mouse domains, respectively. The active site is indicated by a blue box.

5.III.1.b Chick ADAMTS9

The cDNA of chick ADAMTS9 was cloned in seven fragments (1_ADAMTS9 to 7_ADAMTS9). These overlapping fragments covered the entire open reading frame. Similar to the ADAMTS1 cDNA, the ADAMTS9 cDNA clones differed slightly from the predicted Ensembl sequence (Fig.22). In particular, the coding sequence for the TSP like 1 motifs close to the 3'- end lacked 332 nucleotides encoding the TSP-1 domain 12 and the C- or N-terminal halves of the TSP-1 repeats 11 and 13, correspondingly. The absence of these structural elements was confirmed by analysing multiple sub-clones originating from diverse embryo RNA templates. Consequently, the chick ADAMTS9 from embryonic fibroblasts contains only thirteen thrombospondin type-1 repeats instead of fifteen as described for the human and mouse orthologues.

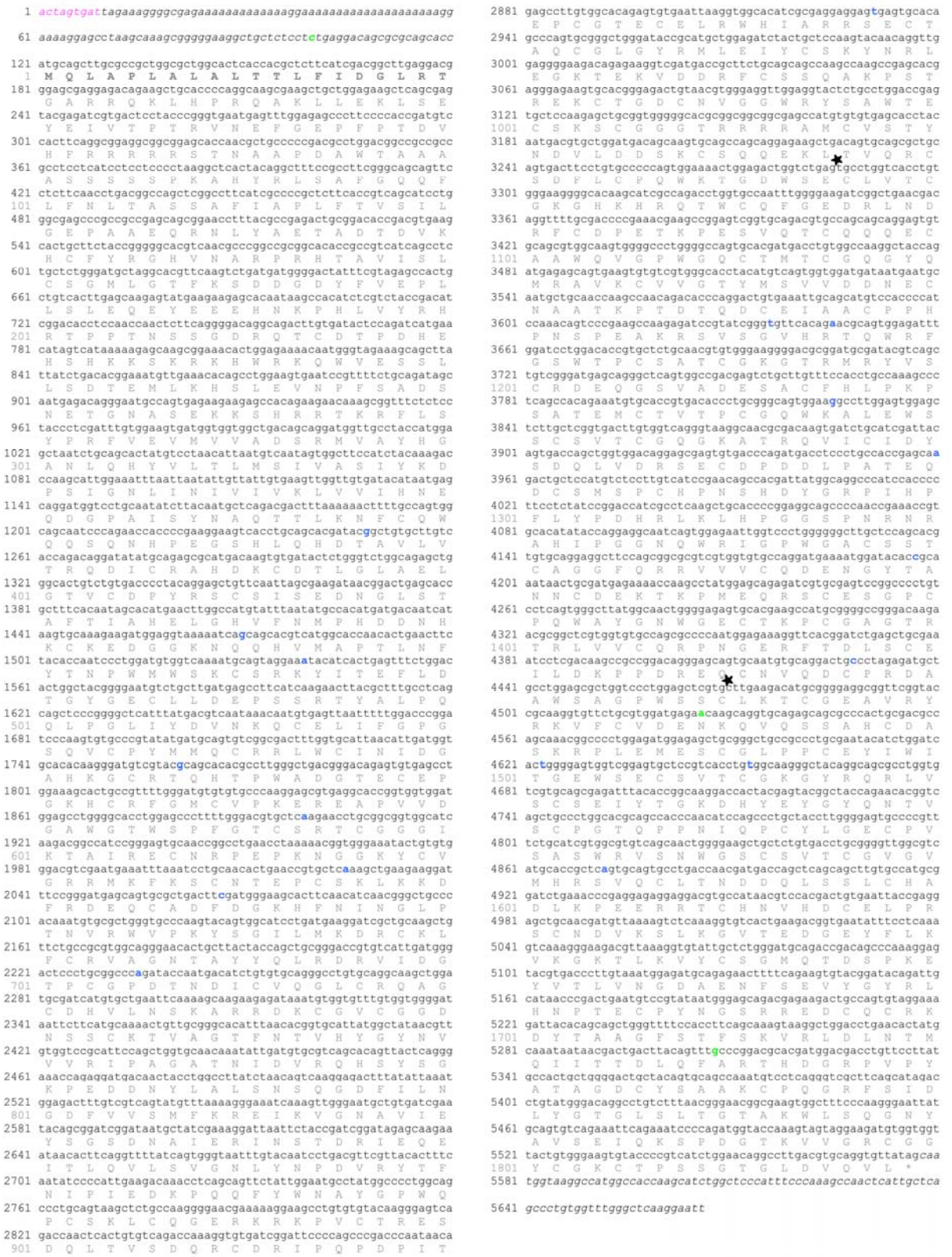

Figure 22. cDNA and deduced peptide sequence of chick ADAMTS9.

The ADAMTS9 cDNA was assembled by aligning the Ensembl sequences of the predicted chick gene, the chick cDNA and the transcript of the human orthologue. The cloned and confirmed cDNA sequence is typed in black font. Italic letters indicate the 5' and 3' UTR regions. A portion of the 5'-UTR not covered by our clones is written in pink letters. Synonymous mutations are depicted by blue characters (positions 1248, 1470, 1539, 1761, 1899, 2025, 2067, 2235, 2931, 3636, 3645, 3825, 3960, 4197, 4428, 4623, 4653, 4872; all silent mutations), while non-synonymous variations (positions

4526, 5308) also found in the Ensembl chick genome project and a mutation in the 5'UTR (position 100) are marked in green. Deletions indicated by an asterisk at positions 3285/3286 (ccctggcag) and 4469/4470 were observed only in our cloned cDNA, but were not described in the Ensembl prediction. The 332 bp-stretch, which is absent at position 4469/4470 (asterisk), corresponds to the sequence encoding the TSP-1 repeat number 12 and half of the domains 11 and 13 of the human orthologue. The amino acid sequence deduced from chick ADAMTS9 peptide (1818 residues) is depicted below the cDNA sequence. The predicted signal peptide is indicated in bold font. Single-letter amino acid codes are used.

The chick ADAMTS9 shared at the cDNA and peptide levels 72% and 77% identity, respectively, with the human orthologue or 71% and 75% identity with the mouse orthologue. Although the chick catalytic domain was highly similar to the human and mouse enzymes (80 and 81% identity, respectively), it included an insertion of two amino-acids and other minor variations within this element. The active site, however, was completely conserved (Fig.23).

```
human           FLSYPRFVEVLVVADNRMVSYHGENLQHYILTLMSIVASIYKDPSIGNLINIVIVNLIVI 60
mouse           FLSYPRFVEVMVVADHRMVLYHGANLQHYILTLMSIVASIYKDSSIGNLINIVIVNLVVI 60
chick           FLSYPRFVEVMVVADSRMVAYHGANLQHYVLTLMSIVASIYKDPSIGNLINIVIVKLVVI 60
                **********:**** *** *** *****:*************.***********:*:**

human           HNEQDGPSISFNAQTTLKNFCQWQHSKNSPGG--IHHDTAVLLTRQDICRAHDKCDTLGL 118
mouse           HNEQEGPYINFNAQTTLKNFCQWQHSKNYLGG--IQHDTAVLVTREDICRAQDKCDTLGL 118
chick           HNEQDGPAISYNAQTTLKNFCQWQQSQNHPEGSHLQHDTAVLVTRQDICRAHDKCDTLGL 120
                ****:** *.:*************:*:*   *  ::******:**:*****:********

human           AELGTICDPYRSCSISEDSGLSTAFTIAHELGHVFNMPHDDNNKCKEEGVKSPQHVMAPT 178
mouse           AELGTICDPYRSCSISEDSGLSTAFTIAHELGHVFNMPHDDSNKCKEEGVKSPQHVMAPT 178
chick           AELGTVCDPYRSCSISEDNGLSTAFTIAHELGHVFNMPHDDNHKCKEDGGKNQQHVMAPT 180
                *****:************.**********************.:****:* *. *******

human           LNFYTNPWMWSKCSRKYITEFLDTGYGECLLNEPESRPYPLP 220
mouse           LNFYTNPWMWSKCSRKYITEFLDTGYGECLLNEPASRTYPLP 220
chick           LNFYTNPWMWSKCSRKYITEFLDTGYGECLLDEPSSRTYALP 222
                ******************************:** **.*.**
```

Figure 23. Comparison of ADAMTS9 catalytic domains in human, mouse and chick.
The amino sequences of the catalytic domains of ADAMTS9 in human, mouse and chick were aligned. The chick catalytic domain shows 80% and 81% identity with the human and mouse domains, respectively. The active site is indicated by a blue box. The presumed chick catalytic domain is two residues longer than the human or mouse counterpart.

The location of the overlapping cDNA clones and the modular organisation of the deduced peptide sequences of chick ADAMTS1 and ADAMTS9 are shown in figure 24.

A)

Chick ADAMTS1

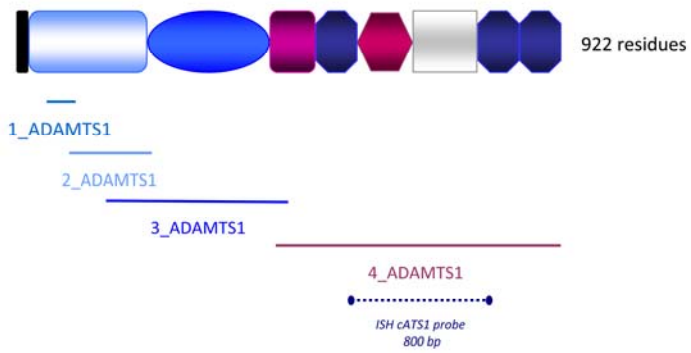

B)

Chick ADAMTS9

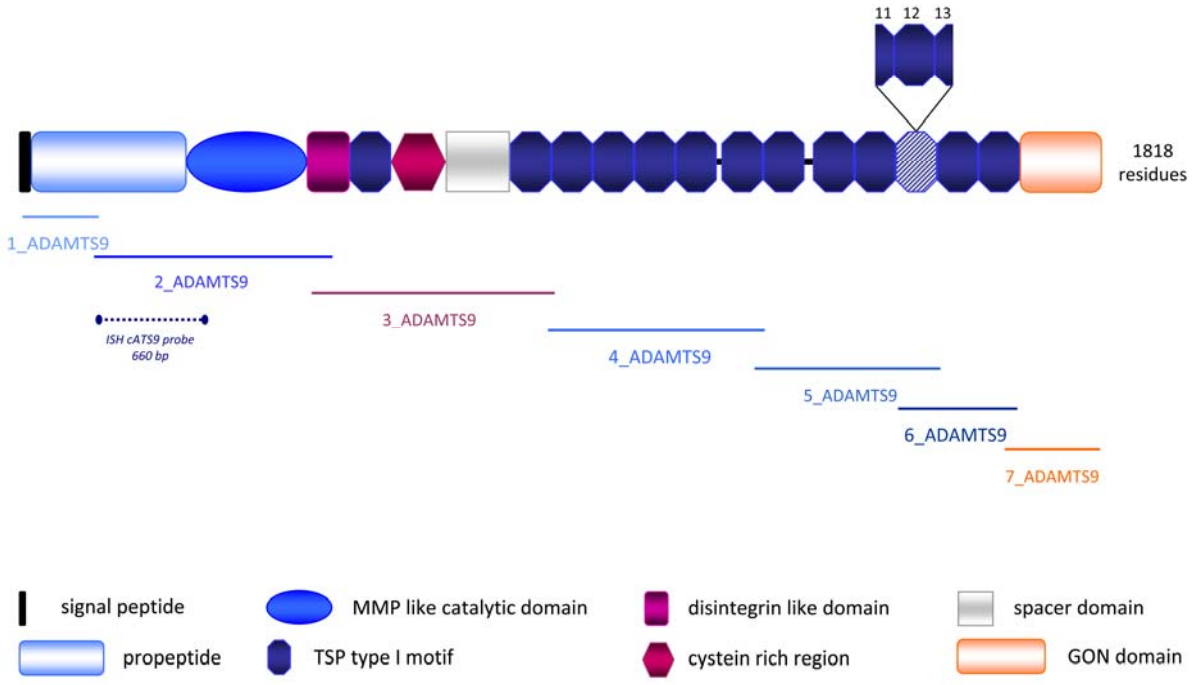

Figure 24. Schematic representation of cloned PCR-fragments of chick ADAMTS1 and ADAMTS9 cDNAs and the domain structures of the deduced peptides.
The fragments for chick ADAMTS1 (A) and ADAMTS9 (B) cDNAs are aligned to the peptide domains they encode. The chick ADAMTS9 characterised in our cloning experiments lacks two TSP type-1 motifs in relation to the human and mouse orthologues (see insert). The positions of the riboprobes employed in our *in situ* hybridisations are represented by a dotted line.

5.III.2 Distribution of chick ADAMTS1 and ADAMTS9 transcripts

Previous studies in man and mouse described the expression of ADAMTS1 and ADAMTS9 in some adult and embryonic tissues. During mouse embryogenesis, the

expression patterns of both enzymes appeared rather wide and mostly complementary to each other being present in developing organs such as lung, heart and kidney as well as in different mesenchymal tissues including the limb buds (Jungers et al., 2005; Thai and Iruela-Arispe, 2002). However, despite indications that both enzymes exert some proteolytic activity towards versicans (Somerville et al., 2003), no comparative analysis of ADAMTS1 and ADAMTS9 expression in relation to the versican turnover have been described so far. Hence, we focused our ADAMTS expression studies on the developing hind limb, where the rapidly changing distribution of versicans inversely correlates with the routes taken by peripherally extending axons (Landolt et al., 1995). For our developmental expression studies, we chose the chicken as model organism because of obvious advantages in regard to easy timing and accessibility of differently staged embryos. The initial *in situ* hybridisations detecting ADAMTS1 and ADAMTS9 mRNAs were performed on embryos staged between HH23 to HH27.

The transcripts of the two enzymes were both found in chick limb anlage, but not at the same development stages and not at the same level of expression (Fig.25 and 26). Surprisingly, ADAMTS1 mRNA was only minimally present in chick embryos at early stages of development. No expression was detectable at HH23. Later from HH25, the staining was weakly visible in the neural tube and in DRG, in the dermomyotomes and also in the hind limb bud, where it was found primarily around the condensing mesenchyme of the cartilage primordia (Fig.25B and C).

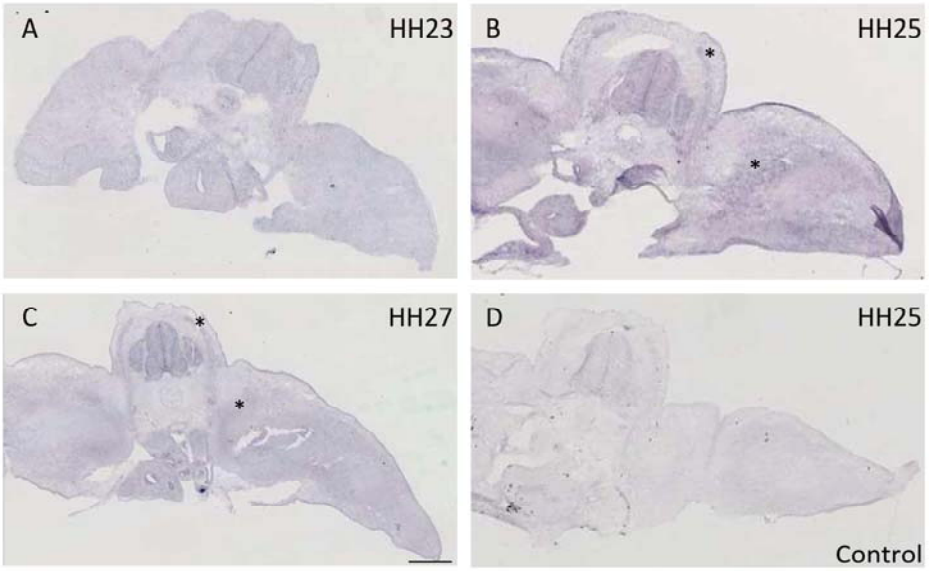

Figure 25. ADAMTS1 is weakly expressed in hind limb of chick embryo during early development.
The expression patterns of ADAMTS1 transcripts were analysed by *in situ* hybridisation on 20 µm cryosections of chick embryos. No expression of ADAMTS1 was observable at HH23 stage (A). At HH25 a weak expression was detectable in the dermomyotomes and in the centre of the limb mesenchyme (B, asterisk). This staining was slightly more pronounced at HH27 (C, asterisk). Panel D shows a control section of an HH25 embryo hybridised with the corresponding sense probe. Scale bar: 200 µm.

In contrast, ADAMTS9 mRNA expression initiated already around HH23 in the dermomyotomes and became at the level of the hind limbs more prominent at later stages (Fig.26D). At HH25 the staining was particularly noticeable in the pelvic girdle precursor and in the dermomyotomes (Fig.26E). Finally, at HH27 a well defined signal detected ADAMTS9 expression within the connective tissue localised between the epidermis and the precartilage mesenchyme of the hind limb (Fig.26F).

Double immunofluorescence staining for versican V0/V1 and neurofilaments on sections successive to the ISH displayed a complementary distribution of versican protein and ADAMTS9 mRNA, while the neurofilament-positive axons were absent from versican-rich mesenchymal areas extending exclusively into the ADAMTS9 expressing zone. In detail, at an early stage of development (HH23), when ADAMTS9 expression is mainly absent, versican is abundant in the entire limb bud (Fig.26G) and to a lesser extent around the notochord and the neural tube. At this time, axons have extended into the plexus region, but are restrained from entering the limb bud (Fig.26J). Around HH25, the proteoglycan progressively disappears from the connective tissue of the limb (Fig.26H) and is, except for the pelvic girdle precursor and other prechondrogenic areas, finally cleared from the future axonal pathways (HH27; Fig.26I). During this period, ADAMTS9 is consistently expressed in the mesenchymal zones that loose the versican immunostaining (Fig.26E and F). Until HH27 the axons have invaded the base of the limb, they have bifurcated into a ventral and dorsal branch and they continue to grow along ADAMTS9 expressing versican-free zones that border the condensing mesenchyme of the cartilage and bone primordia (Fig.26L).

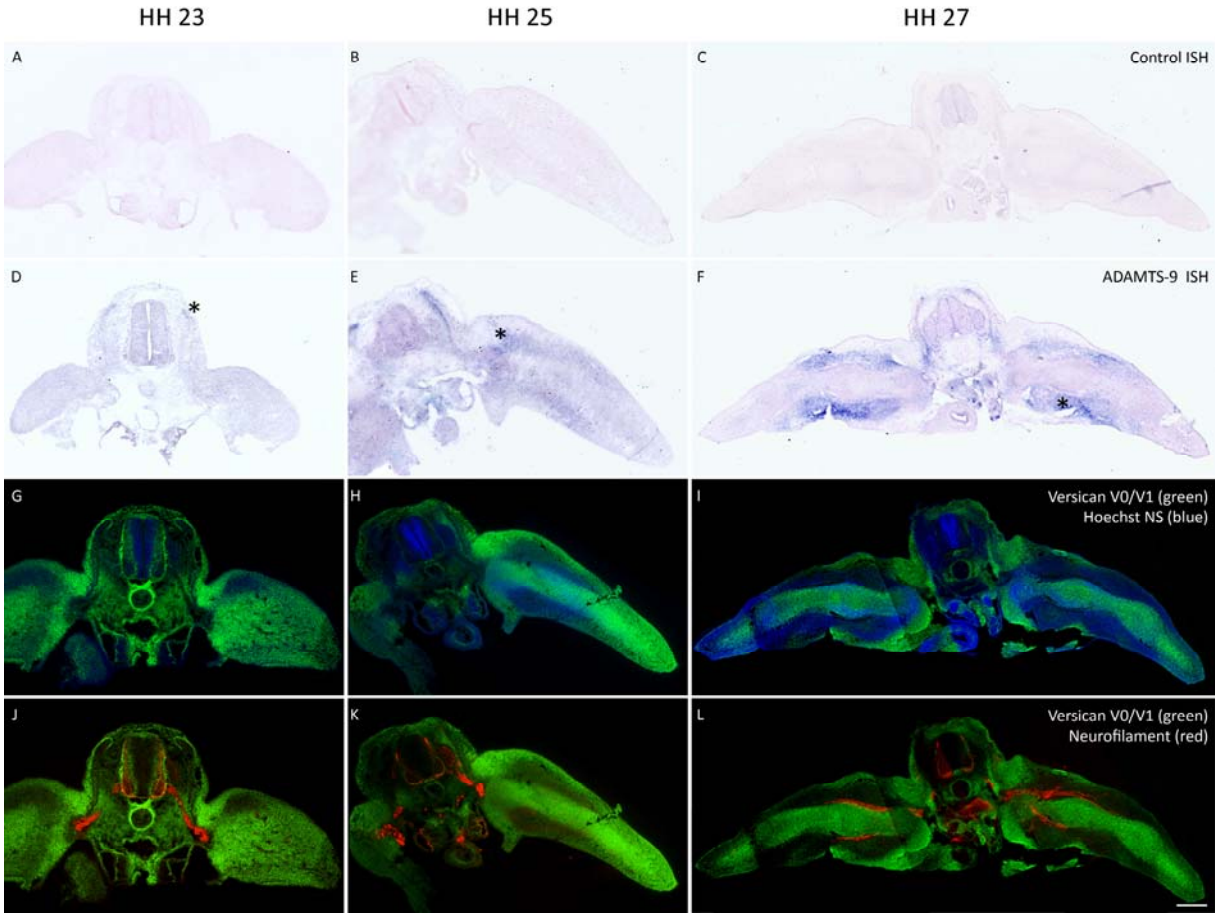

Figure 26. Modulated expression of ADAMTS9 in correlation with the versican disappearance and the extension of axons in chick limb bud during development.
Distribution of the ADAMTS9 expression detected by *in situ* hybridisation (ISH) in chick embryos at HH23 (D), HH25 (E), HH27 (F) and comparison with the localisation of versican V0/V1 and neurofilaments at the respective stages by double immunofluorescence (Cifuentes-Diaz et al.) stainings (HH23: G, J; HH25: H, K; HH27: I, L, respectively). Panels A, B, C show the corresponding sense probe control for the ADAMTS9 ISH. Successive 20 µm cryosections from the same embryos were processed for ISH labelling and IF staining.
ADAMTS9 expression is detectable in the dermomyotomes starting from HH23 (D, asterisk). Between HH25 and HH27, it becomes more prominent in the dorsal and ventral mesenchyme near the pelvic girdle precursor (E, asterisk) and along the prechondrogenic condensations of the leg bone primordia (F, asterisk).
Versican is rather uniformly distributed in the limb bud of chick embryos at HH23 stage (G). It subsequently disappears from the dorsal and ventral mesenchyme (H) being finally restricted to the prechondrogenic areas and a narrow subepidermal zone within the developing hind limb (I). Motoraxons growing out from the neural tube and sensory axons extending from the DRG join and invade the limb in areas that are cleared from versican (J, K, L). Scale bar: 200 µm.

In summary, the temporospatial expression patterns indicate, that ADAMTS9 expression may function in the control of hind limb innervation, whereas an involvement of ADAMTS1 in this process appears rather unlikely. The ADAMTS9 expression correlates well with areas of versican clearance and outlines zones of future axonal growth in the limb.

5.IV. Discussion

In the course of development, different timely and spatially coordinated processes have to occur to allow the neuronal network to be correctly formed. One of these crucial events consists in the specific remodelling of an originally non-permissive extracellular matrix in order to permit axonal growth along precisely delineated pathways. In this project, we were particularly interested in the potential link between the turnover of versican and the expression of distinct ADAMTS proteases in the embryonic hind limb during chick peripheral nervous system development. Indeed, steadily accumulating evidence has supported the hypothesis that, among the components present in axonal barrier tissues, versican may take an active part in the guidance of growing axons by acting as non-permissive guidance cue. On one hand, the isoforms V0/V1 co-localised with the barrier tissues in chick embryos, while growing axons move forward along paths freed from this hyalectan (Landolt et al., 1995). On the other hand, isolated versicans are potent axonal growth inhibitors *in vitro* and *in ovo* (Schmalfeldt et al., 2000; Dutt et al. see part IV of this thesis). Furthermore, also early neural crest stem cells migration is inhibited by versicans in stripe-choice assays *in vitro* (Dutt et al., 2006). All these inhibitory functions seem to emanate from the core glycoprotein. The blocking capacity of various boundary tissues in the limb anlage is temporally restrained suggesting that the non-permissive properties of versican are accurately modulated alongside. Prime candidates for regulating the activity of versicans are different members of the ADAMTS metalloprotease family, which exert various levels of hyalectanase activity. Consequently, we have directed our main focus on ADAMTS1 and ADAMTS9, which are widely expressed in mouse embryos (Jungers et al., 2005; Thai and Iruela-Arispe, 2002) and have been described to cleave versican *in vitro* (Sandy et al., 2001; Somerville et al., 2003).

To investigate the expression patterns of ADAMTS1 and -9 during the crucial phases of limb innervation, we started with the full-length cDNA cloning of the chick orthologues of the known human and mouse proteases. Comparisons of sequences of our chick cDNAs clones with the predicted sequences from the chick genome project and with the published human and mouse sequences displayed one major and several minor deviations. Some of the differences to the chick gene predictions might be explained by certain sequence errors in the database, which currently is incomplete and has not yet been manually curated. Even after the release of multiple updates during the elaboration of this study, the published sequences still appeared only partly accurate. Especially the predicted Exon I of the chick ADAMTS1 gene, theoretically including the 5' UTR and the translational start codon, could only be aligned for a minimal stretch with its human counterpart. A putative start codon was listed in the annotation, but a suitable sequence carrying the Kozak sequence was missing and no TATA box could be identified in the predicted sequence. We therefore tried to circumvent this problem by manually aligning an upstream sequence in the chick Exon I with

the well-described human and mouse ADAMTS1 sequences. In spite of the extensive testing of the selected guessmer primers under different RT-PCR conditions, we were still not able to completely elucidate the sequence corresponding to the 5'UTR of chick ADAMTS1. Nevertheless, even if the 5'- end of the chick ADAMTS1 cDNA is missing in our overlapping cDNA clones, it most likely lacks only a small portion at the 5'- end, which encodes the translational start codon, the secretory signal sequences and less then 20 N-terminal amino acids of the propeptide, but it contains the entire open-reading frame of the mature enzyme. In addition, we observed in our ADAMTS1 cDNA six silent mutations and one in frame-deletion of six nucleotides in the translated part. Since the current annotation in Ensembl seems to be based on only a few genomic sequences and is not derived from a large cohort of different chicken breeds, it seems likely that the variations observed in our cDNAs reflect natural polymorphisms.

The sequence of our chick ADAMTS9 cDNA clones, coding for the whole proenzyme, showed apart from annotated SNPs and hitherto unknown silent single nucleotide exchanges one major difference in comparison to the gene sequence published in the Ensembl database. Two predicted exons (29 and 30) were consistently skipped in our cDNA fragments independent of the embryonic RNA preparations tested. In consequence, our cloned cDNA is two TSP-1 motifs shorter than the predicted chick ADAMTS9 and to the curated human and mouse orthologues. Due to the genomic constellation the N-terminal half of the TSP-1 repeat 11 and the C-terminal half of the repeat 13 are fused, while the stretch in between is lacking. The shortened ADAMTS9 in chicken may either correspond to a not yet described splice-variant or may reflect a particularity of the chick HISEX breed or the chick genome in general, although the splice donors and receptors of the skipped exons appeared intact in the gene annotation. Further screening of different breeds coming from different hatchery should be performed in order to confirm this observation. Finally, another much smaller deletion was observed at position 3285/3286 affecting a nonamer sequence, which was duplicated in the Ensembl gene prediction.

The chick genome annotation misses currently parts of the promoter region including the canonical TATA box, which was identified in the human gene, and around 30 bp of the transcribed portion up to the transcription initiation site (Yaykasli et al., 2009). Besides, the promoter sequence described in Ensembl for the chick ADAMTS9 promoter contains at least one putative binding site for the transcription factor, Nuclear Factor of Activated T cells (NFAT), with the consensus sequence (GGAAA) (Rao et al., 1997). In order to be able to analyse the regulation of the ADAMTS9 gene in detail and to establish a relation to the control of versican gene expression, the identification and cloning of the entire promoter would be required, however. Whether the chick ADAMTS9 expression is regulated by cytokines via the NFATc1 transcription factor, as described for human chondrocytes

(Yaykasli et al., 2009), would have to be first verified, but may have consequences for the turnover of versican and/or aggrecan during morphogenesis and inflammatory process as arthritis.

Finally, the primary structures deduced from the cloned cDNAs of both, chick ADAMTS1 and ADAMTS9, contained the characteristic catalytic domain with the specific active site, which was highly similar to the catalytic domain of their respective orthologues in human and mouse and to other members of the ADAMTS family.

The analysis of the expression profiles by *in situ* hybridisation suggested a distinct regulation of ADAMTS1 and -9 in the developing chick limbs, which, particularly in regard to ADAMTS1, seemed to differ from the previously described pattern in mouse embryos. In mice, whole mount *in situ* hybridisations had revealed ADAMTS1 expression in the apical epithelial ridge starting from E9. At E11 the expression remained limited to the most distal part of the limb bud, and was finally restricted to the interdigital zone at E12 (Thai and Iruela-Arispe, 2002). At the corresponding stage in the chick (E12 mouse - HH27 chick), we detected in *in situ* hybridisation of thin sections only little ADAMTS1 transcripts in mesenchymal areas of the developing limb and none at the distal rim. In contrast, we observed a moderate staining in the DRG and in the neural tube starting from HH25. This location of ADAMTS1 expression has been described in mouse embryos too, albeit at later stages of development. These discrepancies between the mouse and the chick models could be first explained by the technique itself. The signal of our ADAMTS1 ISH experiments on cryo-sections was extremely weak. It is possible that our short riboprobe was staining less efficiently than the whole mount *in situ* probe of Thai and colleagues, which hybridised to almost the entire coding sequence of the mature peptide bearing however, an increased risk for cross-hybridisations (Thai and Iruela-Arispe, 2002). Secondly, by analysing sections, we may have missed the proper plane that included the developing toes and their interdigital zones. Thirdly, the timing and distribution of ADAMTS1 expression might differ from one organism to another during development. In fact, we studied only a restricted period of the chick embryogenesis (up to HH27). It seems possible that the high levels of the ADAMTS1 expression observed in mice become apparent only later in avian development. Finally, one could imagine that another member of the ADAMTS family has taken over the function of ADAMTS1 in the chick, because of a certain redundancy of the substrate specificities. Irrespective of the explanations mentioned above, the expression of ADAMTS1 initiates well after the time frame of the early limb innervation. It therefore seems rather unlikely the ADAMTS1 is the key enzyme that clears versican from the axonal pathways at this stage.

No such species differences were evident regarding the spatial and temporal regulation of ADAMTS9 expression during limb development. Jungers *et al.*, who previously determined the expression in mouse embryos (Jungers et al., 2005), showed a wide and timely

distribution of ADAMTS9 throughout the development. Within the developing limbs, ADAMTS9 was predominantly expressed in the mesenchyme around the cartilage at E13.5. In the present study on chick embryos, the expression of ADAMTS9 was also confirmed in hind limb mesenchyme at comparable developmental stages. Moreover, immunofluorescence stainings for versican on sections successive to the sections processed for ADAMTS9-specific ISH revealed a clear correlation of ADAMTS9 expression and versican disappearance in the developing hind limb. Notably, ADAMTS9 expression was present on all future routes taken by the axons to innervate the limb.

During development, the extracellular matrix undergoes an active remodelling permitting the growing axons to invade spaces that were previously non-permissive to their extension. Since ADAMTS9 was described to have versicanase activity *in vitro*, the nearly perfect complementarity of the distribution of ADAMTS9 transcripts and the proteoglycan disappearance may be of great significance. These findings let us therefore, speculate that the ADAMTS9 protease is crucial for the versican turnover during the mesenchymal remodelling in chick embryos and consequently may neutralise the inhibitory properties of early axonal growth barriers. Nevertheless, combined functional studies with versican and ADAMTS9 are necessary to confirm this intriguing hypothesis.

6. *In vitro* and *in vivo* studies to analyse ADAMTS9 function on versican turnover

6.I. Introduction

The ADAMTSs (a disintegrin and metalloproteinase with thrombospondin type 1 motifs) comprise a superfamily of extracellular proteases forming frequently an integral part of the extracellular matrix (ECM) themselves. They are involved in various biochemical and biological processes, such as maturation of von Willebrand factor and procollagen, as well as proteolysis of extracellular matrix proteoglycans in the context of ovulation, morphogenesis, angiogenesis, cancer and arthritis (Kuno et al., 2000; Levy et al., 2001; Shindo et al., 2000; Tortorella et al., 1999; Wang et al., 2003). Together with other proteases, the ADAMTS have a potential function in the degradation and turnover of ECM components in a broad range of tissues. Among them, ADAMTS1, -4, -5, -8, -9, -15 and -20 exert hyalectanase activity cleaving aggrecan, versican and/or brevican at specific sites (Abbaszade et al., 1999; Kuno et al., 2000; Somerville et al., 2003; Tortorella et al., 1999; Westling et al., 2004).

In our previous experiments (part 5), we have shown that ADAMTS9 expression correlates particularly well with the disappearance of versican during chick development. Versican, which is strongly expressed in the entire hind limb mesenchyme at early stages of development, rapidly disappears between HH23 to HH25 to remain finally only present in the condensing mesenchyme of the future cartilage and bone forming tissues. This swift remodelling of the mesenchymal areas in the hind limb is likely connected to an active turnover of the versican proteoglycan. Due to its matching spatiotemporal expression, ADAMTS9 is the prime candidate for the initialisation of the versican degradation. Further evidence for this notion is provided by *in vitro* experiments, in which a versican preparation from bovine aorta was specifically processed at the Glu(441)-Ala(442) bond by incubation with COS-1 cells expressing recombinant human ADAMTS9 (Somerville et al., 2003). Moreover, different studies led by Apte and colleagues have recently shown a direct implication of versican cleavage in various morphogenetic processes. While homozygous ADAMTS9 knockout mice die early at E7.5, heterozygous Adamts9$^{(+/-)}$ mice survive, but display cardiac and aortic anomalies or, in case of ADAMTS9$^{(+/-)}$/ADAMTS20$^{(-/-)}$ double knockouts, cleft palates (Enomoto et al., 2010; Kern et al., 2010). Both of these defects have been directly attributed to reduced versican processing and accumulation of this proteoglycan as a result of ADAMTS9 haploinsufficiency. Different combinations of partial or complete suppression of ADAMTS5, -9 and -20 have also been linked to defects in interdigital web regression during embryogenesis and consequent syndactyly (McCulloch et al., 2009b). Taken together, these observations suggest a potential role of ADAMTS9 in the regulation of versican functions during development of the hind limb in chick embryos via an

active processing of its core protein. The aims of this part of our project were to verify the cleavage activity of ADAMTS9 towards versican and to study the function of this processing during peripheral nervous system development *in vitro* and *in vivo*. For this purpose, we prepared different expression vectors containing the full-length chick ADAMTS9 and its inactive form carrying a mutation in the active site (E427A). We established stable cell lines expressing the recombinant chick ADAMTS9 and the mutant E427A_ATS9. In parallel, we generated specific anti-sera recognising the chick ADAMTS9 peptide. We then examined the activity of these recombinant enzymes on purified chick versican and we attempted to test the *in vivo* effect of injections and electroporations of ADAMTS9 cDNA in early chick embryos.

6.II. Material and methods

6.II.1 Generation of antibodies against chick ADAMTS9

6.II.1.a Preparation of recombinant ADAMTS9 fragments for immunization

Two different chick ADAMTS9 cDNA fragments covering nucleotides 1414 to 1740 (fragment A) and 1474 to 1740 (fragment B) were PCR-amplified from a cloned cDNA template (construct F_Ab) (Fig.27). The construct F_Ab had previously been prepared by inserting a *SacII* and *BamHI* fragment from 2_ADAMTS9 into the 3_ADAMTS9 plasmid (ref Figure 19. Cloning strategy for assembling the full length ADAMTS9 cDNA).

The primers for amplification were specifically modified for in frame insertion into the pDS9-cassette expression vector (Zimmermann et al., 1994). The forward primers carried at their 5' end a *SfiI* restriction site and the codons for the tetrapeptide of the factor Xa cleavage site, while the reverse primers included the inverse complementary sequence for a translational stop codon followed by a *NotI* site. PCR amplifications were done from 20 ng of F_Ab template in a 50 µl reaction volume containing 1 X TaqGOLD buffer, 2.5 mM $MgCl_2$, 0.2 mM dNTPs, 0.2 µM primers, 1.25 U Taq GOLD Polymerase (Roche) (initial denaturation: 10 min at 95°C, cycling conditions repeated 25 times: 1 min at 94°C, 1 min at annealing temperature, 1 min 30 sec at 72°C, final extension: 8 min at 72 °C then final hold at 4°C, Table.4).

The amplification products were digested with *NotI* and *SfiI* and inserted into the expression vector. The resulting constructs were verified by DNA sequencing and used for the production of recombinant peptides that served as antigens.

The His-tagged fusion proteins were expressed in E.Coli M15 [pREPA] (Qiagen) grown in LB medium at 30°C (PepA) or at 37°C (PepB). The expression and purification under denaturing conditions was performed according to the manufacturer's recommendations (Qiagen).

Table 4. Primer sequences and conditions used for amplification of fragments PepA and PepB

Fragment name	Primer name	Primer sequence	Product length	Annealing Temp. °C
Fragment PepA	SfiI-ATS9 2 up	taggccttattggccattgaaggtcgtAGGAAATACATCACTGAGTTT	370 bp	68.5
	NotI-ATS9 1 low	atgcggccgctcaATCCACCACCGGTGCCTCACG		
Fragment PepB	SfiI-ATS9 1 up	taggccttattggccattgaaggtcgtTCATCAAGAACTTACGCTTTG	297 bp	71
	NotI-ATS9 1 low	atgcggccgctcaATCCACCACCGGTGCCTCACG		

Nucleotides complementary to ADAMTS9 sequences are written in capital letters. The restriction sites are indicated in purple.

In brief, the expression of recombinant peptides was induced by addition of IPTG to a final concentration of 2 mM in a 500 ml bacterial culture.

After 1.5 hours, the bacteria were centrifuged at 6000 rpm for 18 min at 4°C. To extract the total proteins, the pellet was gently resuspended in buffer A containing 6M guanidium hydrochloride, 0.1M NaH_2PO_4, pH 8 and rocked for 1 hour at room temperature before centrifugation at 20.000 rpm for 10 min. Now cleared from bacterial debris, the supernatant containing the total protein extract was collected, supplemented with 20 mM imidazole and applied to the $Ni2^+$-NTA agarose resin (Qiagen). This adsorption step was done by gentle mixing for at least 16 hours at 4°C. After assembling, the column was extensively washed with buffer B (50mM Tris-HCl, 50mM NaH_2PO_4, 300 mM NaCl, 20 mM imidazole, pH 8). Before the final elution, the non-specifically bound components were washed off with buffer C (50mM Tris-HCl, 50mM NaH_2PO_4, 300 mM NaCl, 50 mM imidazole, pH 8). The recombinant His-tagged peptide was finally eluted with 250 mM imidazole in buffer E (50mM Tris-HCl, 50mM NaH_2PO_4, 300 mM NaCl, pH 8). After extensive dialysis against PBS at 4°C, the fractions were analysed on a 4-25% gradient PhastGel stained with Coomassie blue.

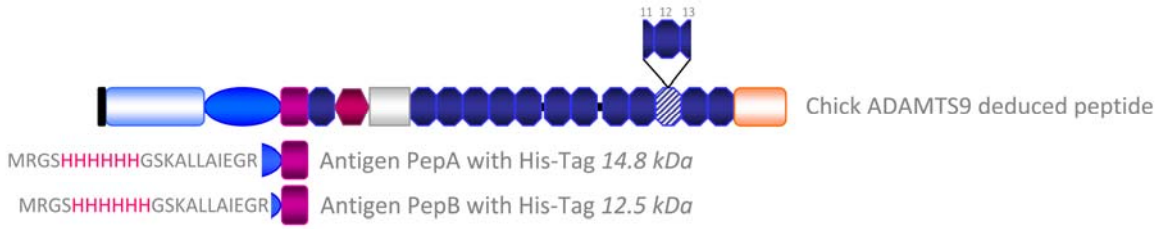

Figure 27. Localisation of antigenic peptides.
Antigenic peptides (PepA and PepB) are depicted under the respective domains of chick ADAMTS9 peptide, the His-Tag is shown in pink.

6.II.1.b Generation of polyclonal antibodies against recombinant chick ADAMTS9 fragments

The polyclonal antisera were prepared at the Institute of Animal Science of the University Zürich Irchel. Rabbits were immunized with 100 - 200 µg of purified antigen emulsified in incomplete Freund adjuvant. After one boost and seven bleedings the rabbits

were sacrificed. Antisera from initial and final bleeding (anti-chick ATS9pepA, anti-chick ATS9pepB) were collected, supplemented with 0.02% sodium azide and stored at -20°C. Aliquots in use were kept at 4°C.

6.II.2 Cloning of mutant form of chick ADAMTS9

A functionally inactive form of ADAMTS9 was prepared by introducing the mutation E427A into the catalytic domain via PCR-amplification/mutagenesis and replacement of the respective *XmaI* fragment in the wild type clone. The strategy was divided into three main steps (Fig. 28).

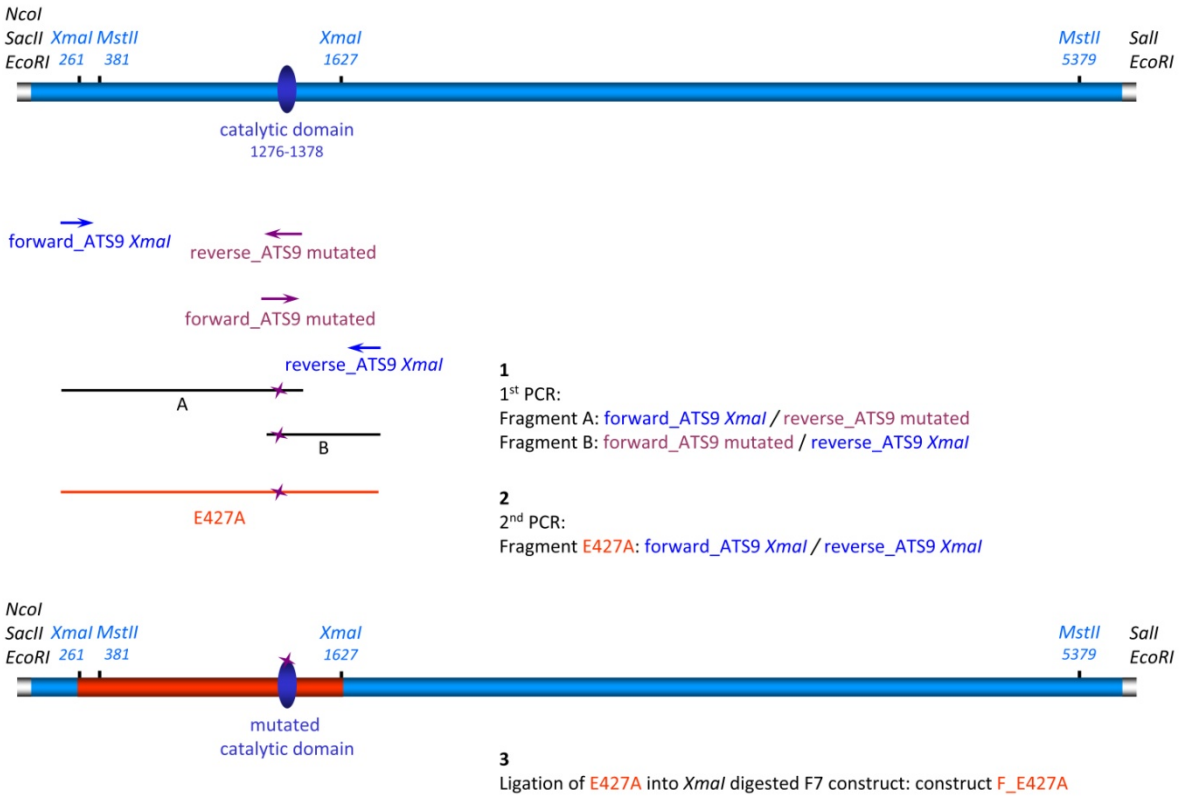

Figure 28. Generation of the mutated chick ADAMTS9 form: E427A
On the upper panel, ADAMTS9 cDNA is represented in blue, the MCS from pGEM ®T-Easy vector in white. The different primers and the fragments generated by PCR amplifications are depicted under their respective positions. The lower panel shows the mutated E427A cDNA in pGEM ®T-Easy with the replaced fragment in orange. Point mutation: purple star.

Firstly, two sub-fragments (A and B) overlapping the catalytic domain were amplified each with a primer carrying the mutation of the catalytic domain and a primer up- or downstream of the corresponding *XmaI* restriction site. Secondly, these overlapping PCR-products A and B were used as templates for a second ligation PCR-amplification now exclusively employing the primers close to the *XmaI* sites. The resulting PCR product carried the mutation E427A in the middle and the two *XmaI* sites near its 5'- and 3'- ends. This product was then first

subcloned in pGEM ®T-Easy (Promega) and further propagated. Following excision by *XmaI* digestion, the mutated fragment was finally inserted into the F construct, from where the wild type *XmaI* fragment had been removed previously. Thus, the plasmid F_E427A containing the full length ADAMTS9 with an inactivating point mutation in the catalytic site was reconstituted. Intermediate and final products were sequenced to verify that no spurious point mutation was introduced during the PCR amplifications.

Following steps and conditions were employed in the amplification experiments:

PCR amplifications of fragments A and B: 5 ng of plasmid F template was added to 1 X TaqGOLD buffer, 2.5 mM $MgCl_2$, 0.2 mM dNTPs, 0.2 µM primers, 1.25 U Taq GOLD Polymerase in a 50 µl reaction volume (initial denaturation: 10 min at 95°C, cycling conditions repeated 20 times: 1 min at 94°C, 1 min at 57°C, 1 min 30 sec at 72°C, final extension: 8 min at 72 °C then hold at 4°C).

PCR amplification of fragment F_E427A: 2 µl of the PCR products A and B were added together to 1 X buffer, 2.5 mM $MgCl_2$, 0.2 mM dNTPs, 0.2 µM primers, 1.25 U Taq GOLD Polymerase in a 50 µl reaction volume (initial denaturation: 10 min at 95°C, cycling conditions repeated 18 times: 1 min at 94°C, 1 min at 54°C, 1 min 30 sec at 72°C, final extension: 8 min at 72 °C then hold at 4°C).

Primers used to generate the mutated form E427A:

forward_ ATS9 *XmaI*: CAGCGAGTACGAGATCGTGA

reverse_ ATS9 mutated: **TATTAAATACATGGCCAAGTGCATGTGCTA**TTGTGAAAGC

forward_ ATS9 mutated: **TAGCACATGCACTTGGCCATGTATTTAATA**TG

reverse_ATS9 *XmaI*: ACATTGTTTATTGACGTCAT

The mutated nucleotides are written in orange, the overlapping complementary sequences amplified in fragments A and B are indicated in bold font.

6.II.3 Generation of eukaryotic expression vectors

Different expression vectors have been used to express ADAMTS9 and its mutant form E427A in mammalian cells *in vitro* and in chick embryos *in viv*o (Fig.29).

A modified pSecTag A vector (Invitrogen) under the control of CMV promoter previously prepared in our lab, has been used for the expression in mammalian cell cultures. It contains a cassette encoding the FLAG tag in the fragment flanked by unique *XbaI* and *PmeI* restriction sites. The cDNA is inserted upstream of this sequence. Thus, the proteins expressed from this vector are fused at their C-terminus to a FLAG-tag.

To prepare the expression constructs, the full length sequence of ADAMTS9 was amplified by long-distance PCR (LD-PCR) to introduce at the 5'-end a *NheI* and at the 3'-end a *XbaI* restriction site (forward_ATS9_NheI and reverse_ATS9_XbaI primer). The PCR product was

cloned into pGEM ®T-Easy vector and sequence-verified. Mutation artefacts caused by the LD-PCR amplification were corrected by exchanging mutated by non-mutated fragments from the F construct. The resulting cDNA was excised and ligated into the *NheI/XbaI* cleaved pSecTag FLAG vector. For the expression of the mutant *E427A*, the *MstII_MstII* fragment of the wild type ADAMTS9 cDNA was replaced by the corresponding fragment from the F_E427A plasmid (Fig.28) prior to subcloning into the pSecTag FLAG vector.

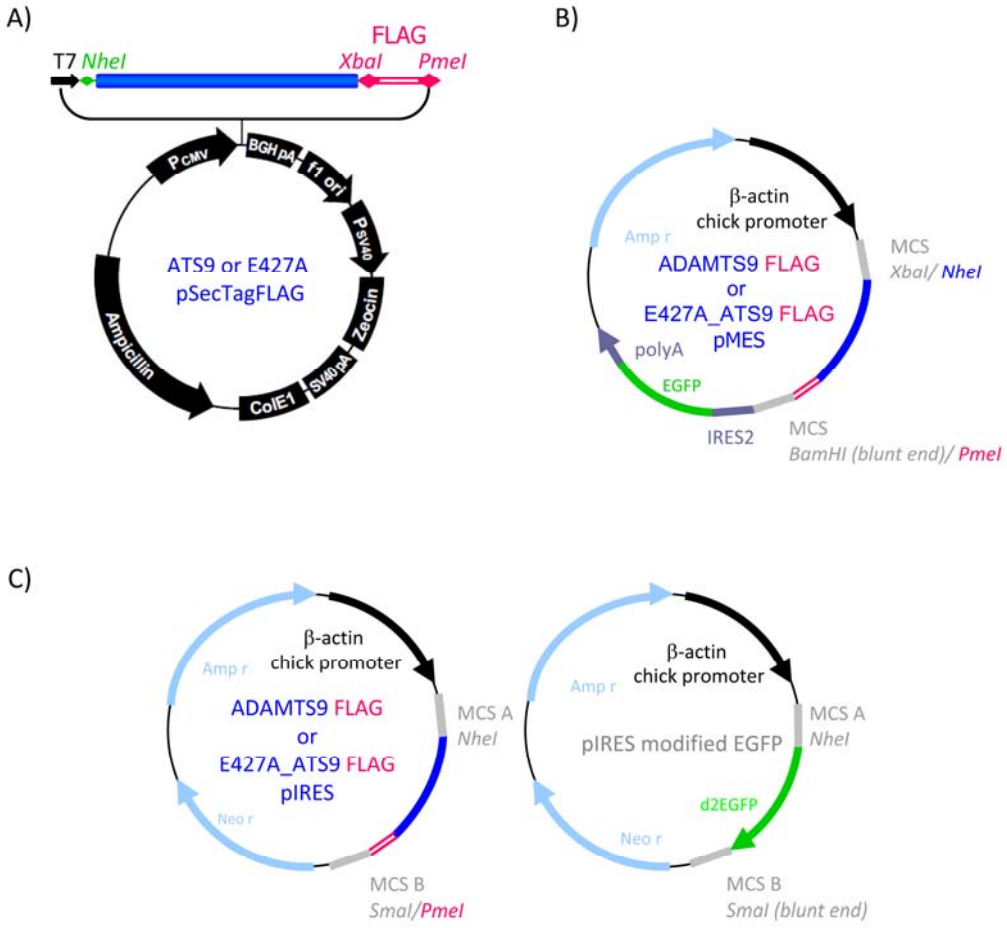

Figure 29. Vectors prepared for eukaryotic expression.
Vectors used for the expression of chick ADAMTS9 and its mutant E427A-variant in mammalian cells (A) or in chick embryos (B and C). The cDNA encoding the ADAMTS9 or the E427A mutant is depicted in navy blue, the FLAG tag in pink. The EGFP modified pIRES was used as marker construct in co-transfection experiments.

Conditions and primers used for LD-PCR amplification were the following:

5 ng of vector F template was added to 1 X LA buffer II, 2.5 mM $MgCl_2$, 0.2 mM dNTPs, 0.2 µM primers, 2.5 U Takara LA Taq Polymerase in a 50 µl reaction volume (initial denaturation: 2 min at 94°C; first cycling conditions repeated 14 times: 30 sec at 94°C, 10 min at 68°C; second cycling conditions repeated 16 times: 30 sec at 94°C, 10 min with 20 sec increment at 68°C; final extension: 10 min at 68 °C then hold at 4°C).

Forward_ ATS9_NheI: TAGCTAGC**GCAGCACCATGCAG**

Reverse_ ATS9_ XbaI: TATCTAGA**TAACACCTGCACGTCAAGGC**

Blue letters indicate the restriction sites, red the start codon; the bases corresponding to the ADAMTS9 cDNA are written in bold font.

For the *in vivo* expression in chick embryos, vectors with the chick β-actin promoter instead of the CMV promoter were used. The pMES vector carrying two IRES sequences expresses green fluorescent protein (GFP) in addition to the inserted cDNA of choice (modified pIRES and pMES plasmids kindly provided by E. Stoeckli).

For our purpose, we digested ADAMTS9_pSec Tag FLAG with *NheI* and *PmeI*. The pMES vector was open with *BamHI* and blunt-ended with the Klenow fragment of the DNA Polymerase I followed by digestion with *XbaI*. The pIRES vector was open with *SmaI* generating blunt-ends and then cut with *XbaI*. The ADAMTS9-FLAG insert was ligated into pMES or pIRES vectors via the *NheI/XbaI* site compatibility at the 5'- end and the junction of the two blunt ends at the 3'- end. The same procedure was employed for cloning of the variant E427A in these expression vectors.

6.II.4 Cloning of C-terminally truncated ADAMTS9-variants

Different variants truncated at the carboxy-end were generated in pSecTag FLAG. The same cloning strategy as for the full length was followed. For each variant specific primer pairs were designed to incorporate at the 5'- end a *NheI* site and at the 3'- end a *XbaI* site. The variants were amplified from the F template by LD-PCR. Spurious mutations incorporated during the amplification were corrected by fragment replacement using non-mutated subclones as a source.

Conditions and primers used for LD-PCR amplification were the following:

8 ng of vector F template was added to 1 X LA buffer II, 2.5 mM $MgCl_2$, 0.2 mM dNTPs, 0.2 µM primers, 2.5 U Takara LA Taq Polymerase in a 50 µl reaction volume (initial denaturation: 2 min at 94°C; first cycling conditions repeated 10 times: 30 sec at 94°C, 10 min at 68°C; second cycling conditions repeated 15 times: 30 sec at 94°C, 10 min with 20 sec increment at 68°C; final extension: 10 min at 68 °C then hold at 4°C).

Forward_ ATS9_NheI: TAGCTAGC**GCAGCACCATGCAGCTTG**

Reverse_ ATS9.1_ XbaI: TATCTAGA**TGAGCACGGTTCAGTGTTGCA**

Reverse_ ATS9.2_ XbaI: TATCTAGA**CCCGCACTGGGCTGTGCACTCA**

Reverse_ ATS9.3_ XbaI: TATCTAGA**GGCTTCGGGACTGT**

Blue letters indicate the restriction sites, red shows the start codon; the nucleotides corresponding to ADAMTS9 cDNA are written in bold font.

6.II.5 Recombinant expression of ADAMTS9 in mammalian cell cultures

6.II.5.a Transient expression of ADAMTS9, E427A and the ADAMTS9 variants

293 FT and 293 F cells (Invitrogen) were used for transient expression of ADAMT9 pSecTagFLAG, E427A pSecTagFLAG and the variants ADAMTS9.1, ADAMTS9.2, ADAMTS9.3.

The 293F cells were grown in complete medium (D-MEM medium, 10% FCS, 1X Glutamax, 100 U/ml penicillin, 100 µg/ml streptomycin; all products from Invitrogen) to reach 80% confluence before transfection. The 293FT cells were cultivated in this complete medium supplemented with 1X MEM Non Essential Amino Acids (Invitrogen), 500 µg/ml Geniticin (Invitrogen). The cultures were kept at 37°C in a humidified atmosphere with 5% CO_2.

The transfections were done with the PolyFect transfection reagent (Qiagen) in 6-well plates. Before transfecting 293F cells, the complete medium was changed for serum-free medium and transfection mix was added to the 293F cells (per plate: 2 µg vector, 15 µl Lipofectamine transfection reagent (Invitrogen), 2 ml D-MEM). The next day, the culture medium was replaced either by complete medium with 5% FCS or by serum free D-MEM with 1X Glutamax, 100 U/ml penicillin, 100 µg/ml streptomycin. Both media were supplemented with 50 µg/ml heparin (Sigma). After 48, 72 or 96 hours the conditioned media was collected and the cells were extracted.

For transfection of 293 FT cells a transfection mix consisting of 1 µg vector, 20 µl PolyFect and 2 ml D-MEM with 5% FCS was used per 6-well plate. The next day, the culture medium was changed for fresh complete medium with 5% FCS supplemented with 50 µg/ml heparin.

6.II.5.b Stable lines expressing chick ADAMTS9 and E427A pSecTag FLAG

To produce stable cell lines, 293 F cells were cultivated and transfected in a 10 cm dish as described above. 24 hours post-transfection, the cells were subjected to Zeocin (Invitrogen) selection, 100 µg/ml selection antibiotic was added to the medium containing D-MEM supplemented with 10 % FCS, 1X Glutamax, 100U/ml penicillin, 100 µg/ml streptomycin and seeded as single clone in 96 well-plates. The isolated clones have been maintained under selection for 2 months.

6.II.5.c Suspension culture of stable lines

Apart from maintaining the newly generated stable 293F cell lines in adherent monolayers, they were also cultivated in suspension to facilitate the production and purification of the potentially secreted recombinant enzymes. For this purpose, 293 SFM-II and FreeStyle 293 Expression media from Invitrogen were tested. All media were supplemented with 1X Glutamax, 100U/ml penicillin and 100 µg/ml streptomycin with or without addition of 50 µg/ml heparin.

6.II.6 Immunofluorescence staining on cells

For immunofluorescence stainings stably transfected cells were cultivated in ChamberSlides (BD-Falcon). When the adherent cultures reached 80% confluence, they were carefully rinsed in PBS and fixed for 30 min in 4% PFA at room temperature. After a short rinsing and three successive washes for 5 min in PBS, the cells were permeabilized in methanol for 20 min at -20°C. They were then rehydrated in PBS and non-specific binding sites were blocked for at least 30 min in blocking buffer (0.5% BSA, 0.2% gelatine, 0.02% NaN_3 in PBS) at room temperature. Primary antibody incubations (pepA anti-serum 1/100 diluted in blocking buffer) were performed for at least 16 hours at 4°C in a humidified chamber. After successive washings for 10 min in PBS, the highly cross-absorbed Alexa Fluor 488 goat anti rabbit IgG (H+L) secondary antibodies (Molecular Probes, Invitrogen) were applied on the slides and incubated for 1 hour at room temperature under light-protection. The preparations were subsequently rinsed again in PBS and counterstained with Hoechst H33258 bis-benzimide (Invitrogen). Finally the slides were washed three times in PBS for 5 minutes and cover-slipped with fluorescence mounting medium (Dako).

The transiently transfected cells were imbedded in paraffin using a cell block technique (Schmid et al., 2010). 5 µm thick sections were cut on a microtome and mounted on SuperFrost Plus glass slides (Menzel Gläser). Standard dewaxing by xylene followed by rehydration in a descending ethanol series were performed. Epitopes were recovered by steam-cooking for two minutes in citrate buffer (1.8 mM monohydrated citric acid, 12,2 mM tri-sodium citrate, pH 6) in an antigen retrieval device (FSG 120_T/T from Milestone). The subsequent immunofluorescence staining was done as mentioned above.

Fluorescence images were collected as described in the part V section “Immunofluorescence pictures and *in situ* hybridisation images”.

6.II.7 Fast purification of chick versican

Conditioned medium from chick fibroblast primary culture was centrifuged at 10000 rpm for 10 min to remove cellular debris. The NaCl concentration in the conditioned medium was adjusted to 300 mM. 25 ml of this solution was applied by gravity flow on a column previously packed with 1.5 ml Sepharose Fast Flow DEAE resin (GE Healthcare), which had been equlibrated in wash buffer (300 mM NaCl, 50 mM Tris-Hcl, pH 7.5). The first 5 ml of wash buffer running through the column was collected for control. The washing step was continued until the UV-absorbance reached baseline. The bound versican-enriched proteoglycan fraction was finally eluted with 15 ml of elution buffer (NaCl 3 M, Tris-HCl 50 mM, pH 7.5). The collected fractions were extensively dialysed against ATS buffer (150 mM NaCl, 50 mM Tris-HCl, 3 mM $CaCl_2$, pH 7.5) for 16 hours at 4°C. The samples were then digested with chondroitinase ABC lyase (MP Biomedicals) before analysis by Phastgel electrophoresis and immunoblotting.

6.II.8 Preparation and processing of cell extracts and conditioned medium of ADAMTS-expressing cell cultures

Conditioned media were collected and cleared from cellular debris by centrifugation at 15000 rpm for 30 min at 4 °C. The proteins were then concentrated with Amicon Ultra-15 Centrifugal Filter Units 10,000 NMWL (Millipore) according to manufacturer's recommendations. The samples destined for activity assays were dialysed against ATS buffer and processed without delay.

After trypsinization and washing with PBS, cells were lysed and extracted for 10 min on ice with extraction buffer (10 mM Tris, 1 mM EDTA, 2% SDS, pH 8). The lysates were centrifuged at 14 000 rpm for 30' at 4°C. The supernatant was transferred to a fresh tube.

6.II.9 Assay to test the potential versican-cleavage activity of recombinant ADAMTS9

To test the activity of the recombinant enzyme and its variants, 20 µl of purified chick versican dialysed against ATS buffer (150 mM NaCl, 50 mM Tris-HCl, 3 mM $CaCl_2$, pH 7.5) was combined with concentrated conditioned media (total protein content 20-40 µg) from stable or transiently transfected cells in digestion buffer (1X ATS buffer, 1 µM leupeptin, 1 µM pepstatin, 1 mM pefablock, pH 7.5) supplemented with 10 or 250 µM $ZnCl_2$ in a final volume of 30 µl. These samples were incubated at 37 °C for 16-20 hours. The glycosaminoglycan chains were removed by chondroitinase ABC lyase digestion (MP Biomedicals) either simultaneously or subsequently to the ADAMTS treatment. The processed samples were run on a Phastgel system and analysed by immunoblotting.

6.II.10 Electrophoresis and Immunoblotting

Protein samples from cell extracts or conditioned media were denatured in loading buffer (100 mM Tris-HCl, 10 mM EDTA, 20 % SDS, 3 % β-mercaptoethanol, 0.1 % bromophenol blue) for 5 min at 95°C. Following electrophoresis on PHAST polyacrylamide gels (Pharmacia), proteins were detected with immunoblotting. For this purpose, the proteins were transferred onto Immobilon P membranes (Millipore) by diffusion blotting at 70 °C for 30 min. The membranes were then blocked in blocking buffer (3 % milk in PBS) for 1 hour and incubated with primary antibody solutions in blocking buffer for at least 12 hours at room temperature. After three washes in PBST buffer, the alkaline-phosphatase conjugated secondary antibodies were incubated for 1 hour. After three successive washes in PBST, the blots were subjected to chromogenic detection with WesternBlue substrate (Promega).

Following antibodies and dilutions were used in these immunoblotting experiments: anti-chick versican GAG α, anti-chick versican GAG β, anti-chick ATS9pepA, anti-chick ATS9pepB (all rabbit polyclonal antibodies produced in our lab; diluted 1:1000), anti-FLAG M2 monoclonal antibody (purified IgG; 1:1000; Sigma) and alkaline phosphatase conjugated goat anti-mouse and goat anti-rabbit IgG (both 1:15000 diluted; Jackson ImmunoResearch Europe).

6.II.11 In vivo injections into the hind limb and into the central canal of the spinal cord

6.II.11.a Embryos preparation

Fertilised eggs (Hisex, Hendrix Genetics) were obtained from a local hatchery. After 3 days of incubation at 38.5 °C a small hole was made at either end of the eggs and 5 ml of egg white was withdrawn with a syringe. The holes were then sealed with paraffin. After that, a window of about 1.5 x 1.5 cm was cut into the side of the eggshell. Subsequently, the window was closed with tape allowing monitoring of the development and repeated opening and closing of the egg for *in ovo* manipulations.

6.II.11.b Injection of plasmids and electroporation in ovo

All embryos were staged according to Hamburger and Hamilton (Hamburger and Hamilton, 1951). The injection procedures followed the protocol previously described by Stoeckli *et al.* (Stoeckli and Landmesser, 1995). Briefly, the shell windows were opened and the extra-embryonic membrane was cut and removed from the hind limb region of the embryo. The injections were done with pointed glass capillaries with a tip diameter of about 5 µm. Test samples (1 to 5 µg plasmid in 10 µl injection mix) were mix supplement with 0.04% (vol/vol) Trypan Blue (Invitrogen) to control volume and localisation of the injection. In a small extra test series 0.5 or 4 µl lipofectamine transfection reagent was additionally included in the injection mix.

Injections at stage 18 to 23 were targeted to the right hind limb mesenchyme near the upper part of the plexus region (injection volume at least 1 µl). Alternatively, less than 1 µl were injected directly into the central canal of the spinal cord at stage HH14/15. Platinum electrodes (BTX, Genetronics) of 4 µm length were positioned next to the injection spot. The number of pulses and the applied voltage was adapted to the age of the embryos. Usually 10 pulses of 50 ms duration with 1 second interpulse interval were delivered at 25 V for the hind limb experiments in HH20 embryos, only 5 to 7 pulses at 22 V were applied to the embryos injected into the central canal. Before and after electroporation a few drops of cold, sterile PBS were added to cool the embryos. The eggs were again closed after every injection and incubated at 38.5 °C until the embryo reached the desired stage for analysis. Embryos injected with the marker plasmids encoding EGFP or YFP (under control of the β-actin promoter) alone were used as controls.

6.II.12 Whole mount staining of chick embryos

Chick embryos were sacrificed and dissected under the dissecting microscope at stage 22 to 26. They were placed into a silica agar plate containing PBS, the membranes around the embryos were removed. After decapitation, the embryos laying on their back were pinned down at the neck, tail and fore limbs. The hind limbs were kept intact for further analysis. The embryos were opened from the ventral side, cleaned of all the internal organs and blood,

fixed in 4% PFA at 4°C overnight and then subjected to whole mount immunofluorescence staining. After fixation in 4% PFA at 4°C overnight, the embryos were washed in PBS, subsequently transferred to a 24 well plate and permeabilized with 1% Triton in PBS for 2 h at room temperature. This and all following incubations were done under gentle and constant shaking. The embryos were then rinsed with PBS and incubated in 20 mM lysine in 0.1 M sodium phosphate, pH 7.4 for 1 h. After washing the embryos 5 times for 10 min each in PBS, blocking step was performed with 10% FCS in PBS for 2 h at room temperature. The incubation with primary antibodies diluted in blocking buffer (mAb RMO-270 against neurofilaments, 1:1500; Invitrogen and FITC-conjugated goat anti-GFP, 1:500; Rockland Immunochemicals) was done at 4°C for at least 48 h. After washing with 5 changes of PBS and an additional incubation in PBS for 12 h, embryos were incubated again with blocking buffer for 2 h prior to the addition of secondary Cy-3 conjugated AffiniPure goat anti-mouse IgG antibody (diluted 1:500 in blocking buffer, Jackson ImmunoResearch Europe) overnight at 4°C. This incubation was followed by 5 times extensive PBS-washing steps, two of which proceeding for more than 2 h, and a sixth incubation in PBS overnight. Finally the embryos were dehydrated with successive incubations in 25%, 50%, 75% and 100% ethanol for at least 30 min and then transferred to glass vials containing BBBA (benzyl benzoate and benzyl alcohol 2:1). Embryos were analysed under the fluorescence microscope while still in BBBA solution.

6.III. Results

6.III.1 Generation of polyclonal antibodies against chick ADAMTS9

For the immunological detection of the chick ADAMTS9 protein, we first had to generate monospecific antibodies. To direct the antibody-binding to a unique sequence near the catalytic domain, we prepared peptide fragments in a bacterial expression system. This way, we ascertained that the antibodies would specifically recognise the enzymatically active form of ADAMTS9 even after propetide- and putative C-terminal cleavage, but would not cross-react with other ADAMTS family members. Furthermore, by selecting epitopes in close proximity to the highly conserved catalytic site, we increased the chances that the antibodies would eventually exert some ADAMTS9-specific function blocking activity. Two rabbit antisera against a longer (PepA) and a shorter recombinant antigen (PepB) were generated and initially tested on immunoblots containing the bacterial fusion peptides (Fig.30). Both antisera reacted strongly with their respective HIS-tagged fusion peptides, while the pre-immune sera displayed only weak interactions with a few bacterial proteins unrelated to the fusion peptides pepA or pepB. Slower migrating components exclusively detected in extracts of bacteria expressing the fusion proteins most likely represented multimeric forms. To verify the reactivity and specificity of our antisera against the complete zymogen and the mature

enzymatic forms of ADAMTS9, we analysed extracts of 293FT cells transiently transfected with a full length cDNA construct (see below).

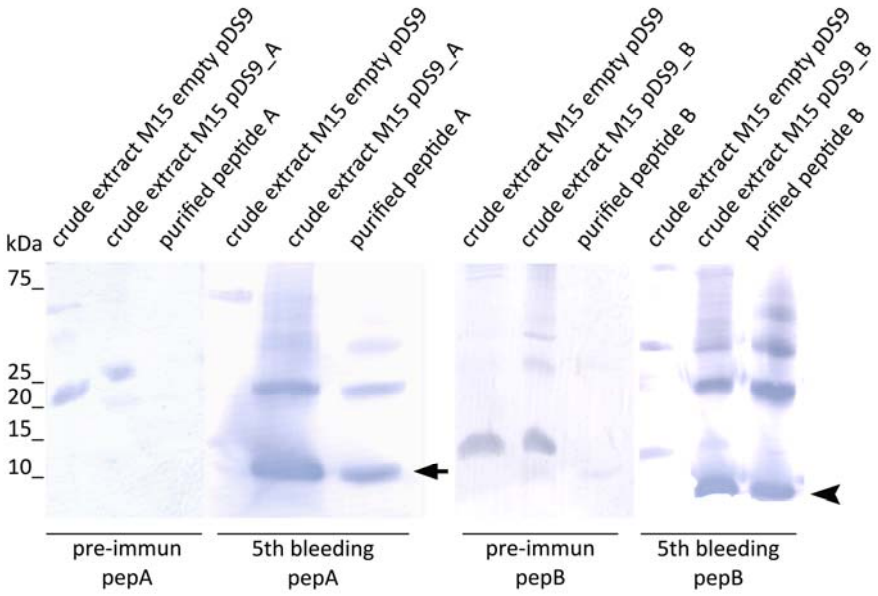

Figure 30. Characterisation of antisera against bacterially expressed chick ADAMTS9 fusion peptides.
The anti-pepA and anti-pepB rabbit antisera were tested against their purified peptides and the crude extracts of bacteria carrying the pDS9_A or pDS9_B expression vectors. Pre-immune sera showed some reactivity against bacterial proteins but not against the fusion proteins. The anti-pepA antiserum detected the purified pepA of 13.2 kDa (arrow) and the anti-pepB antiserum the purified pepB of 10.8 kDa (arrowhead). The proteins were separated under reducing conditions.

6.III.2 Recombinant expression of chick ADAMTS9 and its mutant E427A_ATS9

6.III.2.a Analysis of ADAMTS9 and E427A_ATS9 protein production in transiently and in stably expressing mammalian cells

The full length ADAMTS9 and the mutant form E427A_ATS9 were cloned into the pSecTagFLAG plasmid for expression in mammalian cells. First, HEK293 FT cells were transiently transfected with these constructs and analysed by immunoblotting using either our ADAMTS9 specific polyclonal antibodies or a monoclonal antibody against the C-terminal Flag-tag (Fig.31). In crude cell extracts, the anti-Flag and the anti-chick ATS9pepA antibodies reacted exclusively with the recombinant zymogen (calculated molecular mass: 204 kDa; activated enzyme after propetide cleavage: 173 kDa), whereas the anti-chick ATS9pepB antiserum recognised an additional band migrating on SDS-PAGE faster than the full-length pro-enzyme. This unspecific reactivity was also observable in the untransfected sample. Consequently, only the mono-specific anti-chick ATS9pepA antiserum was used for further experiments.

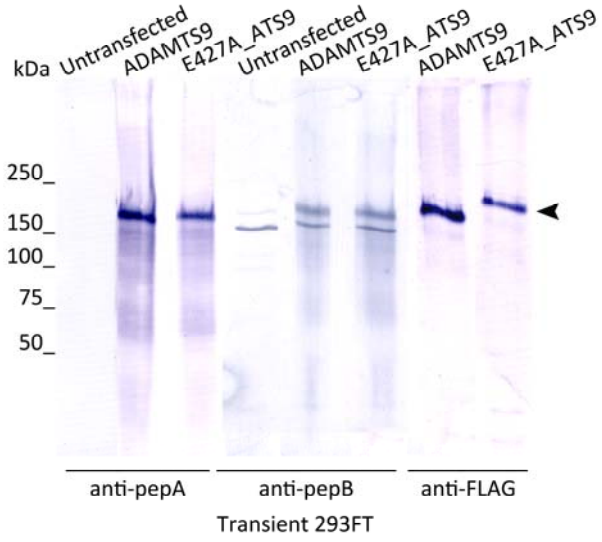

Figure 31. Characterisation of antisera against eukaryotically expressed chick ADAMTS9.
The anti-pepA and anti-pepB antisera were tested against the cell extracts from transiently transfected 293FT cells. The monoclonal antibody anti-FLAG detecting the FLAG tag at the C-terminal end of the recombinant enzymes was used to verify the expression of the transfected plasmids. Both antisera recognised the recombinant enzymes (arrowhead), but the serum anti-pepB showed an additional unspecific reactivity. SDS-PAGE was run under reducing conditions.

Stable expression lines were then established in 293F cells. The choice of 293F cell line was based on a previous work with human recombinant ADAMTS9 (Koo et al., 2007). After two months of selection, total cell extracts were prepared and analysed by immunoblotting with the rabbit antiserum anti-chick ATS9pepA (Fig.32).

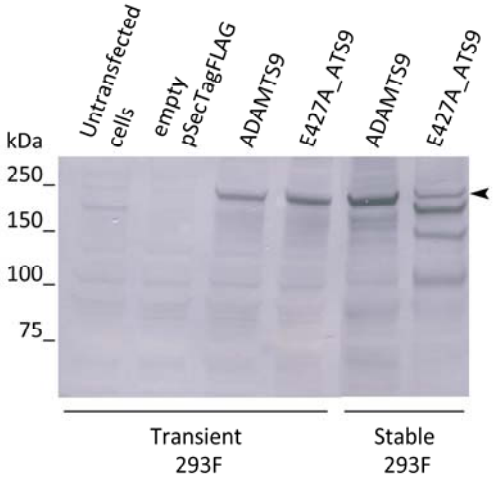

Figure 32. Analysis of ADAMTS9 and mutant E427A_ATS9 expressions in cell extracts of transiently transfected or stable cell lines by immunoblotting with the anti-pepA antiserum.
293F cells were transiently or stably transfected with the expression vectors encoding ADAMTS9, E427A_ATS9 or the control vector alone. The 204 kDa proenzyme was recognised in extracts of both ADAMTS9 and E427A_ATS9 expression systems (arrowhead). SDS-PAGE was run under reducing conditions.

The analyses revealed that both, wildtype and mutant cell lines, stably expressed the zymogen form of ADAMTS9. Unlike in cell extracts of transiently transfected cells, other smaller fragments were detectable in the stably expressing mutant line with our antiserum. These smaller peptides may reflect either breakdown products or result from random linearisation and cDNA fragmentation followed multicopy genomic incorporation of the expression construct in these cells.

We also examined the expression in the different cell lines by immunofluorescence stainings of cell preparations (Fig.33). The recombinant chick ADAMTS9 and the mutant form E427A_ATS9 were primarily detected as strong punctate stainings in the perinuclear area and with decreasing intensity towards the cellular membrane expected for synthesis and transport via endoplasmatic reticulum and secretory pathway.

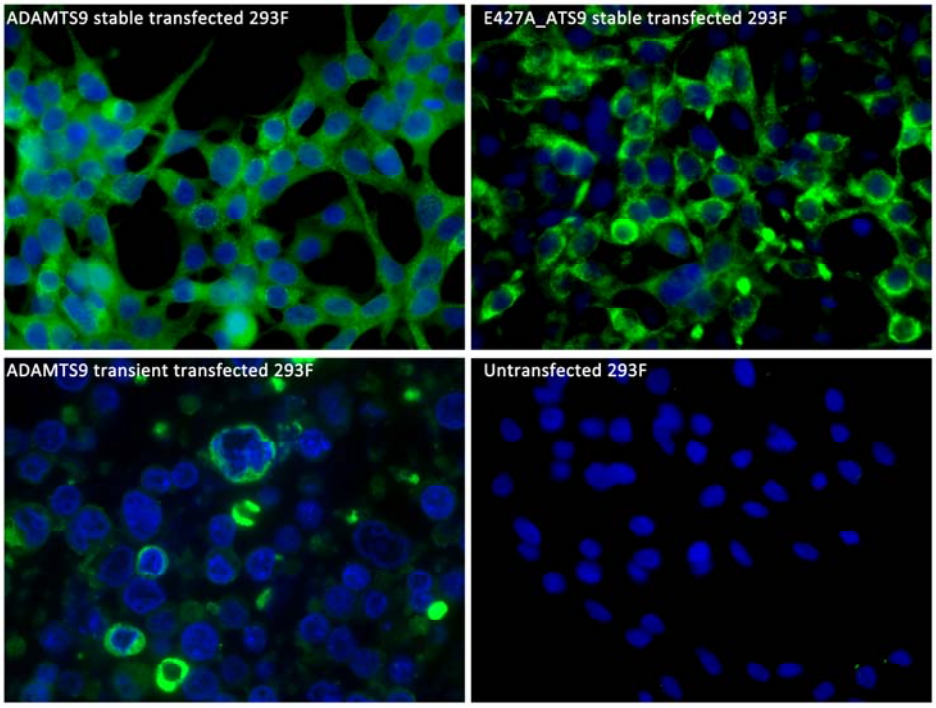

Figure 33. Analysis of ADAMTS9 and mutant E427A_ATS9 expressions in transient and stable cell lines by immunofluorescence staining of permeabilised cells.
The enzyme was detected intracellularly in stable and transiently transfected 293F cells with the antiserum anti-pepA combined with the Alexa 488-conjugated secondary antibody (green). Nucleus were stained in blue with the Hoechst nuclear counterstain.

This pattern was observed in all 293F cell lines stably expressing ADAMTS9 or E427A_ATS9 confirming the proper incorporation of the expression vector and the homogeneity of the selected clone. In contrast, only a minor proportion of the transiently transfected 293FT cells showed a clear staining. These few cells seemed to express however, substantial amounts of recombinant protein as judged by the strong immunofluorescence signal.

6.III.2.b Analysis of the expression of ADAMTS9 and E427A_ATS9 in conditioned media

Next, we attempted to detect the expression of the enzyme and its mutant form in conditioned media of adherent cell cultures, which required FCS in the medium (at least 5% for 293FT cultures). Under these conditions, the level of secreted protein turned out too low to be detectable with the monoclonal anti-FLAG M2 antibody. Besides, the identification with our antiserum was difficult. Furthermore, a concentration of the medium was hampered by the presence of serum proteins. Consequently, we had to adapt the cells to different serum-free suspension culture media.

The different conditioned media of the suspension cultures were collected, fifty times concentrated and together with the corresponding cell extracts subjected to analysis by immunoblotting. Under all culture conditions tested, the 200 kDa-band of the zymogen was again detectable in the cell extracts of stably expressing ADAMTS9 and E427A_ATS9 cell lines (Fig.34A). In addition, a band of around 150 kDa was present in the extracts. Both, wild-type and mutant cell lines also secreted several immunoreactive ADAMTS9 fragments independent of the medium (serum-free DMEM, SFMII or FreeStyle media) utilised for the suspension culture. The proportion and fragment pattern of the secreted fraction differed according to the culture condition, however. For instance, cultures maintained in FreeStyle medium retained most of the recombinant ADAMTS9 within the cells, while cells grown in SFMII medium appeared more adapted for the secretion of the enzyme. We therefore continued to focus onto the SFMII-cultures. Although a 170 kDa- fragment (expected size for the enzyme form after removal of N-terminal propeptide) was not detectable in the conditioned SFMII medium of the wild type ADAMTS9 cell line, strongly immunoreactive bands were always perceptible around 100, 50 and 37 kDa and to a smaller extent also around 150 and 75 kDa (Fig.34B). In the medium of the mutant line, the 100 kDa-band was particularly prominent.

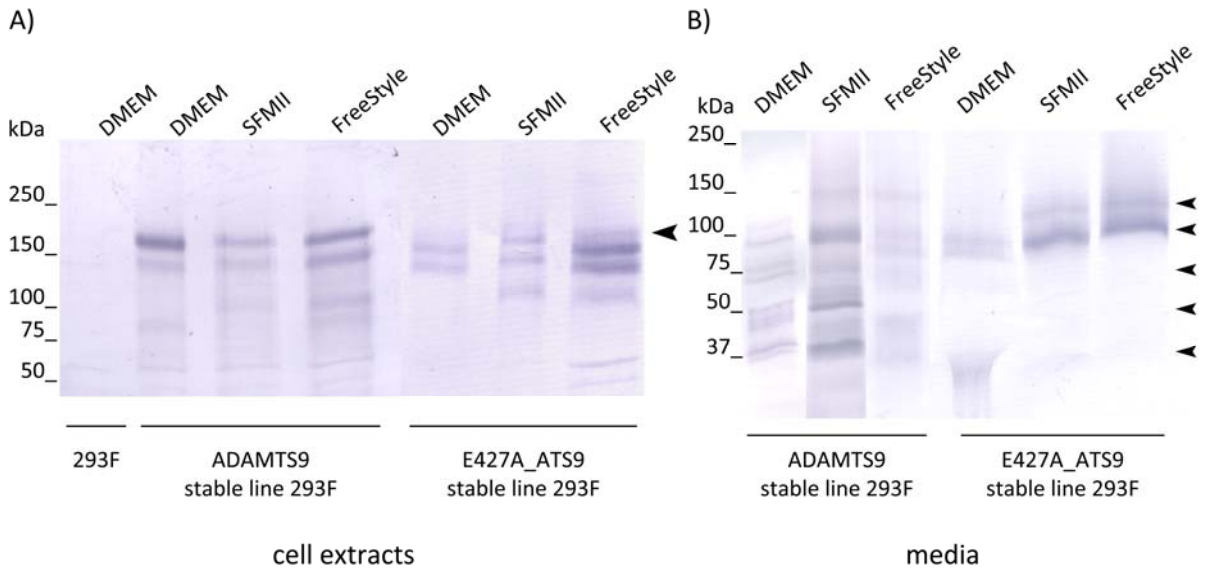

Figure 34. Analysis of the expression of ADAMTS9 and E427A_ATS9 in different culture media by immunoblotting with the antiserum anti-pepA.
293F cells were stably transfected with the expression vectors encoding ADAMTS9 or E427A_ATS9.
A) Cell extracts. The ADAMTS9 proenzyme and its E427A_ATS9 mutant form with a size of about 200 kDa are stronger expressed when cells are cultivated in FreeStyle medium (arrowhead).
B) Conditioned media. Several fragments of about 150, 100, 75, 50 and 40 kDa size were detected in the different conditioned media from ADAMTS9 stable lines and more intensively in SFMII medium (arrowheads). In conditioned media of the mutant form, only the bands of 150 and 100 kDa were consistently detected.

Since we repeatedly detected these fragments in the conditioned media, we assumed that they originate from a physiological process. Consequently, we tried to match the fragment sizes with our deduced peptide sequence in order to locate the potential cleavage region and to possibly identify protease recognition sites (Annexe 1). As all fragments contained the epitopes near the catalytic site, we concluded that they most likely represent C-terminally truncated forms of ADAMTS9, which might maintain the proteolytic activity. In relation to the deduced peptide sequence, the 150 kDa-band detected in media would, for instance, correspond to a fragment, from which the N-terminal pro-peptide has been removed and an additional cleavage has occurred between the last thrombospondin-like repeat and the GON-1 homology domain. Similarly, the prominent product around 100 kDa could be generated by furin processing at positions 277 (pro-peptide cleavage) and 1168 (between 6th and 7th thrombospondin-like repeat). A third putative furin cleavage site, which has been identified near the N-terminus of the pro-peptide, is most likely not present anymore in this fragment.

6.III.3 Enzymatic activity assays: chick ADAMTS9 / versican substrate

We subsequently tested the versicanase activity of chick recombinant ADAMTS9 on versican purified from the supernatant of chick embryonic fibroblast cultures. These versican preparations, containing mainly the largest V0 isoform, were incubated in ATS buffer with

concentrated and dialysed conditioned SFMII-media from ADAMTS9 or E427A_ATS9 293F cells cultures. Similarly processed media from 293FT cells stably expressing a recombinant fragment of mouse ADAMTS4 with known versican cleavage activity (Matasci et al. unpublished data) was used as positive control and its mutant E358A_ATS4.3 form as supplementary negative control. Subsequent or in parallel to the ADAMTS treatment, the samples were subjected to enzymatic removal of the glycosaminoglycan chains and putative core protein processing by the ADAMTSs was assessed by immunoblotting (Fig.35). As expected, samples incubated with the recombinant mouse ADAMTS4.3 fragment, showed a major proteolytic fragment well above the 250 kDa marker and some remaining traces of the intact V0 and V1 versican core proteins. Neither the samples treated with medium preparations from E358A_ATS4.3 cells nor from E427A_ATS9 cells gave rise to additional bands. Unexpectedly, however, also the medium from ADAMTS9 293F cells did not exhibit any versicanase activity. Only the intact chick versican substrate was detected by the rabbit antiserum against the GAGβ domain in samples treated with the medium fraction.

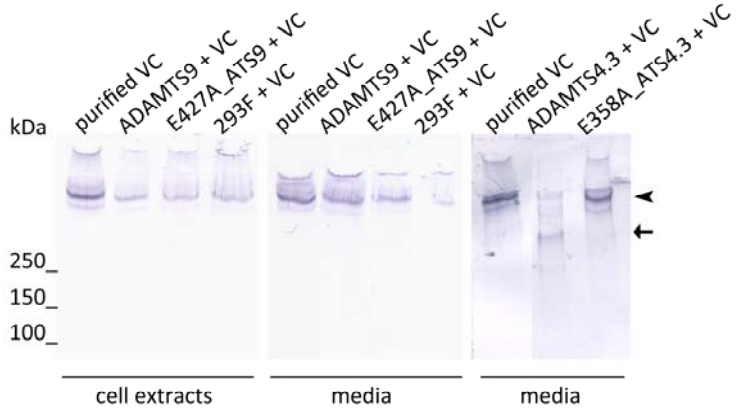

Figure 35. Analysis of proteolytic activity of recombinant ADAMTS9 and E427A_ATS9 mutant towards purified chick V0/V1 versican.
Medium-treated chick V0/V1 versican (VC) samples were recognised with a rabbit antiserum against the GAG-β domain of chick versican. Samples were chondroitinase-digested before running in SDS-PAGE under reducing conditions. Cleaved versican was detected in ADAMTS4.3-treated sample (arrow), while the mutant form of ADAMT4.3 (E358A_ATS4.3) did not cleave versican. In this assay neither ADAMTS9 in the cell extracts nor in the conditioned media showed versicanase activity (arrowhead).

6.III.4 Expression of truncated variants ADAMTS9.1, ADAMTS9.2, ADAMTS9.3

As no versicanase activity could be demonstrated using our full length ADAMTS-9 construct and as different sub-fragments were regularly present in conditioned media, we focused on the recombinant expression of truncated ADAMTS9 mimetics. In fact, similar approaches performed with C-terminally truncation of human ADAMTS1 and -4 showed previously clear aggrecanase and/or versicanase activities of some of these fragments (Gao et al., 2004; Kuno et al., 2000, Matasci et al unpublished data). According to our analysis

described in section 6.III.2.b the location of the chick ADAMTS9 fragments observed in the conditioned media were estimated (Fig.36).

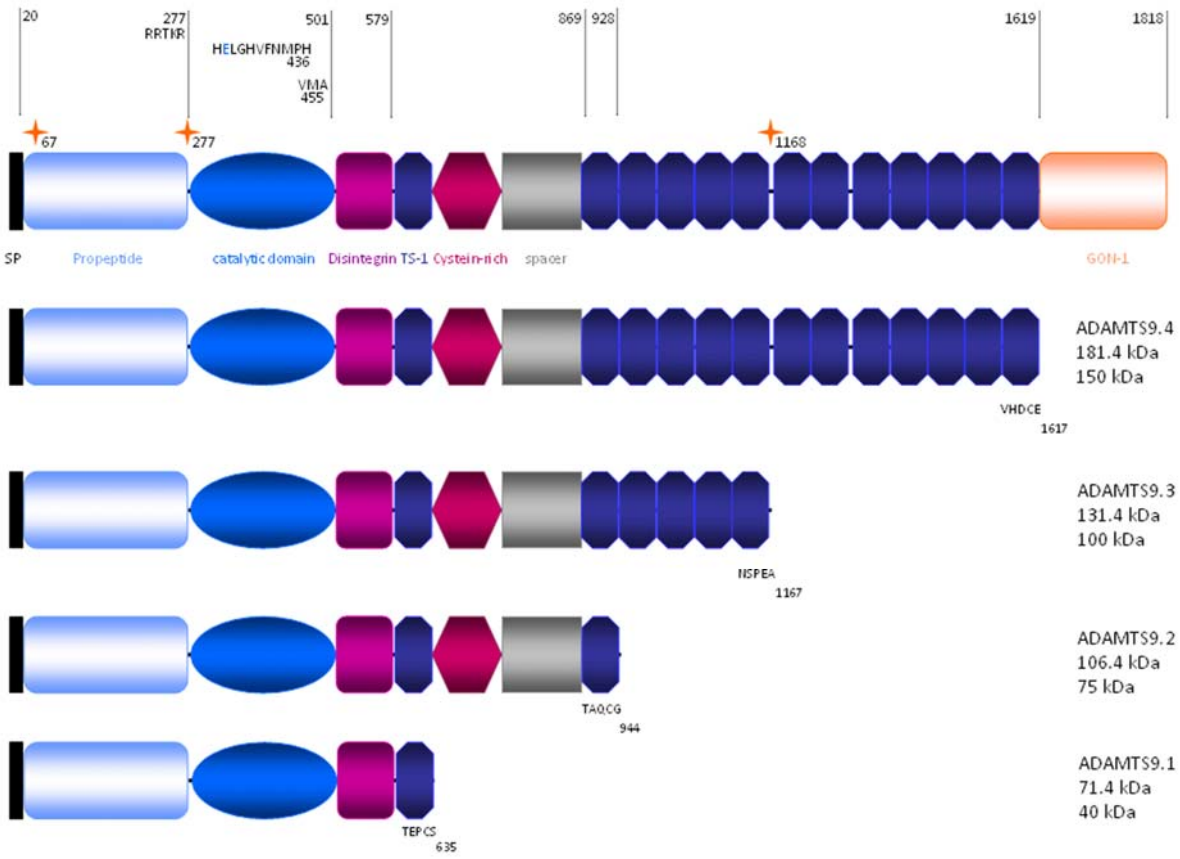

Figure 36. Schematic representation of ADAMTS9 fragments potentially secreted into the medium. Different variants ADAMTS9.1 to ADAMTS9.4 are depicted below the deduced full-length chick ADAMTS9 (zymogen: 204 kDa, active form after removal of the propeptide: 173 kDa). Respective fragment sizes before and after propeptide processing are indicated. Putative furin cleavage sites are marked with an orange asterisk. The numbers on the top represent the amino-acid positions. The carboxy- terminal amino-acids and the total number of residues are mentioned under each variant. The sequence of the active site and the met-turn (VMA) are noted on top of the catalytic domain. Further details about ADAMTS9 domain features are described in annexe 1.

For the expression experiments, we concentrated our efforts on the variants ADAMTS9.1 to ADAMTS9.3. One of the truncated forms (ADAMTS9.1) corresponded structurally to the ADAMTS4 fragment ADAMTS4.3, which displayed versicanase activity in previous experiments of our lab (Matasci et al., unpublished data) and was therefore regularly used as positive control of the assay. In human ADAMTS1, the aggrecanase activity was shown to be dependent on the presence of the spacer domain (Kuno et al., 2000). Due to this observation and due to the existence of a corresponding secretion fragment, we generated the intermediate ADAMTS9.2 truncation-mimetic carrying the spacer domain and the adjacent TSP-1 motif number 2. Finally, the ADAMTS9.3 variant ending at the potential furin cleavage site between the TSP-1 repeats six and seven was included in the test series.

These three variants were cloned into pSecTagFLAG vector and transiently expressed in 293F cells. The zymogen forms of the three variants were clearly detected with the rabbit anti-pepA antiserum on immunoblots of cell extracts (Fig.37). The predicted sizes of 71 kDa (ADAMTS9.1), 106 kDa (ADAMTS9.2) and 131 kDa (ADAMTS9.3) matched well with the corresponding migration properties in SDS-polyacrylamide gels (arrowheads in Fig.37A). Similarly, the pro-peptide lacking forms of ADAMTS9.1, ADAMTS9.2 and ADAMTS9.3 with expected molecular masses of 40kDa, 75 kDa, 100 kDa, respectively were recognised on blots of conditioned medium preparations (arrowheads in Fig37.B). In all cell extracts and media samples, intermediary fragments were consistently detected with the anti-serum anti-pepA in addition to the predicted recombinant products. For ADAMTS9.1, the band in the cell extract migrating around 40 kDa was strongly reactive against the anti-pepA serum (arrow in Fig.37A). This band was always seen with different intensities in cell extracts and conditioned media of all three mimetic cultures. Furthermore, a 70 kDa-component was present in extracts of ADAMTS9.2 and ADAMTS9.3 cells, and an additional 100 kDa peptide was detected in the ADAMTS9.3 preparation. These bands correspond in size to processed forms of the distinct recombinant variants. In conditioned media of the ADAMTS9.2 and ADAMTS9.3 cultures, the additional 70 kDa-component was consistently present suggesting that the enzyme has been subjected to intra- or pericellular C-terminal cleavage. Some differently processed minor products of chick recombinant ADAMTS9 are apparently also released into the medium. For instance, we often observed that bands weakly immunostained with the anti-serum anti-pepA were migrating above the predicted mature enzyme forms in the medium preparations providing evidence that a small proportion of the variants carry still their propeptides. Whether this release of the nascent forms results from a physiological process or is caused accidentally by limited cell lysis during culturing remains open.

Regarding the immunoblots with the anti-FLAG antibody, only the full length proteins in cell extracts of the three variant cultures (Fig.37A) and the secreted forms of ADAMTS9.1 and ADAMTS9.3 in conditioned medium preparations (Fig.37B) were detectable. The secreted form of ADAMTS9.1 became always visible, while the other forms were not reproducibly observed. In conclusion, the weak sensitivity of the monoclonal anti-FLAG antibody did not allow us to identify the precise nature of the intermediary fragments present in cell extracts and media.

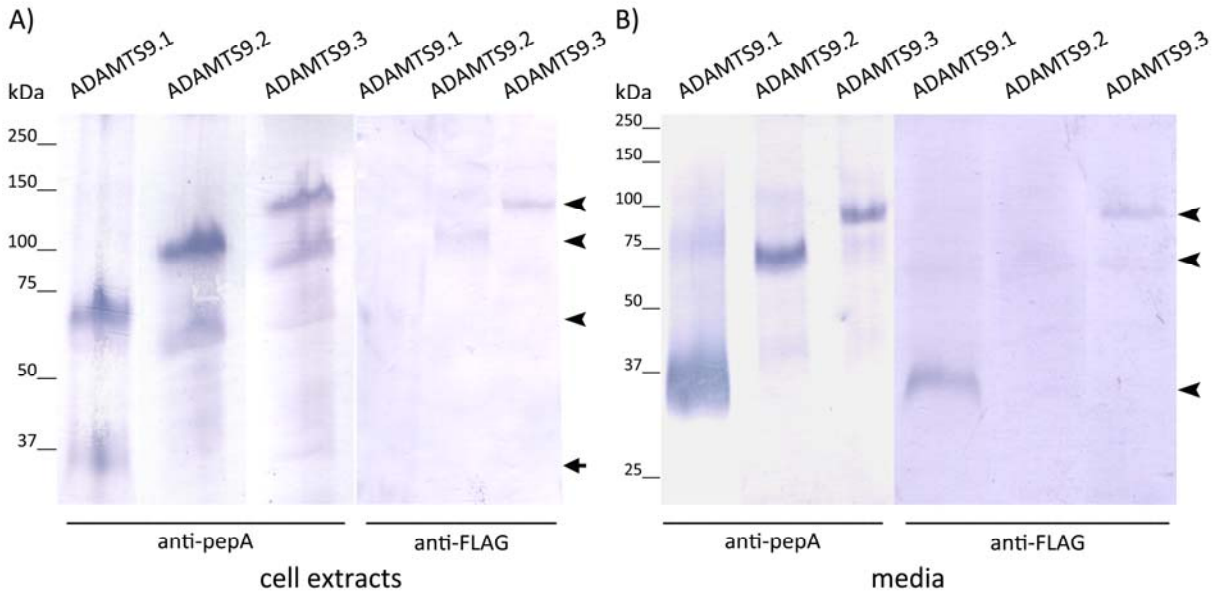

Figure 37. Analysis of the expression of the truncated chick ADAMTS9 variants in cell extracts and conditioned media by immunoblotting.

The three variants cloned into pSecTagFLAG vector were transiently expressed in 293F cells and detected with the rabbit anti-pepA antiserum or the monoclonal anti-FLAG M2 antibody. The zymogen forms were all detected in cell extracts (arrowheads in A), while the conditioned media contained faster migrating fragments most likely lacking the N-terminal propeptide (arrowheads in B). In cell extracts and in media, additional intermediary fragments were recognised with the anti-serum anti-pepA. The different variants were weakly detected by the monoclonal anti-FLAG antibody. Calculated sizes of ADAMTS9.1: zymogen 71.6 kDa, secreted form 40.1 kDa; ADAMTS9.2: zymogen 106.4 kDa, secreted form 74.9 kDa; ADAMTS9.3: zymogen 131.5 kDa, secreted form 100.1 kDa.

6.III.5 Enzymatic activity assays: chick ADAMTS9 variants / versican substrate

In order to test the versicanase activity of the three mimetics, the same protocol as described in the subpart 6.II.9 was used. Briefly, conditioned and concentrated media of 293F cells transiently transfected with the pSecTagFLAG vectors coding for the variants ADAMTS9.1, ADAMTS9.2 or ADAMT9.3 were incubated in presence of purified versican and then choindroitinase treated before analysis on SDS gels. As controls, the media from stable 293FT lines expressing the ADAMTS4.3, the mutant form E358A_ATS4.3 and the medium from the transient transfected 293F with the ADAMTS4.3_pSecTagFLAG vector were processed under identical conditions. In all samples treated with the shorter variants of chick ADAMTS9, the intact versican was present (arrowhead Fig.38). Versican was undetectable in both media containing the ADAMTS4.3 peptide, while in the negative control using the mutant E358A_ATS4.3 form, the intact versican core glycoprotein was detected by the rabbit antiserum against the chick GAGβ domain of versican. Hence, we found no evidence for a versicanase activity of recombinant full-length ADAMTS9 and its smaller mimetics under these experimental conditions.

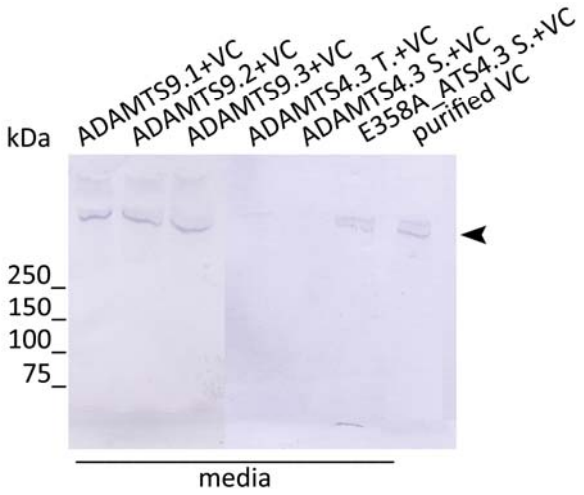

Figure 38. Analysis of the proteolytic activity of recombinant variants ADAMTS9.1, ADAMTS9.2 and ADAMTS9.3 towards purified chick V0/V1 versican.
Medium-treated chick V0/V1 versican (VC) samples were recognised with a rabbit antiserum against the GAG-β domain of chick versican. Samples were chondroitinase-digested before running on SDS-PAGE under reducing conditions. In ADAMTS4.3-treated samples from transiently (T) or stably (S) transfected cells, no intact versican core proteins were detected (empty lanes), while the mutant form of ADAMT4.3 (E358A_ATS4.3) did not cleave versican. In this assay ADAMTS9 variants expressed in the conditioned media did not show any versicanase activity (arrowhead).

6.III.6 *In vivo* studies of the effect of ADAMTS9 over-expression on axonal guidance in chick embryos. Preliminary data with ADAMTS9 DNA injection and electroporation

6.III.6.a ADAMTS9 injection and electroporation into the hind limb bud

In parallel to the functional studies *in vitro*, we investigated the function of ADAMTS9 *in vivo* in chick embryos. We hypothesised that a preterm ADAMTS9 expression in the hind limb during development would result in an early processing of versican and consequently in a premature extension of axons. For this purpose, pIRES and pMES expression vectors containing the full-length chick ADAMTS9 and/or a fluorescent marker protein (eGFP, YFP) were injected into the right hind limb bud next to the sciatic plexus and electroporated into the cells of the region. Different stages of development at the time of injection and diverse parameters utilised for limb bud electroporation were tested (Table.5). The non-injected limb bud served as control. To assess the efficiency of the electroporation and to visualize possible effects on axonal growth, the embryos were processed by whole mount staining of GFP-expressing cells and neurofilaments.

The survival rate was variable depending on the egg batches. We observed that the injection of the plasmids was easier at stage HH20/22, as embryos older than HH22 reacted by briskly moving, when the pipette was introduced into the hind limb. In all development stages tested, the diffusion of the injected mix within the whole hind limb was very fast and wide-spread.

Table 5. Conditions tested for injection and electroporation of plasmids into cells of the hind limb

Injection conditions vectors - development stage - electroporation parameters			Observations development stage - survival ratio - green cells
control eGFP_pIRES or ADAMTS9_pMES	HH19	25 V - 10 pulses	HH25/26 - 18.5% - few cells with control vector
control eGFP_pIRES + Lipofectamine	HH18	25 V - 5 pulses	HH25/26 - 45% - few cells
control YFP_pIRES	HH21/22	25 V - 5/7 pulses	HH25/26 - 75% - few cells
control YFP_pIRES or ADAMTS9_pIRES and E427A_pIRES + eGFP_pIRES	HH19/20	25 V - 5/7 pulses	HH25/26 - 80% - few cells with eGFP_pIRES
control eGFP_pIRES or ADAMTS9_pMES or ADAMTS9_pIRES + eGFP_pIRES	HH19/20	25 V - 5/7 pulses	HH25/26 - 64% - few cells with each construct
ADAMTS9_pMES or E427A_pMES	HH21/22	25 V - 5/7 pulses	HH25/26 - 30% - few cells with each construct
ADAMTS9_pMES or E427A_pMES	HH22/23	26 V - 5/10 pulses	HH26 - 27% - few cells with each construct

Among the embryos injected and electroporated with the ADAMTS9_pMES construct only 3% survived and displayed green epifluorescence (Fig.39). Despite the co-expression of ADAMTS9 in these fluorescent cells, no obvious difference in axonal growth was noticeable in the injected versus the control leg anlage. In general, it appeared that only a few cells had incorporated the plasmid and that the GFP expression was limited to the surface of the limb bud. Unfortunately, even though the functionality of the tested plasmids could be confirmed by detecting the GFP expression, the classical electroporation technique was under the various conditioned tested in this series too inefficient for an over-expression of our constructs in the developing hind limb.

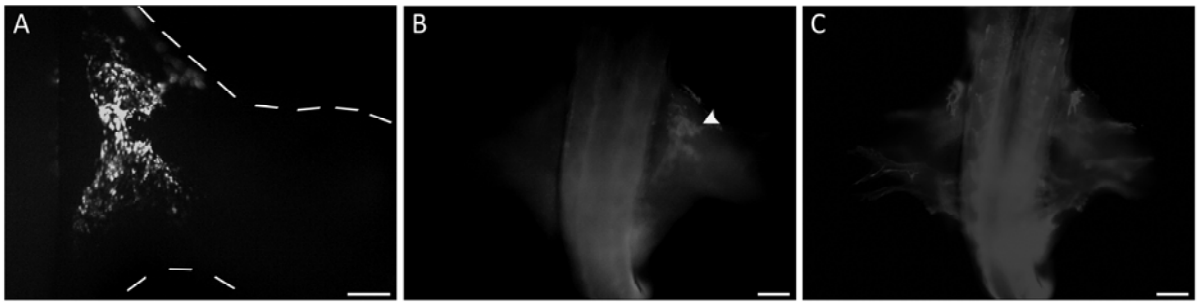

Figure 39. Injection and electroporation of ADAMTS9_pMES into the chick limb bud.
The ADAMTS9_pMES construct was injected and electroporated into the right hind limb of chick embryo (HH19). Epifluorescence of GFP was detected at the surface of the hind limb above the plexus region (panel A) in the HH21 chick embryo. In panel B, the expression of ADAMTS9_pMES detected by whole mount staining for the GFP revealed a weak expression in the hind limb (arrowhead). The whole mount immunostaining of neurofilaments showed no difference between the injected, electroporated hindlimb and the non-treated limb bud (panel C). The hind limb of the embryo in panel A is outline by a dotted line. Scale bar 200 µm.

6.III.6.b ADAMTS9 injection and electroporation into the central canal of the spinal cord

Since the standard electroporation method was inappropriate for over-expressing our constructs in the mesenchymal cells of the limb, the injection and electroporation of the expression vectors into the central canal of the spinal cord was used as alternative approach. This way, we investigated the effect of ADAMTS9 over-expression by the neurons themselves. We hypothesised that the forced ADAMTS9 expression in neurons would help to directly clear versican from the presumptive nerve pathways and thus, would permit their axons to extend earlier than normal into the limb bud. Among the injected embryos 67% survived. Despite the moderate GFP-expression observable by epifluorescence along the spinal cord (Fig.40A), GFP was not detectable in the neural cell bodies by the less sensitive immunofluorescence staining of cryosections or whole-mounts (data not shown). Of note, these embryos did not show any particular changes of axonal growth during limb innervation (Fig.40B-E). For these analyses treated and untreated sides of the electroporated embryos were compared.

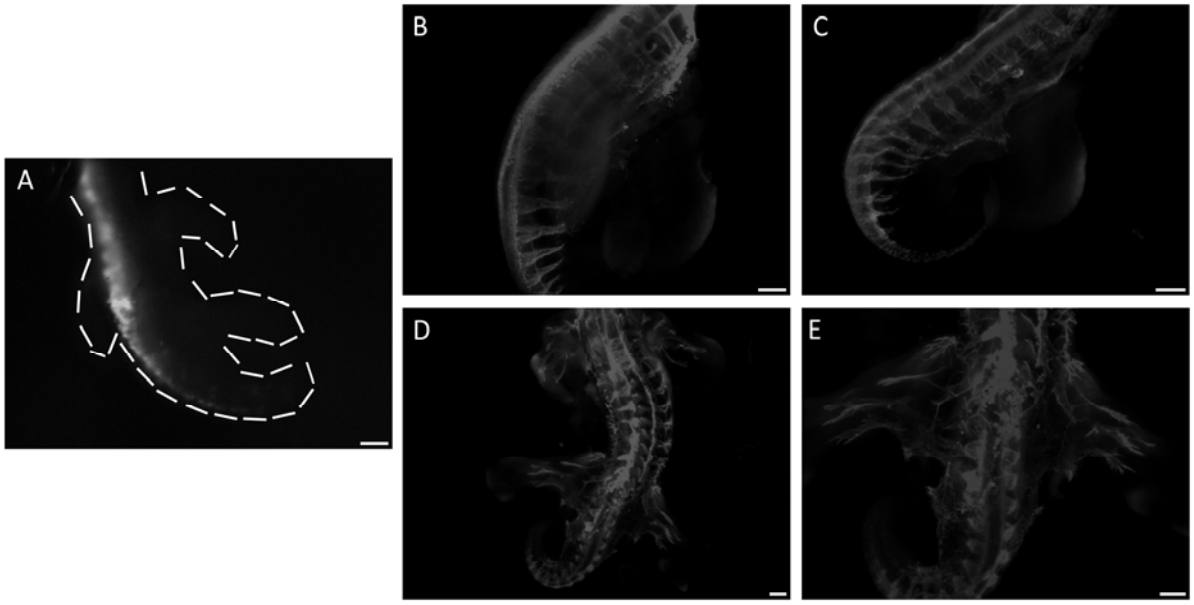

Figure 40. Injection and electroporation of ADAMTS9_pMES into the spinal cord.
The ADAMTS9_pMES construct was injected and electroporated into the central canal of the spinal cord at stage HH15. The epifluorescence of GFP expressed in the spinal cord was observed at HH22 (panel A). Whole mount staining of the neurofilaments was processed in embryos at stage HH22 (panel B), HH23 (panel C), HH26 (panels D and E). In panel C, a control embryo at HH23 is shown. The chick embryo is outlined by a dotted-line in panel A. Scale bar 200 µm.

From these different *in ovo* experiments, it appears that the classical injection/electroporation method is not yet optimally adapted to over-express our constructs in the hind limb. Further experiments with a more efficient gene transfer system such as sonoporation should also be

considered to finally achieve an effective ectopic expression of recombinant DNA in mesenchymal tissues *in vivo* (Ohta et al., 2008).

6.IV. Discussion

During development of the peripheral nervous system, active remodelling of the extracellular matrix occurs to allow the extension of growing axons through previously non-permissive regions (reviewed in (Barros et al., 2010)). In the previous chapter, the exact correlation between ADAMTS9 expression and the distribution of versican proteoglycan has been clearly demonstrated in hind limb throughout development of chicken embryos. Besides, different members of the ADAMTS metalloprotease family including ADAMTS9 were described to display hyalectanase properties in recent *in vitro* studies (reviewed in (Apte, 2009)). In this context, we hypothesised that ADAMTS9 plays a major role in the turnover of versican when expressed in barrier-tissues to growing axons. Thus, in this study, we focused our efforts on ADAMTS9 protease function in a regulated and active catabolism of versican.

First, expression vectors for the chick recombinant ADAMTS9 and the respective E427A_ATS9 mutant form were cloned and stable lines expressing these constructs were established. In order to detect the recombinant chick ADAMTS9, specific rabbit anti-sera (anti-pepA and anti-pepB antisera) directed against an epitope close to the catalytic domain of ADAMTS9 were developed. After testing the two antisera on purified peptides and on cell extracts of transiently transfected cells in western blot, the highly specific anti-pepA antiserum was selected for all subsequent analyses. A former *E.coli* exposure of the rabbit immunized with our peptide B might explain the reactivity of the anti-pepB antiserum against bacterial host proteins.

The expression of ADAMTS9 and its mutant variant in transient and stable mammalian cell lines were subsequently controlled by western-blot analyses and immunofluorescence staining.

The full length form of the enzyme and the inactive variant were detected in cell extracts of transient cell lines by two antibodies directed against different regions of the peptide, the anti-FLAG antibody recognising the C-terminal flag-tag of the recombinant proteins and the specific anti-pepA antiserum. In stable cell lines, additional non-characterised bands were detected by the anti-pepA antiserum in cell extracts of ADAMTS9 and E427A_ATS9 cell lines. These bands probably corresponded to degradation products of the recombinant protein. The integrity and homogeneity of the selected clones were demonstrated by an invariably ubiquitous fluorescent immunostain of ADAMTS9 or mutant peptides in stable cell lines preparations.

Afterwards, the expression of the enzymes in the selected stable lines was analysed in more detail in order to pursue functional studies. Among the different tested culture media, the SFMII medium appeared to be the most appropriate medium to express recombinant ADAMTS9. However, even though the full-length ADAMTS9 was expressed in cell extracts and different peptides were repeatedly identified in the media with the anti-pepA antiserum, the expected fragment corresponding to the pro-peptide lacking active form could not be detected in any of the tested media. Besides, the expression of the recombinant proteins was too weak to allow detection by the monoclonal anti-FLAG antibody in the cell extracts and concentrated media of stable lines. Consequently no purification via FLAG tag was feasible. It should be noted that in a recent study, similar problems to purify the full-length form of recombinant human ADAMTS9 has been reported (Koo et al., 2007).

To investigate the putative catalytic activity of the recombinant ADAMTS9, activity assays were designed with concentrated conditioned media of stable lines cultivated in suspension. The functionality of the activity assay was confirmed by the use of the medium of stable cells expressing the recombinant mouse ADAMTS4.3 variant, previously tested in our laboratory as a positive control. The concentrated medium containing recombinant mouse ADAMTS4.3 variant displayed proper hyalectanase activity towards chick purified versican. However, no activity could be demonstrated with ADAMTS9 medium. This unexpected result can partly be explained by insufficient levels of active peptide expressed in conditioned media. As mentioned above, the expression of recombinant ADAMTS9 was extremely weak in conditioned media from stable line, making its detection by immunoblot rather challenging even after medium concentration. The recombinant full-length ADAMTS9 is a 200 kDA long peptide. This large size may affect expression efficiency of the transfected cells. Expression might be enhanced in other alternative expression systems e.g employing adenoviruses, which are well known to confer high protein level expression levels in mammalian cells.

Hence, we decided to orientate the functional studies of ADAMTS9 to the expression of mimetics corresponding to potentially active truncated forms of the enzyme. In our previous experiments, diverse fragments were constantly detected in media of stable cells cultivated in suspension. The detailed analysis of these peptides revealed that they might correspond to products from specific processes of ADAMTS9. Indeed, different putative furin cleavage sites (at arginine residues n° 67, 277 and 1168) were identified in the chick ADAMTS9 peptide sequence. Moreover, previous works led by different groups have shown catalytic activity for shorter variants of the ADAMTS1, ADAMTS4 (Flannery et al., 2002; Gao et al., 2002; Kuno et al., 2000). In this context, the corresponding truncated variants (ADAMTS9.1, ADAMTS9.2 and ADAMTS9.3) carrying a FLAG-tag at their carboxyl terminus were cloned and transiently expressed in 293F cells.

As confirmed by immunoblots with the anti-pepA antiserum and the monoclonal anti-FLAG antibody, the zymogen forms of ADAMTS9.1, ADAMTS9.2 and ADAMTS9.3 were present in cell lysates. According to the fragment sizes, the respective mature enzymes corresponding to the pro-peptide lacking forms were also constantly recognised in media with the anti-pepA antiserum. However, only the putative ADAMTS9.1 mature form was always detected with the monoclonal anti-FLAG antibody, probably due to weak sensitivity of the anti-FLAG antibody. In the cell extracts of ADAMTS9.1, ADAMTS9.2 and ADAMTS9.3, additional smaller bands corresponding in size to the variants depleted of their pro-peptides were also identified with the anti-pepA antiserum. In addition, a band of about 70 kDa was visible in ADAMTS9.2 and ADAMTS9.3 cell extract preparations. These smaller fragments always present in cell extracts let suppose that intracellular or peri-cellular processing occurred for the recombinant forms of chick ADAMTS9 variants.

Apte and co-workers suggested a completely new mechanism regarding the processing regulation of the human ADAMTS9 enzyme (Koo et al., 2006). Like for other proteases, the ADAMTS9 pro-domain is removed from the zymogen form by the furin proprotein convertase. However, conversely to previous furin-mediated cleavages that have hitherto been described for other metalloproteases, the cleavage of human ADAMTS9 protease seems not to occur in the trans-Golgi compartment, but at the cell-surface of the 293F cells. Moreover, no intracellular processing of the prodomain could be identified in different cell types. These results were obtained with the recombinant full-length and a truncated form of human ADAMTS9 including the signal peptide, the prodomain and the catalytic domain, suggesting that the processing regulation was independent of the ancillary domain.

To confirm the nature and to precisely establish the origin of the diverse fragments of chick ADAMTS9 variants in cell lysates and media preparations, complementary experiments are needed. The immuno-precipitation with the anti-pepA antibody of peptides present in cell extracts and media preparations, followed by an immuno-detection with the anti-FLAG antibody would allow to identify which fragments are subject to C-terminal processing. Furthermore, it would allow a more sensitive detection of potential forms present, which are only weakly or not all visualised by the anti-FLAG antibody in conjunction with direct immunoblotting. Further experiments would be required to assess, whether the processed forms identified in cell extracts of all three chick recombinant variants are physiological products from furin and/or other proprotein convertases. For instance, use of specific proprotein convertases inhibitors such as dec-RVKR-cmk could be considered.

Since bands corresponding to the expected secreted forms were robustly recognised by the anti-pepA antiserum in media of all three variant cultures, we performed activity assays to test versicanase function of the variants with the respective concentrated conditioned media. Unexpectedly, none of the variants (ADAMTS9.1, ADAMTS9.2 or ADAMTS9.3) displayed

protease activity towards chick purified versican. While human ADAMTS9 has been described to cleave versican, no versicanase activity could be demonstrated with the diverse recombinant variants of chick ADAMTS9 in our various assays.

Initially, Apte and co-workers provide evidences of versicanase property for human recombinant ADAMTS9 in a cell-assay (Somerville et al., 2003). In this experiment, cells that transiently expressed ADAMTS9 or the truncated catalytic variant were rinsed and put in fresh serum free medium before adding purified bovine versican. The cleavage product, a processed versican fragment of 70 kDa was detected after overnight incubation. In another set of experiments (Koo et al., 2007), either conditioned media from transient cultures to test activity of the different ADAMTS9 constructs towards versican containing medium were used or a comparable cell-assay was employed. This frequent alteration of the experimental procedures used by this group may point to some difficulties they have encountered in handling ADAMTS9 protease and in analysing its putative activity. Furthermore, analyses of versicanase activity emanating from different constructs for human ADAMTS9 revealed a unique characteristic regarding metalloprotease activity regulation that has not been described yet (Koo et al., 2007). The recombinant full-length ADAMTS9 zymogen was catalytically active and even more efficient in cleaving versican than the processed form missing the N-terminal propeptide domain, although the propetide-lacking forms usually correspond to the active form of metalloproteases. Again, this astonishing result showed the unpredictability and the complexity of mechanisms controlling ADAMTS9 functions. In a recent study, an original mechanism for ADAMTS9 proenzyme processing regulation has been suggested (Koo and Apte, 2010). In this paper, they showed that ADAMTS9 proenzyme and furin convertase associate together at the cell surface in a complex including members of the HSP90 chaperones family. Furthermore, these chaperone proteins participate by interacting very likely with furin in modulating the propeptide domain cleavage and in the secretion of the ADAMTS9 catalytic form.

In summary, these data and our results lead to the hypothesis that ADAMTS9 is subject to a unique regulation mechanism differing from the activation pocess known from other metalloproteases. Furthermore, we can assume that its versicanase function should be accurately regulated.

Beside the functional *in vitro* studies, we investigated in parallel the putative role of ADAMTS9 *in vivo* during development of chicken embryos. In the second chapter, we have demonstrated an obvious correlation between ADAMTS9 expression and versican distribution in developing hind limb, at particular points in time when nerve invasion should take place. Thus, we hypothesised that an early induced expression of ADAMTS9 in the hind limb would engender premature versican cleavage and therefore provoke precocious extension of axons in the limb bud.

For this purpose, different expression vectors containing our deduced chick ADAMTS9 or the E427A_ATS9 mutant construct under control of the chick β-actin promoter were generated. Then the vectors were injected and electroporated into the hind limb of chicken embryos at different stages of development. Either our construct was expressed simultaneously with a fluorescent marker protein (eGFP) from a bicistronic vector (pMES), or a separate vector coding for a fluorescent marker protein (YFP_pIRES or eGFP_pIRES) was used in parallel of our construct to visualise the site of injection/electroporation. Despite multiple attempts employing different parameters of injection and electroporation, only a few cells in some embryos displayed green epifluorescence. Analyses of injected embryos by whole mount staining of GFP-expressing cells and neurofilaments did not reveal any difference between the injected limb bud and the non-treated side of embryos. Because no evidence of a potential ADAMTS9 effect on axon growth could be established by these means, another experimental approach was tested to evaluate the impact of ADAMTS9 over-expression *in vivo*. The expression vectors were injected into the central canal of the spinal cord. In this setting, we hypothesised that ADAMTS9 overexpressing neurons would clear up their routes from versican and in consequence extend their axons earlier than usually observed in normal hind limb. Despite the fact that the functionality of expression vectors was again proven by the presence of green-cells, no consequence on axon growth was observed, when comparing axon routing on both sides of the spinal cord at the entrance of limb buds.

In our set of *in vivo* experiments, different technical problems were regrettably encountered, making the observations and drawing conclusions from this part of the study rather difficult. Even though the functionality of expression vectors was proven by the presence of green cells in electroporated regions, the epifluorescence coming from cells transfected with the eGFP_pIRES or eGFP_pMES vectors were less intense than that one observed with the YFP_pIRES control vector. Thus, use of the YFP_pIRES vector in parallel of the tested construct should be preferred in future trials. In spite of numerous injected and electroporated embryos, only a small number survived and could be processed up to the final whole mount staining treatment, restraining considerably the panel of analysable specimens. Another major difficulty seemed to be associated with the technique itself. Injections and electroporations of the plasmids in the hind limb were largely inefficient. Indeed, the mesenchymal tissue permits considerable and rapid diffusion of the preparation mix into the extracellular space, thus impeding the correct and precise integration of the plasmids into cells. Another gene transfer approach should be seriously considered in order to efficiently express specific constructs into mesenchymal tissues of the limb bud. Lately, a couple of studies emphasized the efficiency and accuracy of gene transduction by sonoporation in different types of cells, tissues and organisms (Fischer et al., 2006; Li et al., 2009; Liu et al., 2006). Interestingly, the injection of DNA-microbubble mixture preparation into the region of

interest followed by exposure of the ultrasound to the targeted tissues, allowed to obtain successful gene expression especially in the developing limb bud of chicken embryos (reviewed in (Ohta et al., 2008)). Therefore, the use of sonoporation might be of great interest to express recombinant cDNAs and to study roles of specific proteins in axonal guidance, in particular in the hind limb during chick development.

7. General discussion

During the development of vertebrates, the migrating neural precursor cells and growing axons are orientated towards their appropriate target regions through a coordinated action of repelling and attracting guidance forces. Among the different signals playing a role in these processes, the hyalectan versican is believed to participate as a non-permissive component for growing axons in development of chick embryos.

Indeed, previous work from our laboratory showed that versican V0/V1 isoforms are selectively expressed in barriers tissues of neural crest cells and outgrowing axons (Landolt et al., 1995). In addition, versicans V0/V1 were shown to inhibit the migration of neural crest cells *in vitro*, and this function was mostly triggered by the core protein of the hyalectans (Dutt et al., 2006). Together, these studies provided evidence for a versican role in guiding neural crest cells and extending axons throughout embryonic trunk development.

Thus, the general aim of the presented project was to assess more specifically the putative role of versican in axonal guidance of the peripheral nervous system during development of chick embryos. Towards this aim, functional studies regarding sensory-motor innervation of the hind limb were carried out in *in vitro* assays and in *in vivo* experiments.

We confirmed that versican was the main proteoglycan expressed in transient mesenchymal barriers from limb bud and trunk of chick embryos. Furthermore, the stripe choice assays and analyses by time-lapse microscopy of neurite growth clearly proved the overriding inhibitory effect of versican on axonal growth of DRG neurons *in vitro*, whereas neuronal cells were cultivated in neurite growth promotion supporting substrates. Likewise *in vivo*, we could demonstrate that repeated ectopical deposition of versican V1 and V0/V1 splice-variants in the nerve pathways caused severe disturbances of growing nerves in the hind limb, such as aberrant axon routings and defasciculation of extending neurites from the sciatic nerve *in ovo*.

The inhibitory property of versican V0/V1 induced, in a concentration dependent way, conformational changes leading to growth cone collapse and axonal retraction. This observation suggests that versican does not only act as a simple physical barrier but might activate downstream signalling pathways involved in the rapid remodelling of the cytoskeleton at the leading edge. Especially, downstream effectors/modulators of the RhoGTPases pathways have been shown to mediate inhibitory effects of the chondroitin sulphates proteoglycans (CSPGs). For instance, CSPG activation of the Rho pathway resulted in the expression of different protein kinase C isoforms which transduced the inhibitory signal blocking axonal regeneration (Sivasankaran et al., 2004). Besides, the activation of RhoA by versican V2 via independent p75NTR/NgR pathways was also shown to inhibit axonal growth (Schweigreiter et al., 2004). Currently, no specific receptor for

versican has been identified. Versican might interact with the epidermal growth factor receptor (EGFR) by the EGF-like sequence in the G3 domain. The EGFR has also been proposed to mediate the inhibition of axon regeneration by CSPGs (Koprivica et al., 2005). However in another study, the expression of the recombinant versican G3 domain alone promoted neurite growth by activation of the EGFR (Xiang et al., 2006), suggesting that other domains might be involved in evoking the inhibitory response towards versicans.

From our experiments, it appears that the core protein of versican is mainly conferring the inhibitory property, while the GAG chains possibly modulate the versican function by interacting with putative partners and by preserving structural stability. Moreover, the distribution of versican is tempo-spatially inversely related to the extension of growing axons from the crural and sciatic plexi into the hind limb. Indeed, the distribution of versican appears to be specifically regulated throughout the development, since in early chick embryos, the entire limb bud expresses the V0/V1 isoforms, while only a few stages later, the versican localisation is restricted to the prechondrogenic zone of the forming pelvic girdle and the femur (Landolt et al., 1995). These data let us hypothesise that an active turnover by specific proteases might regulate the function of the versican core protein and therefore influences the axonal guidance processes. Additionally, specific ADAMTS metalloproteases were described to cleave hyalectans in *in vitro* assays (reviewed in (Apte, 2009)). Interestingly, ADAMTS1 and ADAMTS9, potential versicanases, were shown to be expressed in embryos throughout mouse development (Jungers et al., 2005; Thai and Iruela-Arispe, 2002).

In this context, we first determined the expression patterns of the ADAMTS candidates in chick embryos with *in situ* hybridisation. Akin to the expression pattern of ADAMTS9 in mice, we detected a wide expression of ADAMTS9 in chick embryos. As described before (Landolt et al., 1995), we confirmed by immunofluorescence stainings that versican disappeared from the limb anlage, while nerve fibres from the plexus regions grew into the limb bud. Furthermore, the ADAMTS9 expression profile was perfectly matching with the distribution of versican during limb bud development. Since ADAMTS1 expression in chick embryos was not relevant after analysis by *in situ* hybridisation, we focused our attention on the putative role of ADAMTS9. After cloning the full-length of chick ADAMTS9 cDNA, differences were observed between our sequence and the reported cDNA sequence in the chick genome (ENSGALT00000011955). Although ADAMTS9 is the most highly conserved member of the ADAMTS-family (Somerville et al., 2003), these discrepancies between the sequences might be explained by inter-hatchery strain variability.

In order to identify ADAMTS9 as a specific protease of versican, recombinant full-length ADAMTS9 or variants were expressed together with versican *in vitro*. Although the versicanase function of recombinant human ADAMTS9 was demonstrated *in vitro*

(Somerville et al., 2003) and the profile expression of the metalloprotease correlated with the distribution of versican in chick embryos, no enzymatic activity of our recombinant full-length ADAMTS9 or variants could be observed towards purified chick versican. This might be linked to the possibility that chick ADAMTS9 is only a minor protease involved in versican turnover or that this metalloprotease interacts with other ADAMTS members to process versican. Indeed, recent genetic studies in mice revealed a cooperative function of *Adamts9* and two other versicanases, the close homologues *Adamts20* and *Adamts5* (Longpre et al., 2009; Silver et al., 2008). Silver and colleagues showed that *Adamts20* mediated survival of neural crest derived melanoblasts via Kit signalling and that *Adamts9* also participated in the development of the melanoblasts in the trunk and in the head (Silver et al., 2008). Besides, they demonstrated that medium from cells expressing recombinant ADAMTS20 cleaved versican and that *Adamts20* was required for versican processing in the skin. Analyses of single and double deleted mice for *Adamts9* and *Adamst20* provided evidence for the collaborative function in the closure of the secondary palate (Enomoto et al., 2010). The authors suggested that ADAMTS9 expressed in capillaries and ADAMTS20 expressed in the mesenchyme collaborate in the proteolysis of versican to ensure correct palatogenesis. In another development process, the combinatory functions of *Adamts5*, *Adamts9* and *Adamts20* were demonstrated to be involved in interdigital web regression (McCulloch et al., 2009b). In this publication, they showed that these three metalloproteases interacted to cleave versican and generate active versican fragments that mediate apoptosis to eliminate cells in the interdigital web. Interestingly, versican cleavage appears to be required in web regression and in palatogenesis at the same developmental age.

From analysis of ADAMTS5 expression patterns in mouse, ADAMTS5 appears to be the most promising partner of ADAMTS9 in limb bud remodelling and appears to constitute the sole metalloprotease directly involved in versican turnover during limb innervation (McCulloch et al., 2009a). Actually, ADAMTS5 is associated to several peripheral nervous system components. During development, it is expressed in trunk segmental nerves, from E12.5 to E14.5 in emerging nerves in hind limb, in developing root ganglia, and in neural-associated Schwann cells precursors (McCulloch et al., 2009a). In adults, ADAMTS5 is present in dorsal root ganglia and their associated spinal nerve roots, in the perinerium and in nerve fibres of the sciatic nerve and in Schwann cells (McCulloch et al., 2009a). In the chick, innervation of the hind limb starts after HH24, corresponding to stage E12.5 in the mouse. In parallel, versican disappears from HH24-25 to be extremely restricted at stage HH27, which is comparable to E13.5. From these data, we speculate that ADAMTS5 expressed by peripheral nerves contributes towards cleavage of versican and regulation of axonal guidance. This ADAMTS5 function might take place through interaction with

ADAMTS9 expressed in mesenchymal tissues. Thus, ADAMTS5 represents an interesting candidate for future investigation.

Using the chick model for studying the different processes during development has many advantages, due to the easy access to embryos (reviewed in (Stern, 2005)). However, the incomplete sequencing of the chick genome still forms a certain obstacle, which we were also confronted with during this project. Once the chick genome sequencing is completed, it should be easier to study the exact role of different genes, in particular those which are fine-tuned during embryogenesis. The findings collected from the chick-model could be of general importance to understand the development of a functional neuronal network which could also pertain to vertebrates including humans.

8. Abbreviations

ADAM	A Disintegrin And Metalloprotease
ADAMTS	A Disintegrin And Metalloprotease with Thrombospondin type 1 motifs
BDNF	Brain-Derived Neurotrophic Factor
BMP	Bone Morphogenic Protein
CAM	Cell Adhesion Molecule
CHL1	Close Homologue of L1
Comm	Commissureless
COS	CV-1 in Origin and carrying the SV40
Cos2	kinesin Costal 2
CNS	Central Nervous System
CRP	Complement Regulatory Protein
CS	Chondroitin Sulphate
CSPG	Chondroitin Sulphate Proteoglycans
DCC	Deleted in Colorectal Cancer
DRG	Dorsal Root Ganglia
DREZ	Dorsal Root Entry Zone
DS	Dermatan Sulphate
DSCAM	Down Syndrome Cell Adhesion Molecule
ECM	Extracellular Matrix
EGF	Epidermal Growth Factor
EGFR	Epidermal Growth Factor Receptor
ERK	Extracellular-signal-Regulated Kinase
FGF	Fibroblast Growth Factor
FGFR	Fibroblast Growth Factor Receptor
Fu	Fused protein
Fz	Frizzled
GAG	Glycosaminoglycan
GDGF	Glial-Derived Growth Factor
GHAP	Glial Hyaluronate binding protein
GPI	Glycosylphosphatidylinositol
HA	Hyaluronic Acid
HEK	Human Embryonic Kidney
HGF	Hepatocyte Growth Factor
HH	Hamburger and Hamilton
HS	Heparan Sulphate
HSPG	Heparan Sulphate Proteoglycans
KS	Keratan Sulphate
LMC	Lateral Motor Columns
LMCm	medial Lateral Motor Columns
LTP	Long Term Potentiation
mdDA	mesodiencephalon DopAminergic neurons
NCC	Neural Crest Cell
NGF	Nerve Growth Factor
Npn	Neuropilin
NRG	Neuregulin
NT	Neurotrophin
PCP	Planar Cell Polarity
PKC	Protein Kinase C
PI3K	Phosphatidylinositol 3-kinase
PNA	Peanut Agglutinin
PNN	Perineural net
PNS	Peripheral Nerve System
Ptc	Patched

$p75^{NTR}$	p75 neurotrophin receptor
RGC	Retinal Ganglion Cells
Robo	Roundabout
SCF	Stem Cell Factor
SFK	Src-Family Kinase
Sfrp	Secreted frizzled-related protein
Shh	Sonic hedgehog
Smo	Smoothened
SLRP	Small Leucin-Rich Protein
TGFβ	Transforming Growth Factor β
TN	Tenascin
TSP-1	Thrombospondin type-1 like repeat
Trk	Tropomyosin-related kinase
UNC	Uncoordinated
vWF	von Willebrand Factor

9. Lists of figures and tables

9.I. List of figures

Figures article:

9.II. List of tables

10. Annexes

```
Ensembl ADAMTS9 MQLAPLALALTTLFIDGLRTGARRQKLHPRQAKLLEKLSEYEIVTPTRVNEFGEPFPTDV 60
cloned ADAMTS9  MQLAPLALALTTLFIDGLRTGARRQKLHPRQAKLLEKLSEYEIVTPTRVNEFGEPFPTDV 60
               ************************************************************

Ensembl ADAMTS9 HFRRRRRSTNAAPDAWTAAAASSSSSPKAHYRLSAFGQQFLFNLTASSAFIAPLFTVSIL 120
cloned ADAMTS9  HFRRRRRSTNAAPDAWTAAAASSSSSPKAHYRLSAFGQQFLFNLTASSAFIAPLFTVSIL 120
               ************************************************************

Ensembl ADAMTS9 GEPAAEQRNLYAETADTDVKHCFYRGHVNARPRHTAVISLCSGMLGTFKSDDGDYFVEPL 180
cloned ADAMTS9  GEPAAEQRNLYAETADTDVKHCFYRGHVNARPRHTAVISLCSGMLGTFKSDDGDYFVEPL 180
               ************************************************************

Ensembl ADAMTS9 LSLEQEYEEEHNKPHLVYRHRTPPTNSSGDRQTCDTPDHEHSHKKSKRKHWRKQWVESSL 240
cloned ADAMTS9  LSLEQEYEEEHNKPHLVYRHRTPPTNSSGDRQTCDTPDHEHSHKKSKRKHWRKQWVESSL 240
               ************************************************************

Ensembl ADAMTS9 LSDTEMLKHSLEVNPFSADSNETGNASEKKSHRRTKRFLSYPRFVEVMVVADSRMVAYHG 300
cloned ADAMTS9  LSDTEMLKHSLEVNPFSADSNETGNASEKKSHRRTKRFLSYPRFVEVMVVADSRMVAYHG 300
               ************************************************************

Ensembl ADAMTS9 ANLQHYVLTLMSIVASIYKDPSIGNLINIVIVKLVVIHNEQDGPAISYNAQTTLKNFCQW 360
cloned ADAMTS9  ANLQHYVLTLMSIVASIYKDPSIGNLINIVIVKLVVIHNEQDGPAISYNAQTTLKNFCQW 360
               ************************************************************

Ensembl ADAMTS9 QQSQNHPEGSHLQHDTAVLVTRQDICRAHDKCDTLGLAELGTVCDPYRSCSISEDNGLST 420
cloned ADAMTS9  QQSQNHPEGSHLQHDTAVLVTRQDICRAHDKCDTLGLAELGTVCDPYRSCSISEDNGLST 420
               ************************************************************

Ensembl ADAMTS9 AFTIAHELGHVFNMPHDDNHKCKEDGGKNQQHVMAPTLNFYTNPWMWSKCSRKYITEFLD 480
cloned ADAMTS9  AFTIAHELGHVFNMPHDDNHKCKEDGGKNQQHVMAPTLNFYTNPWMWSKCSRKYITEFLD 480
               ************************************************************

Ensembl ADAMTS9 TGYGECLLDEPSSRTYALPQQLPGLIYDVNKQCELIFGPGSQVCPYMMQCRRLWCINIDG 540
cloned ADAMTS9  TGYGECLLDEPSSRTYALPQQLPGLIYDVNKQCELIFGPGSQVCPYMMQCRRLWCINIDG 540
               ************************************************************
                         disintegrin
Ensembl ADAMTS9 AHKGCRTQHTPWADGTECEPGKHCRFGMCVPKEREAPVVDGAWGTWSPFGTCSRTCGGGI 600
cloned ADAMTS9  AHKGCRTQHTPWADGTECEPGKHCRFGMCVPKEREAPVVDGAWGTWSPFGTCSRTCGGGI 600
               ************************************************************
                                                  TSP-1 1
Ensembl ADAMTS9 KTAIRECNRPEPKNGGKYCVGRRMKFKSCNTEPCSKLKKDFRDEQCADFDGKHFNINGLP 660
cloned ADAMTS9  KTAIRECNRPEPKNGGKYCVGRRMKFKSCNTEPCSKLKKDFRDEQCADFDGKHFNINGLP 660
               ************************************************************

Ensembl ADAMTS9 TNVRWVPKYSGILMKDRCKLFCRVAGNTAYYQLRDRVIDGTPCGPDTNDICVQGLCRQAG 720
cloned ADAMTS9  TNVRWVPKYSGILMKDRCKLFCRVAGNTAYYQLRDRVIDGTPCGPDTNDICVQGLCRQAG 720
               ************************************************************

Ensembl ADAMTS9 CDHVLNSKARRDKCGVCGGDNSSCKTVAGTFNTVHYGYNVVVRIPAGATNIDVRQHSYSG 780
cloned ADAMTS9  CDHVLNSKARRDKCGVCGGDNSSCKTVAGTFNTVHYGYNVVVRIPAGATNIDVRQHSYSG 780
               ************************************************************
                                  spacer
Ensembl ADAMTS9 KPEDDNYLALSNSQGDFILNGDFVVSMFKREIKVGNAVIEYSGSDNAIERINSTDRIEQE 840
cloned ADAMTS9  KPEDDNYLALSNSQGDFILNGDFVVSMFKREIKVGNAVIEYSGSDNAIERINSTDRIEQE 840
               ************************************************************

Ensembl ADAMTS9 ITLQVLSVGNLYNPDVRYTFNIPIEDKPQQFYWNAYGPWQPCSKLCQGERKRKPVCTRES 900
cloned ADAMTS9  ITLQVLSVGNLYNPDVRYTFNIPIEDKPQQFYWNAYGPWQPCSKLCQGERKRKPVCTRES 900
               ************************************************************
                                        2
Ensembl ADAMTS9 DQLTVSDQRCDRIPQPDPITEPCGTECELRWHIARRSECTAQCGLGYRMLEIYCSKYNRL 960
cloned ADAMTS9  DQLTVSDQRCDRIPQPDPITEPCGTECELRWHIARRSECTAQCGLGYRMLEIYCSKYNRL 960
               ************************************************************
                                        3

Ensembl ADAMTS9 EGKTEKVDDRFCSSQAKPSTREKCTGDCNVGGWRYSAWTECSKSCGGGTRRRRAMCVSTY 1020
```

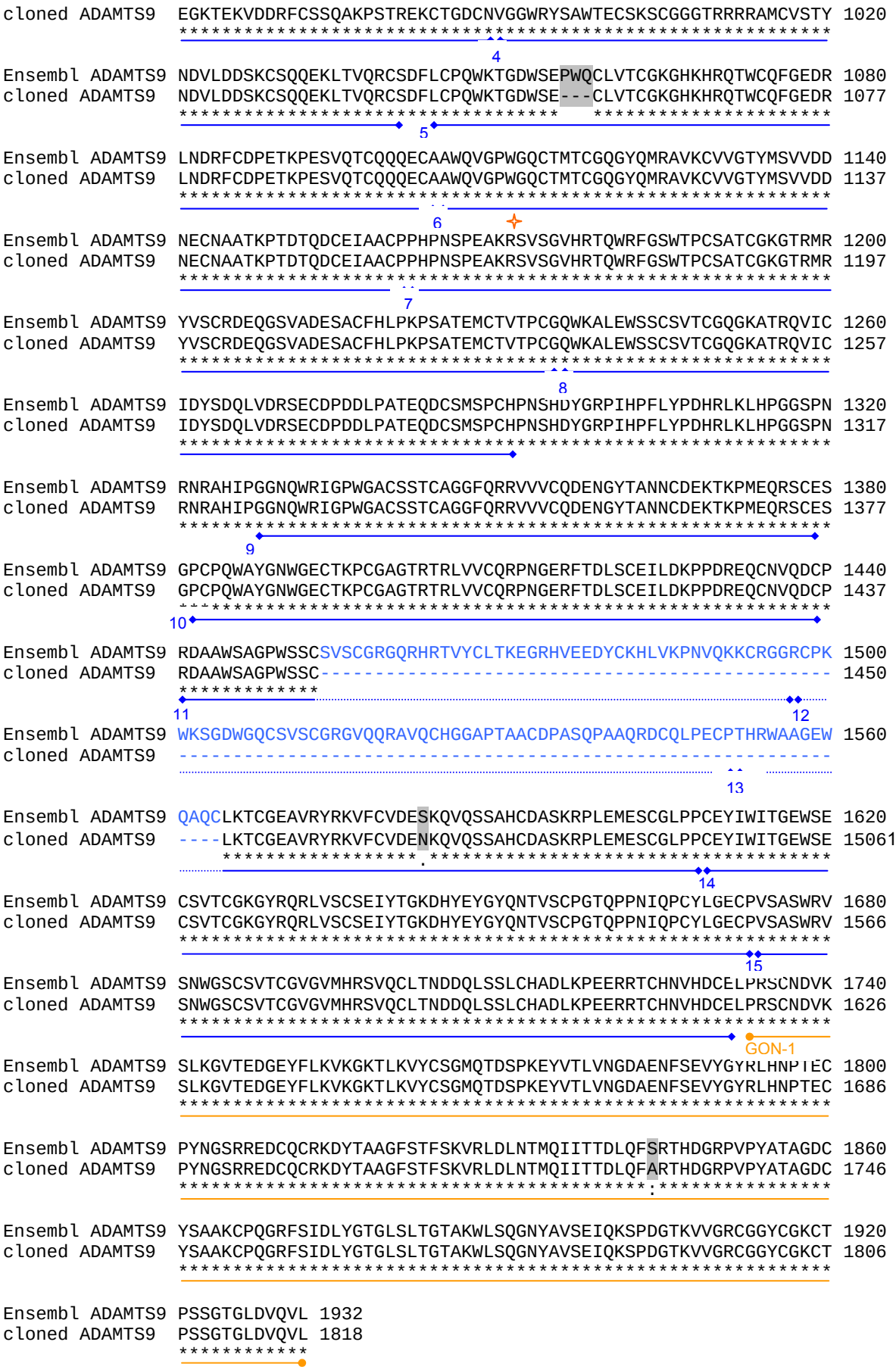

Annexe 1. Alignment of the chick ADAMTS9 translated sequences obtained from predicted cDNA sequence from Ensembl and from cloned cDNA. The prodomain is indicated in bold font, the

consensus sequence of the catalytic site is written in blue and the start of the different subsequent domains are identified with an arrow under the corresponding sequence. TSP1: Thrombospondin type 1 like domain with the related number. GON-1 domain is underlined in orange. GON-1 refers to the product of *gon-1* gene in *C.Elegans.* The putative furin cleavage sites are indicated by an asterisk. The mismatched amino-acids between the predicted sequence from Ensembl and the obtained cDNA in chick are shaded. The TSP sequence corresponding to the missing part in the cloned ADAMTS9 is written in light blue. Single letter code is used for amino-acids sequences.

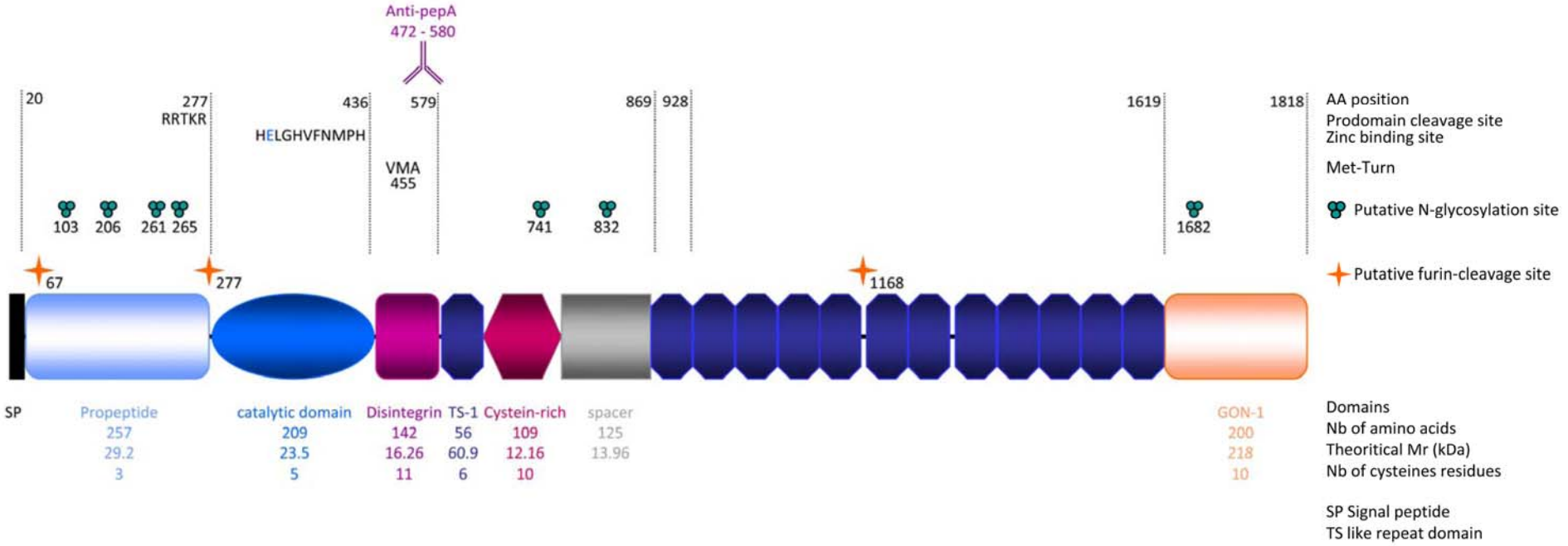

Annexe 2. The domain structure and features of chick deduced ADAMTS9 peptide.

The schematic shows the structural motifs in chick ADAMTS9 with corresponding theoretical Mr, number of amino acids and cysteine residues, the zinc-binding sequence and putative furin cleavage sites. The location of the epitope recognized by the rabbit anti-pepA antiserum is depicted by an antibody symbol. Amino acid sequences are written in single-letter code. Abbreviations: ADAMTS, a disintegrin and metalloproteinase with thrombospondin motifs; Mr, molecular weight; TS-1, thrombospondin type 1 motif (named as well TS like repeat domain or TSP-1).

11. Bibliography

A

Abbaszade, I., Liu, R. Q., Yang, F., Rosenfeld, S. A., Ross, O. H., Link, J. R., Ellis, D. M., Tortorella, M. D., Pratta, M. A., Hollis, J. M. et al. (1999). Cloning and characterization of ADAMTS11, an aggrecanase from the ADAMTS family. *J Biol Chem* **274**, 23443-50.
Andrews, G. L., Tanglao, S., Farmer, W. T., Morin, S., Brotman, S., Berberoglu, M. A., Price, H., Fernandez, G. C., Mastick, G. S., Charron, F. et al. (2008). Dscam guides embryonic axons by Netrin-dependent and -independent functions. *Development* **135**, 3839-48.
Ang, L. C., Zhang, Y., Cao, L., Yang, B. L., Young, B., Kiani, C., Lee, V., Allan, K. and Yang, B. B. (1999). Versican enhances locomotion of astrocytoma cells and reduces cell adhesion through its G1 domain. *J Neuropathol Exp Neurol* **58**, 597-605.
Apte, S. S. (2009). A disintegrin-like and metalloprotease (reprolysin-type) with thrombospondin type 1 motif (ADAMTS) superfamily: functions and mechanisms. *J Biol Chem* **284**, 31493-7.
Arikawa-Hirasawa, E., Watanabe, H., Takami, H., Hassell, J. R. and Yamada, Y. (1999). Perlecan is essential for cartilage and cephalic development. *Nat Genet* **23**, 354-8.
Asher, R. A., Morgenstern, D. A., Fidler, P. S., Adcock, K. H., Oohira, A., Braistead, J. E., Levine, J. M., Margolis, R. U., Rogers, J. H. and Fawcett, J. W. (2000). Neurocan is upregulated in injured brain and in cytokine-treated astrocytes. *J Neurosci* **20**, 2427-38.
Asher, R. A., Morgenstern, D. A., Shearer, M. C., Adcock, K. H., Pesheva, P. and Fawcett, J. W. (2002). Versican is upregulated in CNS injury and is a product of oligodendrocyte lineage cells. *J Neurosci* **22**, 2225-36.
Aspberg, A., Binkert, C. and Ruoslahti, E. (1995). The versican C-type lectin domain recognizes the adhesion protein tenascin-R. *Proc Natl Acad Sci U S A* **92**, 10590-4.
Aspberg, A., Miura, R., Bourdoulous, S., Shimonaka, M., Heinegard, D., Schachner, M., Ruoslahti, E. and Yamaguchi, Y. (1997). The C-type lectin domains of lecticans, a family of aggregating chondroitin sulfate proteoglycans, bind tenascin-R by protein-protein interactions independent of carbohydrate moiety. *Proc Natl Acad Sci U S A* **94**, 10116-21.
Asundi, V. K., Erdman, R., Stahl, R. C. and Carey, D. J. (2003). Matrix metalloproteinase-dependent shedding of syndecan-3, a transmembrane heparan sulfate proteoglycan, in Schwann cells. *J Neurosci Res* **73**, 593-602.
Augsburger, A., Schuchardt, A., Hoskins, S., Dodd, J. and Butler, S. (1999). BMPs as mediators of roof plate repulsion of commissural neurons. *Neuron* **24**, 127-41.

B

Barnea, G., Grumet, M., Milev, P., Silvennoinen, O., Levy, J. B., Sap, J. and Schlessinger, J. (1994). Receptor tyrosine phosphatase beta is expressed in the form of proteoglycan and binds to the extracellular matrix protein tenascin. *J Biol Chem* **269**, 14349-52.
Barnes, S. H., Price, S. R., Wentzel, C. and Guthrie, S. C. (2010). Cadherin-7 and cadherin-6B differentially regulate the growth, branching and guidance of cranial motor axons. *Development* **137**, 805-14.
Barros, C. S., Franco, S. J. and Muller, U. (2010). Extracellular Matrix: Functions in the Nervous System. *Cold Spring Harb Perspect Biol*.
Beggah, A. T., Dours-Zimmermann, M. T., Barras, F. M., Brosius, A., Zimmermann, D. R. and Zurn, A. D. (2005). Lesion-induced differential expression and cell association of Neurocan, Brevican, Versican V1 and V2 in the mouse dorsal root entry zone. *Neuroscience* **133**, 749-62.
Bekku, Y., Vargova, L., Goto, Y., Vorisek, I., Dmytrenko, L., Narasaki, M., Ohtsuka, A., Fassler, R., Ninomiya, Y., Sykova, E. et al. (2010). Bral1: its role in diffusion barrier formation and conduction velocity in the CNS. *J Neurosci* **30**, 3113-23.

Bespalov, M. M., Sidorova, Y. A., Tumova, S., Ahonen-Bishopp, A., Magalhaes, A. C., Kulesskiy, E., Paveliev, M., Rivera, C., Rauvala, H. and Saarma, M. (2011). Heparan sulfate proteoglycan syndecan-3 is a novel receptor for GDNF, neurturin, and artemin. *J Cell Biol*.
Bloechlinger, S., Karchewski, L. A. and Woolf, C. J. (2004). Dynamic changes in glypican-1 expression in dorsal root ganglion neurons after peripheral and central axonal injury. *Eur J Neurosci* **19**, 1119-32.
Bode-Lesniewska, B., Dours-Zimmermann, M. T., Odermatt, B. F., Briner, J., Heitz, P. U. and Zimmermann, D. R. (1996). Distribution of the large aggregating proteoglycan versican in adult human tissues. *J Histochem Cytochem* **44**, 303-12.
Bonanomi, D. and Pfaff, S. L. (2010). Motor axon pathfinding. *Cold Spring Harb Perspect Biol* **2**, a001735.
Bourikas, D., Pekarik, V., Baeriswyl, T., Grunditz, A., Sadhu, R., Nardo, M. and Stoeckli, E. T. (2005). Sonic hedgehog guides commissural axons along the longitudinal axis of the spinal cord. *Nat Neurosci* **8**, 297-304.
Bovolenta, P., Rodriguez, J. and Esteve, P. (2006). Frizzled/RYK mediated signalling in axon guidance. *Development* **133**, 4399-408.
Brakebusch, C., Seidenbecher, C. I., Asztely, F., Rauch, U., Matthies, H., Meyer, H., Krug, M., Bockers, T. M., Zhou, X., Kreutz, M. R. et al. (2002). Brevican-deficient mice display impaired hippocampal CA1 long-term potentiation but show no obvious deficits in learning and memory. *Mol Cell Biol* **22**, 7417-27.
Brew, K. and Nagase, H. (2010). The tissue inhibitors of metalloproteinases (TIMPs): an ancient family with structural and functional diversity. *Biochim Biophys Acta* **1803**, 55-71.
Brose, K., Bland, K. S., Wang, K. H., Arnott, D., Henzel, W., Goodman, C. S., Tessier-Lavigne, M. and Kidd, T. (1999). Slit proteins bind Robo receptors and have an evolutionarily conserved role in repulsive axon guidance. *Cell* **96**, 795-806.
Bruckner, G., Grosche, J., Schmidt, S., Hartig, W., Margolis, R. U., Delpech, B., Seidenbecher, C. I., Czaniera, R. and Schachner, M. (2000). Postnatal development of perineuronal nets in wild-type mice and in a mutant deficient in tenascin-R. *J Comp Neurol* **428**, 616-29.
Bulow, H. E. and Hobert, O. (2006). The molecular diversity of glycosaminoglycans shapes animal development. *Annu Rev Cell Dev Biol* **22**, 375-407.
Butler, S. J. and Dodd, J. (2003). A role for BMP heterodimers in roof plate-mediated repulsion of commissural axons. *Neuron* **38**, 389-401.

C

Cal, S., Obaya, A. J., Llamazares, M., Garabaya, C., Quesada, V. and Lopez-Otin, C. (2002). Cloning, expression analysis, and structural characterization of seven novel human ADAMTSs, a family of metalloproteinases with disintegrin and thrombospondin-1 domains. *Gene* **283**, 49-62.
Canoll, P. D., Barnea, G., Levy, J. B., Sap, J., Ehrlich, M., Silvennoinen, O., Schlessinger, J. and Musacchio, J. M. (1993). The expression of a novel receptor-type tyrosine phosphatase suggests a role in morphogenesis and plasticity of the nervous system. *Brain Res Dev Brain Res* **75**, 293-8.
Canoll, P. D., Petanceska, S., Schlessinger, J. and Musacchio, J. M. (1996). Three forms of RPTP-beta are differentially expressed during gliogenesis in the developing rat brain and during glial cell differentiation in culture. *J Neurosci Res* **44**, 199-215.
Carulli, D., Rhodes, K. E., Brown, D. J., Bonnert, T. P., Pollack, S. J., Oliver, K., Strata, P. and Fawcett, J. W. (2006). Composition of perineuronal nets in the adult rat cerebellum and the cellular origin of their components. *J Comp Neurol* **494**, 559-77.
Carulli, D., Rhodes, K. E. and Fawcett, J. W. (2007). Upregulation of aggrecan, link protein 1, and hyaluronan synthases during formation of perineuronal nets in the rat cerebellum. *J Comp Neurol* **501**, 83-94.

Chan, S. S., Zheng, H., Su, M. W., Wilk, R., Killeen, M. T., Hedgecock, E. M. and Culotti, J. G. (1996). UNC-40, a C. elegans homolog of DCC (Deleted in Colorectal Cancer), is required in motile cells responding to UNC-6 netrin cues. *Cell* **87**, 187-95.
Charron, F., Stein, E., Jeong, J., McMahon, A. P. and Tessier-Lavigne, M. (2003). The morphogen sonic hedgehog is an axonal chemoattractant that collaborates with netrin-1 in midline axon guidance. *Cell* **113**, 11-23.
Chedotal, A. (2010). Further tales of the midline. *Curr Opin Neurobiol*.
Chedotal, A. and Richards, L. J. (2010). Wiring the brain: the biology of neuronal guidance. *Cold Spring Harb Perspect Biol* **2**, a001917.
Chen, D., Zhao, M. and Mundy, G. R. (2004). Bone morphogenetic proteins. *Growth Factors* **22**, 233-41.
Chen, H., Chedotal, A., He, Z., Goodman, C. S. and Tessier-Lavigne, M. (1997). Neuropilin-2, a novel member of the neuropilin family, is a high affinity receptor for the semaphorins Sema E and Sema IV but not Sema III. *Neuron* **19**, 547-59.
Chen, Z., Gore, B. B., Long, H., Ma, L. and Tessier-Lavigne, M. (2008). Alternative splicing of the Robo3 axon guidance receptor governs the midline switch from attraction to repulsion. *Neuron* **58**, 325-32.
Chen, Z. J., Ughrin, Y. and Levine, J. M. (2002). Inhibition of axon growth by oligodendrocyte precursor cells. *Mol Cell Neurosci* **20**, 125-39.
Chilton, J. K. (2006). Molecular mechanisms of axon guidance. *Dev Biol* **292**, 13-24.
Cifuentes-Diaz, C., Faille, L., Goudou, D., Schachner, M., Rieger, F. and Angaut-Petit, D. (2002). Abnormal reinnervation of skeletal muscle in a tenascin-C-deficient mouse. *J Neurosci Res* **67**, 93-9.
Cirulli, V. and Yebra, M. (2007). Netrins: beyond the brain. *Nat Rev Mol Cell Biol* **8**, 296-306.
Clark, M. E., Kelner, G. S., Turbeville, L. A., Boyer, A., Arden, K. C. and Maki, R. A. (2000). ADAMTS9, a novel member of the ADAM-TS/ metallospondin gene family. *Genomics* **67**, 343-50.
Colamarino, S. A. and Tessier-Lavigne, M. (1995). The axonal chemoattractant netrin-1 is also a chemorepellent for trochlear motor axons. *Cell* **81**, 621-9.
Colavita, A. and Culotti, J. G. (1998). Suppressors of ectopic UNC-5 growth cone steering identify eight genes involved in axon guidance in Caenorhabditis elegans. *Dev Biol* **194**, 72-85.
Colavita, A., Krishna, S., Zheng, H., Padgett, R. W. and Culotti, J. G. (1998). Pioneer axon guidance by UNC-129, a C. elegans TGF-beta. *Science* **281**, 706-9.
Colige, A., Nuytinck, L., Hausser, I., van Essen, A. J., Thiry, M., Herens, C., Ades, L. C., Malfait, F., Paepe, A. D., Franck, P. et al. (2004). Novel types of mutation responsible for the dermatosparactic type of Ehlers-Danlos syndrome (Type VIIC) and common polymorphisms in the ADAMTS2 gene. *J Invest Dermatol* **123**, 656-63.
Colige, A., Vandenberghe, I., Thiry, M., Lambert, C. A., Van Beeumen, J., Li, S. W., Prockop, D. J., Lapiere, C. M. and Nusgens, B. V. (2002). Cloning and characterization of ADAMTS-14, a novel ADAMTS displaying high homology with ADAMTS-2 and ADAMTS-3. *J Biol Chem* **277**, 5756-66.
Collins-Racie, L. A., Flannery, C. R., Zeng, W., Corcoran, C., Annis-Freeman, B., Agostino, M. J., Arai, M., DiBlasio-Smith, E., Dorner, A. J., Georgiadis, K. E. et al. (2004). ADAMTS-8 exhibits aggrecanase activity and is expressed in human articular cartilage. *Matrix Biol* **23**, 219-30.
Costell, M., Gustafsson, E., Aszodi, A., Morgelin, M., Bloch, W., Hunziker, E., Addicks, K., Timpl, R. and Fassler, R. (1999). Perlecan maintains the integrity of cartilage and some basement membranes. *J Cell Biol* **147**, 1109-22.
Couchman, J. R. (2010). Transmembrane signaling proteoglycans. *Annu Rev Cell Dev Biol* **26**, 89-114

D

Davies, J. E., Tang, X., Denning, J. W., Archibald, S. J. and Davies, S. J. (2004). Decorin suppresses neurocan, brevican, phosphacan and NG2 expression and promotes axon growth across adult rat spinal cord injuries. *Eur J Neurosci* **19**, 1226-42.
de Castro, R., Jr., Tajrishi, R., Claros, J. and Stallcup, W. B. (2005). Differential responses of spinal axons to transection: influence of the NG2 proteoglycan. *Exp Neurol* **192**, 299-309.
Derijck, A. A., Van Erp, S. and Pasterkamp, R. J. (2010). Semaphorin signaling: molecular switches at the midline. *Trends Cell Biol* **20**, 568-76.
Dickson, B. J. (2002). Molecular mechanisms of axon guidance. *Science* **298**, 1959-64.
Dickson, B. J. and Gilestro, G. F. (2006). Regulation of commissural axon pathfinding by slit and its Robo receptors. *Annu Rev Cell Dev Biol* **22**, 651-75.
Doege, K. J., Sasaki, M., Kimura, T. and Yamada, Y. (1991). Complete coding sequence and deduced primary structure of the human cartilage large aggregating proteoglycan, aggrecan. Human-specific repeats, and additional alternatively spliced forms. *J Biol Chem* **266**, 894-902.
Doherty, P., Williams, G. and Williams, E. J. (2000). CAMs and axonal growth: a critical evaluation of the role of calcium and the MAPK cascade. *Mol Cell Neurosci* **16**, 283-95.
Domanitskaya, E., Wacker, A., Mauti, O., Baeriswyl, T., Esteve, P., Bovolenta, P. and Stoeckli, E. T. (2010). Sonic hedgehog guides post-crossing commissural axons both directly and indirectly by regulating Wnt activity. *J Neurosci* **30**, 11167-76.
Domowicz, M., Krueger, R. C., Li, H., Mangoura, D., Vertel, B. M. and Schwartz, N. B. (1996). The nanomelic mutation in the aggrecan gene is expressed in chick chondrocytes and neurons. *Int J Dev Neurosci* **14**, 191-201.
Domowicz, M. S., Sanders, T. A., Ragsdale, C. W. and Schwartz, N. B. (2008). Aggrecan is expressed by embryonic brain glia and regulates astrocyte development. *Dev Biol* **315**, 114-24.
Dou, C. L. and Levine, J. M. (1994). Inhibition of neurite growth by the NG2 chondroitin sulfate proteoglycan. *J Neurosci* **14**, 7616-28.
Dours-Zimmermann, M. T., Maurer, K., Rauch, U., Stoffel, W., Fassler, R. and Zimmermann, D. R. (2009). Versican V2 assembles the extracellular matrix surrounding the nodes of ranvier in the CNS. *J Neurosci* **29**, 7731-42.
Dours-Zimmermann, M. T. and Zimmermann, D. R. (1994). A novel glycosaminoglycan attachment domain identified in two alternative splice variants of human versican. *J Biol Chem* **269**, 32992-8.
Durbeej, M. (2010). Laminins. *Cell Tissue Res* **339**, 259-68.
Dutt, S., Kleber, M., Matasci, M., Sommer, L. and Zimmermann, D. R. (2006). Versican V0 and V1 guide migratory neural crest cells. *J Biol Chem* **281**, 12123-31.

E

Ebendal, T., Bengtsson, H. and Soderstrom, S. (1998). Bone morphogenetic proteins and their receptors: potential functions in the brain. *J Neurosci Res* **51**, 139-46.
Ebens, A., Brose, K., Leonardo, E. D., Hanson, M. G., Jr., Bladt, F., Birchmeier, C., Barres, B. A. and Tessier-Lavigne, M. (1996). Hepatocyte growth factor/scatter factor is an axonal chemoattractant and a neurotrophic factor for spinal motor neurons. *Neuron* **17**, 1157-72.
Eberhart, J., Barr, J., O'Connell, S., Flagg, A., Swartz, M. E., Cramer, K. S., Tosney, K. W., Pasquale, E. B. and Krull, C. E. (2004). Ephrin-A5 exerts positive or inhibitory effects on distinct subsets of EphA4-positive motor neurons. *J Neurosci* **24**, 1070-8.
Endo, Y. and Rubin, J. S. (2007). Wnt signaling and neurite outgrowth: insights and questions. *Cancer Sci* **98**, 1311-7.

Engel, M., Maurel, P., Margolis, R. U. and Margolis, R. K. (1996). Chondroitin sulfate proteoglycans in the developing central nervous system. I. cellular sites of synthesis of neurocan and phosphacan. *J Comp Neurol* **366**, 34-43.
Enomoto, H., Nelson, C. M., Somerville, R. P., Mielke, K., Dixon, L. J., Powell, K. and Apte, S. S. (2010). Cooperation of two ADAMTS metalloproteases in closure of the mouse palate identifies a requirement for versican proteolysis in regulating palatal mesenchyme proliferation. *Development* **137**, 4029-38.
Esko, J. D., Kimata, K. and Lindahl, U. (2009). Proteoglycans and Sulfated Glycosaminoglycans.
Ethell, I. M., Irie, F., Kalo, M. S., Couchman, J. R., Pasquale, E. B. and Yamaguchi, Y. (2001). EphB/syndecan-2 signaling in dendritic spine morphogenesis. *Neuron* **31**, 1001-13.
Ethell, I. M. and Yamaguchi, Y. (1999). Cell surface heparan sulfate proteoglycan syndecan-2 induces the maturation of dendritic spines in rat hippocampal neurons. *J Cell Biol* **144**, 575-86.

F

Faissner, A., Pyka, M., Geissler, M., Sobik, T., Frischknecht, R., Gundelfinger, E. D. and Seidenbecher, C. (2010). Contributions of astrocytes to synapse formation and maturation - Potential functions of the perisynaptic extracellular matrix. *Brain Res Rev* **63**, 26-38.
Fazeli, A., Dickinson, S. L., Hermiston, M. L., Tighe, R. V., Steen, R. G., Small, C. G., Stoeckli, E. T., Keino-Masu, K., Masu, M., Rayburn, H. et al. (1997). Phenotype of mice lacking functional Deleted in colorectal cancer (Dcc) gene. *Nature* **386**, 796-804.
Ferguson, B. A. (1983). Development of motor innervation of the chick following dorsal-ventral limb bud rotations. *J Neurosci* **3**, 1760-72.
Fidler, P. S., Schuette, K., Asher, R. A., Dobbertin, A., Thornton, S. R., Calle-Patino, Y., Muir, E., Levine, J. M., Geller, H. M., Rogers, J. H. et al. (1999). Comparing astrocytic cell lines that are inhibitory or permissive for axon growth: the major axon-inhibitory proteoglycan is NG2. *J Neurosci* **19**, 8778-88.
Flannery, C. R. (2006). MMPs and ADAMTSs: functional studies. *Front Biosci* **11**, 544-69.
Fredette, B. J., Miller, J. and Ranscht, B. (1996). Inhibition of motor axon growth by T-cadherin substrata. *Development* **122**, 3163-71.
Friedlander, D. R., Milev, P., Karthikeyan, L., Margolis, R. K., Margolis, R. U. and Grumet, M. (1994). The neuronal chondroitin sulfate proteoglycan neurocan binds to the neural cell adhesion molecules Ng-CAM/L1/NILE and N-CAM, and inhibits neuronal adhesion and neurite outgrowth. *J Cell Biol* **125**, 669-80.
Frisen, J., Yates, P. A., McLaughlin, T., Friedman, G. C., O'Leary, D. D. and Barbacid, M. (1998). Ephrin-A5 (AL-1/RAGS) is essential for proper retinal axon guidance and topographic mapping in the mammalian visual system. *Neuron* **20**, 235-43.

G

Gao, G., Plaas, A., Thompson, V. P., Jin, S., Zuo, F. and Sandy, J. D. (2004). ADAMTS4 (aggrecanase-1) activation on the cell surface involves C-terminal cleavage by glycosylphosphatidyl inositol-anchored membrane type 4-matrix metalloproteinase and binding of the activated proteinase to chondroitin sulfate and heparan sulfate on syndecan-1. *J Biol Chem* **279**, 10042-51.
Gao, G., Westling, J., Thompson, V. P., Howell, T. D., Gottschall, P. E. and Sandy, J. D. (2002). Activation of the proteolytic activity of ADAMTS4 (aggrecanase-1) by C-terminal truncation. *J Biol Chem* **277**, 11034-41.
Garwood, J., Heck, N., Reichardt, F. and Faissner, A. (2003). Phosphacan short isoform, a novel non-proteoglycan variant of phosphacan/receptor protein tyrosine phosphatase-beta, interacts with neuronal receptors and promotes neurite outgrowth. *J Biol Chem* **278**, 24164-73.

Garwood, J., Rigato, F., Heck, N. and Faissner, A. (2001). Tenascin glycoproteins and the complementary ligand DSD-1-PG/ phosphacan--structuring the neural extracellular matrix during development and repair. *Restor Neurol Neurosci* **19**, 51-64.
Gary, S. C. and Hockfield, S. (2000). BEHAB/brevican: an extracellular matrix component associated with invasive glioma. *Clin Neurosurg* **47**, 72-82.
Gary, S. C., Zerillo, C. A., Chiang, V. L., Gaw, J. U., Gray, G. and Hockfield, S. (2000). cDNA cloning, chromosomal localization, and expression analysis of human BEHAB/brevican, a brain specific proteoglycan regulated during cortical development and in glioma. *Gene* **256**, 139-47.
Gautam, M., Noakes, P. G., Moscoso, L., Rupp, F., Scheller, R. H., Merlie, J. P. and Sanes, J. R. (1996). Defective neuromuscular synaptogenesis in agrin-deficient mutant mice. *Cell* **85**, 525-35.
Geisbrecht, B. V., Dowd, K. A., Barfield, R. W., Longo, P. A. and Leahy, D. J. (2003). Netrin binds discrete subdomains of DCC and UNC5 and mediates interactions between DCC and heparin. *J Biol Chem* **278**, 32561-8.
Gendron, C., Kashiwagi, M., Lim, N. H., Enghild, J. J., Thogersen, I. B., Hughes, C., Caterson, B. and Nagase, H. (2007). Proteolytic activities of human ADAMTS-5: comparative studies with ADAMTS-4. *J Biol Chem* **282**, 18294-306.
Gherardi, E., Love, C. A., Esnouf, R. M. and Jones, E. Y. (2004). The sema domain. *Curr Opin Struct Biol* **14**, 669-78.
Giamanco, K. A., Morawski, M. and Matthews, R. T. (2010). Perineuronal net formation and structure in aggrecan knockout mice. *Neuroscience* **170**, 1314-27.
Giger, R. J., Urquhart, E. R., Gillespie, S. K., Levengood, D. V., Ginty, D. D. and Kolodkin, A. L. (1998). Neuropilin-2 is a receptor for semaphorin IV: insight into the structural basis of receptor function and specificity. *Neuron* **21**, 1079-92.
Gilestro, G. F. (2008). Redundant mechanisms for regulation of midline crossing in Drosophila. *PLoS One* **3**, e3798.
Giros, A., Morante, J., Gil-Sanz, C., Fairen, A. and Costell, M. (2007). Perlecan controls neurogenesis in the developing telencephalon. *BMC Dev Biol* **7**, 29.
Gore, B. B., Wong, K. G. and Tessier-Lavigne, M. (2008). Stem cell factor functions as an outgrowth-promoting factor to enable axon exit from the midline intermediate target. *Neuron* **57**, 501-10.
Grako, K. A., Ochiya, T., Barritt, D., Nishiyama, A. and Stallcup, W. B. (1999). PDGF (alpha)-receptor is unresponsive to PDGF-AA in aortic smooth muscle cells from the NG2 knockout mouse. *J Cell Sci* **112 (Pt 6)**, 905-15.
Grumet, M., Milev, P., Sakurai, T., Karthikeyan, L., Bourdon, M., Margolis, R. K. and Margolis, R. U. (1994). Interactions with tenascin and differential effects on cell adhesion of neurocan and phosphacan, two major chondroitin sulfate proteoglycans of nervous tissue. *J Biol Chem* **269**, 12142-6.
Gundersen, R. W. and Barrett, J. N. (1979). Neuronal chemotaxis: chick dorsal-root axons turn toward high concentrations of nerve growth factor. *Science* **206**, 1079-80.

H

Hacker, U., Nybakken, K. and Perrimon, N. (2005). Heparan sulphate proteoglycans: the sweet side of development. *Nat Rev Mol Cell Biol* **6**, 530-41.
Hagino, S., Iseki, K., Mori, T., Zhang, Y., Hikake, T., Yokoya, S., Takeuchi, M., Hasimoto, H., Kikuchi, S. and Wanaka, A. (2003). Slit and glypican-1 mRNAs are coexpressed in the reactive astrocytes of the injured adult brain. *Glia* **42**, 130-8.
Hamburger, V. and Hamilton, H. (1951). A series of normal stages in the development of the chick embryo. *Journal of Morphology* **88**, 49-92.
Hansen, M. J., Dallal, G. E. and Flanagan, J. G. (2004). Retinal axon response to ephrin-as shows a graded, concentration-dependent transition from growth promotion to inhibition. *Neuron* **42**, 717-30.

Hao, J. C., Yu, T. W., Fujisawa, K., Culotti, J. G., Gengyo-Ando, K., Mitani, S., Moulder, G., Barstead, R., Tessier-Lavigne, M. and Bargmann, C. I. (2001). C. elegans slit acts in midline, dorsal-ventral, and anterior-posterior guidance via the SAX-3/Robo receptor. *Neuron* **32**, 25-38.
Harroch, S., Furtado, G. C., Brueck, W., Rosenbluth, J., Lafaille, J., Chao, M., Buxbaum, J. D. and Schlessinger, J. (2002). A critical role for the protein tyrosine phosphatase receptor type Z in functional recovery from demyelinating lesions. *Nat Genet* **32**, 411-4.
Harroch, S., Palmeri, M., Rosenbluth, J., Custer, A., Okigaki, M., Shrager, P., Blum, M., Buxbaum, J. D. and Schlessinger, J. (2000). No obvious abnormality in mice deficient in receptor protein tyrosine phosphatase beta. *Mol Cell Biol* **20**, 7706-15.
Hashimoto, G., Shimoda, M. and Okada, Y. (2004). ADAMTS4 (aggrecanase-1) interaction with the C-terminal domain of fibronectin inhibits proteolysis of aggrecan. *J Biol Chem* **279**, 32483-91.
Hedgecock, E. M., Culotti, J. G. and Hall, D. H. (1990). The unc-5, unc-6, and unc-40 genes guide circumferential migrations of pioneer axons and mesodermal cells on the epidermis in C. elegans. *Neuron* **4**, 61-85.
Heldin, C. H., Miyazono, K. and ten Dijke, P. (1997). TGF-beta signalling from cell membrane to nucleus through SMAD proteins. *Nature* **390**, 465-71.
Henderson, D. J., Ybot-Gonzalez, P. and Copp, A. J. (1997). Over-expression of the chondroitin sulphate proteoglycan versican is associated with defective neural crest migration in the Pax3 mutant mouse (splotch). *Mech Dev* **69**, 39-51.
Hindges, R., McLaughlin, T., Genoud, N., Henkemeyer, M. and O'Leary, D. D. (2002). EphB forward signaling controls directional branch extension and arborization required for dorsal-ventral retinotopic mapping. *Neuron* **35**, 475-87.
Holt, C. E. and Dickson, B. J. (2005). Sugar codes for axons? *Neuron* **46**, 169-72.
Hsueh, Y. P. and Sheng, M. (1999). Regulated expression and subcellular localization of syndecan heparan sulfate proteoglycans and the syndecan-binding protein CASK/LIN-2 during rat brain development. *J Neurosci* **19**, 7415-25.
Huber AB, K. A., Tran TS, Gu C, De Marco Garcia N, Lieberam I, Johnson D, Jessell TM, Ginty DD, Kolodkin AL. (2005). Distinct roles for secreted semaphorin signaling in spinal motor axon guidance. *Neuron* **48**, 949-64.
Hubert, T., Grimal, S., Carroll, P. and Fichard-Carroll, A. (2009). Collagens in the developing and diseased nervous system. *Cell Mol Life Sci* **66**, 1223-38.
Hunanyan, A. S., Garcia-Alias, G., Alessi, V., Levine, J. M., Fawcett, J. W., Mendell, L. M. and Arvanian, V. L. (2010). Role of chondroitin sulfate proteoglycans in axonal conduction in Mammalian spinal cord. *J Neurosci* **30**, 7761-9.

I

Ilic, M. Z., East, C. J., Rogerson, F. M., Fosang, A. J. and Handley, C. J. (2007). Distinguishing aggrecan loss from aggrecan proteolysis in ADAMTS-4 and ADAMTS-5 single and double deficient mice. *J Biol Chem* **282**, 37420-8.
Inatani, M., Irie, F., Plump, A. S., Tessier-Lavigne, M. and Yamaguchi, Y. (2003). Mammalian brain morphogenesis and midline axon guidance require heparan sulfate. *Science* **302**, 1044-6.
Ingham, P. W. and McMahon, A. P. (2001). Hedgehog signaling in animal development: paradigms and principles. *Genes Dev* **15**, 3059-87.
Irving, C., Malhas, A., Guthrie, S. and Mason, I. (2002). Establishing the trochlear motor axon trajectory: role of the isthmic organiser and Fgf8. *Development* **129**, 5389-98.
Ishii, N., Wadsworth, W. G., Stern, B. D., Culotti, J. G. and Hedgecock, E. M. (1992). UNC-6, a laminin-related protein, guides cell and pioneer axon migrations in C. elegans. *Neuron* **9**, 873-81.
Ito, K., Shinomura, T., Zako, M., Ujita, M. and Kimata, K. (1995). Multiple forms of mouse PG-M, a large chondroitin sulfate proteoglycan generated by alternative splicing. *J Biol Chem* **270**, 958-65.

Itoh, A., Miyabayashi, T., Ohno, M. and Sakano, S. (1998). Cloning and expressions of three mammalian homologues of Drosophila slit suggest possible roles for Slit in the formation and maintenance of the nervous system. *Brain Res Mol Brain Res* **62**, 175-86.
Ivins, J. K., Litwack, E. D., Kumbasar, A., Stipp, C. S. and Lander, A. D. (1997). Cerebroglycan, a developmentally regulated cell-surface heparan sulfate proteoglycan, is expressed on developing axons and growth cones. *Dev Biol* **184**, 320-32.

J

Jaworski, D. M., Kelly, G. M. and Hockfield, S. (1995). The CNS-specific hyaluronan-binding protein BEHAB is expressed in ventricular zones coincident with gliogenesis. *J Neurosci* **15**, 1352-62.
Jen, Y. H., Musacchio, M. and Lander, A. D. (2009). Glypican-1 controls brain size through regulation of fibroblast growth factor signaling in early neurogenesis. *Neural Dev* **4**, 33.
Jessell, T. M. (2000). Neuronal specification in the spinal cord: inductive signals and transcriptional codes. *Nat Rev Genet* **1**, 20-9.
Joester, A. and Faissner, A. (2001). The structure and function of tenascins in the nervous system. *Matrix Biol* **20**, 13-22.
Johnson, K. G., Ghose, A., Epstein, E., Lincecum, J., O'Connor, M. B. and Van Vactor, D. (2004). Axonal heparan sulfate proteoglycans regulate the distribution and efficiency of the repellent slit during midline axon guidance. *Curr Biol* **14**, 499-504.
Johnston, P., Chojnowski, A. J., Davidson, R. K., Riley, G. P., Donell, S. T. and Clark, I. M. (2007). A complete expression profile of matrix-degrading metalloproteinases in Dupuytren's disease. *J Hand Surg Am* **32**, 343-51.
Jones, G. C. and Riley, G. P. (2005). ADAMTS proteinases: a multi-domain, multi-functional family with roles in extracellular matrix turnover and arthritis. *Arthritis Res Ther* **7**, 160-9.
Jones, L. L., Sajed, D. and Tuszynski, M. H. (2003). Axonal regeneration through regions of chondroitin sulfate proteoglycan deposition after spinal cord injury: a balance of permissiveness and inhibition. *J Neurosci* **23**, 9276-88.
Jones, L. L., Yamaguchi, Y., Stallcup, W. B. and Tuszynski, M. H. (2002). NG2 is a major chondroitin sulfate proteoglycan produced after spinal cord injury and is expressed by macrophages and oligodendrocyte progenitors. *J Neurosci* **22**, 2792-803.
Jungers, K. A., Le Goff, C., Somerville, R. P. and Apte, S. S. (2005). Adamts9 is widely expressed during mouse embryo development. *Gene Expr Patterns* **5**, 609-17.

K

Kashiwagi, M., Enghild, J. J., Gendron, C., Hughes, C., Caterson, B., Itoh, Y. and Nagase, H. (2004). Altered proteolytic activities of ADAMTS-4 expressed by C-terminal processing. *J Biol Chem* **279**, 10109-19.
Keino-Masu, K., Masu, M., Hinck, L., Leonardo, E. D., Chan, S. S., Culotti, J. G. and Tessier-Lavigne, M. (1996). Deleted in Colorectal Cancer (DCC) encodes a netrin receptor. *Cell* **87**, 175-85.
Keleman, K., Rajagopalan, S., Cleppien, D., Teis, D., Paiha, K., Huber, L. A., Technau, G. M. and Dickson, B. J. (2002). Comm sorts robo to control axon guidance at the Drosophila midline. *Cell* **110**, 415-27.
Kennedy, T. E., Serafini, T., de la Torre, J. R. and Tessier-Lavigne, M. (1994). Netrins are diffusible chemotropic factors for commissural axons in the embryonic spinal cord. *Cell* **78**, 425-35.
Kern, C. B., Wessels, A., McGarity, J., Dixon, L. J., Alston, E., Argraves, W. S., Geeting, D., Nelson, C. M., Menick, D. R. and Apte, S. S. (2010). Reduced versican cleavage due to Adamts9 haploinsufficiency is associated with cardiac and aortic anomalies. *Matrix Biol* **29**, 304-16.
Kiani, C., Chen, L., Wu, Y. J., Yee, A. J. and Yang, B. B. (2002). Structure and function of aggrecan. *Cell Res* **12**, 19-32.

Kidd, T., Bland, K. S. and Goodman, C. S. (1999). Slit is the midline repellent for the robo receptor in Drosophila. *Cell* **96**, 785-94.
Kidd, T., Brose, K., Mitchell, K. J., Fetter, R. D., Tessier-Lavigne, M., Goodman, C. S. and Tear, G. (1998). Roundabout controls axon crossing of the CNS midline and defines a novel subfamily of evolutionarily conserved guidance receptors. *Cell* **92**, 205-15.
Killeen, M. T. and Sybingco, S. S. (2008). Netrin, Slit and Wnt receptors allow axons to choose the axis of migration. *Dev Biol* **323**, 143-51.
Kimata, K., Oike, Y., Tani, K., Shinomura, T., Yamagata, M., Uritani, M. and Suzuki, S. (1986). A large chondroitin sulfate proteoglycan (PG-M) synthesized before chondrogenesis in the limb bud of chick embryo. *J Biol Chem* **261**, 13517-25.
Klein, R. (2004). Eph/ephrin signaling in morphogenesis, neural development and plasticity. *Curr Opin Cell Biol* **16**, 580-9.
Kolk, S. M., Gunput, R. A., Tran, T. S., van den Heuvel, D. M., Prasad, A. A., Hellemons, A. J., Adolfs, Y., Ginty, D. D., Kolodkin, A. L., Burbach, J. P. et al. (2009). Semaphorin 3F is a bifunctional guidance cue for dopaminergic axons and controls their fasciculation, channeling, rostral growth, and intracortical targeting. *J Neurosci* **29**, 12542-57.
Kolodkin, A. L., Levengood, D. V., Rowe, E. G., Tai, Y. T., Giger, R. J. and Ginty, D. D. (1997). Neuropilin is a semaphorin III receptor. *Cell* **90**, 753-62.
Kolodkin, A. L., Matthes, D. J., O'Connor, T. P., Patel, N. H., Admon, A., Bentley, D. and Goodman, C. S. (1992). Fasciclin IV: sequence, expression, and function during growth cone guidance in the grasshopper embryo. *Neuron* **9**, 831-45.
Kolodkin, A. L. and Tessier-Lavigne, M. (2010). Mechanisms and Molecules of Neuronal Wiring: A Primer. *Cold Spring Harb Perspect Biol*.
Kolodziej, P. A., Timpe, L. C., Mitchell, K. J., Fried, S. R., Goodman, C. S., Jan, L. Y. and Jan, Y. N. (1996). frazzled encodes a Drosophila member of the DCC immunoglobulin subfamily and is required for CNS and motor axon guidance. *Cell* **87**, 197-204.
Koo, B. H., Longpre, J. M., Somerville, R. P., Alexander, J. P., Leduc, R. and Apte, S. S. (2007). Regulation of ADAMTS9 secretion and enzymatic activity by its propeptide. *J Biol Chem* **282**, 16146-54.
Koprivica, V., Cho, K. S., Park, J. B., Yiu, G., Atwal, J., Gore, B., Kim, J. A., Lin, E., Tessier-Lavigne, M., Chen, D. F. et al. (2005). EGFR activation mediates inhibition of axon regeneration by myelin and chondroitin sulfate proteoglycans. *Science* **310**, 106-10.
Kramer, E. R., Knott, L., Su, F., Dessaud, E., Krull, C. E., Helmbacher, F. and Klein, R. (2006). Cooperation between GDNF/Ret and ephrinA/EphA4 signals for motor-axon pathway selection in the limb. *Neuron* **50**, 35-47.
Kuhn, T. B., Schmidt, M. F. and Kater, S. B. (1995). Laminin and fibronectin guideposts signal sustained but opposite effects to passing growth cones. *Neuron* **14**, 275-85.
Kuno, K., Kanada, N., Nakashima, E., Fujiki, F., Ichimura, F. and Matsushima, K. (1997). Molecular cloning of a gene encoding a new type of metalloproteinase-disintegrin family protein with thrombospondin motifs as an inflammation associated gene. *J Biol Chem* **272**, 556-62.
Kuno, K. and Matsushima, K. (1998). ADAMTS-1 protein anchors at the extracellular matrix through the thrombospondin type I motifs and its spacing region. *J Biol Chem* **273**, 13912-7.
Kuno, K., Okada, Y., Kawashima, H., Nakamura, H., Miyasaka, M., Ohno, H. and Matsushima, K. (2000). ADAMTS-1 cleaves a cartilage proteoglycan, aggrecan. *FEBS Lett* **478**, 241-5.
Kuno, K., Terashima, Y. and Matsushima, K. (1999). ADAMTS-1 is an active metalloproteinase associated with the extracellular matrix. *J Biol Chem* **274**, 18821-6.

L

Landolt, R. M., Vaughan, L., Winterhalter, K. H. and Zimmermann, D. R. (1995). Versican is selectively expressed in embryonic tissues that act as barriers to neural crest cell migration and axon outgrowth. *Development* **121**, 2303-12.

Lee, J. S. and Chien, C. B. (2004). When sugars guide axons: insights from heparan sulphate proteoglycan mutants. *Nat Rev Genet* **5**, 923-35.
Lemons, M. L., Sandy, J. D., Anderson, D. K. and Howland, D. R. (2003). Intact aggrecan and chondroitin sulfate-depleted aggrecan core glycoprotein inhibit axon growth in the adult rat spinal cord. *Exp Neurol* **184**, 981-90.
Leonardo, E. D., Hinck, L., Masu, M., Keino-Masu, K., Ackerman, S. L. and Tessier-Lavigne, M. (1997). Vertebrate homologues of C. elegans UNC-5 are candidate netrin receptors. *Nature* **386**, 833-8.
Leung, K. M., Margolis, R. U. and Chan, S. O. (2004). Expression of phosphacan and neurocan during early development of mouse retinofugal pathway. *Brain Res Dev Brain Res* **152**, 1-10.
Levi-Montalcini, R. and Cohen, S. (1956). In Vitro and in Vivo Effects of a Nerve Growth-Stimulating Agent Isolated from Snake Venom. *Proc Natl Acad Sci U S A* **42**, 695-9.
Levy, G. G., Nichols, W. C., Lian, E. C., Foroud, T., McClintick, J. N., McGee, B. M., Yang, A. Y., Siemieniak, D. R., Stark, K. R., Gruppo, R. et al. (2001). Mutations in a member of the ADAMTS gene family cause thrombotic thrombocytopenic purpura. *Nature* **413**, 488-94.
Levy, J. B., Canoll, P. D., Silvennoinen, O., Barnea, G., Morse, B., Honegger, A. M., Huang, J. T., Cannizzaro, L. A., Park, S. H., Druck, T. et al. (1993). The cloning of a receptor-type protein tyrosine phosphatase expressed in the central nervous system. *J Biol Chem* **268**, 10573-81.
Li, H., Domowicz, M., Hennig, A. and Schwartz, N. B. (1996). S103L reactive chondroitin sulfate proteoglycan (aggrecan) mRNA expressed in developing chick brain and cartilage is encoded by a single gene. *Brain Res Mol Brain Res* **36**, 309-21.
Li, H. S., Chen, J. H., Wu, W., Fagaly, T., Zhou, L., Yuan, W., Dupuis, S., Jiang, Z. H., Nash, W., Gick, C. et al. (1999). Vertebrate slit, a secreted ligand for the transmembrane protein roundabout, is a repellent for olfactory bulb axons. *Cell* **96**, 807-18.
Liang, Y., Annan, R. S., Carr, S. A., Popp, S., Mevissen, M., Margolis, R. K. and Margolis, R. U. (1999). Mammalian homologues of the Drosophila slit protein are ligands of the heparan sulfate proteoglycan glypican-1 in brain. *J Biol Chem* **274**, 17885-92.
Little, C. B., Mittaz, L., Belluoccio, D., Rogerson, F. M., Campbell, I. K., Meeker, C. T., Bateman, J. F., Pritchard, M. A. and Fosang, A. J. (2005). ADAMTS-1-knockout mice do not exhibit abnormalities in aggrecan turnover in vitro or in vivo. *Arthritis Rheum* **52**, 1461-72.
Litwack, E. D., Ivins, J. K., Kumbasar, A., Paine-Saunders, S., Stipp, C. S. and Lander, A. D. (1998). Expression of the heparan sulfate proteoglycan glypican-1 in the developing rodent. *Dev Dyn* **211**, 72-87.
Litwack, E. D., Stipp, C. S., Kumbasar, A. and Lander, A. D. (1994). Neuronal expression of glypican, a cell-surface glycosylphosphatidylinositol-anchored heparan sulfate proteoglycan, in the adult rat nervous system. *J Neurosci* **14**, 3713-24.
Liu, C. J. (2009). The role of ADAMTS-7 and ADAMTS-12 in the pathogenesis of arthritis. *Nat Clin Pract Rheumatol* **5**, 38-45.
Liu, G., Li, W., Wang, L., Kar, A., Guan, K. L., Rao, Y. and Wu, J. Y. (2009). DSCAM functions as a netrin receptor in commissural axon pathfinding. *Proc Natl Acad Sci U S A* **106**, 2951-6.
Livesey, F. J. (1999). Netrins and netrin receptors. *Cell Mol Life Sci* **56**, 62-8.
Long, H., Sabatier, C., Ma, L., Plump, A., Yuan, W., Ornitz, D. M., Tamada, A., Murakami, F., Goodman, C. S. and Tessier-Lavigne, M. (2004). Conserved roles for Slit and Robo proteins in midline commissural axon guidance. *Neuron* **42**, 213-23.
Longpre, J. M., McCulloch, D. R., Koo, B. H., Alexander, J. P., Apte, S. S. and Leduc, R. (2009). Characterization of proADAMTS5 processing by proprotein convertases. *Int J Biochem Cell Biol* **41**, 1116-26.
Lowery, L. A. and Van Vactor, D. (2009). The trip of the tip: understanding the growth cone machinery. *Nat Rev Mol Cell Biol* **10**, 332-43.
Lum, L. and Beachy, P. A. (2004). The Hedgehog response network: Sensors, switches, and routers. *Science* **304**, 1755-1759.

Luo, Y., Raible, D. and Raper, J. A. (1993). Collapsin: a protein in brain that induces the collapse and paralysis of neuronal growth cones. *Cell* **75**, 217-27.
Luria, V., Krawchuk, D., Jessell, T. M., Laufer, E. and Kania, A. (2008). Specification of motor axon trajectory by ephrin-B:EphB signaling: symmetrical control of axonal patterning in the developing limb. *Neuron* **60**, 1039-53.
Ly, A., Nikolaev, A., Suresh, G., Zheng, Y., Tessier-Lavigne, M. and Stein, E. (2008). DSCAM is a netrin receptor that collaborates with DCC in mediating turning responses to netrin-1. *Cell* **133**, 1241-54.
Lyuksyutova, A. I., Lu, C. C., Milanesio, N., King, L. A., Guo, N., Wang, Y., Nathans, J., Tessier-Lavigne, M. and Zou, Y. (2003). Anterior-posterior guidance of commissural axons by Wnt-frizzled signaling. *Science* **302**, 1984-8.

M

Ma, L. and Tessier-Lavigne, M. (2007). Dual branch-promoting and branch-repelling actions of Slit/Robo signaling on peripheral and central branches of developing sensory axons. *J Neurosci* **27**, 6843-51.
MacNeil, L. T., Hardy, W. R., Pawson, T., Wrana, J. L. and Culotti, J. G. (2009). UNC-129 regulates the balance between UNC-40 dependent and independent UNC-5 signaling pathways. *Nat Neurosci* **12**, 150-5.
Maeda, N., Hamanaka, H., Oohira, A. and Noda, M. (1995). Purification, characterization and developmental expression of a brain-specific chondroitin sulfate proteoglycan, 6B4 proteoglycan/phosphacan. *Neuroscience* **67**, 23-35.
Maeda, N. and Noda, M. (1996). 6B4 proteoglycan/phosphacan is a repulsive substratum but promotes morphological differentiation of cortical neurons. *Development* **122**, 647-58.
Maeda, N. and Noda, M. (1998). Involvement of receptor-like protein tyrosine phosphatase zeta/RPTPbeta and its ligand pleiotrophin/heparin-binding growth-associated molecule (HB-GAM) in neuronal migration. *J Cell Biol* **142**, 203-16.
Magill-Solc, C. and McMahan, U. J. (1988). Motor neurons contain agrin-like molecules. *J Cell Biol* **107**, 1825-33.
Mann, F., Chauvet, S. and Rougon, G. (2007). Semaphorins in development and adult brain: Implication for neurological diseases. *Prog Neurobiol* **82**, 57-79.
Mann, F., Ray, S., Harris, W. and Holt, C. (2002). Topographic mapping in dorsoventral axis of the Xenopus retinotectal system depends on signaling through ephrin-B ligands. *Neuron* **35**, 461-73.
Mann, F. and Rougon, G. (2007). Mechanisms of axon guidance: membrane dynamics and axonal transport in semaphorin signalling. *J Neurochem* **102**, 316-23.
Margolis, R. K., Rauch, U., Maurel, P. and Margolis, R. U. (1996). Neurocan and phosphacan: two major nervous tissue-specific chondroitin sulfate proteoglycans. *Perspect Dev Neurobiol* **3**, 273-90.
Marillat, V., Sabatier, C., Failli, V., Matsunaga, E., Sotelo, C., Tessier-Lavigne, M. and Chedotal, A. (2004). The slit receptor Rig-1/Robo3 controls midline crossing by hindbrain precerebellar neurons and axons. *Neuron* **43**, 69-79.
Marthiens, V., Gavard, J., Padilla, F., Monnet, C., Castellani, V., Lambert, M. and Mege, R. M. (2005). A novel function for cadherin-11 in the regulation of motor axon elongation and fasciculation. *Mol Cell Neurosci* **28**, 715-26.
Marti, E. and Bovolenta, P. (2002). Sonic hedgehog in CNS development: one signal, multiple outputs. *Trends Neurosci* **25**, 89-96.
Matsui, F., Watanabe, E. and Oohira, A. (1994). Immunological identification of two proteoglycan fragments derived from neurocan, a brain-specific chondroitin sulfate proteoglycan. *Neurochem Int* **25**, 425-31.
Matsumoto, K., Kamiya, N., Suwan, K., Atsumi, F., Shimizu, K., Shinomura, T., Yamada, Y., Kimata, K. and Watanabe, H. (2006). Identification and characterization of versican/PG-M aggregates in cartilage. *J Biol Chem* **281**, 18257-63.

Matthews, R. T., Kelly, G. M., Zerillo, C. A., Gray, G., Tiemeyer, M. and Hockfield, S. (2002). Aggrecan glycoforms contribute to the molecular heterogeneity of perineuronal nets. *J Neurosci* **22**, 7536-47.
Maurel, P., Rauch, U., Flad, M., Margolis, R. K. and Margolis, R. U. (1994). Phosphacan, a chondroitin sulfate proteoglycan of brain that interacts with neurons and neural cell-adhesion molecules, is an extracellular variant of a receptor-type protein tyrosine phosphatase. *Proc Natl Acad Sci U S A* **91**, 2512-6.
Mayanil, C. S., George, D., Freilich, L., Miljan, E. J., Mania-Farnell, B., McLone, D. G. and Bremer, E. G. (2001). Microarray analysis detects novel Pax3 downstream target genes. *J Biol Chem* **276**, 49299-309.
Mayanil, C. S., Pool, A., Nakazaki, H., Reddy, A. C., Mania-Farnell, B., Yun, B., George, D., McLone, D. G. and Bremer, E. G. (2006). Regulation of murine TGFbeta2 by Pax3 during early embryonic development. *J Biol Chem* **281**, 24544-52.
McCulloch, D. R., Le Goff, C., Bhatt, S., Dixon, L. J., Sandy, J. D. and Apte, S. S. (2009a). Adamts5, the gene encoding a proteoglycan-degrading metalloprotease, is expressed by specific cell lineages during mouse embryonic development and in adult tissues. *Gene Expr Patterns* **9**, 314-23.
McCulloch, D. R., Nelson, C. M., Dixon, L. J., Silver, D. L., Wylie, J. D., Lindner, V., Sasaki, T., Cooley, M. A., Argraves, W. S. and Apte, S. S. (2009b). ADAMTS metalloproteases generate active versican fragments that regulate interdigital web regression. *Dev Cell* **17**, 687-98.
McLaughlin, T., Hindges, R., Yates, P. A. and O'Leary, D. D. (2003). Bifunctional action of ephrin-B1 as a repellent and attractant to control bidirectional branch extension in dorsal-ventral retinotopic mapping. *Development* **130**, 2407-18.
Melendez-Vasquez, C., Carey, D. J., Zanazzi, G., Reizes, O., Maurel, P. and Salzer, J. L. (2005). Differential expression of proteoglycans at central and peripheral nodes of Ranvier. *Glia* **52**, 301-8.
Milev, P., Chiba, A., Haring, M., Rauvala, H., Schachner, M., Ranscht, B., Margolis, R. K. and Margolis, R. U. (1998a). High affinity binding and overlapping localization of neurocan and phosphacan/protein-tyrosine phosphatase-zeta/beta with tenascin-R, amphoterin, and the heparin-binding growth-associated molecule. *J Biol Chem* **273**, 6998-7005.
Milev, P., Fischer, D., Haring, M., Schulthess, T., Margolis, R. K., Chiquet-Ehrismann, R. and Margolis, R. U. (1997). The fibrinogen-like globe of tenascin-C mediates its interactions with neurocan and phosphacan/protein-tyrosine phosphatase-zeta/beta. *J Biol Chem* **272**, 15501-9.
Milev, P., Friedlander, D. R., Sakurai, T., Karthikeyan, L., Flad, M., Margolis, R. K., Grumet, M. and Margolis, R. U. (1994). Interactions of the chondroitin sulfate proteoglycan phosphacan, the extracellular domain of a receptor-type protein tyrosine phosphatase, with neurons, glia, and neural cell adhesion molecules. *J Cell Biol* **127**, 1703-15.
Milev, P., Maurel, P., Chiba, A., Mevissen, M., Popp, S., Yamaguchi, Y., Margolis, R. K. and Margolis, R. U. (1998b). Differential regulation of expression of hyaluronan-binding proteoglycans in developing brain: aggrecan, versican, neurocan, and brevican. *Biochem Biophys Res Commun* **247**, 207-12.
Milev, P., Maurel, P., Haring, M., Margolis, R. K. and Margolis, R. U. (1996). TAG-1/axonin-1 is a high-affinity ligand of neurocan, phosphacan/protein-tyrosine phosphatase-zeta/beta, and N-CAM. *J Biol Chem* **271**, 15716-23.
Miner, J. H. (2008). Laminins and their roles in mammals. *Microsc Res Tech* **71**, 349-56.
Monschau, B., Kremoser, C., Ohta, K., Tanaka, H., Kaneko, T., Yamada, T., Handwerker, C., Hornberger, M. R., Loschinger, J., Pasquale, E. B. et al. (1997). Shared and distinct functions of RAGS and ELF-1 in guiding retinal axons. *EMBO J* **16**, 1258-67.

N

Nakamoto, M., Cheng, H. J., Friedman, G. C., McLaughlin, T., Hansen, M. J., Yoon, C. H., O'Leary, D. D. and Flanagan, J. G. (1996). Topographically specific effects of ELF-1 on retinal axon guidance in vitro and retinal axon mapping in vivo. *Cell* **86**, 755-66.
Naso, M. F., Zimmermann, D. R. and Iozzo, R. V. (1994). Characterization of the complete genomic structure of the human versican gene and functional analysis of its promoter. *J Biol Chem* **269**, 32999-3008.
Nawabi, H., Briancon-Marjollet, A., Clark, C., Sanyas, I., Takamatsu, H., Okuno, T., Kumanogoh, A., Bozon, M., Takeshima, K., Yoshida, Y. et al. (2010). A midline switch of receptor processing regulates commissural axon guidance in vertebrates. *Genes Dev* **24**, 396-410.
Ngo, S. T., Noakes, P. G. and Phillips, W. D. (2007). Neural agrin: a synaptic stabiliser. *Int J Biochem Cell Biol* **39**, 863-7.
Niederost, B. P., Zimmermann, D. R., Schwab, M. E. and Bandtlow, C. E. (1999). Bovine CNS myelin contains neurite growth-inhibitory activity associated with chondroitin sulfate proteoglycans. *J Neurosci* **19**, 8979-89.
Niisato, K., Fujikawa, A., Komai, S., Shintani, T., Watanabe, E., Sakaguchi, G., Katsuura, G., Manabe, T. and Noda, M. (2005). Age-dependent enhancement of hippocampal long-term potentiation and impairment of spatial learning through the Rho-associated kinase pathway in protein tyrosine phosphatase receptor type Z-deficient mice. *J Neurosci* **25**, 1081-8.
Nishiyama, A., Dahlin, K. J., Prince, J. T., Johnstone, S. R. and Stallcup, W. B. (1991). The primary structure of NG2, a novel membrane-spanning proteoglycan. *J Cell Biol* **114**, 359-71.
Nishiyama, A., Watanabe, M., Yang, Z. and Bu, J. (2002). Identity, distribution, and development of polydendrocytes: NG2-expressing glial cells. *J Neurocytol* **31**, 437-55.
Nitkin, R. M., Smith, M. A., Magill, C., Fallon, J. R., Yao, Y. M., Wallace, B. G. and McMahan, U. J. (1987). Identification of agrin, a synaptic organizing protein from Torpedo electric organ. *J Cell Biol* **105**, 2471-8.
Niu, S., Antin, P. B., Akimoto, K. and Morkin, E. (1996). Expression of avian glypican is developmentally regulated. *Dev Dyn* **207**, 25-34.
Nutt, C. L., Zerillo, C. A., Kelly, G. M. and Hockfield, S. (2001). Brain enriched hyaluronan binding (BEHAB)/brevican increases aggressiveness of CNS-1 gliomas in Lewis rats. *Cancer Res* **61**, 7056-9.

O-P

O'Connor, R. and Tessier-Lavigne, M. (1999). Identification of maxillary factor, a maxillary process-derived chemoattractant for developing trigeminal sensory axons. *Neuron* **24**, 165-78.
Ohta, S., Suzuki, K., Ogino, Y., Miyagawa, S., Murashima, A., Matsumaru, D. and Yamada, G. (2008). Gene transduction by sonoporation. *Dev Growth Differ* **50**, 517-20.
Okada, A., Charron, F., Morin, S., Shin, D. S., Wong, K., Fabre, P. J., Tessier-Lavigne, M. and McConnell, S. K. (2006). Boc is a receptor for sonic hedgehog in the guidance of commissural axons. *Nature* **444**, 369-73.
Oohashi, T., Hirakawa, S., Bekku, Y., Rauch, U., Zimmermann, D. R., Su, W. D., Ohtsuka, A., Murakami, T. and Ninomiya, Y. (2002). Bral1, a brain-specific link protein, colocalizing with the versican V2 isoform at the nodes of Ranvier in developing and adult mouse central nervous systems. *Mol Cell Neurosci* **19**, 43-57.
Pasquale, E. B. (2004). Eph-ephrin promiscuity is now crystal clear. *Nat Neurosci* **7**, 417-8.
Pasquale, E. B. (2005). Eph receptor signalling casts a wide net on cell behaviour. *Nat Rev Mol Cell Biol* **6**, 462-75.
Peles, E., Nativ, M., Campbell, P. L., Sakurai, T., Martinez, R., Lev, S., Clary, D. O., Schilling, J., Barnea, G., Plowman, G. D. et al. (1995). The carbonic anhydrase domain of

receptor tyrosine phosphatase beta is a functional ligand for the axonal cell recognition molecule contactin. *Cell* **82**, 251-60.
Peles, E., Schlessinger, J. and Grumet, M. (1998). Multi-ligand interactions with receptor-like protein tyrosine phosphatase beta: implications for intercellular signaling. *Trends Biochem Sci* **23**, 121-4.
Perissinotto, D., Iacopetti, P., Bellina, I., Doliana, R., Colombatti, A., Pettway, Z., Bronner-Fraser, M., Shinomura, T., Kimata, K., Morgelin, M. et al. (2000). Avian neural crest cell migration is diversely regulated by the two major hyaluronan-binding proteoglycans PG-M/versican and aggrecan. *Development* **127**, 2823-42.
Perris, R., Perissinotto, D., Pettway, Z., Bronner-Fraser, M., Morgelin, M. and Kimata, K. (1996). Inhibitory effects of PG-H/aggrecan and PG-M/versican on avian neural crest cell migration. *FASEB J* **10**, 293-301.
Pesheva, P., Gloor, S., Schachner, M. and Probstmeier, R. (1997). Tenascin-R is an intrinsic autocrine factor for oligodendrocyte differentiation and promotes cell adhesion by a sulfatide-mediated mechanism. *J Neurosci* **17**, 4642-51.
Placzek, M., Tessier-Lavigne, M., Jessell, T. and Dodd, J. (1990). Orientation of commissural axons in vitro in response to a floor plate-derived chemoattractant. *Development* **110**, 19-30.
Popp, S., Maurel, P., Andersen, J. S. and Margolis, R. U. (2004). Developmental changes of aggrecan, versican and neurocan in the retina and optic nerve. *Exp Eye Res* **79**, 351-6.

R

Rao, A., Luo, C. and Hogan, P. G. (1997). Transcription factors of the NFAT family: regulation and function. *Annu Rev Immunol* **15**, 707-47.
Raper, J. A. (2000). Semaphorins and their receptors in vertebrates and invertebrates. *Curr Opin Neurobiol* **10**, 88-94.
Rauch, U., Feng, K. and Zhou, X. H. (2001). Neurocan: a brain chondroitin sulfate proteoglycan. *Cell Mol Life Sci* **58**, 1842-56.
Rauch, U., Karthikeyan, L., Maurel, P., Margolis, R. U. and Margolis, R. K. (1992). Cloning and primary structure of neurocan, a developmentally regulated, aggregating chondroitin sulfate proteoglycan of brain. *J Biol Chem* **267**, 19536-47.
Reichardt, L. F. (2006). Neurotrophin-regulated signalling pathways. *Philos Trans R Soc Lond B Biol Sci* **361**, 1545-64.
Reizes, O., Benoit, S. C. and Clegg, D. J. (2008). The role of syndecans in the regulation of body weight and synaptic plasticity. *Int J Biochem Cell Biol* **40**, 28-45.
Rhiner, C., Gysi, S., Frohli, E., Hengartner, M. O. and Hajnal, A. (2005). Syndecan regulates cell migration and axon guidance in C. elegans. *Development* **132**, 4621-33.
Rodriguez-Manzaneque, J. C., Westling, J., Thai, S. N., Luque, A., Knauper, V., Murphy, G., Sandy, J. D. and Iruela-Arispe, M. L. (2002). ADAMTS1 cleaves aggrecan at multiple sites and is differentially inhibited by metalloproteinase inhibitors. *Biochem Biophys Res Commun* **293**, 501-8.
Rothberg, J. M., Jacobs, J. R., Goodman, C. S. and Artavanis-Tsakonas, S. (1990). slit: an extracellular protein necessary for development of midline glia and commissural axon pathways contains both EGF and LRR domains. *Genes Dev* **4**, 2169-87.

S

Sabatier, C., Plump, A. S., Le, M., Brose, K., Tamada, A., Murakami, F., Lee, E. Y. and Tessier-Lavigne, M. (2004). The divergent Robo family protein rig-1/Robo3 is a negative regulator of slit responsiveness required for midline crossing by commissural axons. *Cell* **117**, 157-69.
Sakurai, T., Friedlander, D. R. and Grumet, M. (1996). Expression of polypeptide variants of receptor-type protein tyrosine phosphatase beta: the secreted form, phosphacan,

increases dramatically during embryonic development and modulates glial cell behavior in vitro. *J Neurosci Res* **43**, 694-706.
Sakurai, T., Lustig, M., Nativ, M., Hemperly, J. J., Schlessinger, J., Peles, E. and Grumet, M. (1997). Induction of neurite outgrowth through contactin and Nr-CAM by extracellular regions of glial receptor tyrosine phosphatase beta. *J Cell Biol* **136**, 907-18.
Sanchez-Camacho, C. and Bovolenta, P. (2009). Emerging mechanisms in morphogen-mediated axon guidance. *Bioessays* **31**, 1013-25.
Sandy, J. D., Westling, J., Kenagy, R. D., Iruela-Arispe, M. L., Verscharen, C., Rodriguez-Mazaneque, J. C., Zimmermann, D. R., Lemire, J. M., Fischer, J. W., Wight, T. N. et al. (2001). Versican V1 proteolysis in human aorta in vivo occurs at the Glu441-Ala442 bond, a site that is cleaved by recombinant ADAMTS-1 and ADAMTS-4. *J Biol Chem* **276**, 13372-8.
Sango, K., Oohira, A., Ajiki, K., Tokashiki, A., Horie, M. and Kawano, H. (2003). Phosphacan and neurocan are repulsive substrata for adhesion and neurite extension of adult rat dorsal root ganglion neurons in vitro. *Exp Neurol* **182**, 1-11.
Schecterson, L. C. and Bothwell, M. (2008). An all-purpose tool for axon guidance. *Sci Signal* **1**, pe50.
Schmalfeldt, M., Bandtlow, C. E., Dours-Zimmermann, M. T., Winterhalter, K. H. and Zimmermann, D. R. (2000). Brain derived versican V2 is a potent inhibitor of axonal growth. *J Cell Sci* **113 (Pt 5)**, 807-16.
Schmalfeldt, M., Dours-Zimmermann, M. T., Winterhalter, K. H. and Zimmermann, D. R. (1998). Versican V2 is a major extracellular matrix component of the mature bovine brain. *J Biol Chem* **273**, 15758-64.
Schmid, S., Tinguely, M., Cione, P., Moch, H. and Bode, B. (2010). Flow cytometry as an accurate tool to complement fine needle aspiration cytology in the diagnosis of low grade malignant lymphomas. *Cytopathology*.
Schwartz, N. B. and Domowicz, M. (2004). Proteoglycans in brain development. *Glycoconj J* **21**, 329-41.
Schwartz, N. B., Domowicz, M., Krueger, R. C., Jr., Li, H. and Mangoura, D. (1996). Brain aggrecan. *Perspect Dev Neurobiol* **3**, 291-306.
Schweigreiter, R., Walmsley, A. R., Niederost, B., Zimmermann, D. R., Oertle, T., Casademunt, E., Frentzel, S., Dechant, G., Mir, A. and Bandtlow, C. E. (2004). Versican V2 and the central inhibitory domain of Nogo-A inhibit neurite growth via p75NTR/NgR-independent pathways that converge at RhoA. *Mol Cell Neurosci* **27**, 163-74.
Seeger, M., Tear, G., Ferres-Marco, D. and Goodman, C. S. (1993). Mutations affecting growth cone guidance in Drosophila: genes necessary for guidance toward or away from the midline. *Neuron* **10**, 409-26.
Seidenbecher, C. I., Gundelfinger, E. D., Bockers, T. M., Trotter, J. and Kreutz, M. R. (1998). Transcripts for secreted and GPI-anchored brevican are differentially distributed in rat brain. *Eur J Neurosci* **10**, 1621-30.
Seidenbecher, C. I., Richter, K., Rauch, U., Fassler, R., Garner, C. C. and Gundelfinger, E. D. (1995). Brevican, a chondroitin sulfate proteoglycan of rat brain, occurs as secreted and cell surface glycosylphosphatidylinositol-anchored isoforms. *J Biol Chem* **270**, 27206-12.
Serafini, T., Colamarino, S. A., Leonardo, E. D., Wang, H., Beddington, R., Skarnes, W. C. and Tessier-Lavigne, M. (1996). Netrin-1 is required for commissural axon guidance in the developing vertebrate nervous system. *Cell* **87**, 1001-14.
Serafini, T., Kennedy, T. E., Galko, M. J., Mirzayan, C., Jessell, T. M. and Tessier-Lavigne, M. (1994). The netrins define a family of axon outgrowth-promoting proteins homologous to C. elegans UNC-6. *Cell* **78**, 409-24.
Sheng, W., Wang, G., Wang, Y., Liang, J., Wen, J., Zheng, P. S., Wu, Y., Lee, V., Slingerland, J., Dumont, D. et al. (2005). The roles of versican V1 and V2 isoforms in cell proliferation and apoptosis. *Mol Biol Cell* **16**, 1330-40.
Shim, S. and Ming, G. L. (2007). Signaling of secreted semaphorins in growth cone steering. *Adv Exp Med Biol* **600**, 52-60.

Shindo, T., Kurihara, H., Kuno, K., Yokoyama, H., Wada, T., Kurihara, Y., Imai, T., Wang, Y., Ogata, M., Nishimatsu, H. et al. (2000). ADAMTS-1: a metalloproteinase-disintegrin essential for normal growth, fertility, and organ morphology and function. *J Clin Invest* **105**, 1345-52.
Shinomura, T., Nishida, Y., Ito, K. and Kimata, K. (1993). cDNA cloning of PG-M, a large chondroitin sulfate proteoglycan expressed during chondrogenesis in chick limb buds. Alternative spliced multiforms of PG-M and their relationships to versican. *J Biol Chem* **268**, 14461-9.
Shintani, T., Watanabe, E., Maeda, N. and Noda, M. (1998). Neurons as well as astrocytes express proteoglycan-type protein tyrosine phosphatase zeta/RPTPbeta: analysis of mice in which the PTPzeta/RPTPbeta gene was replaced with the LacZ gene. *Neurosci Lett* **247**, 135-8.
Silver, D. L., Hou, L., Somerville, R., Young, M. E., Apte, S. S. and Pavan, W. J. (2008). The secreted metalloprotease ADAMTS20 is required for melanoblast survival. *PLoS Genet* **4**, e1000003.
Sivasankaran, R., Pei, J., Wang, K. C., Zhang, Y. P., Shields, C. B., Xu, X. M. and He, Z. (2004). PKC mediates inhibitory effects of myelin and chondroitin sulfate proteoglycans on axonal regeneration. *Nat Neurosci* **7**, 261-8.
Skaper, S. D. (2005). Neuronal growth-promoting and inhibitory cues in neuroprotection and neuroregeneration. *Ann N Y Acad Sci* **1053**, 376-85.
Smith, M. A., Yao, Y. M., Reist, N. E., Magill, C., Wallace, B. G. and McMahan, U. J. (1987). Identification of agrin in electric organ extracts and localization of agrin-like molecules in muscle and central nervous system. *J Exp Biol* **132**, 223-30.
Somerville, R. P., Longpre, J. M., Jungers, K. A., Engle, J. M., Ross, M., Evanko, S., Wight, T. N., Leduc, R. and Apte, S. S. (2003). Characterization of ADAMTS-9 and ADAMTS-20 as a distinct ADAMTS subfamily related to Caenorhabditis elegans GON-1. *J Biol Chem* **278**, 9503-13.
Spitzweck, B., Brankatschk, M. and Dickson, B. J. (2010). Distinct protein domains and expression patterns confer divergent axon guidance functions for Drosophila Robo receptors. *Cell* **140**, 409-20.
Stallcup, W. B. and Huang, F. J. (2008). A role for the NG2 proteoglycan in glioma progression. *Cell Adh Migr* **2**, 192-201.
Stanton, H., Rogerson, F. M., East, C. J., Golub, S. B., Lawlor, K. E., Meeker, C. T., Little, C. B., Last, K., Farmer, P. J., Campbell, I. K. et al. (2005). ADAMTS5 is the major aggrecanase in mouse cartilage in vivo and in vitro. *Nature* **434**, 648-52.
Steigemann, P., Molitor, A., Fellert, S., Jackle, H. and Vorbruggen, G. (2004). Heparan sulfate proteoglycan syndecan promotes axonal and myotube guidance by slit/robo signaling. *Curr Biol* **14**, 225-30.
Stern, C. D. (2005). The chick; a great model system becomes even greater. *Dev Cell* **8**, 9-17.
Stipp, C. S., Litwack, E. D. and Lander, A. D. (1994). Cerebroglycan: an integral membrane heparan sulfate proteoglycan that is unique to the developing nervous system and expressed specifically during neuronal differentiation. *J Cell Biol* **124**, 149-60.
Stoeckli, E. T. (2006). Longitudinal axon guidance. *Curr Opin Neurobiol* **16**, 35-9.
Stoeckli, E. T. and Landmesser, L. T. (1998). Axon guidance at choice points. *Curr Opin Neurobiol* **8**, 73-9.

T

Takahashi, T., Fournier, A., Nakamura, F., Wang, L. H., Murakami, Y., Kalb, R. G., Fujisawa, H. and Strittmatter, S. M. (1999). Plexin-neuropilin-1 complexes form functional semaphorin-3A receptors. *Cell* **99**, 59-69.
Tamada, A., Kumada, T., Zhu, Y., Matsumoto, T., Hatanaka, Y., Muguruma, K., Chen, Z., Tanabe, Y., Torigoe, M., Yamauchi, K. et al. (2008). Crucial roles of Robo proteins in

midline crossing of cerebellofugal axons and lack of their up-regulation after midline crossing. *Neural Dev* **3**, 29.
Tang, X., Davies, J. E. and Davies, S. J. (2003). Changes in distribution, cell associations, and protein expression levels of NG2, neurocan, phosphacan, brevican, versican V2, and tenascin-C during acute to chronic maturation of spinal cord scar tissue. *J Neurosci Res* **71**, 427-44.
Tear, G., Harris, R., Sutaria, S., Kilomanski, K., Goodman, C. S. and Seeger, M. A. (1996). commissureless controls growth cone guidance across the CNS midline in Drosophila and encodes a novel membrane protein. *Neuron* **16**, 501-14.
Teleman, A. A., Strigini, M. and Cohen, S. M. (2001). Shaping morphogen gradients. *Cell* **105**, 559-62.
Tessier-Lavigne, M. and Goodman, C. S. (1996). The molecular biology of axon guidance. *Science* **274**, 1123-33.
Tessier-Lavigne, M., Placzek, M., Lumsden, A. G., Dodd, J. and Jessell, T. M. (1988). Chemotropic guidance of developing axons in the mammalian central nervous system. *Nature* **336**, 775-8.
Thai, S. N. and Iruela-Arispe, M. L. (2002). Expression of ADAMTS1 during murine development. *Mech Dev* **115**, 181-5.
Tortorella, M. D., Burn, T. C., Pratta, M. A., Abbaszade, I., Hollis, J. M., Liu, R., Rosenfeld, S. A., Copeland, R. A., Decicco, C. P., Wynn, R. et al. (1999). Purification and cloning of aggrecanase-1: a member of the ADAMTS family of proteins. *Science* **284**, 1664-6.
Tosney, K. W. and Landmesser, L. T. (1985). Development of the major pathways for neurite outgrowth in the chick hindlimb. *Dev Biol* **109**, 193-214.
Tosney, K. W. and Oakley, R. A. (1990). The perinotochordal mesenchyme acts as a barrier to axon advance in the chick embryo: implications for a general mechanism of axonal guidance. *Exp Neurol* **109**, 75-89.
Treloar, H. B., Ray, A., Dinglasan, L. A., Schachner, M. and Greer, C. A. (2009). Tenascin-C is an inhibitory boundary molecule in the developing olfactory bulb. *J Neurosci* **29**, 9405-16.
Trotter, J., Karram, K. and Nishiyama, A. (2010). NG2 cells: Properties, progeny and origin. *Brain Res Rev* **63**, 72-82.

U-V-W

Ughrin, Y. M., Chen, Z. J. and Levine, J. M. (2003). Multiple regions of the NG2 proteoglycan inhibit neurite growth and induce growth cone collapse. *J Neurosci* **23**, 175-86.
Varela-Echavarria, A., Tucker, A., Puschel, A. W. and Guthrie, S. (1997). Motor axon subpopulations respond differentially to the chemorepellents netrin-1 and semaphorin D. *Neuron* **18**, 193-207.
Wang, K. H., Brose, K., Arnott, D., Kidd, T., Goodman, C. S., Henzel, W. and Tessier-Lavigne, M. (1999). Biochemical purification of a mammalian slit protein as a positive regulator of sensory axon elongation and branching. *Cell* **96**, 771-84.
Wang, P., Tortorella, M., England, K., Malfait, A. M., Thomas, G., Arner, E. C. and Pei, D. (2004). Proprotein convertase furin interacts with and cleaves pro-ADAMTS4 (Aggrecanase-1) in the trans-Golgi network. *J Biol Chem* **279**, 15434-40.
Wang, W. M., Ge, G., Lim, N. H., Nagase, H. and Greenspan, D. S. (2006). TIMP-3 inhibits the procollagen N-proteinase ADAMTS-2. *Biochem J* **398**, 515-9.
Wang, W. M., Lee, S., Steiglitz, B. M., Scott, I. C., Lebares, C. C., Allen, M. L., Brenner, M. C., Takahara, K. and Greenspan, D. S. (2003). Transforming growth factor-beta induces secretion of activated ADAMTS-2. A procollagen III N-proteinase. *J Biol Chem* **278**, 19549-57.
Waselle, L., Quaglia, X. and Zurn, A. D. (2009). Differential proteoglycan expression in two spinal cord regions after dorsal root injury. *Mol Cell Neurosci* **42**, 315-27.

Westling, J., Fosang, A. J., Last, K., Thompson, V. P., Tomkinson, K. N., Hebert, T., McDonagh, T., Collins-Racie, L. A., LaVallie, E. R., Morris, E. A. et al. (2002). ADAMTS4 cleaves at the aggrecanase site (Glu373-Ala374) and secondarily at the matrix metalloproteinase site (Asn341-Phe342) in the aggrecan interglobular domain. *J Biol Chem* **277**, 16059-66.
Westling, J., Gottschall, P. E., Thompson, V. P., Cockburn, A., Perides, G., Zimmermann, D. R. and Sandy, J. D. (2004). ADAMTS4 (aggrecanase-1) cleaves human brain versican V2 at Glu405-Gln406 to generate glial hyaluronate binding protein. *Biochem J* **377**, 787-95.
Whitelaw, V. and Hollyday, M. (1983). Neural pathway constraints in the motor innervation of the chick hindlimb following dorsoventral rotations of distal limb segments. *J Neurosci* **3**, 1226-33.
Whitford, K. L., Marillat, V., Stein, E., Goodman, C. S., Tessier-Lavigne, M., Chedotal, A. and Ghosh, A. (2002). Regulation of cortical dendrite development by Slit-Robo interactions. *Neuron* **33**, 47-61.
Wight, T. N. (2002). Versican: a versatile extracellular matrix proteoglycan in cell biology. *Curr Opin Cell Biol* **14**, 617-23.
Winberg ML, N. J., Tamagnone L, Comoglio PM, Spriggs MK, Tessier-Lavigne M, Goodman CS. (1998). Plexin A is a neuronal semaphorin receptor that controls axon guidance. *Cell* **95**, 903-16.
Wolf, A. M., Lyuksyutova, A. I., Fenstermaker, A. G., Shafer, B., Lo, C. G. and Zou, Y. (2008). Phosphatidylinositol-3-kinase-atypical protein kinase C signaling is required for Wnt attraction and anterior-posterior axon guidance. *J Neurosci* **28**, 3456-67.
Wong, J. T., Wong, S. T., O'Connor, T.P. (1999). Ectopic semaphorin-1a functions as an attractive guidance cue for developing peripheral neurons. *Nat Neurosci.* **2**, 798-803.
Wong, J. T., Yu W.T, O'Connor, T.P. (1997). Transmembrane grasshopper Semaphorin I promotes axon outgrowth in vivo. *Development* **124**, 3597-607.
Wu, Y., Sheng, W., Chen, L., Dong, H., Lee, V., Lu, F., Wong, C. S., Lu, W. Y. and Yang, B. B. (2004). Versican V1 isoform induces neuronal differentiation and promotes neurite outgrowth. *Mol Biol Cell* **15**, 2093-104.
Wu, Y. J., La Pierre, D. P., Wu, J., Yee, A. J. and Yang, B. B. (2005). The interaction of versican with its binding partners. *Cell Res* **15**, 483-94.

X-Y-Z

Xiang, Y. Y., Dong, H., Wan, Y., Li, J., Yee, A., Yang, B. B. and Lu, W. Y. (2006). Versican G3 domain regulates neurite growth and synaptic transmission of hippocampal neurons by activation of epidermal growth factor receptor. *J Biol Chem* **281**, 19358-68.
Yam, P. T., Langlois, S. D., Morin, S. and Charron, F. (2009). Sonic hedgehog guides axons through a noncanonical, Src-family-kinase-dependent signaling pathway. *Neuron* **62**, 349-62.
Yamada, H., Fredette, B., Shitara, K., Hagihara, K., Miura, R., Ranscht, B., Stallcup, W. B. and Yamaguchi, Y. (1997). The brain chondroitin sulfate proteoglycan brevican associates with astrocytes ensheathing cerebellar glomeruli and inhibits neurite outgrowth from granule neurons. *J Neurosci* **17**, 7784-95.
Yamada, H., Watanabe, K., Shimonaka, M. and Yamaguchi, Y. (1994). Molecular cloning of brevican, a novel brain proteoglycan of the aggrecan/versican family. *J Biol Chem* **269**, 10119-26.
Yamagata, M., Saga, S., Kato, M., Bernfield, M. and Kimata, K. (1993a). Selective distributions of proteoglycans and their ligands in pericellular matrix of cultured fibroblasts. Implications for their roles in cell-substratum adhesion. *J Cell Sci* **106 (Pt 1)**, 55-65.
Yamagata, M. and Sanes, J. R. (2005). Versican in the developing brain: lamina-specific expression in interneuronal subsets and role in presynaptic maturation. *J Neurosci* **25**, 8457-67.

Yamagata, M., Shinomura, T. and Kimata, K. (1993b). Tissue variation of two large chondroitin sulfate proteoglycans (PG-M/versican and PG-H/aggrecan) in chick embryos. *Anat Embryol (Berl)* **187**, 433-44.
Yamaguchi, Y. (2000). Lecticans: organizers of the brain extracellular matrix. *Cell Mol Life Sci* **57**, 276-89.
Yamakawa, K., Huot, Y. K., Haendelt, M. A., Hubert, R., Chen, X. N., Lyons, G. E. and Korenberg, J. R. (1998). DSCAM: a novel member of the immunoglobulin superfamily maps in a Down syndrome region and is involved in the development of the nervous system. *Hum Mol Genet* **7**, 227-37.
Yamauchi, K., Phan, K. D. and Butler, S. J. (2008). BMP type I receptor complexes have distinct activities mediating cell fate and axon guidance decisions. *Development* **135**, 1119-28.
Yang, B. L., Zhang, Y., Cao, L. and Yang, B. B. (1999). Cell adhesion and proliferation mediated through the G1 domain of versican. *J Cell Biochem* **72**, 210-20.
Yang, Z., Suzuki, R., Daniels, S. B., Brunquell, C. B., Sala, C. J. and Nishiyama, A. (2006). NG2 glial cells provide a favorable substrate for growing axons. *J Neurosci* **26**, 3829-39.
Yaykasli, K. O., Oohashi, T., Hirohata, S., Hatipoglu, O. F., Inagawa, K., Demircan, K. and Ninomiya, Y. (2009). ADAMTS9 activation by interleukin 1 beta via NFATc1 in OUMS-27 chondrosarcoma cells and in human chondrocytes. *Mol Cell Biochem* **323**, 69-79.
Yazdani, U. and Terman, J. R. (2006). The semaphorins. *Genome Biol* **7**, 211.
Yi, X. N., Zheng, L. F., Zhang, J. W., Zhang, L. Z., Xu, Y. Z., Luo, G. and Luo, X. G. (2006). Dynamic changes in Robo2 and Slit1 expression in adult rat dorsal root ganglion and sciatic nerve after peripheral and central axonal injury. *Neurosci Res* **56**, 314-21.
Yuan, W., Matthews, R. T., Sandy, J. D. and Gottschall, P. E. (2002). Association between protease-specific proteolytic cleavage of brevican and synaptic loss in the dentate gyrus of kainate-treated rats. *Neuroscience* **114**, 1091-101.
Zako, M., Shinomura, T. and Kimata, K. (1997a). Alternative splicing of the unique "PLUS" domain of chicken PG-M/versican is developmentally regulated. *J Biol Chem* **272**, 9325-31.
Zako, M., Shinomura, T., Miyaishi, O., Iwaki, M. and Kimata, K. (1997b). Transient expression of PG-M/versican, a large chondroitin sulfate proteoglycan in developing chicken retina. *J Neurochem* **69**, 2155-61.
Zallen, J. A., Yi, B. A. and Bargmann, C. I. (1998). The conserved immunoglobulin superfamily member SAX-3/Robo directs multiple aspects of axon guidance in C. elegans. *Cell* **92**, 217-27.
Zeng, W., Corcoran, C., Collins-Racie, L. A., Lavallie, E. R., Morris, E. A. and Flannery, C. R. (2006). Glycosaminoglycan-binding properties and aggrecanase activities of truncated ADAMTSs: comparative analyses with ADAMTS-5, -9, -16 and -18. *Biochim Biophys Acta* **1760**, 517-24.
Zhang, H., Kelly, G., Zerillo, C., Jaworski, D. M. and Hockfield, S. (1998). Expression of a cleaved brain-specific extracellular matrix protein mediates glioma cell invasion In vivo. *J Neurosci* **18**, 2370-6.
Zhou, X. H., Brakebusch, C., Matthies, H., Oohashi, T., Hirsch, E., Moser, M., Krug, M., Seidenbecher, C. I., Boeckers, T. M., Rauch, U. et al. (2001). Neurocan is dispensable for brain development. *Mol Cell Biol* **21**, 5970-8.
Zhou, Z., Nguyen, T. C., Guchhait, P. and Dong, J. F. (2010). Von Willebrand factor, ADAMTS-13, and thrombotic thrombocytopenic purpura. *Semin Thromb Hemost* **36**, 71-81.
Zimmermann, D. R. and Dours-Zimmermann, M. T. (2008). Extracellular matrix of the central nervous system: from neglect to challenge. *Histochem Cell Biol* **130**, 635-53.
Zimmermann, D. R., Dours-Zimmermann, M. T., Schubert, M. and Bruckner-Tuderman, L. (1994). Versican is expressed in the proliferating zone in the epidermis and in association with the elastic network of the dermis. *J Cell Biol* **124**, 817-25.
Zimmermann, D. R. and Ruoslahti, E. (1989). Multiple domains of the large fibroblast proteoglycan, versican. *EMBO J* **8**, 2975-81.

12. Acknowledgements

First, I would like to thank Prof. Dr. Dieter Zimmermann who gave me the opportunity to do my thesis on a very entertaining topic. I thank him for his supervision and guidance along this project.

I am grateful to Prof. Dr. Esther Stoeckli for being in my committee thesis, for her insightful advices and her continuous kind availability. I am also thankful to Prof. Dr. Stephan Neuhauss for accepting to be part of this committee and for his interest in my work. I would like to thank as well Prof. Dr. Uwe Rauch of the University of Lund in Sweden to review my thesis as an external referee.

I would like to express many thanks to Dr. Mattia Matasci who initiated me into versican purification method, to Dr. Elena Domanitskaya for introducing me to the *in situ* hybridisation technique on chick tissues and to Dr. Marc Debrunner for his expertise in *in ovo* injection.

Many thanks as well to all the former and current members of the Diagnostic Molecular Pathology lab, in particular to Marie-Therese, Claudia, Kristina, Sabrina, Nathali, Regula, Nicole, Barbara and Katharina. Girls, your happy and extremely friendly tempers make our lab life lighter! I thank as well Dr. Maria Teresa Zimmermann for her very nice support in the lab.

I would like to sincerely say a big 'thank you' for the nice time shared in and around the lab, to Marion Bawohl, Gunther Boysen, Silvia Casagrande, Josefine Gerhardt, Duc Luu, Ana Nowicka, Dorothee Pflüger and Martin Weisstanner. Especially, my thoughts go to Markus Rechsteiner for his joyful and fruitful comments, also for his precious assistance along the thesis and in the very last moments.

I also thank my Swiss and non-Swiss friends I met in Zürich and who let me have a real great time out the lab, the enthusiastic Noemi, the cheerful Thomas, the fantastic members and "associates" of the Villa (Saskia, Greg, Christine, Madda,… Gionata and Sophie you won the Palme of good listeners!); and of course, the Grenoblois (still around or expat'), your close and warm support despite the distance was extremely pleasant.

Moreover, I deeply thank my friends Dorothée and Gaëlle. Their friendships, with perpetual encouragements and remarkable aid supported me a lot throughout the thesis. I hope we will continue to share great adventures.

Last but not least, I would like to express my deepest gratitude to my parents for accompanying me in all my projects and my brothers, Vincent and Philippe, for their constant and caring support in everything I do.

13. Fundings

This project has been supported by the Swiss National Science Foundation and the Velux foundation.

14. Curriculum Vitae

Personal data

Surname	Cassoly
Name	Estelle
Date of birth	04.03.1979
Place of birth	Bron (France)
Citizenship	French

Education

1995-1998	High School, Lycée de Kerneuzec, Quimperlé - France, Scientific section
1998-1999	Medecine entrance examination, UBO University, Brest - France
1999-2001	Undergraduate studies in Biology, UBO University, Brest and UJF University, Grenoble – France
2001-2003	Graduate studies in Physiology and Cell biology, UJF University, Grenoble – France
2003-2004	Master of Cell Biology, speciality Neurosciences 1st year, University Laval, Quebec – Canada
2004-2005	Master of Cell Biology, speciality Neurosciences 2nd year, UJF University, Grenoble – France M.Sc Dissertation work in the lab of Prof R. Sadoul, Neurodegeneration and Plasticity, University Hospital/INSERM, Grenoble – France Tittle: Studies of the intracellular traffic of the amyloid precursor protein (APP). Supervisor: Dr. Veronique Boyer
November 2005	Registration at the University of Zurich and at the Neuroscience Center Zürich (ZNZ)
Nov. 2005 - to date	PhD student in the lab of Prof D. Zimmermann at the Diagnostic Molecular Pathology department, Institute of Clinical Pathology, University Hospital Zürich. Title of the dissertation: *S*tudies of the role of versican expression and turnover in the control of axonal growth in the chick embryo.

List of publications

- Frequent coexpression of the vesicular glutamate transporter 1 and 2 genes, as well as coexpression with genes for choline acetyltransferase or glutamic acid decarboxylase in neurons of rat brain. *M. Danik, E.Cassoly, F.Manseau, F.Sotty, D.Mouginot, S. Williams.* J Neurosci Res. 2005 Aug 15;81(4):506-21.

- The pronuclei – 20 years later. *S. Nonchev and E. Cassoly*, Biotechnol. & Biotechnol. 2009 Nov; 23 (1) Eq. 23/2009/1. Diagnosis Press. ISSN 1310-2818.

- Versican V0 and V1 direct the growth of peripheral axons in the developing chick hind limb. *S. Dutt, E. Cassoly, M.T Dours-Zimmermann, M. Matasci, E.T. Stoeckli, D.R. Zimmermann*. J Neurosci. (accepted February 2011).